

SYNTHESIS OF DIENE LIGANDS WITH *H*-BONDING CAPABILITIES FOR BIOIMAGING APPLICATIONS

By Paulina Glowacka

Doctoral Thesis

Submitted in partial fulfilment of the requirement for the award of
Doctor of Philosophy.



University of East Anglia

Department of Chemistry

March 2015

© This Copy of the thesis has been supplied on condition that anyone who consults it is understood to recognise that its copyright rests with the author and that no quotation from the thesis, nor any information derived there from, may be published without the author's prior, without consent.

Preface.

The research in this thesis is, to the best of my knowledge, original except where due reference has been made.

P.Glowacka

September 2014

"Music does not influence research work, but both are nourished by the same sort of longing, and they complement each other in the release they offer."

Albert Einstein

"What Artistic and Scientific Experience Have in Common - Where the world ceases to be the scene of our personal hopes and wishes, where we face it as free beings admiring, asking, and observing, there we enter the realm of Art and Science. If what is seen and experienced is portrayed in the language of logic, we are engaged in science. If it is communicated through forms whose connections are not accessible to the conscious mind but are recognized intuitively as meaningful, then we are engaged in art. Common to both is the loving devotion to that which transcends personal concerns and volition."

Albert Einstein

I wish to dedicate this PhD Thesis to my grandmother Marianna Kowalczyk (1933-2012), and my two cousins Adrian Federowicz (1994-2013) and Mateusz Kowalczyk (1991-2013).

Acknowledgments

“The journey of our lives is not just about the destinations we have reached. Our wisdom, education and personal growth will come from the people we meet, the paths we choose to follow and the lessons we have learned along the way.” Unknown

During my long journey which is called PhD, I have met many valuable people whom I would like to thank.

Firstly, I wish to thank my supervisors, Dr G. Richard Stephenson, for giving me the opportunity to carry out my project in Norwich. You were supportive and helpful. I would also like to thank Prof. Pierre-Yves Renard for our collaboration, great support and for the opportunity to work in Rouen. Thanks to Prof Anthony Romieu for help and advice during my stay in Rouen. I would also like to thank my secondary supervisor Prof. Andy Cammidge. Thanks as well to my examiners Dr Chris Richards from University of East Anglia and Dr Simon Lewis from University of Bath.

I am very grateful to Dr Kenneth Hamilton for his help especially when I started my PhD and all the way through and for correcting my English.

I would like to thank all the members of the Stephenson's group, past, present and future. Many thanks to people with whom I worked in the lab 3.16 and 3.13 for creating such amazing atmosphere and all the people from 3rd floor. In particular, I wish to thanks: Ketan (for lots of fires and cool times with a bit of respect), Francesca, Oliver (for being you crazy self), Dominika, Luis, Doyle, James T. (for making me laugh), Johanna, Hemin, Sonia, Daniel, Ian, Cesar, Ryan, James H., Edmond, Dr Yohan, Dr Jamal, Dr. Julien Doulcet (for support and precise help) and many others. It is actually difficult to name you all. But definitely, thanks a lot to all of you, guys.

Thanks as well to all the technical staff of the department, in particular: Peter Mayes, Liz Suveg and Colin Mcdonald for the NMR.

I wish to thank all my friends from Norwich, in particular: Dr Fabiola Gomez- Lopez (Fabiki) for huge support and great heart, Sarah Delf (small lion) for being more than labmate and our real trips, Iskander (Scandal) for long discussion about life and “scandals”.

My housemates who have made me feel at home during staying in Norwich. In particular, big thanks to: Gabriela Bianchi (Brazilian beauty) for huge support and teaching me the management of life and being for me whenever I need, Dr Kim Findlay Cooper (Kimi) for nice advice and crazy times, Cristina Macarov for crazy kindness and support. Definitely, thanks a lot to all of you, guys. You are all unique.

As well, I wish to thank my teacher and in the same time cool friend without whom I would have never reach this place; Dr Fabrice Bisaro you are one of the best person whom I met during this “trip”. Cheers for helping me to understand and appreciate the organic chemistry with the Bob Dylan songs in the background and as well for your support in critical situations.

I wish to thank all my friends from Poland without whom I would have ever come to Norwich. In particular, many thanks to Piotr Socha (Pitus) for beautiful smile, nice advices, and making me laugh; Iwona Nowak (Iwonia) for great support and being sensitive, Katarzyna Bielawska (Kate B) for the best times with Gutek, Boguslaw Kowalczyk (Bobo) for great support and, Daniel Bernacki (Berni) for advices, Gabriela Rybak (Gaba) for support and being crazy. Although we don’t meet that often but I always know that you are there for me. You are all very special to me.

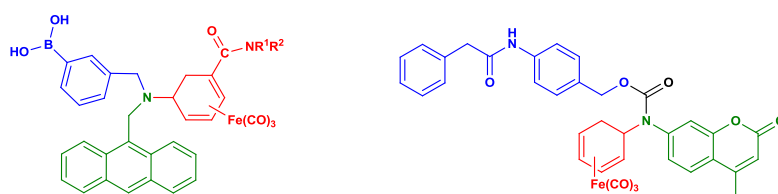
Special thanks to Dr Konrad Kowalski, who encourage me to come to Norwich to work with Richard. That was a very good move and I owe you a lot.

I wish to thank Antoni Socha and Zofia Kalkowska for all support and advices especially during critical situations. You are like family to me.

Finally, I wish to thank the families Glowacki and Kowalczyk for their love and support at all levels. In particular, many thanks to my mother Irena Stanislaw Glowacka, my father Ryszard Andrzej Glowacki, my brother Daniel Bartosz Glowacki. Finally I would like to thank my handsome blue eyed Simon James Hawkes for love, support during the last part of my PhD and not only. Without you I will never be at this place.

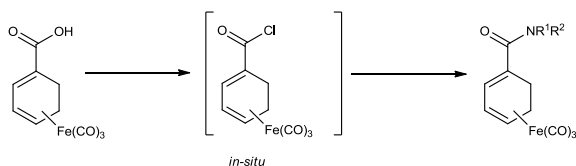
ABSTRACT: The synthesis of diene ligands with *H*-bonding capabilities for bioimaging applications

Investigations of the synthesis of novel bioprobes (Scheme A), potentially useful in bioreactions and sugar sensing, are described. A preliminary study is reported that aims to validate the feasibility of tricarbonyl iron complexes and their derivatives in applications as a constituent part of IR/fluorescent bioprobes. Infrared spectroscopy has significant potential in studying these carbonylmetal-based bioprobes, as the M-CO signals fall in a window in the water background spectrum at about 2000 cm^{-1} where absorptions of most of organic functional groups are absent. Their narrow vibrational stretching modes provide information about the iron complex and its environment.



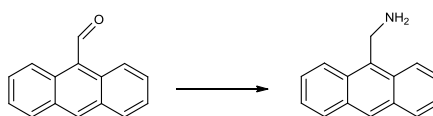
Scheme A

In the first project, novel tricarbonyliron complexes were synthesised by *N*-acylation with various amines. This procedure allowed direct access to novel amide products. (Scheme B).



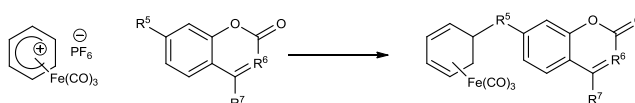
Scheme B

Work towards the development of reactions for the preparation of 9-aminomethylantracene is described. An improved preparation of this fluorophore in good yield from readily available precursors (Scheme C) was developed.



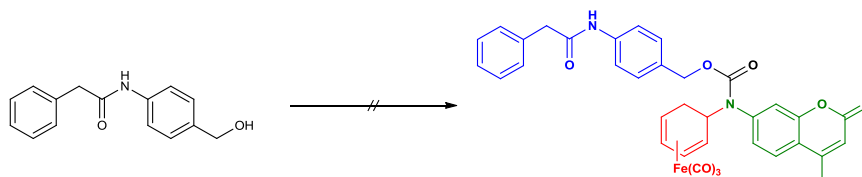
Scheme C

Furthermore, the synthesis of bioprobes suitable for sugar analytes using 9-aminomethylantracene derivatives containing boronic acids were also investigated. The synthesis of bioprobes with self-immolative linkers that also contain both fluorophores and tricarbonyliron complexes and a study of their enzymatic cleavage reactions is also described. The reaction of an electrophilic cyclohexadienyliron(1+) complex with 7-amino-4-methylcoumarin gave a new fluorescent compound, Scheme D. The methodology was then applied to the preparation of a novel series of fluorescent compounds which are valuable precursors in prodrug applications.



Scheme D

Finally, a study was made of the reaction of PABA derivatives with different protecting groups to incorporate the carbonyl group followed by attempted reactions with these new fluorescent compounds to give fully-functional target molecules, but this was unsuccessful (Scheme E).



Scheme E

Contents.

CHAPTER 1:	1
Introduction	1
1.1 About bioprobes in general	2
1.1.1 Methods for bioprobes applications	3
1.1.2 Approaches for the read-out of information	3
1.1.3 Advantages of IR-based read-out method based on organometallic chemistry	6
1.1.4 The selectivity of responses in IR-based read-out methods	10
1.1.4.1 How solvent affects the IR spectrum	10
1.1.4.2 How IR spectrum responds to changes in pH	12
1.1.4.3 How IR spectrum is affected by π –stacking interactions between organic structures	13
1.1.5 How to use of organometallic bioprobes with proteins	14
1.1.6 IR-based bioprobes	15
1.1.7 References:	19
1.2. Introduction to iron carbonyls and diene-Fe(CO) ₃	22
1.2.1. Preparation of iron tricarbonyl complexes.....	22
1.2.2. Synthesis of tricarbonyliron complexes	23
1.2.2.1. Tricarbonyliron transfer reagents	24
1.2.3. Applications of tricarbonyliron complexes.....	26
1.2.3.1. As a stereochemical control group	27
1.2.3.2. As a protecting group	27
1.2.3.3. As an activating Group	28
1.2.3.4. Stabilising capacity of the tricarbonyliron unit	28
1.2.4. Cationic forms of tricarbonyliron complexes.....	29
1.2.5. Reactions of cations.....	33
1.2.6. Decomplexation of tricarbonyliron complexes.....	37
1.2.7. References:	39
1.3. Fluorescence	42
1.3.1. Characterisation of the fluorescence	44
1.3.1.1. Fluorescence absorption and emission spectra (Stokes Shift)	44

1.3.1.2.	Fluorescence lifetime	45
1.3.1.3.	Quantum yield	45
1.3.1.4.	Absorption coefficient.....	46
1.3.1.5.	Fluorescence quenching	46
1.3.2.	Types of fluorophores	47
1.3.3.	Organic fluorophores with emission spectra up to 500 nm.....	48
1.3.3.1.	Coumarin.....	48
1.3.3.2.	Anthracene based fluorophores	50
1.3.4.	Organic fluorophores with emission spectra beyond 500 nm	51
1.3.4.1	Rhodamines.....	51
1.3.4.2.	Fluorescein	55
1.3.4.3.	Cyanines	57
1.3.4.4.	BODIPY	58
1.3.5.	Fluorescent bioprobes	61
1.3.5.1.	Fluorescent bioprobes with a cleavable phosphoester bond.....	62
1.3.5.2.	Fluorescent bioprobes with amide cleavable bonds	64
1.3.5.3.	Fluorescent probes with lactamase-cleavable active bonds	65
1.3.5.4.	Fluorescent bioprobe with cleavable bond by metal ions	66
1.3.5.5.	Fluorescent bioprobes: bonds which are cleavable by reactive oxygen species ...	67
1.3.6.	References:	69
1.4.	Bioprobes based on boron-diol interactions	73
1.4.1.	Boron-saccharide interactions.....	73
1.4.2.	Bioprobes based on the complexes of boronic acids with diols.....	76
1.4.2.1.	The events which can influence the binding event	79
1.4.2.1.1.	The pH and pKa of boronic acids	79
1.4.2.1.2.	The pKa of the boronic esters and the stability of the boronic-acid-diol complex	81
1.4.2.1.3.	Buffer effects	81
1.4.3.	The bioprobes based on fluorescent boronic acid reporter.....	81

1.4.3.1.	Photoinduced Electron Transfer (PET) types of bioprobes.....	82
1.4.4.	Internal Charge Transfer (ICT) in bioprobes.....	90
1.4.5.	Bioprobes for glucose binding	91
1.4.6.	Boron-cell surface interactions.....	97
1.4.7.	References:	99

CHAPTER 2:	102
2.1. Aim of the project 1	103
2.1.1. The Photoinduced Electron Transfer (PET) effect on the target bioprobe	104
2.1.2. Hydrogen bonding interaction observed by IR upon binding	106
2.2. Results and discussion	106
2.2.1. The choice and synthesis of IR reporting group	107
2.2.1.1. Preparation of tricarbonyliron salts	114
2.2.2. Choice and synthesis of sugar sensor	116
2.2.3. Choice and the synthesis of fluorescent reporting group	118
2.2.4. Synthesis of the main part of the target molecule (pathway A)	121
2.2.5. Reaction of tricarbonyliron salt with nucleophile (pathway B)	123
2.2.6. Preparation of target molecule (\pm)-228 and modified target molecules (\pm)-228d and (\pm)-267	124
2.3. Conclusions	129
2.4. References	130

CHAPTER 3:	131
3.1. Aim of the project 2	132
3.1.1. Choice of the self-immolative linker	135
3.1.2. Choice of the enzyme and fluorophore	139
3.2. Results and discussion	140
3.2.1. Preparation of 7-amino-4-methylcoumarin	141
3.2.2. Preparation of tricarbonyl complex and its cation	142
3.2.3. Preparation of the core of the molecule	146
3.2.4. Preparation of PABA linker	153
3.2.5. Preparation of target molecule (\pm)-268	154
3.3. Conclusion	159
3.4. References	160

CHAPTER 4:	162
4.1. General Methods	163
4.2. References	207

Abbreviations

Ac	Acetyl
AMC	7-Amino-4-methylcoumarin
APCI	atmospheric pressure chemical ionisation
aq.	aqueous
Ar	argon
atm	atmosphere
ATR-IR	Attenuated Total Reflection Infrared
br.	broad
BrMOZPhC	4-Bromomethylcoumarin-7-phenyl[6,7-b](6,9)oxazine
Bu	butyl
calcd.	calculated
cat.	catalytic
CDI	N,N'-Carbonyldiimidazole
CMIA	Carbonyl Metallo ImmunoAssay
d	doublet
dba	dibenzylideneacetone
DCE	1,2-dichloroethane
DCM	Dichloromethane
dd	doublet of doublet
ddd	doublet of doublet of doublet
dddd	doublet of doublet of doublet of doublet
DIEA	N,N-Diisopropylethylamine
dist.	distorted
DMAM-PS	Dimethylamionomethyl-polystyrene
DMAP	<i>N,N</i> -4-dimethylaminopyridine
DME	1,2-dimethoxyethane
DMF	<i>N,N</i> -dimethylformamide
DMSO	dimethylsulfoxide
DMSO-d6	deuteriated dimethylsulfoxide
DNA	Deoxyribonucleic Acid
DSC	N,N'-Disuccinimidyl Carbonate
dt	doublet of triplets
ELISA	Enzyme-Linked Immunosorbent Assay
eq	equivalents
ESI	electrospray ionisation
Et	ethyl
Et ₃ N	triethylamine
FITC	Fluorescein Isothiocyanate
FT-IR	fourier transformed infrared spectroscopy

GC	gas chromatography
HPLC	high pressure liquid chromatography
hr(s)	hour(s)
HRMS	high resolution mass spectrometry
IPA	2-propanol
<i>i</i> -Pr	iso-propyl
IR	infrared
<i>J</i>	coupling constant
lit.	literature
m	multiplet
M	molar
<i>m</i>	meta
Me	methyl
MeOH	Methanol
MHz	Megahertz
min	minute(s)
mol	mole(s)
Mp.	melting point
multi	multiple
<i>n</i> -	normal
NBS	<i>N</i> -bromosuccinimide
NMR	Nuclear Magnetic Resonance Spectroscopy
Nuc	nucleophile
<i>p</i>	para
PABA	p-Aminobenzyl Alcohol
PCA	Principal Component Analysis
PGA	Penicilin G Acylase
Ph	phenyl
ppm	Parts Per Million
pyr.	pyridine
q	quartet
Rho 110	Rhodamine 110
RNA	Ribonucleic acid
RT	room temperature
s	singlet
sat.	saturated
t	triplet
<i>t</i> -	tertiary
Temp.	temperature
THF	Tetrahydrofuran
TIS	triisopropylsilane
TLC	Thin Layer Chromatography
TMP	2,2,6,6-tetramethylpiperidine
TMS	trimethylsilyl

UV	Ultraviolet (254nm)
v	volume

CHAPTER 1:

Introduction

1.1 About bioprobes in general

The history of bioprobes began with the development of enzyme-coated electrodes by Leland C. Clark, in 1962.¹ From that point on, research in the fields of biology, chemistry, medicine, and agriculture have come together to discover and develop more sophisticated systems, consisting of biosensing devices for applications which extend even to military uses for bioterrorism detection and prevention. There are many different definitions and terminologies used depending on the field of application, but biosensors are known variously as: immunosensors, optrodes, chemical canaries, resonant mirrors, glucometers, biochips, and biocomputers.² A generally cited classification is the one accepted by IUPAC: “an electrochemical biosensor is a self-contained integrated device, which is capable of providing specific quantitative or semi-quantitative analytical information using a biological recognition element (biochemical receptor) which is retained in direct spatial contact with an electrochemical transduction element”.³

Bioprobes must include a mode to read out the information from the molecular recognition event. Typically, bioprobes have three parts (Figure 1): a binding site for an analyte molecule; a signal transduction portion of the molecule; and a responsive portion of the molecule which provides a read-out of the information. This design is restricted by the selectivity of the receptor where parallel analytes can compete for binding in the receptor. This methodology requires a time consuming process of design and synthesis of an optimized receptor for each analyte.⁴

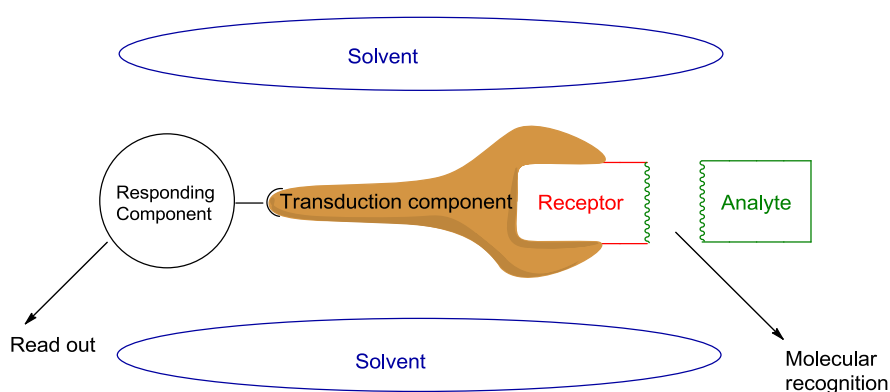


Figure 1 Representation of bioprobe.

Biosensors can be applied to many biotechnological uses, for example, in blood glucose sensing, expressing abundant market potential. Moreover, biosensors have great potential for commercialization in other application areas, but unfortunately commercial acceptance has been slow because of several technological challenges, such as complexity of the real samples, the need for reduction and simplification of the technology, selectivity and stability of the recognizing element.⁵

1.1.1 Methods for bioprobes applications

More advanced biosensors can enable remote and automated environmental monitoring. The biorecognition elements used include enzymes, whole cell receptors, DNA, or antibodies. They are linked with a transducer, such as: an electrochemical, optical, piezoelectric, or thermal device, which changes the biorecognition event into a quantifiable signal. Fluorophores or enzymes are often used to increase and generate detectible signals. The transduced signal is recorded as a digital output, normally on a computer facilitated by dedicated software. The biosensor is also responsible for detecting the analytes of interest and converting a biorecognition event into a digital output. The main purpose in building effective biosensors is to create technology which is user-friendly, sensitive, precise, reliable, and inexpensive.

1.1.2 Approaches for the read-out of information

The most well-known methods for signal transduction and read-out of information use spectroscopic methods such as UV, fluorescence spectroscopy and electrochemistry.

In a UV experiment, the binding of a guest molecule in the receptor changes the spectroscopic properties of a chromophore and so the spectrum of the molecule changes. This kind of spectrum then can be measured in the presence and the absence of the analyte, and comparing the results can give the basis for analytical measurements, and calibration curves can be defined.⁶

Fluorescence spectroscopy can be used in a similar manner to UV/visible methods, but has the important advantages of greater sensitivity.⁷

The molecular design of probes constructed to use fluorescence spectroscopy is often problematical. Figure 1 shows a fluorophore (responding component) which is covalently linked to the molecular receptor to separate the design of the binding component and the read-out component. Signal transduction, in both UV/visible and fluorescence-based systems, occurs between full and empty π / π^* orbitals (or n / π^* orbitals). Modifications in the molecule to optimize signal transduction vary the spectroscopic and fluorescence properties of the molecule. Even though there are some disadvantages to both of these spectroscopic techniques, they are very popular and have many successful applications in research. Advanced designs such as those employing fluorescence quenching have been devised to provide large changes in the spectroscopic responses upon binding of the analyte.⁸

Electrochemistry is also used as a read-out method.⁹ The experiment involves the measurement of changes in redox potentials to identify the binding of the guest analyte. One positive aspect of utilizing redox chemistry is that many subtle molecular factors can impact the electrochemical outputs of the electrophore. Therefore, an array of signal transduction strategies can be used. Organometallic derivatives can offer intense and precise electrochemical responses, and thus it is advantageous to introduce an organometallic structure as the read-out method of the molecular sensor. Ferrocene¹⁰ can be chosen as a good example because it has high levels of chemical stability with a wide selection of synthetic procedures for derivatisation. Ferrocene also has suitable characteristic electrochemical responses that can be used in sensor applications.¹⁰ For example, the binding of lithium and sodium ions in an azacrown has been studied by such an electrochemical approach.¹¹

Although infra-red spectroscopy is not very widely used in molecular sensors, it can show surprisingly many advantages. In the study of biological systems, one of the problems to overcome is the background from water which makes large sections of the IR spectrum unclear, and so not useful in a spectroscopy read-out strategy. It is therefore important to run a background spectrum before the sample spectrum. The most visible features of the background spectrum are strong IR peaks around 3800, 2400, 1600 cm^{-1} . The appearance of these peaks is due to O-H stretch of water and asymmetric stretch of carbon dioxide followed by H-O-H of water, respectively. In IR

spectra, the water bands are made up of many sharp peaks which are the vibrational transitions between different rotational states of water. When a high resolution instrument is used, the CO₂ band shows similar rotational splitting, but the lines are closer together.¹² Rotational splitting only occurs in the gas phase. Within the spectrometer cavity, air contains water and carbon dioxide. To overcome observational problems arising from this, purging the spectrometer has been used, involving the passing of a steady stream of nitrogen through the spectrometer to eliminate the H₂O and CO₂ bands. Despite all this, organometallic chemistry again shows the best answer to this problem. In designing a bioprobe, it is important to achieve a good signal transduction between the receptor site and the responding group, which are less likely to suffer from interference when vibrational spectroscopy provides the read-out process. The key benefits of IR are: 1) minimal background absorbances from biological functional groups in the window in the water background system; 2) this technique can function on a very fast timescale, so it is possible to resolve details of quickly changing events.⁵

To summarise, in order to build good bioprobes, many factors have to be considered, such as high sensitivity in the spectroscopic responses is fundamental. With greater sensitivity, a larger array of biological matters can be distinguished, as method depends on the capability to recognise changing signals from the read-out system in the presence of the background spectra of the biological sample. It needs to be mentioned that low competition from background spectroscopic transitions is crucial. This ensures that when the signal transduction component that conveys information to the responding group changes, or when the structures of the host molecules in the host-guest chemistry of the receptor create change, there are corresponding changes in the spectroscopic responses of the system. The IR-based techniques show that it is possible to cover all requirements and they show great promise as a read-out method for biological applications.

1.1.3 Advantages of IR-based read-out method based on organometallic chemistry

There is a region ($1900\text{--}2100\text{ cm}^{-1}$) in the IR spectrum where organic functional groups do not show vibrational bands, except some very weak overtone bands of bending modes of organic functional groups.¹² The vibrational stretching mode of carbon monoxide (centred on 2143 cm^{-1}) is shifted to lower wavenumbers in carbonylmetal transition metal complexes. Many metal complexes with carbonyl ligands display intense vibrational stretching modes in this window in the background spectrum.⁵ In cases when the complex is connected to a receptor function by a transduction component (Figure 2), a suitable design for bioprobe using IR as a read-out technique can be established. When designing a bioprobe using IR as a read-out technique, it is worth noting that many carbonylmetal complexes show intense vibrational stretching modes in the window in the background spectrum, so they are suitable to be connected to a receptor function by a transduction component (Figure 2).

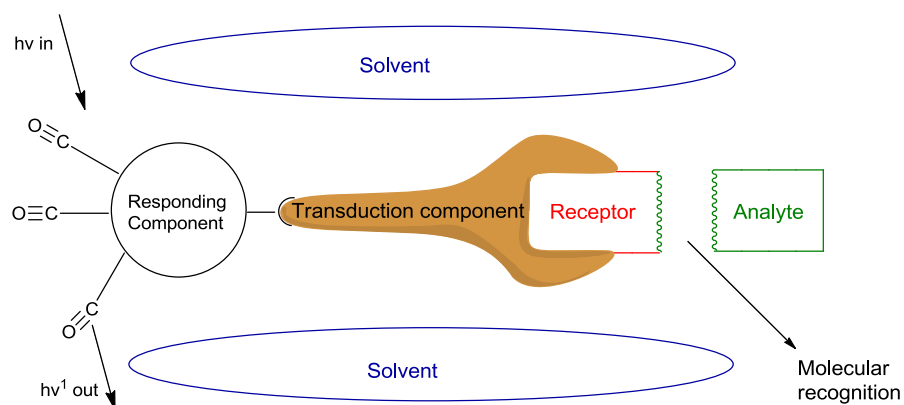


Figure 2 Representation of the complex connected to a reception by transduction component

Furthermore, in the case of the carbonylmetal complexes, the complicated vibration/rotation band structure of carbon monoxide gas is portrayed as single intense vibrational mode. The CO stretching of this mode when attached to the complex normally appears in the $1800\text{--}2100\text{ cm}^{-1}$ region.⁵

The explanation for the shift of the vibrational frequency of free CO into the $1800\text{--}2100\text{ cm}^{-1}$ region in the metal complexes will be now described. A sigma bond (σ) is formed between the carbon of the CO molecule and the metal arising from the overlap

of symmetrical metal orbital and the sp hybrid orbital on carbon (which in the case of free CO holds a non-bonded pair of electrons at carbon). This is called a σ donor interaction which is from the CO carbon lone pair into an empty metal orbital.

The ligands can possess empty antibonding orbitals which have the correct orientation to receive electrons back from the metal to form π bonds, created from the overlap of a π^* orbital of the CO triple bond with a suitable symmetry (antisymmetric) metal-centred atomic orbital (an interaction between the carbonyl ligand and the metal). This can produce a flow of electron density from metal to the ligand which fulfils a π -acceptor function as the metal complex forms.^{12,13}

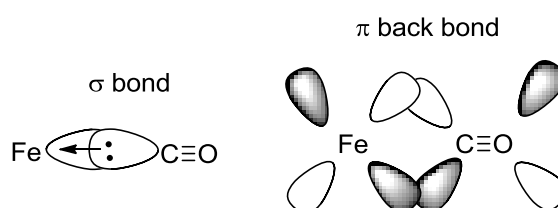


Figure 3 Representation of the σ and π back bond between iron and carbon monoxide.

These properties of the σ -donation and π -acceptance gives a convenient model to recognise the consequences of complexation on the strength of the CO bond, and consequently on the shifts in the vibrational frequency of its stretching mode [$\nu(\text{CO})$]. It is necessary to explain why the cationic carbonyl-metal complexes show $\nu(\text{CO})$ at higher wavenumbers than neutral complexes, and correspondingly why neutral complexes will have $\nu(\text{CO})$ at higher wavenumbers than anionic complexes. It is needed to take into account that anionic complexes possess greater electron density on the metal than a neutral structure, so π -acceptor properties of ligands provide a means for charge delocalization. Greater transfer of electron density from the CO π -bonding system into the orbital which includes the π^* antibonding orbital of the carbonyl ligand, make the triple bond weaker and lowers the vibrational frequency of the stretching mode.

In analogous way, the cationic case can be explained. The lower electron density at the metal results in a smaller tendency to transfer electron density to a π^* antibonding orbital, which avoids making the bond weaker, so the peak for stretching mode appears at higher wavenumbers. If the carbonyl ligand is exchanged for a phosphine

ligand, the vibrational frequency of any remaining carbonyl ligands will be shifted to lower wavenumbers as the phosphines are weaker π -acceptors than carbon monoxide.¹²

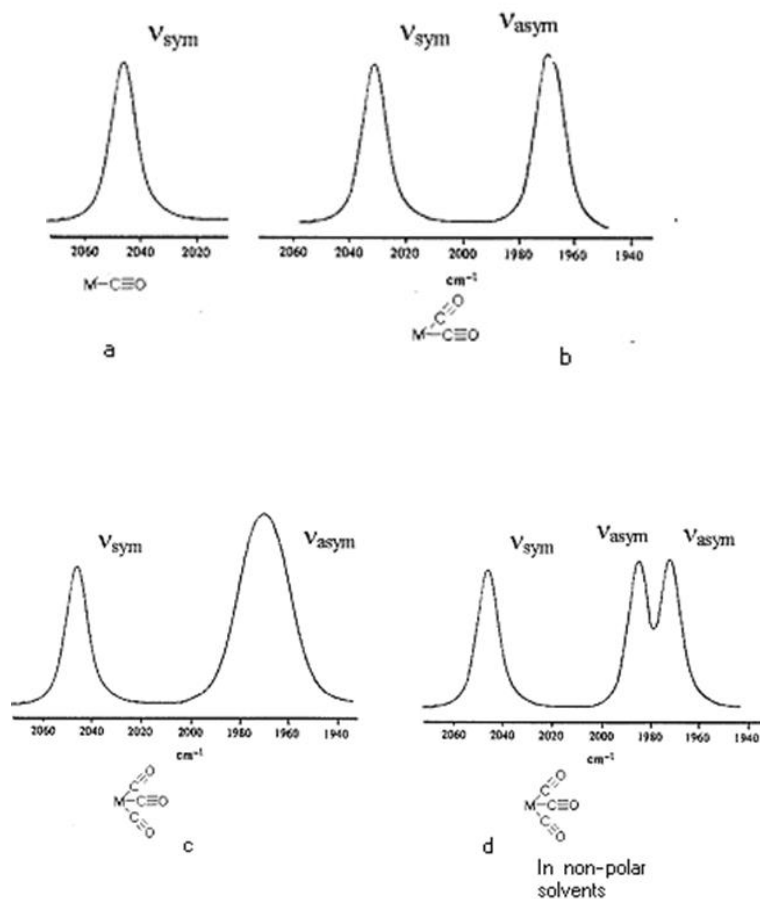


Figure 4 Representation of IR spectra for metal with ligands (adapted from reference 5).

When a metal is connected to several carbonyl ligands, vibrational coupling will produce a more complicated spectrum. Figure 4a is the representation of the IR spectrum as a single sharp band for an isolated $M(CO)$ group. When two carbonyl groups are attached to the metal in an $M(CO)_2$ structure (Figure 4b) this always gives two distinct vibrationally coupled signals, and consequently more information can be read from it. The symmetric vibrational mode of the $M(CO)_2$ corresponds to the higher energy vibrational band, and the antisymmetric mode corresponds to a lower energy vibrational band. The distance between these two bands [$\nu_{sym}(CO)$ and $\nu_{asy}(CO)$] is important because it depends on the efficiency of vibrational coupling. The position of the bands also plays a significant role, as the location of the centre point between the

two band maxima is strongly influenced by the charge on the metal, but the vibrational coupling is most affected by the changes in the geometry of the complex.¹⁴ It is noteworthy that already it is possible to read more information from $M(CO)_2$ than from a $M(CO)$ group, so it is clear that when the three carbonyl groups are attached to the metal even more data is obtained.⁵

In Figure 4c, the IR spectrum for $M(CO)_3$ is presented. There is as before a symmetric stretching mode which shows the highest wavenumber vibrational band. However, there are now two opportunities for antisymmetric stretching modes and often they have the same energy for the vibrational transition – i.e. they are degenerate. In the first instance, Figure 4c, the signals from these therefore appear at the same place in the IR spectrum which shows a smaller $\nu_{sym}(CO)$ band followed at lower frequency by a single $\nu_{asym}(CO)$ band of nearly twice the intensity. In second case, Figure 4d, the $\nu_{asym}(CO)$ bands can sometimes be partially resolved, for example if in non-polar solvents such as cyclohexane. This involves a second vibrational coupling and so provides an additional source of information in the read-out process. Considering bioprobe applications, it is worth notice that the overlapping $\nu_{asym}(CO)$ bands are also of value because loss of degeneracy and the degree of separation of the two bands are consequences of changes in the nature of the complex, which can be assessed by comparing the degree of broadening of the symmetric and antisymmetric signals.¹⁵

The IR based technique using organometallic bioprobes with carbonyl ligand shows promising and unusual features, especially considering the absorption frequencies of $\nu(CO)$ signals (sharp and narrow) can be adjusted by changing other ligands in the complexes. These structures are able to behave in a differential way to a variety of charge/structural effects in the complex. Another great advantage of this method is that the signals of several organometallic complexes can be determined individually in a single spectroscopic experiment. It is also possible to choose to have vibrational bands that do not overlap, which can be very useful in the case of biological systems, where many competing influences on the output of the sensor have to be addressed.⁵

1.1.4 The selectivity of responses in IR-based read-out methods

It has been shown that changing from non-polar solvents both shifts and broadens signals. It can be considered as due to the increased effect of dipole-dipole interaction between the vibrating dipole of the read-out group and dipoles of the solvent molecules, rather than to changes in charge distribution within the structure induced by the greater solvation of charged functionality by more polar solvents. Both cases are possible and substantial because they cause changes to vibrational spectra from the influence of different solvation environments.^{16,17,18}

1.1.4.1 How solvent affects the IR spectrum

Stephenson and Creaser *et al.*¹⁹ showed how to analyse the environment sensitivity of IR-active metal complexes with carbonyl ligands. They used the Bellamy plots²⁰ of $\nu_{\text{sym}}(\text{CO})$ against $\nu_{\text{asym}}(\text{CO})$ vibrational modes and found that the solvents of different polarities give spectra in which the positions of the centres of vibrational bands are shifted substantially relative to one another (Figure 5a). It is worth notice that it correlates to a linear plot in which the responses to each solvent are spread out along a diagonal between hexane and DMA (Figure 5b). The calculation of the diagonal separation (δ) of the extreme points on the plot, corresponding to polar solvents such as dimethylformamide (DMF) and dimethylacetamide (DMA) and non-polar solvents such as hexane and cyclohexane allowed the degree of differentiation of environments shown by each complex to be assessed.

The parameter (δ) was defined (Eq. 1) as:

$$\delta = \{[\nu_{\text{sym}}(\text{hexane}) - \nu_{\text{sym}}(\text{DMA})]^2 + [\nu_{\text{asym}}(\text{hexane}) - \nu_{\text{asym}}(\text{DMA})]^2\}^{1/2} \text{ (Eq. 1)}$$

where the vibrational signals for measurements in hexane and DMA lie at the extremes of the Bellamy plot.

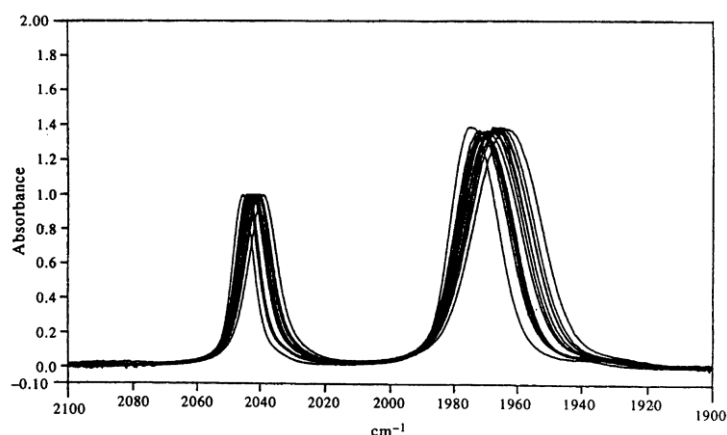


Figure 5a IR spectra influenced by different solvents, reproduced from reference 5.

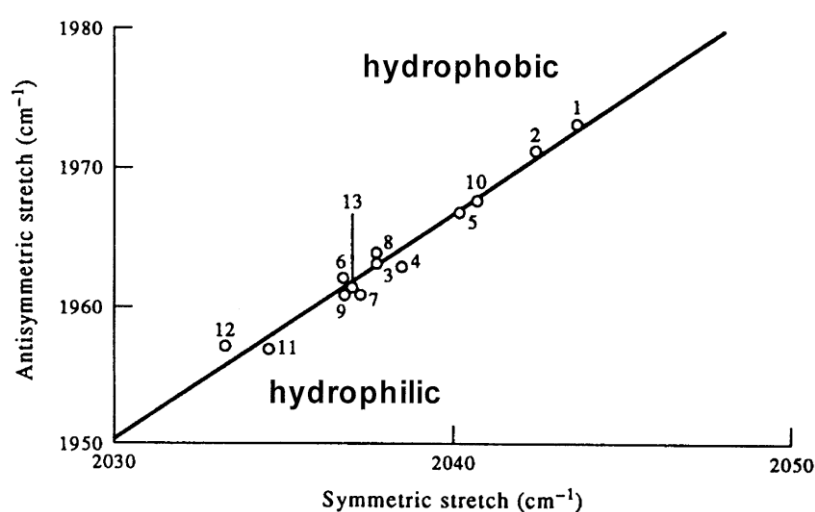
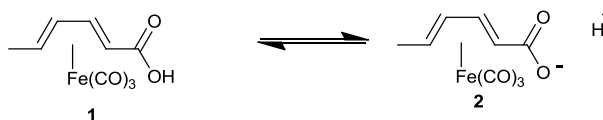


Figure 5b Bellamy plots of symmetric and antisymmetric stretching modes of tricarbonyl(1-methoxy-1,3-cyclohexadiene)iron(0): 1, hexane; 2, cyclohexane; 3, toluene; 4, dichloromethane; 5, diethyl ether; 6, tetrahydrofuran; 7, acetonitrile; 8, ethyl acetate; 9, acetone; 10, 1-octanol; 11, dimethylformamide; 12, dimethylacetamide; 13, acetic anhydride (reproduced from reference 5).

The purpose of this investigation was related to addressing biological applications, as the variation of environment-induced shifts in the IR spectra offers a good read-out tool. In figure 5b, it can be seen that hydrophilic and hydrophobic environments correspond to the ends of the diagonals in the Bellamy plots. Moreover, specific issues that could possibly affect the relative positions of vibrational bands in various environments will provide a more significant to answer specific biological needs.

1.1.4.2 How the IR spectrum responds to changes at different pHs

It has been proved that both the symmetric and antisymmetric modes of the carbonylmetal absorption respond to changes in pH.²¹ The complex **1** (Scheme 1) is a suitable example to show these changes. The $\nu_{\text{sym}}(\text{CO})$ bands gives the simplest one, as the case of $\nu_{\text{asym}}(\text{CO})$, which possess an overlapping pair of antisymmetric modes, is more complicated. The position of the $\nu_{\text{sym}}(\text{CO})$ band of **1** and **2** in a pH range between 3 and 8.6 is represented by filled circles (read against the scale on the left hand vertical axis) in Figure 6.



Scheme 1 Example of the carbonylmetal in response to changes in pH which can be observed by IR.

The pH effect was also studied on derivatives of **1** in which one CO ligand was exchanged for PPh_3 . It is shown in Figure 6 that this change caused the shift of the position of the vibrational bands (Figure 7) and also influences the pK_a of the acid ($\text{Fe}(\text{CO})_2\text{PPh}_3$ complexes are less effective anion stabilizers than their $\text{Fe}(\text{CO})_3$ counterparts, because PPh_3 is a weaker π -acceptor than CO). The data for $\nu_{\text{asym}}(\text{CO})$ of the phosphine complex is represented by white circles also shown in Figure 6 (read against the right-hand axis). These spectra in Figure 6 can give even more information when they are compared with previous ones in Figure 5b where different solvents/solvent mixtures gave shifts of the whole band envelope.

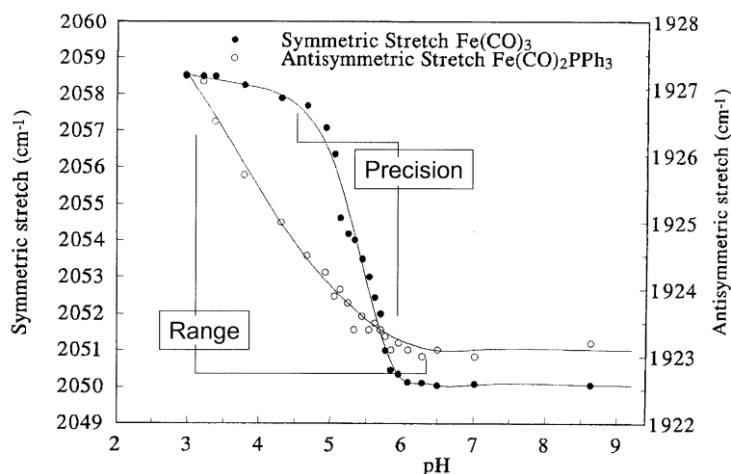


Figure 6 Plot of IR spectra at different pH values (adapted from reference 5)

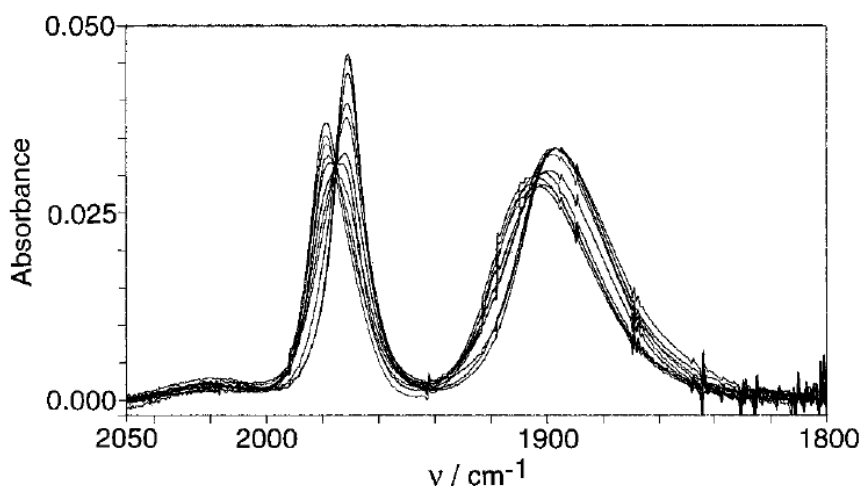


Figure 7 Representation of IR spectra affected by pH values (adapted from reference 5).

1.1.4.3 How the IR spectrum is affected by π -stacking interactions between organic structures

Bioprobes can be based on π -stacking; an effect which is important because of interactions with aromatic side-chains in proteins and between adjacent bases in nucleic acids, and an example has been described by Stephenson *et al.*²² What makes the arene complex perfect for this case is that the aromatic ring is still flat after η^6 -complexation, and the empty antibonding orbitals of the M-C bonding interactions lie in the region above the complexed arene, on the side opposite to the metal. These are envisaged to be suitably placed to form charge transfer interactions with electron rich aromatic rings. The result of π -stacking is that the vibrational bands of

tricarbonylchromium complexes are moved to lower numbers, as seen in benzene when compared with cyclohexane. The results shown in Figure 8 can be explained as follows: in the overlapping vibrational bands for spectra measured in mixtures with dimethoxybenzene in cyclohexane, the positions of the higher wavenumber $\nu_{\text{sym}}(\text{CO})$ and $\nu_{\text{asym}}(\text{CO})$ bands stay constant and reduce in intensity, while a new pair of $\nu_{\text{sym}}(\text{CO})$ and $\nu_{\text{asym}}(\text{CO})$ bands appear at lower wavenumbers, and grow in intensity as the influence of the π -stacking increases. It can be noticed that there is broadening of the new pair of $\nu_{\text{sym}}(\text{CO})$ and $\nu_{\text{asym}}(\text{CO})$ absorptions as they shift more, an effect that can also be affected by gradual addition of a more polar solvent to non-polar (cyclohexane).⁵ This shows that the arene complexes of $\text{Cr}(\text{CO})_3$ are prospective probes with π -stacking effects.

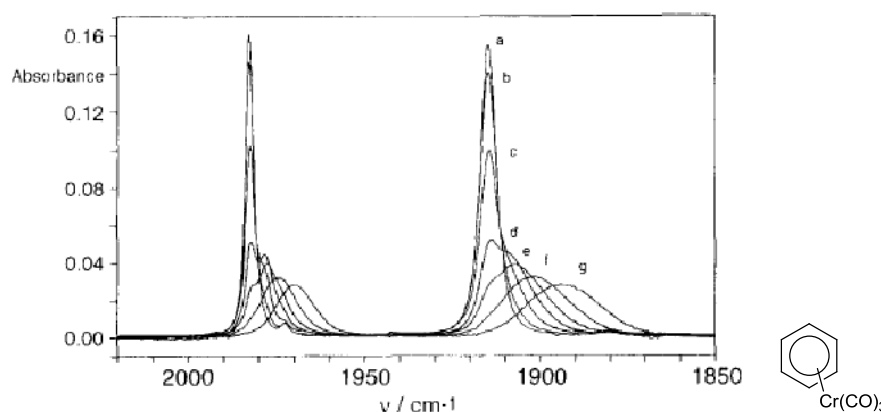
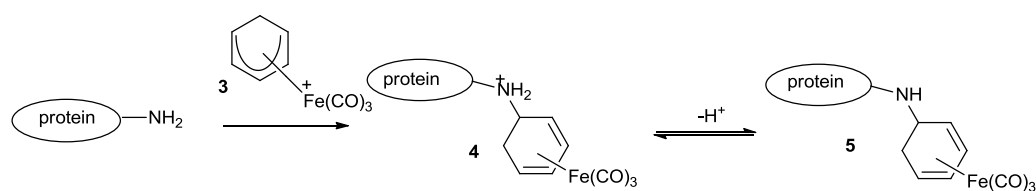


Figure 8 FT-IR spectra of $(\text{benzene})\text{Cr}(\text{CO})_3$ 5 in cyclohexane in the presence of 1,2-dimethoxybenzene (trace a: 39 mM, trace b: 79 mM, trace c: 392 mM, trace d: 785 mM, trace e: 1.57 M, trace f: 3.92 M) (adapted from reference 5).

1.1.5 How to use organometallic bioprobes with proteins

Stephenson *et al.*^{23,24} showed that it is possible to attach carbonylmetal bioprobes to the surfaces of proteins. They used the electrophilic tricarbonyl(cyclohexadienyl)iron(1+) salts **3** to react with nucleophilic groups on the protein, for instance lysine NH_2 groups (Scheme 2). This reaction of the cation with the protein α -chymotrypsin was examined by IR. The bands at 2051 and 1980 cm^{-1} of salt **3** gradually decreased in intensity as higher frequency bands appeared at about 2058 and 1993 cm^{-1} , which are due to formation of compound **4** which is in equilibrium with **5**.



Scheme 2 Use of organometallic reagent **3** to react with proteins.

These results can be explained as the addition of the tricarbonyliron complex to surface lysine groups forming ammonium ions by alkylation of the NH₂ groups. An increase in the concentration of the enzyme results in the appearance of the new signals. The experiment was performed at four different concentrations of α -chymotrypsin (1.96, 2.52, 3.32, and 4.82 mM).²⁴

1.1.6 IR-based bioprobes

There are two distinct ways which are used to develop the organometallic bioprobe structures. The organometallic part can be connected directly to a biological macromolecular structure or to a small molecule which cooperates with a biological receptor system. In studies on oestrogens, Jaouen²⁵ described a method in which steroidal compounds are derivatized at different positions while seeking to maintain biological activity. This research offered the basis for the development of the CarbonylMetalloImmunoAssay^{26,27} (CMIA) method by using metal carbonyl complexes as tracers, organic solvents (ethyl acetate, isopropyl ether) to separate the free and bound fractions, and FT-IR spectroscopy for quantification. Good representatives of this method are **6**^{28,29} and **7**³⁰. The way these two compounds work is different, as **6** is believed to bind competitively to the receptor and **7** is able to make a covalent connection by forming a metal stabilized electrophile by loss of OH from propargylic position.

Another example is the cyclopentadienylrhenium complex **8**³¹ which has been shown by modelling to be suitable to bind the hormone binding domain of the oestradiol receptor. Compounds **9** and **10**³² represent derivatives of zeranol and the natural mycotoxin zearalenone and have also been found to be very useful in a system for the biological recognition of these structures. The compound **11**³³ (a carbonylmanganese

complex) has been found to be suitable as an organometallic tracer³⁴ chemical (derived from the herbicide atrazine). Derivative **12**³⁵ is particularly interesting because the IR experiments for these compound shows non-overlapping IR bands, so it is possible to perform both measurements in a single spectroscopic experiment.

Derivative **13**³⁶ proved effective in binding studies with avidin which is the binding protein produced in the oviducts of birds, reptiles and amphibians.

In designing of the target bioprobes, it is needed to exploit changes in spectroscopic responses upon binding to the target or upon the cleavage of a bond. Whereas the competition assay work targets the determination of binding affinities by measuring attached and removable material. In all cases, it is essential to employ highly efficient spectrometers and to ensure that the organometallic compounds display biological activity. This will allow a precise screening of the biological activity to be performed.

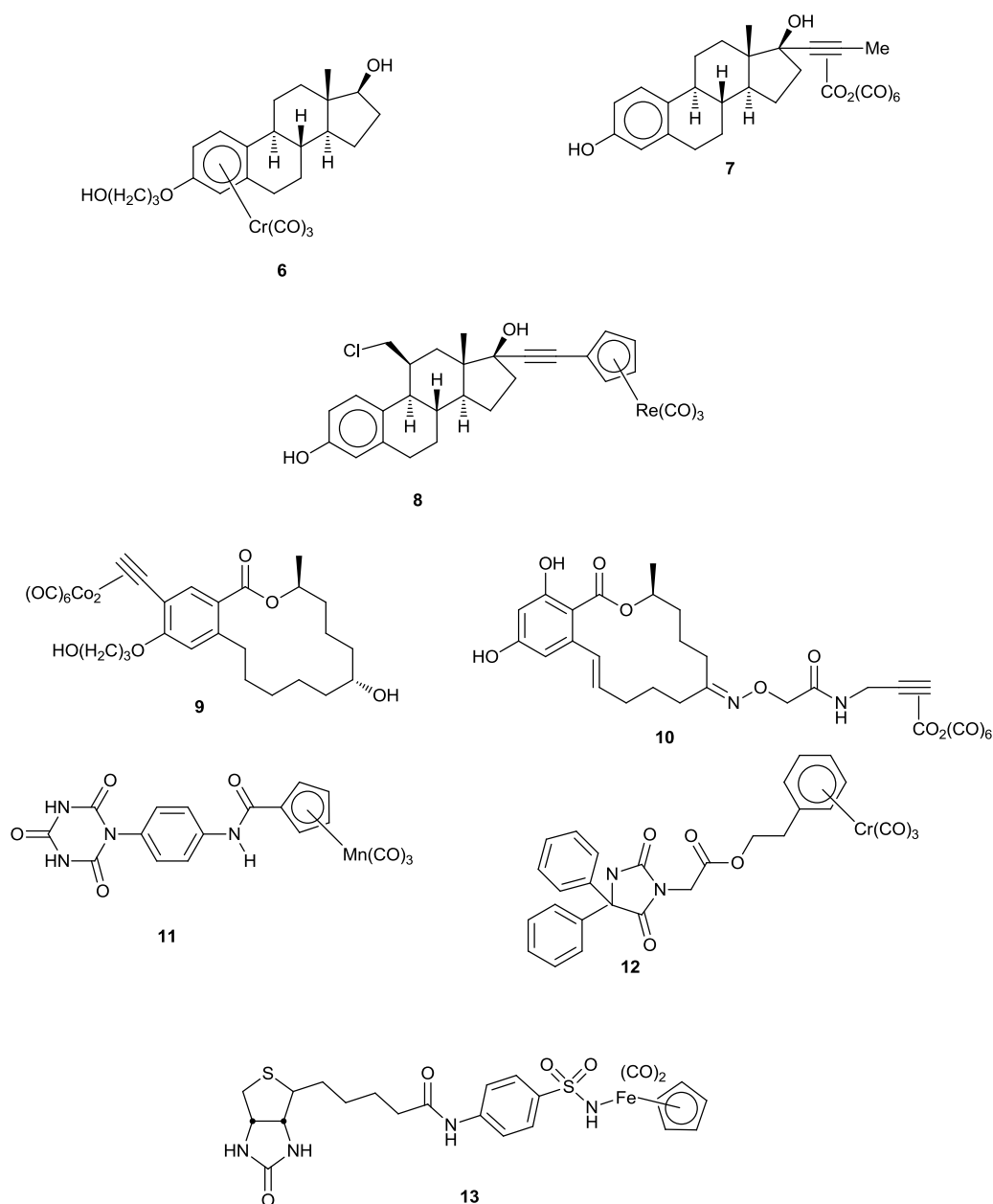


Figure 9 Examples of organometallic bioprobes.

The wide range of examples mentioned above indicates the prospective significance of organometallic carbonylmetal complexes as bioprobes. In our research group, and in collaboration, we are aiming to establish this approach in sugar sensors based on boronic acids, and prodrugs based on peptide “bond cleavage”. Almost all of the current methods utilise fluorescence for reporting the event of binding or cleavage.

There will be detailed descriptions about the structure and synthesis of the target organometallic carbonyliron bioprobes in the Results and Discussion, Chapters 2 and 3. The purpose of this work is to make the high information-content responses of IR-based systems available for the first time in sugar and enzyme-sensing. As a novel development it can lead the way for many new applications.

1.1.7 References:

-
- ¹ L. C. Clark Jr, C. Lyons, *Ann. N. Y. Acad. Sci.*, **1962**, 102, 29-45.
- ² S. P. Mohanty, E. Kougianos, *IEEE Potentials*, **2006**, 25, 35-40.
- ³ D. R. Thevenot, K. Toth, R. A Durst, G. S. Wilson, *Biosens. Bioelectron.*, **2001**, 16, 121-131.
- ⁴ P. M. Saito, K. Kikuchi, *Opt. Rev.*, **1997**, 5, 527.
- ⁵ G. Jaouen (Ed.) *Bioorganometallics*, **2006**, Wiley-VCH Verlag GmbH & Co. KGaA, R. Stephenson, Chapter 7 Organometallic Bioprobes, p:215-262.
- ⁶ a) M. Takuchi, M. Taguchi, H. Shinmori, S. Shinkai, *Bull. Chem. Soc. Jap.*, **1996**, 69, 2613; b) S. Sandanayake, S. Shinkai, *Chem. Commun.*, **1994**, 1083; c) C. J. Ward, P. Patel, P. R. Ashton, T. D. James, *Chem. Commun.*, **2000**, 229-230.
- ⁷ Reviews: a) A. W. Czarnik, *Acc. Chem. Res.*, **1994**, 27, 302; b) A. W. Czarnik (Ed.), *Fluorescent Chemosensors for Ion and Molecule Recognition*, American Chemical Society, Washington DC, **1993**, 538; c) T. D. James, P. Linnana, S. Shinkai, *Chem. Commun.*, **1996**, 281-288.
- ⁸ Reviews: a) A. P. de Silva, H. Q. N. Gunaratne, T. Gunnlaugsson, C. P. McCoy, P. R. S. Maxwell, J. T. Rademacher, T. E. Rice, *Pure. Appl. Chem.*, **1996**, 68, 1443; b) A. P. de Silva, T. Gunnlaugsson, C. P. McCoy, *J. Chem. Edu.*, **1997**, 74, 53; c) R. Narayanaswamy, *Chem. Eng. News*, **1985**, 204.
- ⁹ Reviews: a) S. Takenaka, *Small Mol. DNA RNA Binders*, **2003**, 1, 234; b) S. Subrahmanyam, S. A. Piletski, A. P. F. Turner, *Anal. Chem.*, **2002**, 74, 3942; c) C. N. Campbell, A. Heller, D. J. Caruana, D.W. Schmidtke, *Electroanal. Meth. Biol. Mater.*, **2002**, 74, 3942.
- ¹⁰ Reviews: a) A. Heller, *Acc. Chem. Res.*, **1990**, 23, 128; b) A. D. Ryabov, *Angew. Chem. Int. Ed. Engl.*, **1991**, 23, 931; c) A. N. J. Moore, D. D. M. Wayner, *Can. J. Chem.*, **1999**, 77, 681.
- ¹¹ H. Plenio, D. Burth, *Organometallics*, **1996**, 15, 1151-1156.
- ¹² a) F. A. Cotton, R. M. Wing, *Inorg. Chem.*, **1965**, 4, 314; b) F. A. Cotton, G. Wilkinson, *Advanced Inorganic Chemistry*, 2nd edition, Wiley Interscience, New York, **1966**, 730-

735; c) F. J. Mcquillin, D. G. Parker, G. R. Stephenson, *Transition Metal Organometallics for Organic Synthesis*, Cambridge University Press, Cambridge, **1991**, 19-20.

¹³ L. Pauling, *Nature of the Chemical Bond*, 3rd Edition, Cornell University Press, Ithaca, N. Y., 1964.

¹⁴ T. C. Cheam, S. Krimm, *Chem. Phys. Lett.*, **1984**, 107, 613.

¹⁵ J. K. Burdett, *Inorg. Chem.*, **1981**, 20, 2607-2615.

¹⁶ C. C. Barraclough, J. Lewis, R. S. Nyholm, *J. Chem. Soc.*, **1961**, 2582-2584; W. Beck, K. Lottes, *Z. Naturforsch.*, **1964**, 19b, 987.

¹⁷ D. J. Darensbourg, *Inorg. Chem.*, **1972**, 11, 1606-1609.

¹⁸ L. M. Haines, M. H. B. Stiddard, *Adv. Inorg. Chem. Radiochem.*, **1970**, 12, 53.

¹⁹ C. S. Creaser, M. A. Fey, G. R. Stephenson, *Spectrochim. Acta.*, **1994**, 50A, 1295-1299.

²⁰ L. J. Bellamy, R. L. Williams, *J. Chem. Soc.*, **1957**, 863; L. J. Bellamy, H. E. Hallam, R. L. Williams, *Trans. Faraday Soc.*, **1958**, 54, 1120; L. J. Bellamy, R. L. Williams, *Trans. Faraday Soc.*, **1959**, 55, 14.

²¹ C. E. Anson, T. J. Baldwin, C. S. Creaser, G. R. Stephenson, *Organometallics*, **1996**, 15, 1451-1456.

²² C. E. Anson, C. S. Creaser, G. R. Stephenson, *Spectrochim. Acta*, **1996**, 52A, 1183-1191.

²³ C. E. Anson, C. S. Creaser, G. R. Stephenson, O. Egyed, *Chem. Commun.*, **1994**, 39-40.

²⁴ C. E. Anson, C. S. Creaser, G. R. Stephenson, O. Egyed, *Spectrochim. Acta*, **1997**, 53A, 1867-1877.

²⁵ G. Jaouen, A. Vessièrès, *Pure. Appl. Chem.*, **1985**, 57, 1865-1874.

²⁶ A. Vessièrès, M. Salmain, V. Philmon, G. Jaouen, *Immunoanal. Biol. Spec.*, **1992**, 31, 9.

²⁷ M. Salmain, A. Vessièrès, G. Jaouen, *Bioconjugate Chem.*, **1991**, 1, 59.

²⁸ G. Jaouen, A. Vessièrès, S. Top, A. A. Ismail, I. S. Butler, *J. Am. Chem. Soc.*, **1985**, 107, 4780-4781.

²⁹ G. Jaouen, A. Vessièrès, S. Top, A. A. Ismail, I. S. Butler, *Biochemistry*, **1988**, 27, 6659-6666.

-
- ³⁰ M. Savignac, G. Jaouen, C. A. Rodger, R. E. Perrier, B. G. Sayer, M. J. McGlinchey, *J. Org. Chem.*, **1986**, 51, 2328-2332.
- ³¹ G. Jaouen, A. Vessièrès, I. S. Butler, *Acc. Chem. Res.* **1993**, 26, 361-369.
- ³² M. Gruselle, P. Deprez, A. Vessièrès, S. Greenfield, G. Jaouen, J.-P. Larue, D. Thouvenot, *J. Organomet. Chem.*, **1989**, 359, C53-C56.
- ³³ I. Lavastre, J. Besançon, P. Brossier, C. Moïse, *Appl. Organomet. Chem.*, **1990**, 4, 9.
- ³⁴ M. Salmain, A. Vessièrès, I. S. Butler, *J. Immunol. Methods*, **1992**, 148, 56-75.
- ³⁵ M. Salmain, A. Vessièrès, P. Brossier, G. Jaouen, *Anal. Biochem.*, **1993**, 208, 117.
- ³⁶ B. Rudolf, M. Makowska, A. Domagala, A. Rybarczyk-Pirek, J. Zakrzewski, *J. Organomet. Chem.*, **2003**, 668, 95-100.

1.2. Introduction to iron carbonyls and diene-Fe(CO)₃ complexes

Many metals form complexes which are of great utility for synthetic purposes, including palladium, chromium, magnesium and rhodium. The focus of this project is on organoiron complexes, specifically iron carbonyl complexes which are of special interest due to their high stability, with an iron(0) centre capable of coordinating complex organic ligands - the basis for organoiron chemistry. The most stable and well-known compounds in air are iron(II) complexes. These are readily oxidized to iron(III). Iron(0) can coordinate five or six ligands with trigonal bipyramidal and octahedral geometries. Iron(II) complexes ([Ar]4s⁰3d⁶) bind six ligands with octahedral geometry and for iron(III) ([Ar]4s⁰3d⁵) the coordination number is three to eight with octahedral geometry.¹

1.2.1. Preparation of iron tricarbonyl complexes

The most common procedure for the preparation of tricarbonyliron-diene complexes is based on the complexation of dienes by direct reaction with carbonyliron compounds. The main reagents used are iron pentacarbonyl [Fe(CO)₅] **14**, diironnonacarbonyl [Fe₂(CO)₉] **15**, and triiron dodecacarbonyl [Fe₃(CO)₁₂] **16**. The first of these **14** a yellow liquid, was independently described in 1891 by Mond² and Bertholet³, and was prepared by a direct reaction between finely divided iron and carbon monoxide. The second reagent (small gold flakes) was prepared by photolysis of [Fe(CO)₅] in acetic acid using a medium pressure mercury lamp. The last reagent, triiron dodecacarbonyl [Fe₃(CO)₁₂] **16** (dark green solid), has been prepared by the thermal decomposition of [Fe₂(CO)₉] **15**, Figure 10.

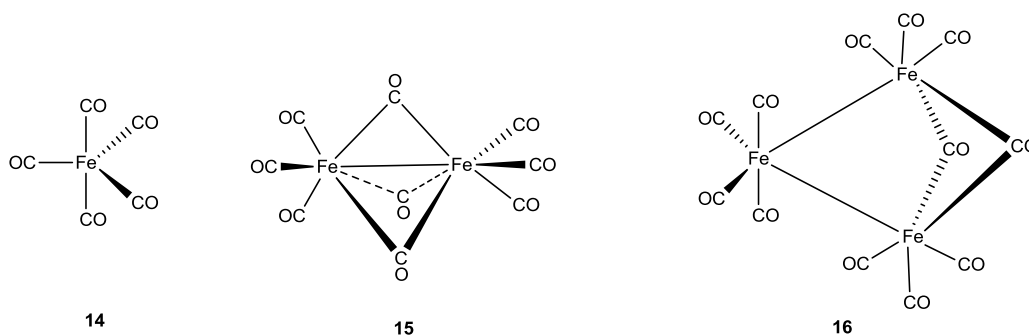
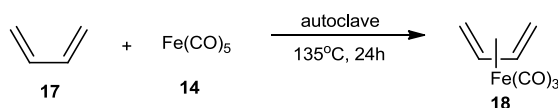


Figure 10 The most common reagents used for preparation of tricarbonyliron complexes.

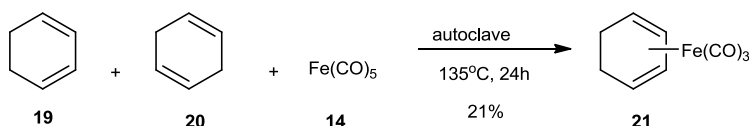
1.2.2. Synthesis of tricarbonyliron complexes

The synthesis of tricarbonyliron complexes was pioneered by Reihlen and his co-workers, although he appears not to have fully appreciated the importance of this innovative discovery in organometallic chemistry. In 1930, Reihlen's group prepared (η^4 -buta-1,3-diene)tricarbonyliron **18** by reaction of buta-1,3-diene **17** with iron pentacarbonyl **14**, Scheme 3.⁴



Scheme 3 Synthetic route towards preparation of **18**.

At the time, this report made no impact as no further papers were published for twenty-eight years in this research area. However, a U.S. patent⁵ was published in 1946, in which Reihlen's method was used for synthesis of the previously described compound **18**. The product was found to be an effective antiknock reagent but unfortunately was unstable - a severe limitation was the need to protect hydrocarbon fuels which contained it from light and oxygen. Hallam and Pauson developed Reihlen's method by refluxing 1,3-cyclohexadiene **19** with pentacarbonyliron to obtain (η^4 -cyclohexa-1,3-diene)tricarbonyliron **21**.⁶



Scheme 4 Synthetic route developed by Hallam and Pauson to obtain **21**.

It is important to note that in the case of unconjugated (1,4)-cyclohexadienes such as **20**, the complexation occurs through an isomerisation mechanism originally reported by Arnet and Pettit in 1961.⁷ A great number of substituted cyclohexa-1,4-dienes are now readily available thanks to the convenient Birch reduction of corresponding benzene derivatives which gave access to a broad range of (η^4 -1,3-cyclohexadiene)tricarbonyliron complexes.⁸

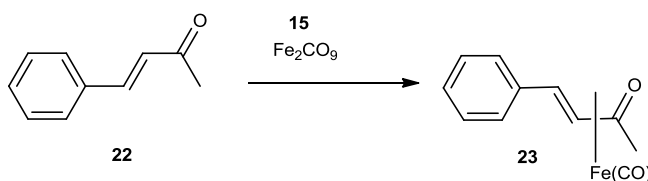
There are now many experimental methods which have been explored for complexation of dienes, as it known that the thermal reaction of Fe_xCO_y ($x=1$ or 2 , $Y=5$ or 9 , respectively) requires a temperature around 135-140 °C for the isomerisation of

1,4 dienes to proceed. The drawback here is the presence of side reactions, especially with reactive diene systems. There is an continuous challenge to find milder conditions to give diene complexes with high selectivity. A huge range of substituents and functional groups are now known to be compatible with the coordination of 1,3-diene ligands to the metal.¹

One of the most curious methods to obtain tricarbonyliron complexes, and one which had a large input in our own creative procedures (see Chapter 3, 3.2 Results and Discussions for Project 2) to prepare tricarbonyliron complex, was performed in the absence of solvent by gentle heating of a mixture of the diene and a preformed mixture of $\text{Fe}_2(\text{CO})_9$ and silica gel, which has advantages during work up. There is still a need to improve the yields for complexation reactions because they are often quite moderate (20-50 %). An important factor is that, in order to obtain high yields, a large excess of the iron carbonyl reagent is necessary, which leads to a hazardous work up due to the building up of pyrophoric iron and the presence of $\text{Fe}(\text{CO})_5$ which is highly toxic. The answer to that was found by using a tricarbonyliron transfer reagent.

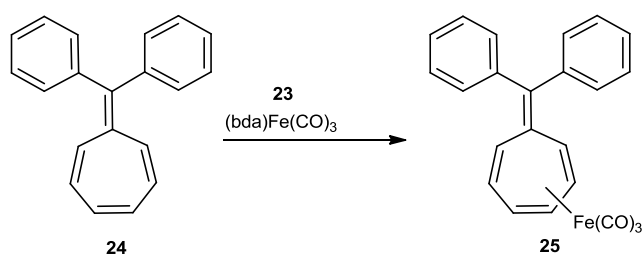
1.2.2.1. Tricarbonyliron transfer reagents

The first (η^4 -1-oxabuta-1,3-diene)tricarbonyliron complexes **23** were reported in 1964 by Weiss *et al.*,⁹ and were employed by Lewis¹⁰ as transfer reagents in 1972. The reagent was prepared by reaction of benzylideneacetone **22** and diironnonacarbonyl **15** as shown in Scheme 5.



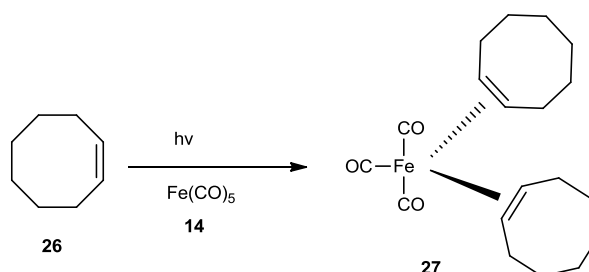
Scheme 5 Synthetic route towards preparation of **23**.

The (bda) $\text{Fe}(\text{CO})_3$ **23** transfer reagent is a suitable source of the tricarbonyliron moiety and was used in the complexation of 8,8-diphenylheptafulvene **24** to yield its tricarbonyliron derivative **25**. A limitation is that this transfer reagent only works in reactions with conjugated dienes.¹¹



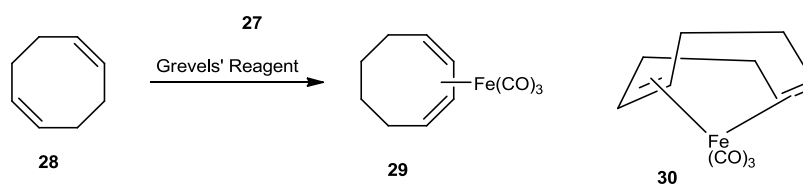
Scheme 6 Synthetic route for preparation of tricarbonyliron derivative **25**.

Subsequently, Grevels in 1984 synthesised the bis(η^2 -cis-cyclooctene)tricarbonyliron complex **27** which has advantages over Weiss's reagent since the reaction conditions do not require high temperatures to transfer the tricarbonyliron fragment to 1,3-dienes.¹² Scheme 7 shows the preparation of Grevel's reagent by photolytic reaction of pentacarbonyliron **14** and *cis*-cyclooctene **26**.



Scheme 7 Photolytic reaction of **15** and **26** to afford **27**.

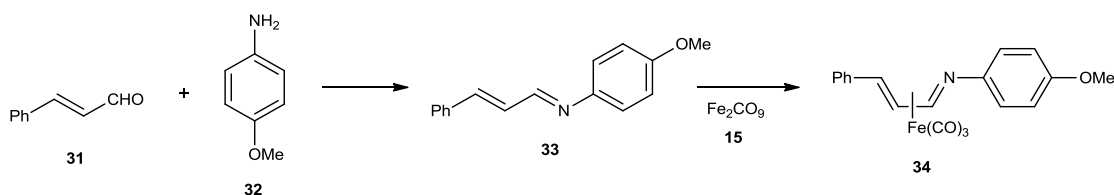
This transfer reagent **27** was used to react with *cis*-cycloocta-1,5-diene **28** which produced two compounds (η^4 -cycloocta-1,3-diene)tricarbonyliron **29** and (η^4 -cycloocta-1,5-diene)tricarbonyliron **30** as a consequence of double-bond migration.



Scheme 8 An application of **27** as a transfer reagent to obtain **29** and **30**.

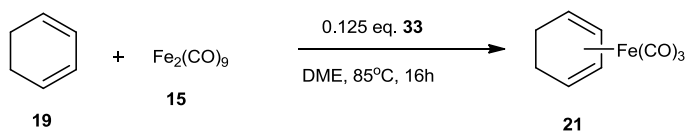
Another type of transfer reagent was first prepared by Otsuka¹³ and Lewis¹⁴ many years ago but in recent times it has been taken up by Knölker *et al.* in an extensive development of this area.^{15,16,17,18} He studied the scope and limitation for their synthesis and we were inspired in our own research by his chemistry.

The most effective transfer reagent was prepared by imine condensation of *trans*-cinnamaldehyde **31** with *p*-anisidine **32** to produce 1-(4-methoxyphenyl)-4-phenyl followed by sonication with diironnonacarbonyl **15** (Scheme 9).¹⁸



Scheme 9 Synthetic route used for preparation of **34**.

The reaction of this complex with 1,3-cyclohexadiene **19** at a suitably high temperature causes transfer of the metal fragment and provides the tricarbonyliron-1,3-cyclohexadiene complex **21** in very good yield. As well as the complexation of conjugated diene, the reaction can be performed in catalytic matter by reaction of pentacarbonyliron **14** or diironnonacarbonyl **15** in the presence of the azabuta-1,3-diene **33**. (Scheme 10)



Scheme 10 Synthetic route used for preparation of **21**.

When comparing the currently reported transfer reagents, the best one is Knölker's compound **34**.¹⁸ The huge benefit of using his compounds compared to others is that when reacting free ligands of type **33** with diironnonacarbonyl, a sub-stoichiometric quantity of the free azadiene ligand may be used in synthesis of cyclobuta-1,4-dienyliron tricarbonyl derivatives such as **21**, and it is possible to recover compound **33** during the work-up of the reaction.

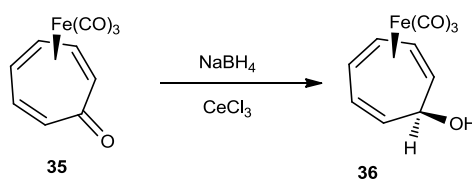
1.2.3. Applications of tricarbonyliron complexes

The synthetic application of the tricarbonyliron complexes is well established in organic synthesis. It is used as a stereochemical control group, a catalyst to isomerize double bonds, a protecting group, and an activating group, or as in this project, for the preparation of advanced biosensors. An outline of some of these will be discussed further.

1.2.3.1. As a stereochemical control group

The application of the iron tricarbonyl moiety as a stereochemical controller is one of the most important synthetic tools.

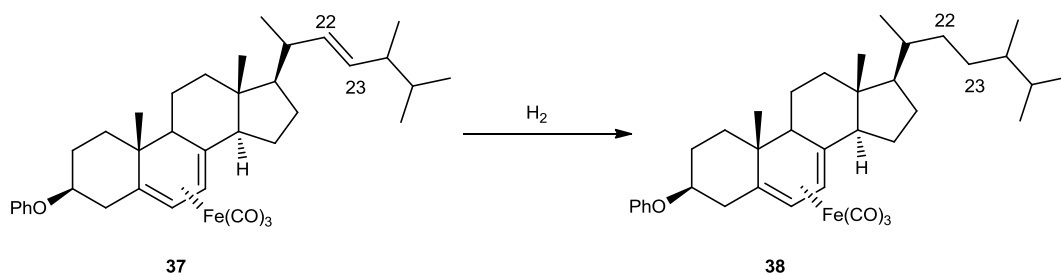
Scheme 11 shows an example of such control, which was reported by Pearson and Srinivasan.¹⁹ Reduction with sodium borohydride of tropone-tricarbonyliron complex **35** formed a single diastereomer **36**. When a ketone located *alpha* to a tricarbonyliron diene is reduced, the reaction is stereochemically controlled. This effect was explained by addition of hydride *anti* to the tricarbonyliron moiety.¹⁹



Scheme 11 Example of stereochemical control using tricarbonyliron group.

1.2.3.2. As a protecting group

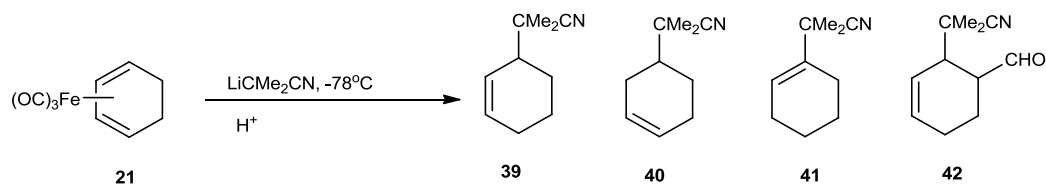
Hallam and Pauson's observations in 1958 on dienes attached to the tricarbonyliron complex, suggest that the iron group could be potentially used as a protecting group.²⁰ For instance, it can survive reactions such as hydroboration, osmylation, hydrogenation, or epoxidation, which are characteristic for the modification of carbon-carbon double bonds. The perfect example of this is exemplified in Scheme 12. The ergosterol benzoate complex **37** goes through these previously mentioned reactions, selectively at the 22,23-double bond, and hydrogenation of this bond is illustrated below. When $\text{Fe}(\text{CO})_3$ is attached to the diene system none of these reactions occur on the ring double bonds.



Scheme 12 Hydrogenation step to obtain **38**.

1.2.3.3. As an activating group

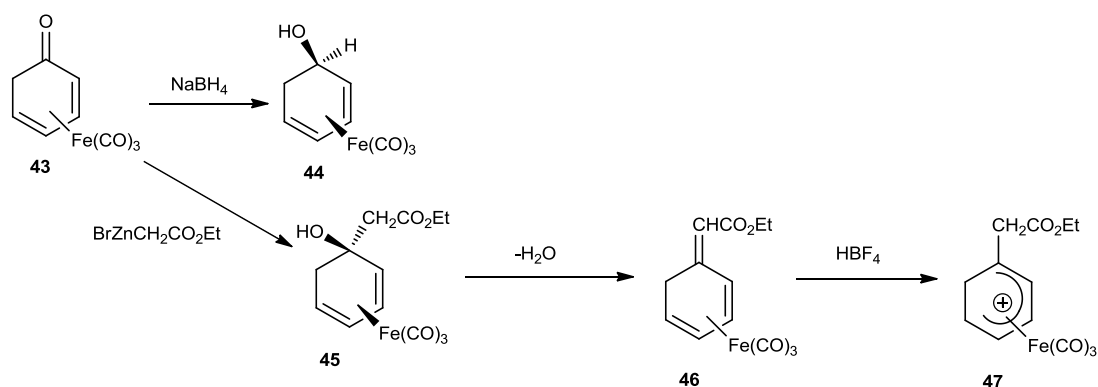
The tricarbonyliron moiety can be used in the formation of new carbon-carbon bonds as it acts as an electron acceptor and opens the possibility for nucleophilic addition to the diene carbon atoms. The nucleophilic addition of 2-lithio-2-methylpropionitrile (LiCMe_2CN) to (η^4 -cyclohexa-1,3-diene)tricarbonyliron **21** and then decomplexation gives four products (**39**, **40**, **41**, **42**) in which compound **39** can be isolated when the reaction mixture is permitted to come to room temperature (Scheme 13).²¹



Scheme 13 Decomplexation step of **21**.

1.2.3.4. Stabilising capacity of the tricarbonyliron unit

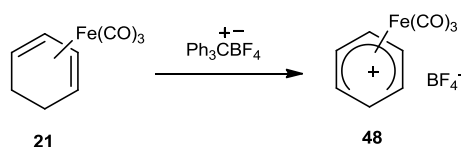
An example of another role in which the tricarbonyliron fragment shows increased stability by coordination is cyclohexa-2,4-dien-1-one, a tautomer of phenol. Cyclohexa-2,4-dien-1-one is the less stable tautomer in the uncomplexed form, however, when the tricarbonyliron fragment is introduced, the compound **43** is stable enough to be used in further synthesis. Scheme 14 shows the limitation in reactivity of the complex with selected nucleophiles. When reduction occurred to form compound **44**, the *endo* hydroxyl complex is favoured as the attack is *anti* to the metal. Similarly, treatment with zinc ethyl bromoacetate resulted in a complex **45** which could undergo dehydration to produce derivative **46**, followed by hydride abstraction, to obtain the highly electrophilic tricarbonyliron cation **47**. This substituted (η^5 -cyclohexadienyl)-tricarbonyliron cation **47** can react with a vast array of nucleophiles.²²



Scheme 14 An example of stabilising role of the tricarbonyliron fragment

1.2.4. Cationic forms of tricarbonyliron complexes

A significant revolution in the organometallic chemistry of iron complexes arose in 1960 with the discovery of the tetrafluoroborate salt of (η^5 -cyclohexa-1,3-dienyl)tricarbonyliron **48**.²³ This highly electrophilic cation was prepared by hydride abstraction from complex **21** with triphenylcarbenium tetrafluoroborate (Scheme 15). It has been proved that iron is bonded to five sp^2 carbon atoms in the cationic complex and they are planar except for the sixth carbon, which in the cyclohexadienyl ring is sp^3 hybridised and lies above (**48a**) or below **48b** the plane, Figure 11.²⁴ Wilkinson *et al.* showed by ^1H -NMR studies that for the (η^5 -cyclohexadienyl)tricarbonyliron tetrafluoroborate complex, the correct conformation is **48b**.²⁵



Scheme 15 Synthetic route towards preparation of salt **48**.

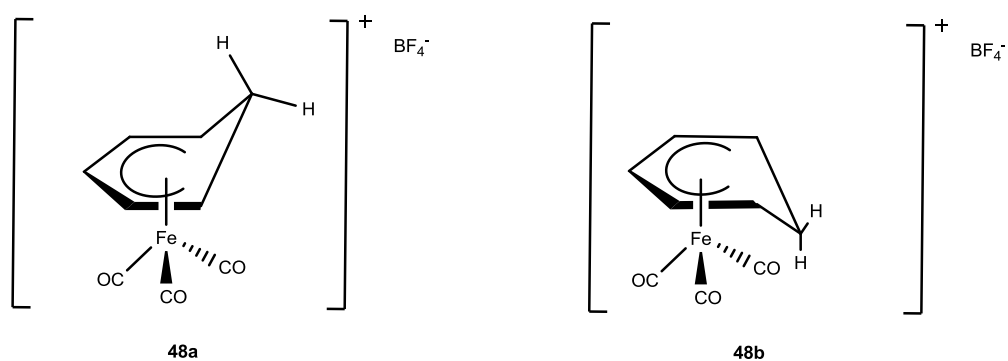
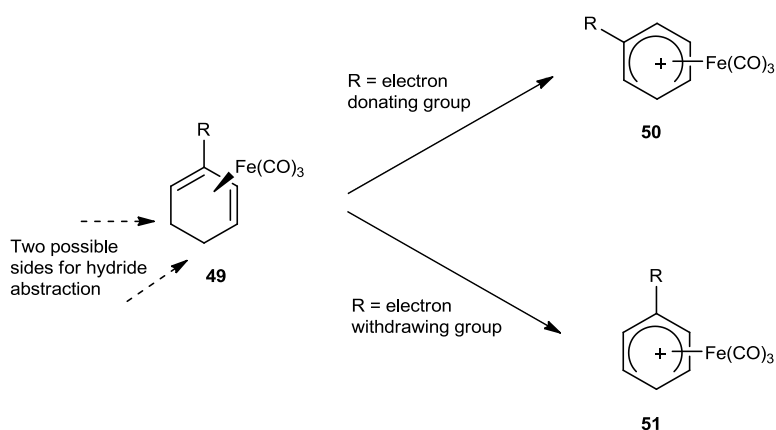


Figure 11 Representation of the conformation of salt **48**

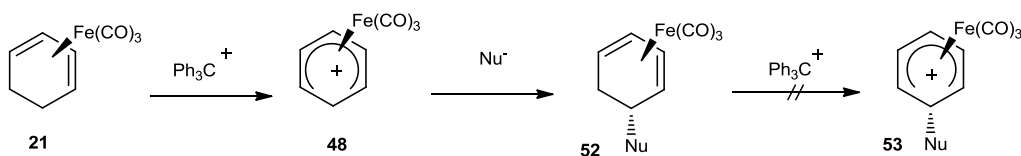
It is no surprise that these cationic complexes opened many gates in organic synthesis due to their strongly electrophilic nature. There was much discussion regarding how nucleophiles could possibly attack the cationic complex (for instance, *anti* or *syn* attack on the ring, attack at the metal). Most evidence to date suggests that in irreversible reactions nucleophilic attack takes place on the ring at the face opposite to the metal, because the products have an *exo* configuration.²⁶

The hydride abstraction reaction for mono- and di- substituted diene complexes is regioselective and the product formed depends on the nature of the substituent (electronic effect) and also on steric effects as the counterion, such as the triphenylmethyl anion, is generally a very bulky group. In substituted cyclohexadiene complexes, there are two methylene groups which can be removed. The electron donating groups preferentially give almost entirely compound **50** and electron-withdrawing groups give complex **51**, but in each case with traces of the other compounds are found, (Scheme 16).²⁷



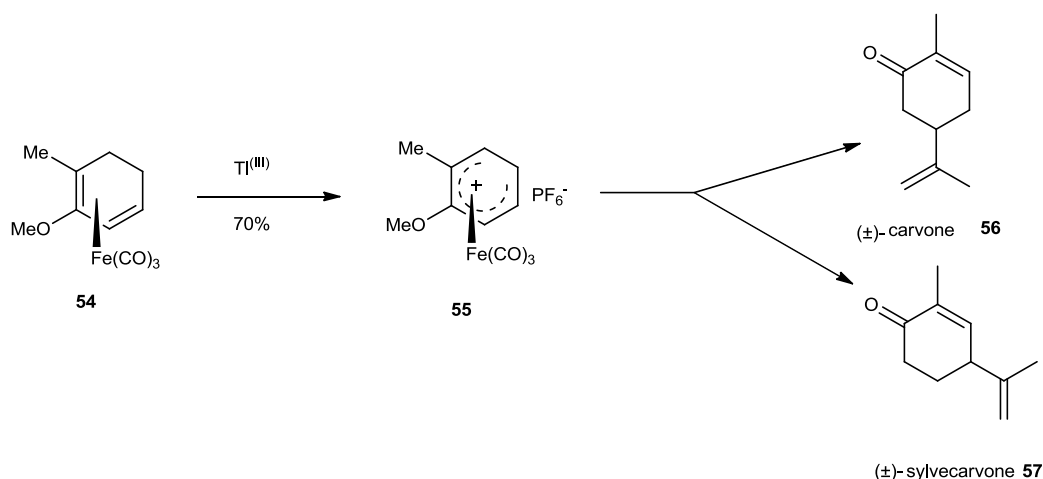
Scheme 16 Hydride abstraction of **49** affording **50** or **51** depends on R substituent.

It is worth noting that it is not possible to perform the hydride abstraction process with cyclohexadiene complexes **52** when a substituent is at the carbon-5 position (*anti* to the metal). This means that after a first addition of nucleophile to a dienyl complex, second addition is not possible, as shown in Scheme 17.²²



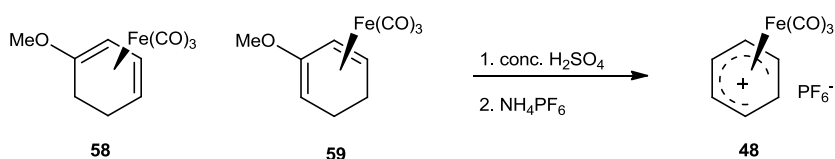
Scheme 17 Representation of hydride abstraction process.

There are a few papers which describe alternative methods to overcome steric hindrance in hydride abstraction, such as oxidation of the neutral 1,2-dimethoxydienyl iron tricarbonyl complex **54** with thallium(III) tris(trifluoroacetate) or activated DDQ- HBF_4 at -78°C . Stephenson and his group used thallium(III) oxidation to prepare (\pm)-carvone **56** and (\pm)-sylvecarvone **57**.²⁸



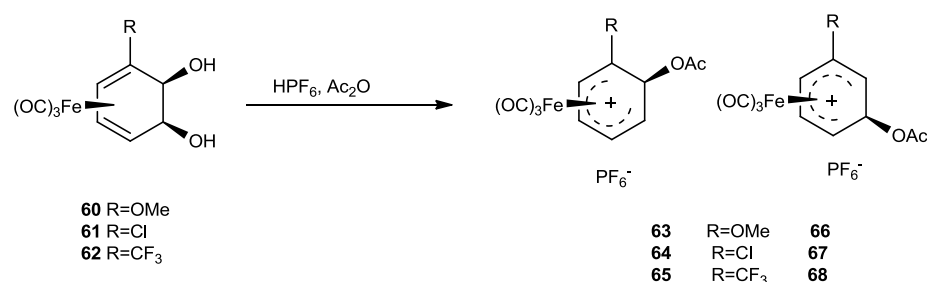
Scheme 18 Synthesis of (±)-carvone and (±)-sylvecarvone

An alternative preparation of η^5 -cyclohexadienyl salts is shown in Scheme 19, involving the reaction of suitable 1- or 2-substituted methoxydienyl or hydroxyl tricarbonyliron complexes under acidic conditions.²⁹



Scheme 19 Preparation of cation **48** under acidic conditions

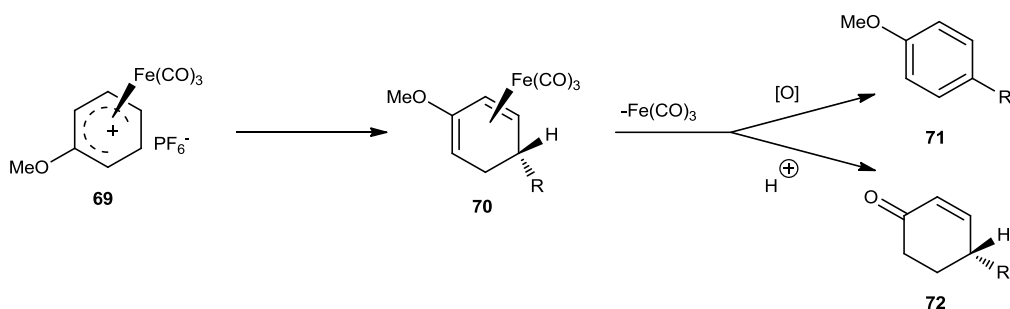
Stephenson *et al.*³⁰ have explored the formation of complexes in acid conditions. These diene diols were primarily used for tricarbonyliron complexation. In Scheme 20, it is shown that depending on the electronic nature of substituent R, cation **63** or **66** is obtained by reaction of 1,2-*cis* dihydrodiol complexes **60**, **61**, **62** with hexafluorophosphoric acid in acetic anhydride. With a trifluoromethyl substituent, compound **68** is formed as the salt, but in the case of methoxy and chloro substituents predominantly **102** and **104** complexes result in a ratio 2:1, and 7:2 respectively.



Scheme 20 The preparation of monosubstituted cations

1.2.5. Reactions of cations

As the cyclohexadienyl-tricarbonyliron complexes are very reactive electrophiles, their reactions with nucleophiles have been well studied, and high regio- and stereo-selectivities have been observed in this type of reaction. Birch *et al.*³¹ demonstrated the reaction of η^5 -methoxy iron cation **69** with nucleophiles and showed that the neutral iron complex **70** can behave differently upon demethylation and dehydrogenation, giving *p*-substituted anisole **71** or under acidic hydrolysis the 4-substituted cyclohex-2-enone **72**.³¹



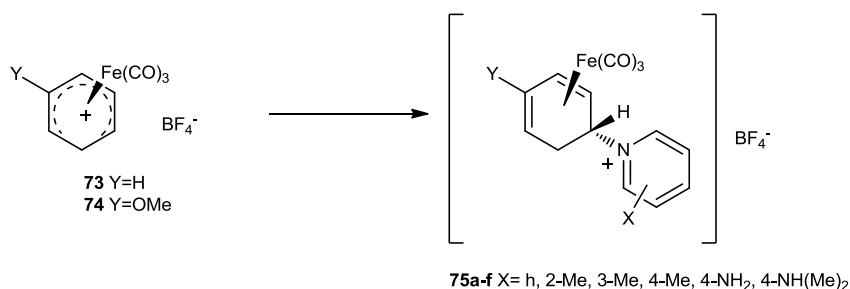
Scheme 21 The superimposed lateral control of reactivity.

There has been a great deal of research on this type of reaction, specifically in the synthesis of natural products but not exclusively, as it is a very useful tool to carry out C-C, C-X (X=N, O, S, etc.) bond formation under mild conditions.³²

These types of salts easily undergo reactions with typical nucleophiles, for example amines, enamines³³, hydroxide, alkoxyanions³⁴, enolizable ketones, thiocyanate, selenocyanate, halide ions, nitrite ions, azide and dithiocarbamates. It is also known

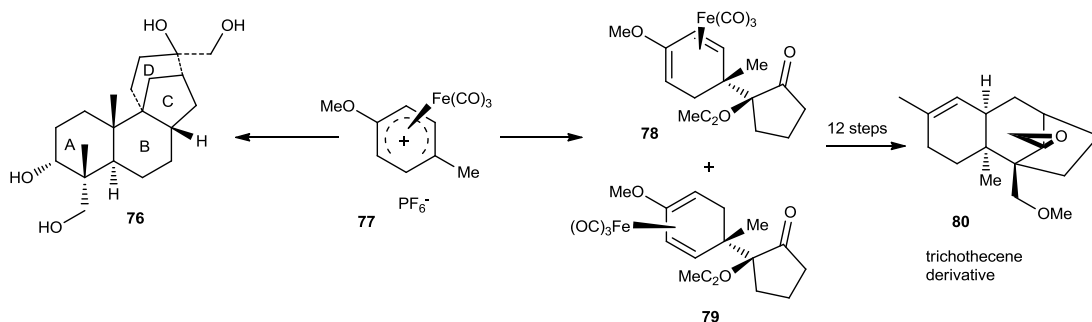
that tricarbonyliron cations react with organocuprates, dialkylzinc, dialkylcadmium, and lithium alkyls in alkylation reactions.^{35,36,37,38}

Adejoro *et al.*³⁹ described the reaction of cations **73** and **74** with pyridine and its derivatives to give new tricarbonyliron pyridino(1,4-η-2-methoxycyclohexa-1,3-diene) complex derivatives (Scheme 22). The reactions were carried out at room temperature in acetonitrile; twelve new products were isolated although yields were not reported.



Scheme 22 Preparation of iron complexes with pyridine and its derivatives

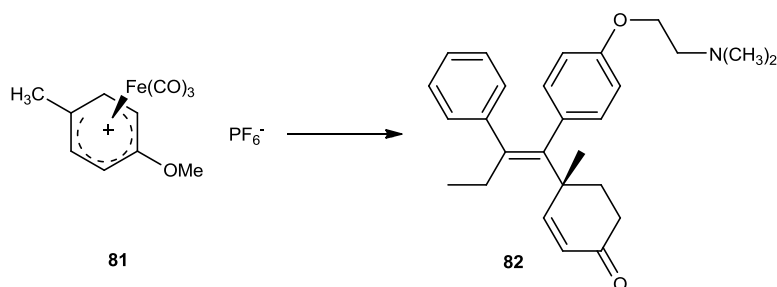
Pearson's group have presented a regio- and stereo- specific method of reaction at the methylated dienyl terminus with the potassium enolate of methyl 2-oxocyclopentanecarboxylate and tricarbonyl(4-methoxy-1-methylcyclohexadienylium)iron hexafluorophosphate **77** to give two diastereoisomers **78** and **79**, which were transformed into 12,13-epoxy-4-methoxytrichothecenes of potential biological interest. This methodology can be applied to the preparation of trichothecene derivatives such as (±)-trichodermol, (±)-trichodiene, (±)-12,13-epoxytrichothec-9-ene.^{40,41}



Scheme 23. Synthesis of aphidicolin and trichothecene dye.

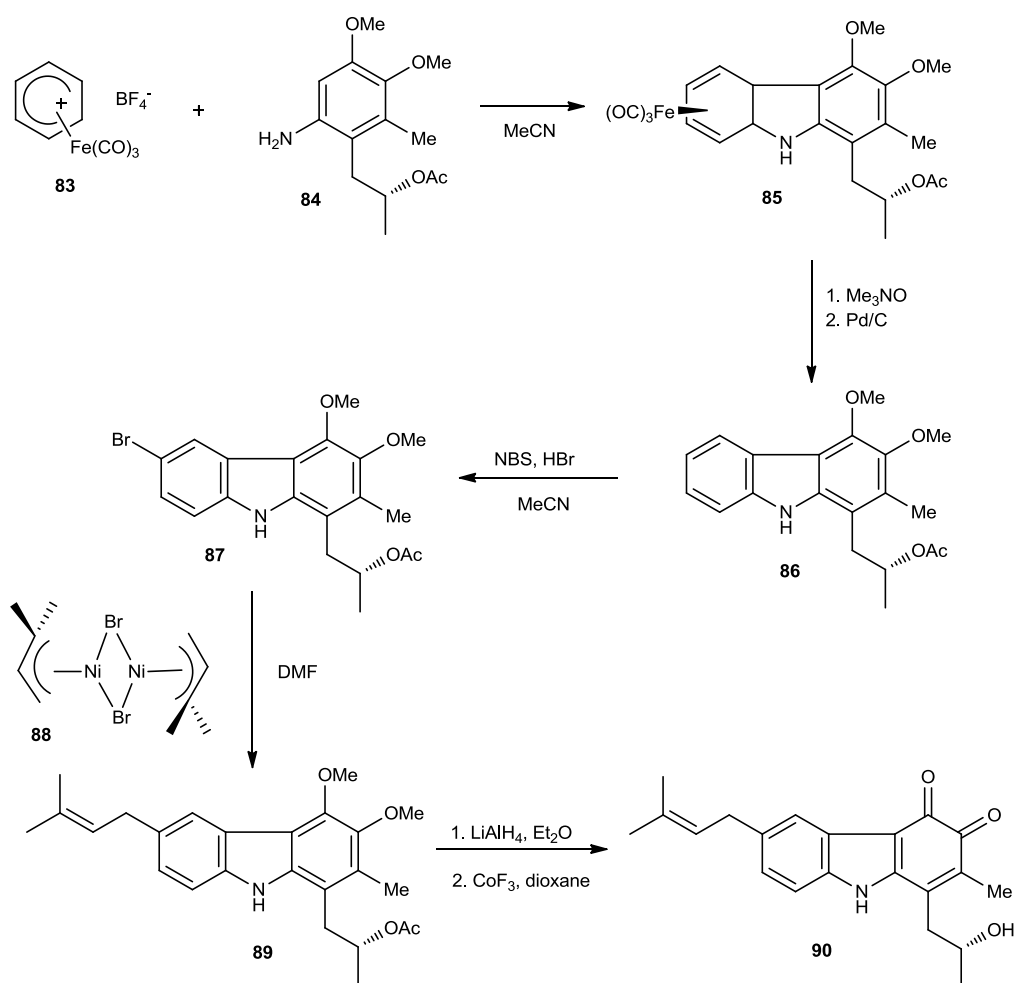
McCague and Potter⁴² reported a new approach to produce potential anticancer drug **82** which is an analogue of tamoxifen (tamadron) by reaction of 2-methoxy-substituted

cyclohexadieneiron complex **81** with low-order organocopper complexes (Scheme 24).⁴²



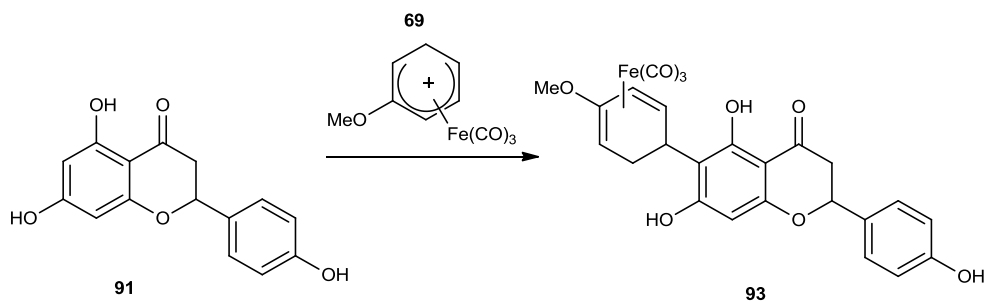
Scheme 24 Synthesis of tamadron **82**.

Carbazoles,⁴³ which are found in certain groups of alkaloids, can show potent neuronal cell protection and display free radical scavenging activity. In 2000, Knolker *et al.*⁴⁴ demonstrated the first enantioselective total synthesis of the carbazole alkaloid carquinostatin A. An enantiopure arylamine was used for nucleophilic trapping of cyclohexadienyl complex **83**, and then oxidative cyclization afforded the tricarbonyliron complex **85**. Simple decomplexation by trimethylamine-*N*-oxide, followed by aromatisation using 10% palladium on activated carbon, gave carbazole **86** which can undergo simple functional group manipulations to obtain the carbazole alkaloid carquinostatin (**90**, Scheme 25).



Scheme 25 Synthesis of alkaloid carquinostatin.

Another interesting example of the use of tricarbonyliron salts was shown by Stephenson *et al.*⁴⁵ His group prepared the organometalcarbonyl probe **93** by reaction of cyclohexadienyl-tricarbonyliron complex **69** with flavanone **91**, Scheme 26.

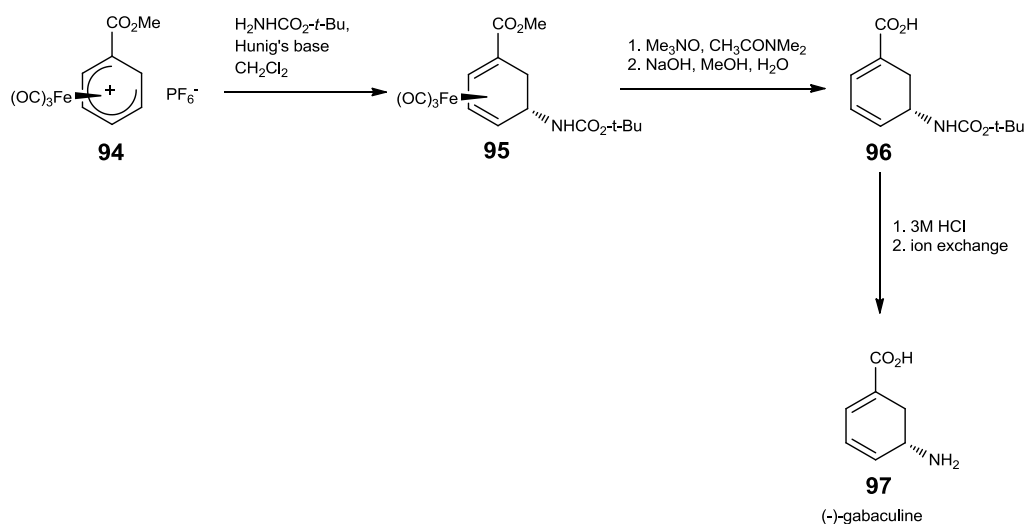


Scheme 26 Synthesis of the organometalcarbonyl probe **93**.

This research shows that the probe can be used to explore the mode of action of nod gene induction in *Rhizobium leguminosarum* by attaching the probe to protein binding

sites. When a tricarbonylmetal complex is bound to target sites, the vibrational modes of its complex undergo environment-induced shifts (see Sections 1.4.1.1-3). These intense vibrational bands of metal carbonyl complexes have also been employed in the CMIA (carbonylmetal immunoassay) method which exploits the low detection limits of the vibrational modes by FT-IR spectroscopy (see Section 1.5).

Birch⁴⁶ used cyclohexadienyl tricarbonyliron complex **94** to prepare (–)-gabaculine **97**, a naturally occurring amino acid which is potentially useful in treatment of Parkinson's disease, schizophrenia and epilepsy. The synthesis included the nucleophilic addition (*anti* to the metal) of *tert*-butyl carbamate to tricarbonyliron cation **94**, to give the neutral complex **95**. After decomplexation by reaction with trimethylamine *N*-oxide, followed by hydroxide ion promoted ester hydrolysis, the last step is a simple acid catalysed hydrolysis of the protected (–)-gabaculine **98** to afford the target compound **97**.⁴⁶

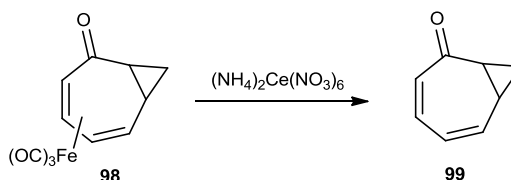


Scheme 27 Synthetic route for preparation of (–)-gabaculine **98**.

1.2.6. Decomplexation of tricarbonyliron complexes

To remove the tricarbonyliron fragment it is common to use one of a variety of different oxidizing reagents, resulting in liberation of ligand without changing its

structure. In 1963, Shvo and Hazum⁴⁷ used trimethylamine-*N*-oxide (Me_3NO) for demetallation and since then, it has been widely used. Other oxidants including iron(III) chloride, copper(II) chloride, pyridinium chlorochromate, $\text{Pb}(\text{OAc})_4$, $\text{H}_2\text{O}_2/\text{NaOH}$, MnO_2 and ceric ammonium nitrate also remove tricarbonyliron complexes, as shown by the example in Scheme 28.²²



Scheme 28 Example of decomplexation step.

The tricarbonyliron complexes conveyed novel reactivity and selectivity providing unique opportunities to design various probes and natural products. The preparation of novel tricarbonyl iron complexes and development of already known examples of these reagents will be described in Chapters 2 and 3 Results and Discussion.

1.2.7. References

-
- ¹ B. Plietker, Iron catalysis in Organic Chemistry Edited by Wiley-VCH, Weinheim, **2008**.
- ² L. Monde, F. Quincke, *J. Chem. Soc.*, **1891**, 59, 604.
- ³ M. Bertholet, *C. R. Hebd. Seances Acad. Sci.*, **1891**, 112, 1343.
- ⁴ H. Reihlen, A. Gruhl, G. Von Hessling, O. Prengle, *J. Liebig Ann. Chem.*, **1930**, 482, 161.
- ⁵ Veltman, P. L. U. S. Patent 2, 409, 167, 1946, *Chem. Abstr.*, **1947**, 41, 595.
- ⁶ B. F. Hallam, P. L. Pauson, *J. Chem. Soc.*, **1958**, 642.
- ⁷ J. E. Arnett, R. Pettit, *J. Am. Chem. Soc.*, **1961**, 83, 2985.
- ⁸ A. J. Birch, P. E. Cross, J. Lewis, D. A. White, S. B. Wild, *J. Chem. Soc. (A)*, **1968**, 332.
- ⁹ K. Stark, J. E. Lancaster, H. D. Murdoch, E. Z. Wiess, *Naturforsch.*, **1964**, 19b, 284.
- ¹⁰ J. A. S. Howell, B. F. G. Johnson, P. L. Josty, J. Lewis, *J. Organometallic Chem.*, **1972**, 39, 329.
- ¹¹ M. Brookhart, G. O. Nelson, *J. Organometallic Chem.*, **1979**, 164, 193.
- ¹² H. Fleckner, F-W. Grevels, D. Hess, *J. Am. Chem. Soc.*, **1984**, 106, 2027.
- ¹³ S. Otsuka, T. Yoshida, A. Nakamura, *Inorg. Chem.*, **1967**, 6, 20.
- ¹⁴ A. M. Brodie, B. F. G. Johnson, P. L. Josty, J. Lewis, *J. Chem. Soc. Dalton Trans.*, **1972**, 2031.
- ¹⁵ H.-J. Knölker, B. Ahrens, P. Gonser, M. Heininger, P. G. Jones, *Tetrahedron*, **2000**, 56, 2259.
- ¹⁶ H.-J. Knölker, P. Gonser, *Synlett*, **1992**, 517.
- ¹⁷ H.-J. Knölker, P. Gonser, P. G. Jones, *Synlett*, **1994**, 405.
- ¹⁸ H.-J. Knölker, P. Gonser, P. G. Jones, H. Röttele, *Eur. J. Inorg. Chem.*, **1998**, 993.
- ¹⁹ A. J. Pearson, K. Srinivasan, *J. Org. Chem.*, **1992**, 57, 3965.
- ²⁰ B. F. Hallam, P. L. Pauson, *J. Chem. Soc.*, **1958**, 642.
- ²¹ M. F. Semmelhack, J. W. Hendon, *Organometallics*, **1983**, 2, 363.
- ²² A. J. Pearson, in Iron Compounds in Organic Synthesis, Academic Press, London, **1994**.
- ²³ E. O. Fischer, R. D. Fischer, *Angew. Chem.*, **1960**, 72, 919.
- ²⁴ R. Petit, G. F. Emerson in Advances in Organometallic Chemistry, R. West, F. G. A. Stone, Academic Press, New York, N. Y. **1964**.

-
- ²⁵ D. Jones, L. Pratt, G. Wilkinson, *J. Chem. Soc.*, **1962**, 4458.
- ²⁶ L. A. P. Kane-Maguire, E. D. Honig, D. A. Sweigart, *Chem. Rev.*, **1984**, 84, 525.
- ²⁷ O. Eisenstein, W. M. Butler, A. J. Pearson, *Organometallics*, **1984**, 3, 1150-1157.
- ²⁸ G. R. Stephenson, *J. Chem. Soc., Perkin Trans. 1*, **1982**, 2449-2456.
- ²⁹ A. J. Birch, M. A. Haas, *J. Chem. Soc., C: Org.*, **1971**, 2465-2467.
- ³⁰ G. R. Stephenson, P. W. Howard, S. C. Taylor, *J. Organomet. Chem.*, **1991**, 419, C14-C17.
- ³¹ A. J. Birch, B. M. R. Bandara, K. Chamberlain, B. Chauncy, P. Dahler, A. I. Day, I. D. Jenkins, L. F. Kelly, T. C. Khor, G. Kretschmer, A. J. Liepa, A. S. Narula, W. D. Raverty, E. Rizzardo, C. Sell, G. R. Stephenson, D. J. Thompson, D. H. Williamson, *Tetrahedron*, **1981**, 37, Supplement 1, 289-302.
- ³² B. M. R. Bandara, A. J. Birch, T.-C. Khor, *Tetrahedron Lett.*, **1980**, 21, 3625-3626.
- ³³ R. E. Ireland, G. G. Brown, R. H. Stanford, T. C. McKenzie, *J. Org. Chem.*, **1974**, 39, 51-59.
- ³⁴ B. R. Reddy, V. Vaughan, J. S. McKennis, *Tetrahedron Lett.*, **1980**, 21, 3639-3642.
- ³⁵ A. J. Pearson, *Aust. J. Chem.*, **1976**, 29, 1101-1103.
- ³⁶ A. J. Pearson, *Aust. J. Chem.*, **1977**, 30, 345-350.
- ³⁷ A. J. Pearson, *Science*, **1984**, 223, 895-901.
- ³⁸ C. E. Anson, M. R. Attwood, T. M. Raynham, D. G. Smyth, G. R. Stephenson, *Tetrahedron Lett.*, **1997**, 38, 505-508.
- ³⁹ T. I. Odiaka, O. F. Akinyele, I. A. Adejoro, *E-Journal of Chemistry*, **2011**, 8, 960-965.
- ⁴⁰ A. J. Pearson, M. K. O'Brien, *J. Org. Chem.*, **1989**, 54, 4663-4673.
- ⁴¹ A. J. Pearson, P. Ham, W. O. Chi, T. R. Perrior, D. C. Rees, *J. Chem. Soc., Perkin Trans. 1*, **1982**, 1527-1534.
- ⁴² G. A. Potter, R. J. McCague, *Chem. Soc., Chem. Commun.*, **1992**, 635-637.
- ⁴³ G. B. Marini-Bettolo, J. Schmutz, *Helv. Chim. Acta*, **1959**, 42, 2146-2155.
- ⁴⁴ a) H. J. Knölker, E. Baum, K. R. Reddy, *Tetrahedron Lett.*, **2000**, 41, 1171; b) H. J. Knölker, W. Fröhner, *Tetrahedron Lett.*, **1997**, 38, 1535; c) H. J. Knölker, M. Wolpert, *Tetrahedron Lett.*, **1997**, 38, 533.

-
- ⁴⁵ A. V. Malkov, L. Mojovic, G. R. Stephenson, A. T. Turner, C. S. Creaser, *J. Organometallic. Chem.*, **1999**, 589, 103.
- ⁴⁶ B. M. R. Bandara, A. J. Birch, L. F. Kelly, *J. Org. Chem.*, **1984**, 49, 2496-2498.
- ⁴⁷ Y. Shvo, E. Hazum, *J. Chem. Soc. Chem. Comm.*, **1974**, 336.

1.3. Fluorescence

Fluorescence (a physical process) is observed as an emission of light by a molecule which has absorbed light of specific wavelength and returned to its ground state by a radiative transition. The absorption and emission of light can be described as being caused by the movement of electrons between different energy levels within the molecule. The fluorescence processes were schematically illustrated by the Polish physicist Alexander Jabłoński in 1933.¹

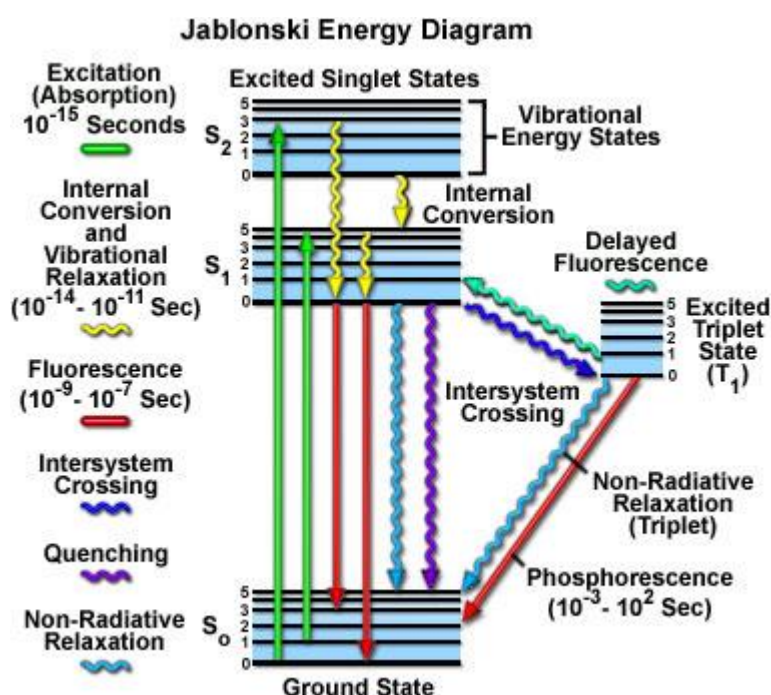


Figure 12. General demonstration of a Jabłoński diagram adapted from <http://molecular.magnet.fsu.edu/primer/java/jablonski/jabintro/index.html>.

This diagram can clearly describe the different energy levels that a single electron can occupy within an atom or molecule. In the middle of the diagram, in Figure 12 are shown singlet states. S_0 corresponds to a singlet ground state, and S_1 and S_2 to first and second singlet excited states, respectively. The excited triplet state, T_1 is shown on the right side. All states have closely separated vibrational and rotational energy levels. A fluorophore can be excited from the lowest vibrational energy level of the ground state ($S_0 = 0$) to a higher orbital in the second excited state ($S_2 = 3$ for instance). Similarly absorption can happen from the second vibrational level ($S_0 = 1$) of the

ground state to the highest vibrational level in the next excited state ($S_1 = 5$). Straightaway after excitation by a photon, there are numerous processes which can occur. The molecule may quickly relax to the lowest vibrational energy level of the first excited state ($S_1 = 0$, Figure 1). This process is named internal conversion or vibrational relaxation (loss of energy in the absence of light emission).² It is a nonradiative process and generally takes place in a picosecond or less. Because a significant number of vibrational cycles can occur during the lifetime of excited states, molecules virtually always undergo complete vibrational relaxation during their excited lifetimes. Alternatively, before relaxation to the ground state $S_0 = 0$, an excited electron can stay in the lowest excited singlet state for periods in the order of nanoseconds. Fluorescence is the process of relaxation from long-lived state to the ground state, the energy being dissipated with the emission of light. Many fluorophores are able to repeat the excitation and emission sequence many times before the exceedingly reactive excited state of the molecule is photobleached (a chemical reaction then occurs, and fluorescence can no longer take place). It is possible to observe other outcomes which compete with the fluorescence emission route. The excited fluorophore can collide with another molecule which results in transfer energy as a non-radiative process, for instance as heat or by a quenching mechanism. Another possibility that can be observed is called intersystem crossing³ (IT) to the lowest excited triplet (T_1), when the electron will change spin orientation. This alternative process is quite rare, but it results in release of a photon through phosphorescence or conversion to the singlet ground state which is called delayed fluorescence. This is an example of a so-called forbidden route. Such forbidden transitions are slower processes, with rate constants for triplet emission many orders of magnitude lower than those for fluorescence. The small chance of intersystem crossing is due to the fact that it is crucial for molecules to undergo spin conversion to yield unpaired electrons, which is not a favourable process. The essential significance of the triplet state is the high chemical reactivity characteristics of molecules in this state, which often results in photobleaching and the creation of destructive free radicals.¹

1.3.1. Characterisation of the fluorescence

A few factors should be taken into consideration in the discussion of fluorescent species, for instance absorption (excitation) and emission spectra, quantum yield, absorption coefficient, fluorescence lifetime, or fluorescence quenching. All of these depend on the configuration of electronic energy states within the molecule. The interactions of fluorophores with their surroundings cause perturbations in the electronic configuration, and, as a consequence fluorescence can be a very sensitive tool to detect these perturbations, and thus the fluorophore's environment. This is one of the reasons why fluorescence is so widely used in analysis. As a consequence, fluorescent measurements are not just able to differentiate between individual species of fluorophores but can additionally provide the information about their surroundings.

1.3.1.1. Fluorescence absorption and emission spectra (Stokes Shift)

The most important characteristic properties of a fluorophore are the absorption and emission spectra. As a consequence of the Boltzmann statistical distribution,⁴ which indicates that at room temperature in any electronic state, the population distribution will be biased towards the lowest vibrational mode of that state and as a result the absorption spectrum will be observed which is caused by broadening from transitions between the lowest energy level in the ground state and different vibrational levels in the excited states. Alternatively, for reflected emission spectra, the probabilities of transition between the lowest energy level in the excited state and different vibrational levels in the ground states are taken into account. The Stokes Shift⁵ defines the separation between the maxima for the wavelengths of excitation and emission, Figure 13.¹

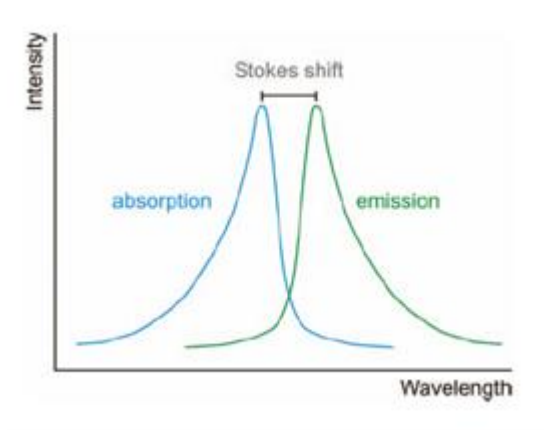


Figure 13 Representation of the Stokes shift.

1.3.1.2. Fluorescence lifetime

First of all, a system which contains a single fluorescent type that is excited by light will be considered. The fluorescence lifetime describes the average time when a molecule can occupy the excited state before returning to the ground state. The number of molecules that stay in the higher energy band will drop exponentially with time. The measured intensity of the fluorescence emission is described by equation

$$I(t) = I_0 \exp(-t/\tau)$$

Where:

$$\tau = 1/(k_R + k_{NR})$$

In the above, t is time¹, τ is the fluorescence lifetime, I_0 is the initial fluorescence at $t=0$, and k are the rates for each decay pathway (radiative and nonradiative). More importantly, the lifetime, τ is independent of the initial intensity of the emitted light. This can be utilized for making non-intensity based measurements in chemical sensing.¹

1.3.1.3. Quantum yield

By definition, the quantum yield describes the number of emitted photons comparative to the number of absorbed photons. It is an indication of how effective spontaneous emission is when competing with nonradiative decay paths.¹

$$\eta = k_R / (k_R + k_{NR})$$

1.3.1.4. Absorption coefficient

The absorption coefficient is defined by the Beer-Lambert Law, which shows the modification in intensity when light goes through an atomiser or solution of the absorbing species. It indicates the number of photons absorbed as a fraction of those which are encountering the fluorophore.¹

$$I = I_0 \exp - (\epsilon b C)$$

where:

ϵ - molar absorption coefficient [$\text{mol}^{-1} \text{cm}^{-1}$]

b – length of atomiser or solution cell

C – concentration of the absorbing species

1.3.1.5. Fluorescence quenching

There are many processes which can cause the reduction in fluorescence intensity, some one of them are gathered in a term named quenching, which gathers different phenomena. Most of these processes take place during the excited state lifetimes. They include: molecular rearrangements, energy transfer, collisional quenching, charge transfer, electron transfer reactions or photochemistry, and also the formation of complexes in the ground state. Quenching experiments are suitable to define the availability of the quencher to a fluorophore and one of the reactants. There are two types of quenching: collisional (dynamic) quenching and static (complex formation) quenching which will be considered. Both involve an interface between fluorophore and quencher.^{1,6}

Collisional quenching is observed when the excited fluorophore diffuses to an atom or molecule which is causing nonradiative returns to the ground state. The best known quenchers included O_2 , I^- , Cs^+ and acrylamide. The Stern-Volmer equation describes the collisional quenching, and shows that the decrease in intensity is due to ratio of the fluorescence in the absence of quenching to that in the presence of quencher.¹

$$I_0/I = 1 + K_{SV} [Q]$$

I_0 and I are the observed fluorescence with and without quencher, $[Q]$ is the quencher concentration and K_{SV} is the Stern-Volmer quenching constant. The value of K_{SV} is given by $k_q\tau_0$ where k_q is the bimolecular quenching rate constant and τ_0 is the excited state lifetime in the absence of quencher. The plot of I_0/I versus $[Q]$ will show the linear dependence of quenching and is known as a Stern-Volmer plot.

Static quenching proceeds by the formation of a stable complex between fluorophore and another molecule and when the excited state of the complex is nonradiative then the fluorophore has been statically quenched.¹ Gregorio Weber⁷ was the first to describe such cases of quenching via complex formation. The dependence of the fluorescence as a function of the quencher concentration is represented by the equation:

$$I_0/I = 1 + K_a [Q]$$

Where K_a is the association constant of the complex.

Noteworthy, the lifetime of the sample is not reduced since fluorophores which are not forming complexes are able to emit after excitation and will have normal excited state properties.

The intensity of the fluorescence for samples is decreased because the quencher is basically reducing the number of fluorophores which can emit.¹

1.3.2. Types of fluorophores

There are numerous useful types of fluorophores which play very important roles in chemistry and also in biology. By definition, fluorophores are fluorescent moiety which can possess contrasting chemical structures, including small organic, organometallic or inorganic molecules, proteins and even semiconductor beads. All the fluorophores possess specific spectral properties. These are directly related to the possible excited states which are due to energies involved when electrons of fluorophores make transitions between states. The fluorophores can be connected via covalent or noncovalent linkages with a sample to be analysed, giving the conjugates or complexes which can show fluorescence from short to very long wavelengths. The current rising interest in the development of new fluorophores is due to the extreme importance

their application to biological investigations. Precisely, fluorophores proved to be very suitable when applied in the case of organic fluorescent markers for labelling of amino acids, peptides, proteins, DNA and other biomolecules.¹ The most common organic fluorophores will be now discussed.

1.3.3. Organic fluorophores with emission spectra up to 500 nm

1.3.3.1. Coumarin

Coumarins are nowadays an important group of organic compounds that are used as drugs,⁸ additives to food and cosmetics,⁹ optical brightening agents,¹⁰ and dispersed fluorescent and laser dyes.¹¹ The derivatives of coumarin usually occur as secondary metabolites present in seeds, root, and leaves of many plant species. Their function is far from clear, although suggestions include waste products, plant growth regulators, fungistats and bacteriostats.¹² It is therefore of utmost importance that the synthesis of coumarin and its derivatives should be achieved by a simple and effective method. The structure of coumarin is shown in Figure 14; the positions 3, 4, 5, 6, 7, 8 are potentially sites for substitution. Substituents introduced on positions 3 and 7 have a relatively stronger electronic effect on the optical properties of the resultant molecules than do substituents at other positions. An important point is that when substituents are attached at different positions they will cause different fluorescence properties of the host fluorophores, but there is still much discussion about exactly how this occurs, and it is difficult to predict the outcomes rationally.

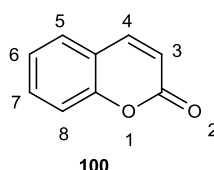
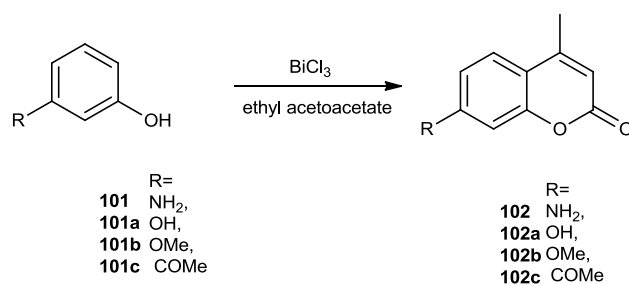


Figure 14 Structure of coumarin.

One quite unusual route was published by Pechmann¹³ and co-workers, where a catalytic approach contributes to the development of clean and green chemical process. This type of reaction is very useful for synthesis of 4-substitued coumarins. It is a simple condensation of resorcinol with ethyl acetoacetate in the presence of BiCl_3 .



Scheme 29 Synthesis of 4-substituted coumarins.

The advantage of this reaction is the use of BiCl_3 as a catalyst which is inexpensive and relatively nontoxic, and almost insensitive to small amounts of water avoiding the need for dry conditions. During this kind of reaction, normally acidic catalysts (sulphuric acid, aluminium chloride, trifluoroacetic acid, etc.) are used in excess. As was mentioned before, coumarins are very useful tools for fluorescent detection. Specifically BrMOZPhC **103** (4-bromomethylcoumarin-7-phenyl[6,7-b](6,9)oxazine)¹⁴ and BrMOZC ¹⁵ **104** are valuable probes for this reason, but they also can be used to determine carboxylic acids by HPLC (Figure 15).¹⁵

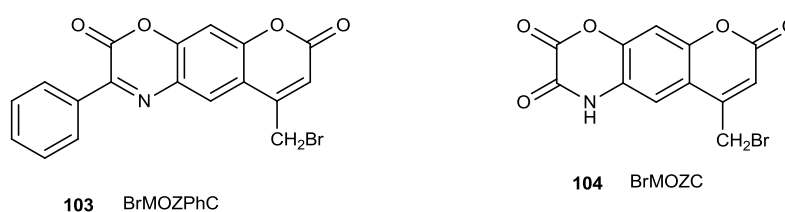


Figure 15 Examples of coumarins used as fluorescent tools.

Another advantage of using coumarin derivatives is that they can be used in ion detection by incorporation of the coumarin chromophore into a larger indicator framework. The first reported ion monitoring coumarin probe is benzothiazolyl-coumarin BTC **105** (Figure 16). This compound is one of the most widely used and is characteristic of a generation of low affinity calcium probes. The APTRA-BTC **106** analogue of BTC dye is more useful to analyse the mixtures of Zn^{2+} and Cd^{2+} .¹⁶

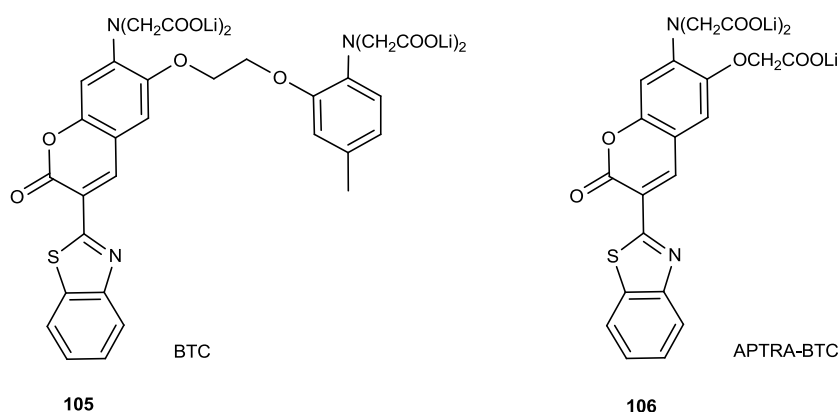
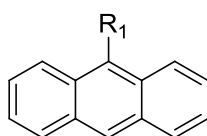


Figure16 Ion monitoring coumarin probes.

These dyes are long-lasting enough to reduce “background” fluorescence of cellular components, tissues and biological fluids. Additionally, a significant fluorescence Stokes shift makes it possible to avoid the overlap of excitation and emission peaks, so improving sensitivity. Fluorescein and rhodamine present large excitation coefficients when compared to coumarin based ion indicators. However, coumarin dyes exhibit a large fluorescence quantum yield which is important in biological applications to permit ion detection at low indicator concentrations, thus allowing coumarins to be introduced to cells either by microinjection or as membrane permeable derivatives without causing death cell.

1.3.3.2. Anthracene based fluorophores

Anthracene based fluorophores possess noteworthy biological activities. They are made up of three planar fused aromatic rings, (Figure 17).



- R =
- 107** CH_2NH_2 ,
 - 107 a** $\text{CH}_2\text{NHCH}_2\text{CH}_2\text{OH}$,
 - 107 b** $\text{CH}_2\text{NH}(\text{CH}_2\text{CH}_2\text{OH})_2$,
 - 107 c** $\text{CH}_2\text{CH}_2\text{CH}_2\text{NH}_2$,
 - 107 d** $\text{CH}_2\text{NH}_2\text{CH}_2\text{CH}_3$

Figure 17 Examples of anthracene based fluorophores.

It is possible to place the anthracene derivatives into the category of fluorescent dye photosensitizers. They are capable of light-reliant chemical reactions that result in damage to biological systems. Anthracenes are good photosensitizers because of their low polarizability, strong fluorescence, good absorption in the near UV region, and a long-lived excited triplet state. Certain anthracene derivatives are also known to be active against specific types of cancers.¹⁷ Specifically, anthracene-based drugs such as Pseudourea (bis-(2-thio(2,2'-(9,10-Anthrylenedimethylene) dihydrochloride) dihydrate)¹⁸ were tested in clinical trials which showed that anthracene itself is effective against specific skin cancer.¹⁹

The planar, linear, three-ring system of the anthracene nucleus has the potential for significant overlap with the DNA base pairs. The versatile chemistry of the anthracene nucleus provides a convenient route to prepare a number of closely related derivatives.²⁰ Additional advantages of the anthracene derivatives are that they have moderate absorption cross-sections in the near-UV region, and good fluorescence quantum yields, which are beneficial for example to monitor ligand binding to DNA by spectroscopic methods.²¹

In 2014, José Berná and co-workers²² reported the synthesis of 9-aminoanthracene which is a part of a [2]rotaxane.²² This design expected to develop a change in the fluorescence of the anthracenyl group of the [2]rotaxane by the competitive binding of an analyte by the hydrazodicarboxamide moiety in which initially resides in a macrocyclic tetralactam ring functionalized with strong electron-withdrawing groups. Another advantage is that the removal of this analyte (by an ion exchange reaction or by oxidation of the hydrazo group) will reset the system to its original state.²²

More details of choosing this type of fluorophore will be discussed in Chapters 1.4 and 2: boronic acid based bioprobes and Results and Discussion for project number 1.

1.3.4. Organic Fluorophores with Emission Beyond 500 nm

1.3.4.1. Rhodamines

Rhodamine dyes are probably the oldest synthetic fluorophores used for dyeing of fabrics, or as fluorescent markers in structural microscopic studies, and they show

good applications in laser dyes. Their derivatives are strongly fluorescent and possess high molar absorptivities in the visible region. This class of fluorophore can have different photophysical properties, depending on the substituent R1, R2, R3, R4, Y or ion X⁻ (Cl⁻, Br⁻, ClO₄⁻) which is shown on Figure 18.²³

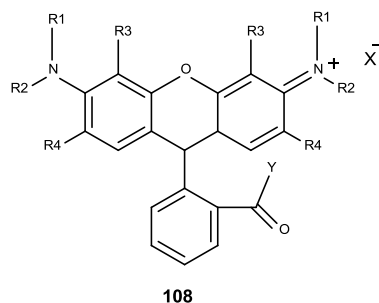


Figure 18 Rhodamine based fluorophore.

There are many rhodamine derivatives used in bioanalysis (covalent or noncovalent labels), but the most modern are Rhodamine 800 and Texas Red, (Figure 19).²¹

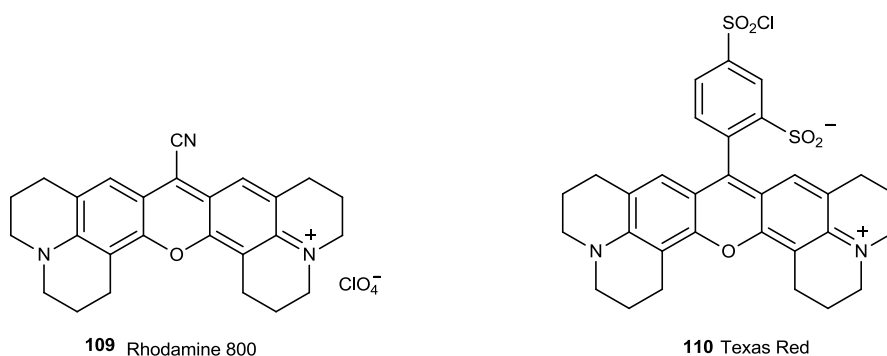
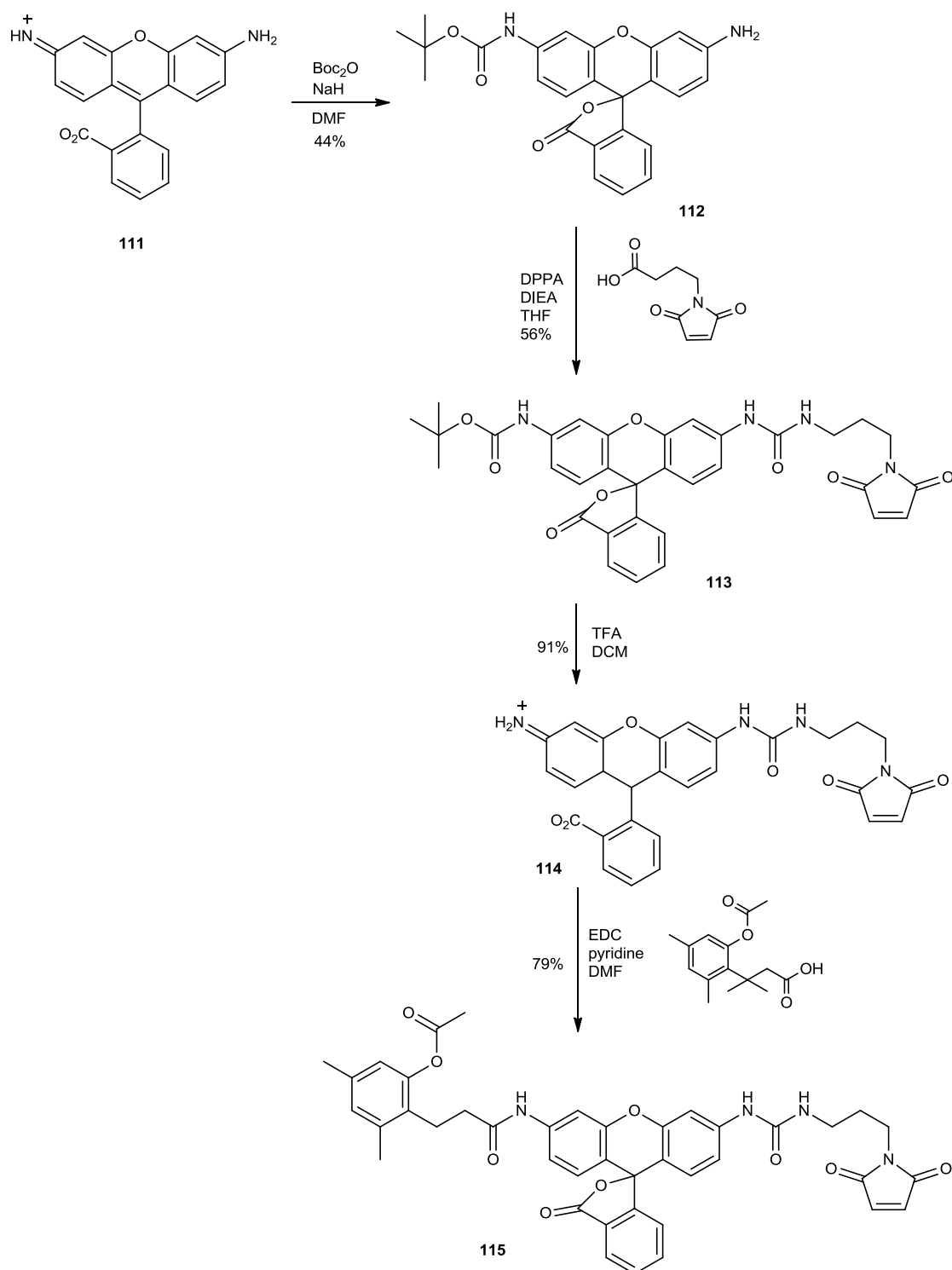


Figure 19 Rhodamine derivatives.

Other xanthene fluorophores such as Rhodamine 110 has been used in studies of enzymatic activity. Raines and co-workers²⁴ described the synthesis of latent fluorophore **115** which was covalently attached to a cationic protein (an RNase, a member of the thiol containing variants of bovine pancreatic ribonuclease). Scheme 30 shows a synthetic route for the preparation of the fluorogenic label **115**. It starts from Boc protection of Rhodamine 110 (**111**), then a coupling reaction using DPPA, DIEA in dry THF to yield urea **113**. Deprotection via iminium salt **114** by using TFA and then

another coupling reaction gives the desired latent fluorophore **115**. Compound **115** is called a latent fluorophore since its fluorescence is quenched through the formation of the cyclic lactone. Yet, when this compound is submitted to esterases enzymes, the acetate moiety is cleaved, and an intramolecular cascade reaction restores the initial fluorescence by formation of the aniline and the subsequent lactone opening.



Scheme 30 Synthetic route for the preparation of the probe **115**.

To increase water solubility and facilitate conjugation of protein with rhodamine derivatives, Burgess *et al.*²⁵ synthesised compound **116** by introducing several carboxylic acid functionalities (Figure 20). This probe also contains an aryl bromide group which can be used for linking other moieties to the fluorescent dye.

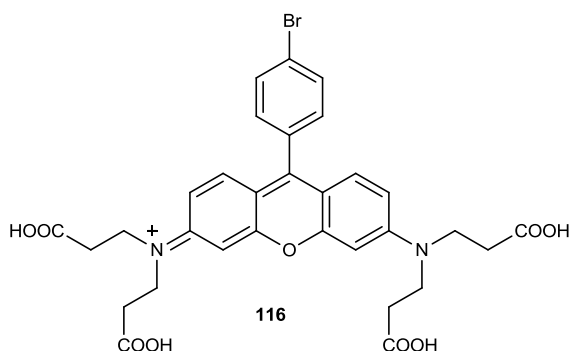
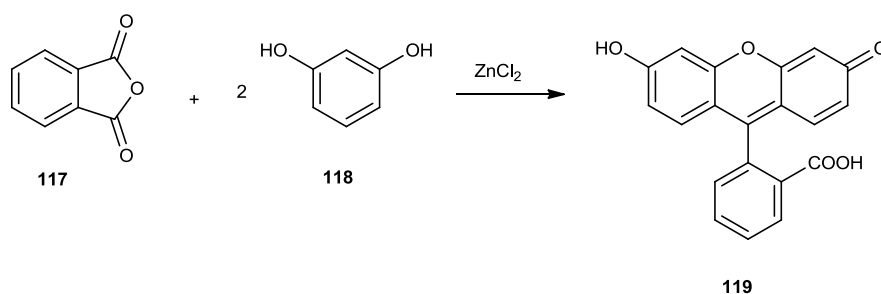


Figure 20 Water soluble rhodamine probe.

1.3.4.2. Fluorescein

Another class of fluorophore which is commercially available and used for labelling proteins, peptides, amino acids is the fluorescein group. The simplest way to synthesise fluorescein involves a Friedel-Crafts type of reaction shown in Scheme 31.^{26,27}



Scheme 31 Synthesis of fluorescein via Friedel-Crafts type reaction.

Fluoresceins have high molar absorptivities and quantum yields, and good solubility in water. Furthermore, fluorescein has an excitation maximum at 494 nm which lies close to the emission line of the argon laser (488 nm); for this reason they are significant fluorophores for applications in laser scanning microscopy and flow cytometry. One of the most widespread fluorophores used in interactions with proteins is fluorescein isothiocyanate (FITC) **120** which is shown on Figure 21.^{28,29}

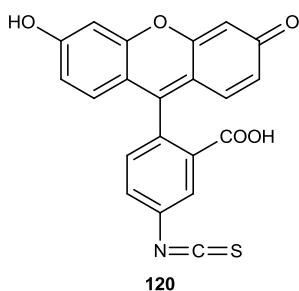
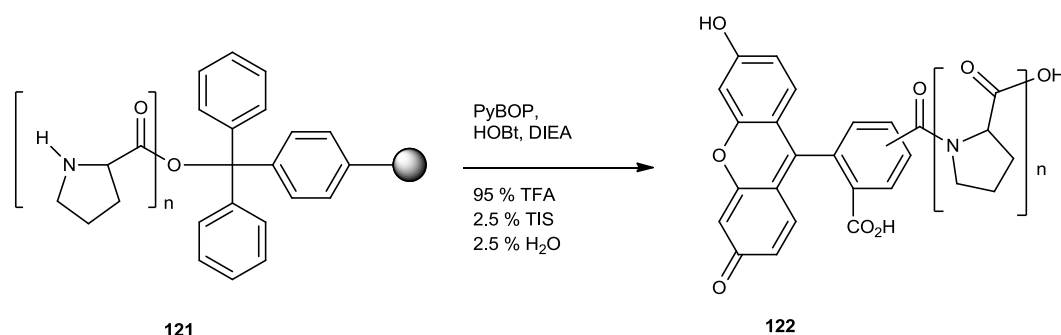


Figure 21 Fluorescein isothiocyanate (FITC).

This fluorophore was for instance used by Kilar and co-workers³⁰ who used it for marking the iron-free human serum transferrin (a glycoprotein binding two ferric ions and responsible for delivery to cells through receptor-mediated endocytosis). This process was observed by using different dye-protein ratios, followed by capillary electrophoresis. This is a very useful technique as the labelled protein can be used as a receptor-mediated endocytosis marker and allows the study of the action of transferrin with FITC.

An excellent example reported by Giralt and Fernandez-Carneado³¹ of solid phase fluorescent labelling of proline peptides in the *N* terminals with 5(6)-carboxyfluorescein, is shown in Scheme 32. This technique can be applied to solid-phase combinatorial synthesis of natural products, polyamides and peptide nucleic acids, where fluorescent labelling for cell biology is very much needed.



Scheme 32 Preparation of fluorescent labelling on solid phase.

A good example of the successful synthesis, photophysical characterization and bioanalytical applications of new fluorescent amino acids is shown in Figure 22. The

compounds **123a** and **123b** have a big advantage over their analogues **123c** based on fluorescein because of significantly better photostability and their pH-independent quantum yields.³²

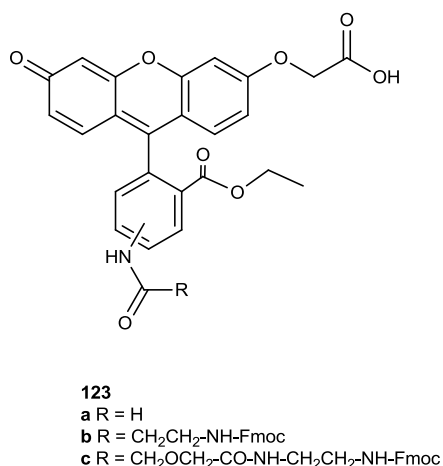


Figure 22 New fluorescent amino acids.

However, sometimes these types of fluorophores can also possess some disadvantages, such as a quite high percentage of photobleaching,^{33,34,35} pH-sensitive fluorescence,^{36,37} and an expansive fluorescence emission spectrum.³⁸ The last problem causes limitation of their utility in multicolour applications. They also have a tendency to self-quench on conjugation to biopolymers, mainly at high levels of substitution.³⁹

1.3.4.3. Cyanines

One of the reasons the cyanine dyes are interesting molecules is their capability to impart light sensitivity to silver halide emulsions in an area of the spectrum at which the silver halide is not usually sensitive. They have found many technical uses since the discovery that they can be used as photographic sensitizers⁴⁰, nonlinear optical materials or more lately as fluorescent probes for bimolecular labelling^{41,42} where in this last field, cyanines have found applications in genetic analysis, DNA sequencing,⁴³ and *in vivo* imaging.⁴⁴

Typically these dyes contain two nitrogen centres, where one has a positive charge and is conjugated with a chain of an odd number of carbon atoms to the other nitrogen. It can be considered as a 'push-pull' polyene which can form the skeleton of the polymethine dyes, which have the streptopolymethine unit as their chromophore. They can be classified as cationic streptopolymethine-cyanine and hemicyanine dyes **124**, anionic streptopolymethine-merooxonol dyes **125**, neutral streptopolymethine-merocyanine dyes **126**, and zwitterionic squaraine-based cyanine dyes **127**, as shown in Figure 23.⁴⁵

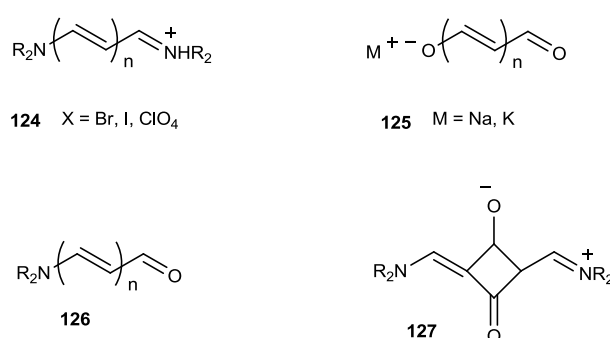
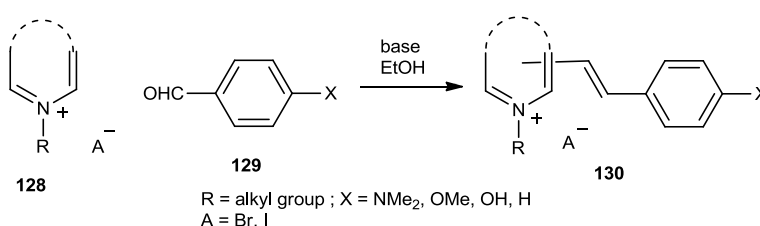


Figure 23 Examples of cyanines dyes.

A common way of preparation of hemicyanines includes the condensation of a 2/4-methyl quaternary salt of the base with a substituted benzaldehyde in presence of a base as shown in Scheme 33.



Scheme 33 Preparation of hemicyanines.

1.3.4.4. BODIPY

4,4-Difluoro-4-bora-3a,4a-diaza-s-indacene, or boron-dipyrromethene (BODIPY) **131**, which is presented in Figure 24, belongs to a group of fluorescent dyes which were first synthesized by Treibs and Kreuzer in 1968.⁴⁶ They can be considered as rigidified

cyanine dyes. They show interesting properties, such as high stability, sharp fluorescence peaks, tunable emission and high quantum yields. The BODIPYs increased in prominence after the publication of a patent in 1988 by Molecular Probes®.⁴⁷

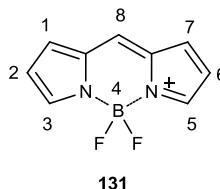


Figure 24 Basic structure of BODIPYs.

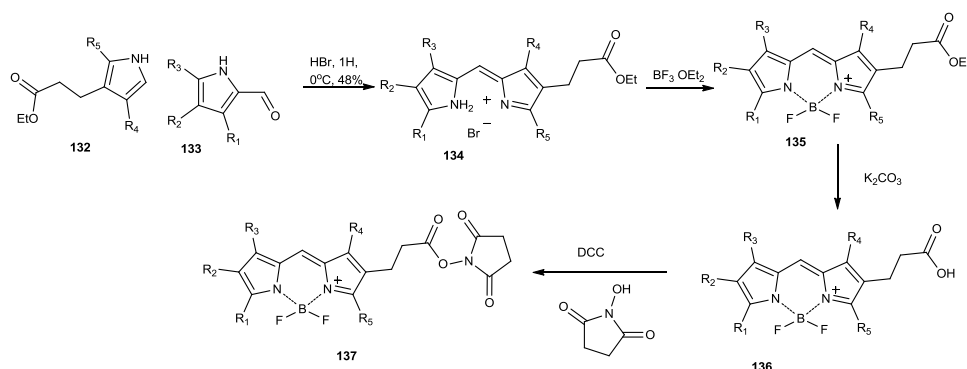
The synthesis of BODIPY can be performed in two ways. To get a symmetrical BODIPY, condensation of two identical pyrrolic units and a carbonyl compound (aldehyde or acyl chloride) is performed in presence of a strong acid [hydrobromic acid (HBr) or trifluoroacetic acid (TFA), see Scheme 34]. Three reaction conditions gave a dipyrromethane which is substituted by the structure previously linked to the carbonyl reagent at the central position (meso position). The dipyrromethane undergoes aromatization with chloranil or DDQ to form a dipyrromethene (or dipyrin), which is followed by complexation with a difluoroboryl derivative in a base-catalyzed reaction with trifluoroboryl etherate ($\text{BF}_3 \cdot \text{OEt}_2$) and triethylamine (TEA) resulting in the expected BODIPY.

Analogously, to obtain non-meso-substituted BODIPYs, it is essential to use two different pyrrolic units but one of them needs to have a carboxyaldehyde group at C2 position of the pyrrolic ring. The reaction is performed in the presence of phosphoryl chloride to achieve the dipyrin, which is subsequently converted into BODIPY as was described for previous example.

This class of fluorophores has been found to be useful in applications in biochemistry, biophysics and biotechnology for protein labelling. There are many examples in the literature, but only a few will be discussed.

BOBIPY derivatives with a succinimidyl ester group were first described in 1988 by Molecular Probes®.⁴⁷ The reaction involved the coupling of an ester-substituted pyrrole with pyrrole carboxyaldehyde dyes to achieve a dipyrromethene, then complexation produces the BODIPY connected to the ethyl ester. The reaction of this

product with an aqueous solution of potassium carbonate released the carboxyl group that was then coupled with *N*-hydroxysuccinimide (Scheme 34). Currently, many succinimidyl ester BODIPY derivatives with different spectral characteristics are commercially available.



Scheme 34 Synthetic route towards the preparation of BODIPYs.

These succinimidyl ester BODIPY dyes are used, for example, in the labelling of casein (a simple protein which serves as a substrate to several endoproteases) or the surfactant protein B (which prevents the alveoli from collapsing).

The synthesis of a BODIPY with an aminooxy reactive group was reported in 2011.⁴⁸ This fluorophore, shown in Figure 25, was synthesised for making quorum sensing chemicals (i.e., 3-oxododecanoyl homoserine lactone) attached to a proteic transcriptional modulator which is present in some bacteria. This can allow bioorthogonal labelling of this protein to be performed.

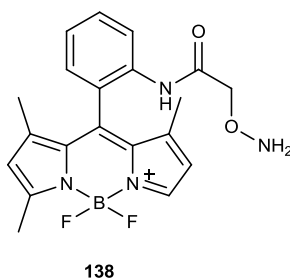
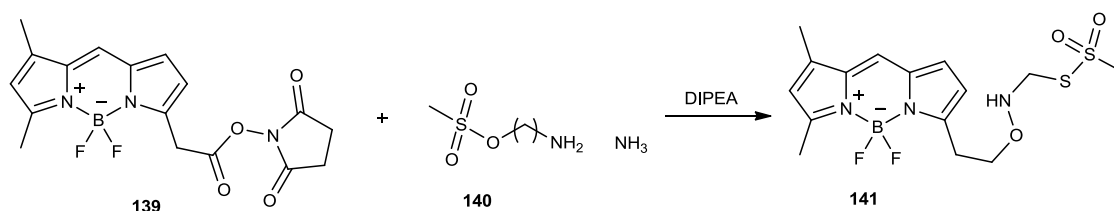


Figure 25 BODIPY with aminooxy reactive group.

Not all synthesised BODIPYs are successful in conjugation. Scheme 35 shows the preparation of a BODIPY dye with a free MTS group. The synthesis includes the reaction of the commercial BODIPY with 3-aminopropyl methanethiosulfonate

hydrobromide, in the presence of diisopropylethylamine (DIPEA) to get the desired BODIPY derivative. The conjugation of this BODIPY with the muscle nicotinic acetylcholine receptor, however, was not successful, despite the fact that this had been achieved with other MTS fluorophores.⁴⁹



Scheme 35 Unsuccessful route for preparation of BODIPY dye.

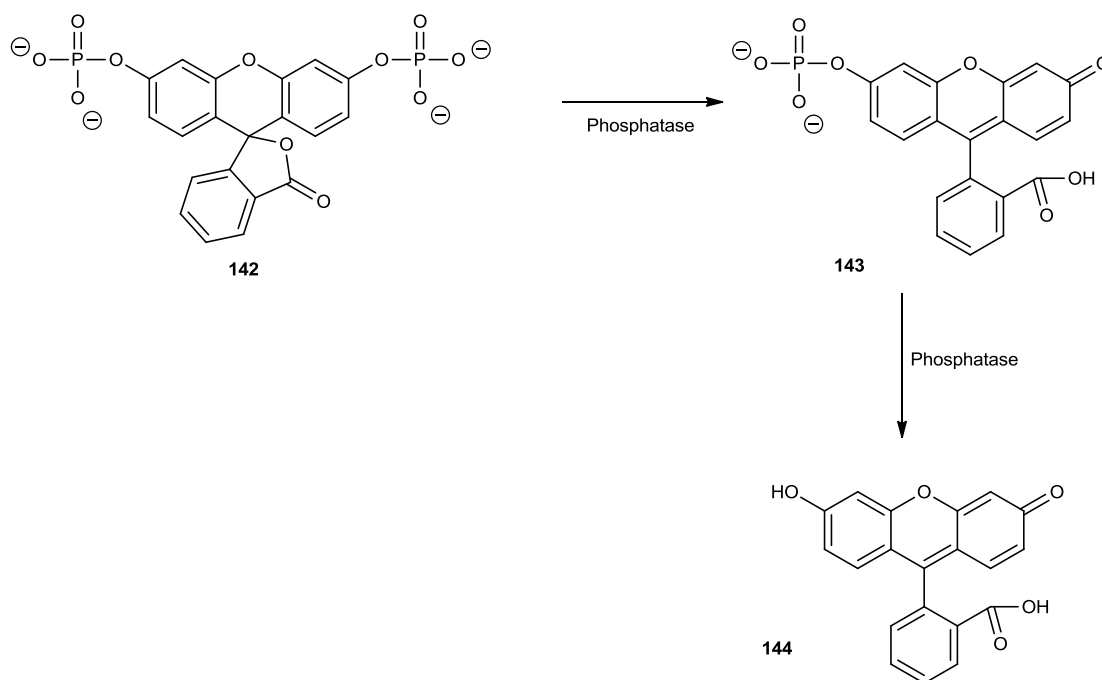
1.3.5. Fluorescent bioprobes

Fluorescent bioprobes are broadly used in many fields as they possess a unique capability to improve the analytical sensitivity. Additionally, they make possible temporal and spatial sampling with a greater proficiency. The main attention in this section will be a focus on fluorescent bioprobes which are designed with cleavable active bond as a linker. In the past few years, the design and development of such probes has received immense attention particularly in the context of the specific determination of analytes with high hydrolytic reactivity (from metal ions to enzyme activity).⁵⁰ Moreover, they allow the monitoring of many biological processes *in situ* and in real time. Many spectroscopic techniques can be used to allow the accurate observation of fluorescent bioprobes with the cleavable active bond providing selectivity for the precise detection of specific analytes. The most famous technique is to use photoinduced electron transfer, photoinduced proton transfer, or fluorescence resonance energy transfer.⁵¹ All these probes can be summarized as “turn on”, latent fluorescent or pro-fluorescent probes, as introduced by R. T. Raines in 2005.⁵²

In project number 2, the target is to synthesise a bioprobe with a peptide cleavage bond as the linker. As an introduction to this topic, the main classes of cleavable types of bond will now be described.

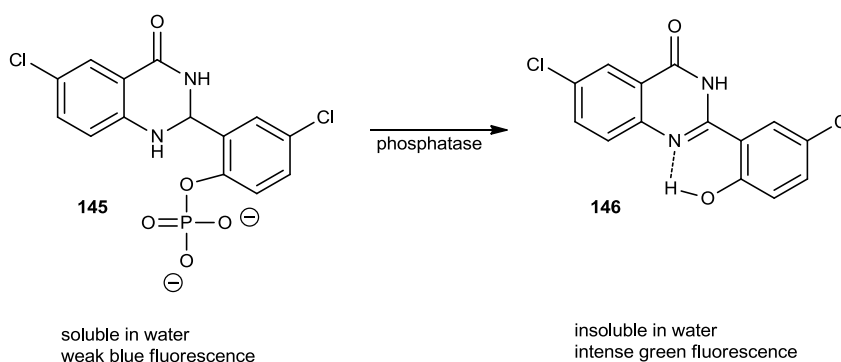
1.3.5.1. Fluorescent bioprobes with a cleavable phosphoester bond

The phosphate and polyphosphate esters have significant roles in cells as enzyme substrates or secondary messengers. Specifically, the metabolism of polyphosphate esters has a big input in the activities of cells. Bioprobes with a cleavable phosphoester bond have been developed to detect the activity of phosphatases and other enzymes (ATPases and DNA/RNA polymerases).⁵³ The main factor which needs to be taken into account is the choice of a fluorophore which is suitable for the design of bioprobes with this type of cleavable bond. The most commonly used fluorophores possess hydroxyl groups (fluorescein, 7-hydroxy-9H-(1,3-dichloro-9,9-dimethylacridin-2-one DDAO, 7-hydroxy-4-methyl-coumarin) which are derivatised as phosphate esters. An interesting example of a sensitive fluorogenic phosphatase substrate **142** (derivative of fluorescein) is shown in Scheme 36. Before the reaction with alkaline phosphatase, dye **142** is colourless and non-fluorescent. Afterwards, this compound is hydrolysed in two steps to fluorescein **144**, with a strong fluorescence, the cleavage of the two phosphate bonds being accompanied with the intramolecular lactone ring opening, restoring the conjugation between the two parts of the fluorescein moiety. The turn on probe displays significant fluorescence enhancement.⁵⁴



Scheme 36 Example of fluorescent bioprobe with cleavable phosphoester bond.

Another phosphatase substrate (**145**, Scheme 37) has been applied to localise the endogenous alkaline phosphatase in tissues and cultured cells with high-resolution.⁵⁵



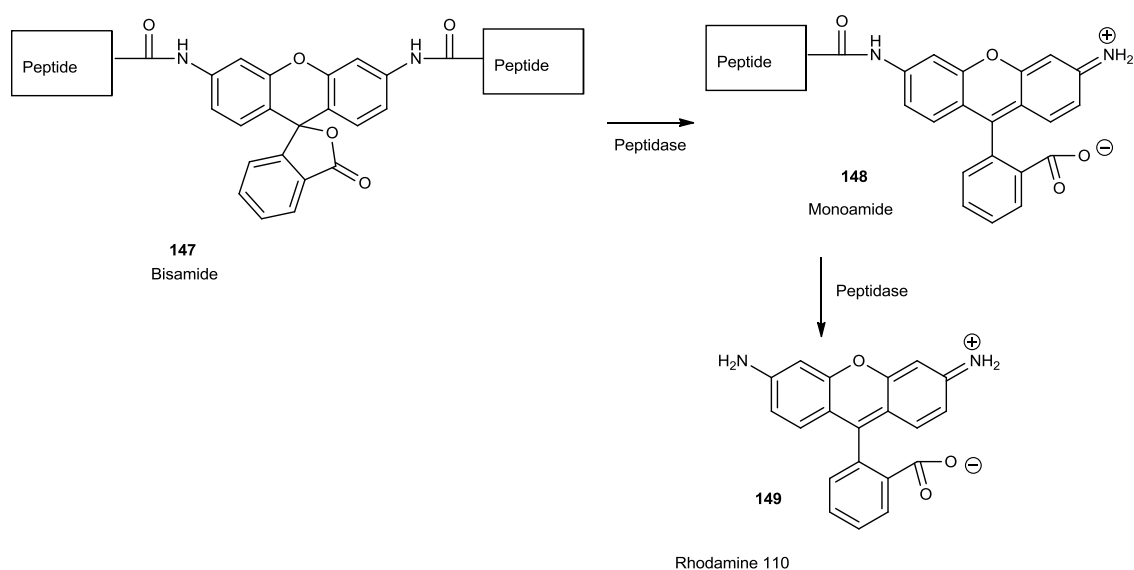
Scheme 37 Phosphatase substrate probe used for detection of alkaline phosphatase.

The substrate **145** has weakly blue-fluorescent properties but after the enzymatic cleavage provides an intensely photostable yellow-green fluorescent product **146** which is a consequence of the recovered hydroxyl which takes part in intramolecular hydrogen bonding and enhances fluorescence through the ESIP⁵⁶ phenomenon (intramolecular proton transfer in the excited state).⁵⁷

1.3.5.2. Fluorescent bioprobes with amide cleavable bonds

In the development of monitoring enzyme activity, peptide substrates containing a pair of fluorescent donor and acceptor groups are important because of the ability of a peptidase to cleave selectively peptide bond.⁵⁸

Bioprobes with amide cleavable bonds are important because of their interaction with enzymes, specifically the peptidases and proteases, which play significant roles in protein activation, cell regulation and signalling, as well as in the generation of amino acids for protein synthesis. These bioprobes most commonly are based on 7-amino-4-methylcoumarin (AMC) to detect enzymatic activity in cells, homogenates and solutions.⁵⁹ Additionally, rhodamine, which is a visible light-excitable dye, is widely used in designs that usually comprise two identical amino acids or peptides attached to single fluorophore, as is shown in Scheme 38. The hydrolysis of bisamide derivatives **147** of Rho 110 by a peptidase occurs in two stages.



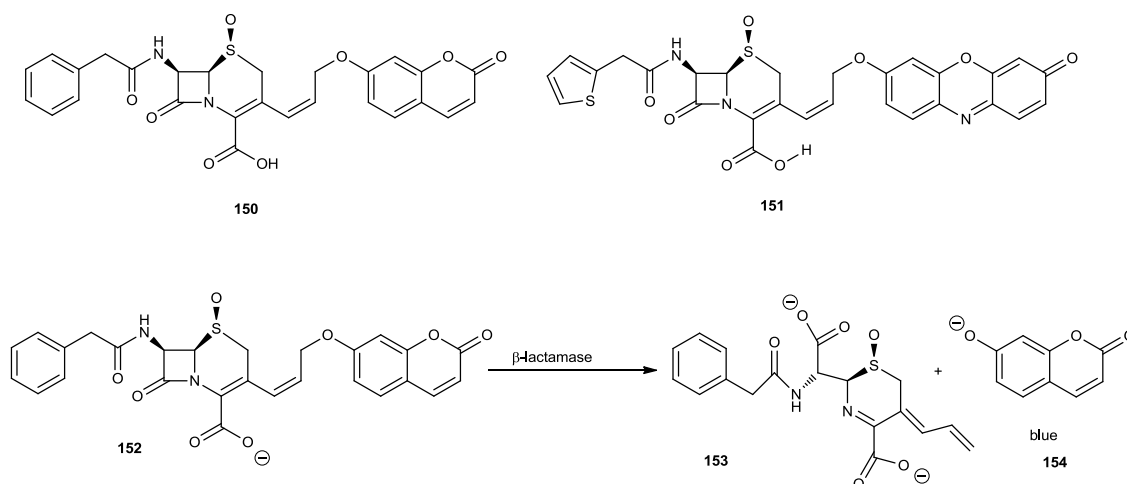
Scheme 38 Representation of hydrolysis of bisamide to afford Rho110.

The enzymatic activity starts with non-fluorescent bisamide **147** which is converted into the monoamide **148** which is fluorescent. Additionally, the hydrolysis of its second amide **148** by the peptidase releases even more fluorescent Rho 110. The fluorophore

149 can be retained within the cell and this fluorescence can be excited by visible light at 495 nm.⁶⁰ Further important designs and coumarin-based probes with a cleavable amide bond, will be discussed in the results and discussion section for project 2.

1.3.5.3. Fluorescent probes with lactamase-cleavable active bonds

The clinical importance of the precise detection of β -lactamases activity in biological samples has led to the development of bioprobes that respond to the presence of antibiotics resistant bacteria strains through development of beta-lactamase activity. These types of bacteria belong to the families which cleave penicillins and cephalosporin with high catalytic efficiency and so are resistant to β -lactam antibiotics. Dyes **150**, **151**, **152** presented in Scheme 39 have been established to detect β -lactamase activity with high sensitivity.⁶¹

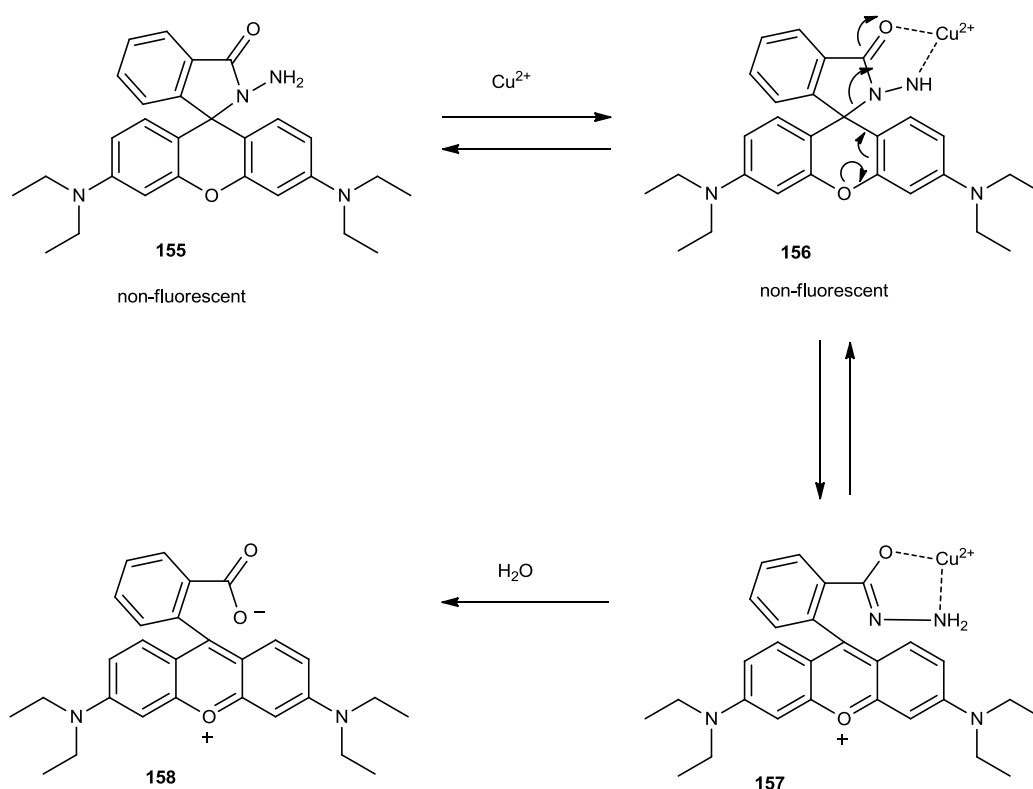


Scheme 39 The detection mechanism for β -lactamases activity employs as a first step the hydrolysis of **150** which gives rise to the release of the fluorophore **152** with enhanced fluorescent signals through a domino 1-6 elimination process.⁶¹

The mechanism of β -lactamase activity is presented in Scheme 39. The hydrolysis of **152** will promote the release of fluorophore **154** with fluorescent signals through a 1-6 elimination process, which is only possible once the beta-lactam ring has been cleaved.

1.3.5.4. Fluorescent bioprobe with cleavable bond by metal ions

The challenge to design and synthesise bioprobes for detection of metal ions required a wide investigation as they resemble and have similar reaction properties to common spectroscopic probes. The answers to the problem rely on novel probes based on fluorophores with selectively hydrolysable groups. A bioprobe for the detection of Cu^{2+} was reported by Czarnik *et al.*⁶² and is shown in Scheme 40. The probe **155** is non-fluorescent, since the gamma lactam ring breaks the conjugation on the rhodamine scaffold, and was based on the hydrolysis mechanism in which the addition of Cu^{2+} results in N,O chelation by hydrazide species followed by redox hydrolysis with release of fluorophore **158**.

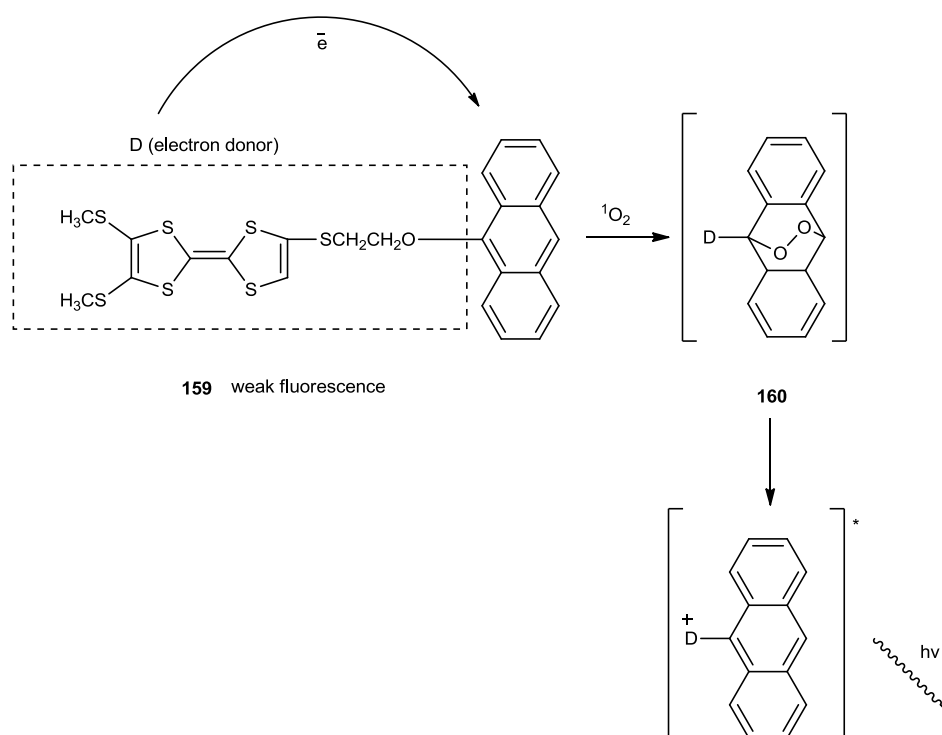


Scheme 40 Example of fluorescent bioprobe with cleavable bond by Cu^{2+} .

1.3.5.5. Fluorescent bioprobes with bonds which are cleavable by reactive oxygen species

The bioprobes based on the detection of reactive oxygen species are important mediators for the pathological conditions of many diseases. The most common reactive oxygen species are hydrogen peroxide, superoxide, hydroxyl radical or singlet oxygen.⁶³

The molecule **159**, designed for singlet oxygen ($^1\text{O}_2$) detection, is shown in Scheme 41. This probe has highly selective and sensitive chemiluminescence. The precise methodology for operation of the probe is through the incorporation of an electron-rich tetrathiafulvalene dye into the luminophore of anthracene which is sensitive to $^1\text{O}_2$. During reaction with hydrogen peroxide or hypochlorite, superoxide, hydroxyl radical, or $^1\text{O}_2$, the probe displays chemiluminescence (CL) outputs.⁶⁴

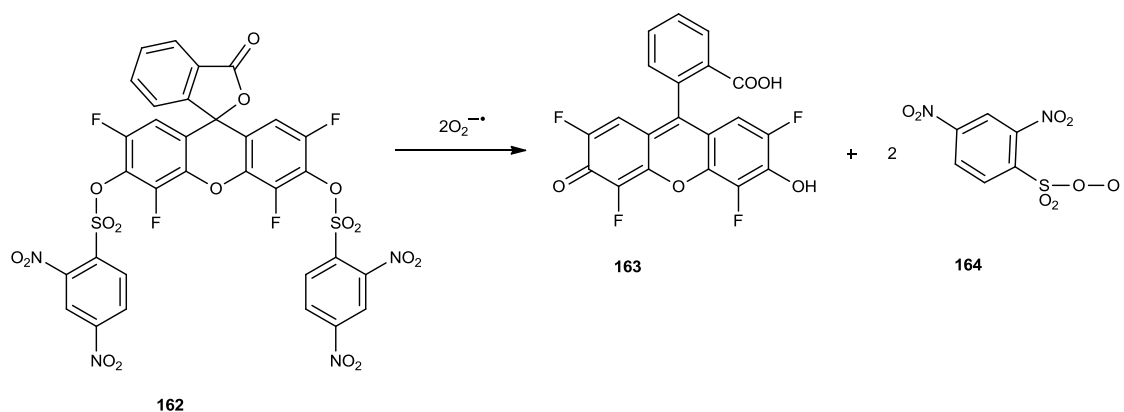


Scheme 41 Example of chemiluminescent bioprobe for singlet oxygen detection.

Importantly, it is a highly sensitive process for reaction with $^1\text{O}_2$ in comparison with other reactive oxygen dyes. As a consequence of this effect, the probe is widely used

for $^1\text{O}_2$ detection in many chemical and biological systems as $^1\text{O}_2$ can be easily differentiated from other reactive oxygen species mentioned above.⁶⁴

Another good example of a novel fluorescent probe **162** for detecting, in this case, the superoxide ion, was reported by Maeda's group.⁶⁵ Scheme 42 shows the mechanism by which this works, which involves the reaction of the non-fluorescent substrate **162** with $\text{O}_2^{\bullet-}$ (nucleophile) followed by cleavage of the sulfonic ester bonds to release the product **163**. Two equivalents of $\text{O}_2^{\bullet-}$ are needed to liberate the desired compound **163**.



Scheme 42 Example of fluorescent probe for detecting of the superoxide ion.

Representative examples of variety fluorescent probes with cleavable bonds for the detection of analytes have been discussed to outline a field which is under investigation in organic and bioanalytical chemistry. The future research in the design of fluorescence bioprobes will seek to establish more precise analytical properties in the sense of the selectivity and sensitivity, which can improve the understanding of mechanism of biomolecular interactions or *in vivo* processes.

1.3.6. References:

-
- ¹ J. R. Lakowicz, Principles of Fluorescence Spectroscopy, Third Edition, Springer Science & Business Media, 5 Dec **2007**.
- ² D. Zhao and T. M. Swager, *Macromolecules*, **2005**, 38, 9377-9384.
- ³ H. Xu, Q. Liu, *Spectrochim. Acta*, **2008**, 70A, 243-246.
- ⁴ C. Tsallis, *J. Statistical Physics*, **1988**, 52, 479-487.
- ⁵ R. Wang, Z. Yu, *Acto Physico-Chimica Sinica*, **2007**, 23, 1353-1359.
- ⁶ P. Zhu, J. P. Clamme, *Biophysics*, **2005**, 89, 37-39.
- ⁷ G. Weber, F. W. J. Teale, *Trans. Faraday Soc.*, **1958**, 54, 640-648.
- ⁸ D. Egan, R. O'Kennedy, E. Morgan, D. Cox, E. Prosser, R. D. Thornes, *Drug Metabolism Reviews*, **1990**, 22, 503-529.
- ⁹ R. O'Kennedy, R. D. Thornes, Coumarins: Biology, Applications and Mode of Action, Wiley & Sons, Chichester, **1997**.
- ¹⁰ M. Zahradnik, The Production and Application of Fluorescent Brightening Agents, Wiley & Sons, **1992**.
- ¹¹ M. Maeda, Laser Dyes, Academic Press, New York, **1994**.
- ¹² R. D. H. Murray, J. Mendez, S. A. Brown, The Natural Coumarins: Occurance, Chemistry and Biochemistry, Wiley & Sons, New York, **1982**.
- ¹³ S. K. De, R. A. Gibbs, *Synthesis*, **2005**, 1231-1233.
- ¹⁴ E. Gikas, M. Parissi-Poulou, M. Kazanis, A. Vavagianis, *Anal. Chim. Acta*, **2003**, 489, 153.
- ¹⁵ E. Gikas, A. Vavayiannis, M. Kazanis, M. Parissi-Poulou, *J. Liq. Chromatogr. Relat. Technol.*, **2003**, 26385.
- ¹⁶ H. E. Katerinopoulos, *Curr. Pharm. Dess.*, **2004**, 10, 3835-3852.
- ¹⁷ a) F. A. Tanious, T. C. Jenkins, S. Neidle, W. D. Wilson, *Biochemistry*, **1992**, 31, 11632-11640; b) R. K. Y. Zee-Cheng, C. C. Cheng, *J. Med. Chem.*, **1978**, 21, 291.
- ¹⁸ S. K. Carter, D. Rall, P. Schein, R. D. Davis, H. B. Wood, R. Engle, J. P. Davignon, J. M. Venditti, S. A. Schepartz, B. R. Murray, C. G. Zubrod, Psuedourea; National Cancer Chemotherapy Institute Clinical, Brochure No. NSC56054, p 2.
- ¹⁹ R. F. Pittillo, C. Woolley, *Appl. Microbiol.*, **1969**, 18, 519-521.

-
- ²⁰ a) W. D. Wilson, F. A. Tanious, R. A. Watson, H. J. Barton, A. Strekowska, D. B. Harden, L. Strekowski, *Biochemistry*, **1989**, 28, 1984-1992; b) T. P. Wunz, R. T. Dorrr, D. S. Alberts, C. L. Tunget, J. Einspahr, S. Milton, W. A. Remers, *J. Med. Chem.*, **1987**, 30, 1313-1321.
- ²¹ C. V. Kumar, E. H. Asuncion, *J. Am. Chem. Soc.*, **1993**, 115, 8547-8553.
- ²² J. Bern, C. Franco-Pujante, M. Alajarin, *Org. Biomol. Chem.*, **2014**, 12, 474-478.
- ²³ M. Beija, C. A. M. Afonso, J. M. G. Martinho, *Chem. Soc. Rev.*, **2009**, 38, 2410-2433.
- ²⁴ L. D. Lavis, T.-Y. Chao, R. T. Raines, *Chem. Biol.*, **2006**, 4, 252-260.
- ²⁵ R. Bandichhor, A. D. Petrescu, A. Vespa, A. B. Kier, F. Schoreder, K. Burgess, *Bioconjugate Chem.*, **2006**, 17, 1219.
- ²⁶ C. E. P. Muller, M.-L. Viriot, M.-C. Carré, *Helv. Chim. Acta*, **2001**, 84, 3735.
- ²⁷ Y. Ueno, G. -S. Jiao, K. Burgess, *Pract. Synth. Proc.*, **2004**, 31, 2591.
- ²⁸ L. Fulop, B. Penke, M. J. Zarandi, *J. Pept. Sci.*, **2001**, 7, 397.
- ²⁹ C. Hoffmann, J. Leroy-Dudal, S. Patel, O. Gallet, E. Pauthe, *Anal. Biochem.*, **2008**, 372, 62.
- ³⁰ T. Konecsni, F. Kilár, *J. Chromatogr. A*, **2004**, 1051, 135.
- ³¹ J. Fernández-Carneado, E. Giralt, *Tetrahedron Lett.*, **2004**, 45, 6079.
- ³² O. N. Burchak, L. Mugherli, F. Chatelain, M. Y. Balakirev, *Bioorg. Med. Chem.*, **2006**, 14, 2559.
- ³³ S. Undenfriend, S. Stein, P. Böhlen, W. Dairman, W. Leimgruber, M. Weigele, *Science*, **1972**, 178, 871.
- ³⁴ M. Talhavini, T. D. Z. Atvars, *J. Photochem. Photobiol. A: Chem.*, **1998**, 114, 65.
- ³⁵ M. Talhavini, T. D. Z. Atvars, *J. Photochem. Photobiol. A: Chem.*, **1999**, 120, 141.
- ³⁶ M. Weigele, S. DeBernardo, W. Leimgruber, *Biochem. Biophys. Res. Commun.*, **1973**, 50, 352.
- ³⁷ M. Carvell, I. D. Robb, P. W. Small, *Polymer*, **1998**, 39, 393.
- ³⁸ M. M. Martin, *Chem. Phys. Lett.*, **1975**, 35, 105.
- ³⁹ M. A. Bridges, K. M. McErlane, E. Kwong, S. Katz, D. A. Applegarth, *Clin. Chim. Acta*, **1986**, 157, 73.
- ⁴⁰ P. Almeida, *Quimica*, **1999**, 73, 9.

-
- ⁴¹ A. Gomez-Hens, M. P. Aguilar-Caballos, *Trends Anal. Chem.*, **2004**, 23, 127.
- ⁴² G. Patonay, J. Salon, J. Sowell, L. Strekowski, *Molecules*, **2004**, 9, 40.
- ⁴³ R. D. Mitra, J. Shendure, J. Olejnik, E. Krzymanska-Olejnik, G. M. Church, *Anal. Biochem.*, **2003**, 320, 55.
- ⁴⁴ R. Weissleder, V. Ntziachristos, *Nat. Med.*, **2003**, 9, 123.
- ⁴⁵ S. J. Mason, S. Balasubramanian, *Org. Lett.*, **2002**, 4, 4261.
- ⁴⁶ A. Treibs, F. H Kreuzer, *Liebigs, Ann. Chem.*, **1968**, 718, 208.
- ⁴⁷ R. P. Haugland, H. C. Kang, US pat. 4,774, 339, **1988**.
- ⁴⁸ J. Rayo, N. Amara, P. Krief, M. M. Meijler, *J. Am. Chem. Soc.*, **2011**, 133, 7469.
- ⁴⁹ T. Kalai, K. Hideg, *Tetrahedron*, **2006**, 62, 10352.
- ⁵⁰ a) I. Johnson, *J. Histochem.*, **1998**, 30, 123-140; b) J. R. Lakowicz, Topics in Fluorescence Spectroscopy, Vol. Volume 4 - Probe Design and Chemical Sensing, **2002**; c) X. Chen, M. Sun, H. Ma, *Curr. Org. Chem.*, **2006**, 10, 477-489; d) N. Johnsson, K. Johnsson, *ACS Chem. Biol.*, **2006**, 31-38; e) T. Terai, T. Nagano, *Curr. Opin. Chem. Biol.*, **2008**, 12, 515-521; f) T. Nagano, *Proc. Jpn Acad. Ser. B Phys. Biol. Sci.*, **2010**, 86, 837-847; g) J. Chan, S. C. Dodani, C. J. Chang, *Nat. Chem.*, **2012**, 4, 973-984; h) J. B. Grimm, L. M. Heckman, L. D. Lavis, *Prog. Mol. Biol. Transl. Sci.*, **2013**, 113, 1-34; i) T. Terai, T. Nagano, *Pflugers Arch.*, **2013**, 465, 347-359; j) X. Li, X. Gao, W. Shi, H. Ma, *Chem. Rev.*, **2014**, 114, 590-659.
- ⁵¹ M. Fernández-Suárez, A. Y. Ting, *Nature Reviews Molecular Cell Biology*, **2008**, 9, 929-943.
- ⁵² R. T. Raines, S. S. Chandran, K. A. Dickson, *J. Am. Chem. Soc.*, **2005**, 127, 1652-1653.
- ⁵³ K. Rurack, M. Kollmannsberger, J. Daub, *Angew. Chem. Int. Ed.*, **2001**, 40, 385.
- ⁵⁴ M. Zimmerman, E. Yurewicz, G. Patel, *Anal. Biochem.*, **1976**, 70, 258-262.
- ⁵⁵ G. B. Irvine, M. Ennis, C. H. Williams, *Anal. Biochem.*, **1990**, 185, 304-307.
- ⁵⁶ a) M. Santra, B. Roy, K. H. Ahn, *Org. Lett.*, **2011**, 13, 3422-3425; b) G. Li, D. Zhu, Q. Liu, L. Xue, H. Jiang, *Org. Lett.*, **2013**, 13, 924-927; c) S. Goswami, S. Das, K. Aich, B. Pakhira, S. Panja, S. K. Mukherjee, S. Sarkar, *Org. Lett.*, **2013**, 15, 5412-5415; d) J. E. Kwon, S. Y. Park, *Adv. Mater.*, **2011**, 23, 3615-3642.
- ⁵⁷ G. Jourquin, J.-M. Kauffmann. *Pharm. Biomed. Anal.*, **1998**, 18, 585-596.

-
- ⁵⁸ J. George, M. L. Teeaar, C. G. Norey, D. D. Burns, *J. Biomol. Screening*, **2003**, 8, 72-80.
- ⁵⁹ C. G. Knight, *Methods Enzymol.*, **1995**, 248, 18-34.
- ⁶⁰ A. F. Johnson, M. D. Struthers, K. B. Pierson, W. F. Mangel, L. Smith, *Anal. Chem.*, **1993**, 65, 2352-2359.
- ⁶¹ W. Gao, B. Xing, R. Y. Tsien, J. J. Rao, *J. Am. Chem. Soc.*, **2003**, 125, 11146-11147.
- ⁶² A. W. Czarnik, V. Dujols, F. Ford, *J. Am. Chem. Soc.*, **1997**, 119, 7386-7387.
- ⁶³ B. Halliwell, J. M. C. Gutteridge, *Free Radicals in Biology and Medicine* (3rd ed), Clarendon Press: Oxford, **1999**.
- ⁶⁴ X. Li, G. Zhang, H. Ma, D. Zhang, J. Li, D. Zhu, *J. Am. Chem. Soc.*, **2004**, 126, 11543-11548.
- ⁶⁵ H. Maeda, K. Yamamoto, Y. Nomura, I. Kohno, L. Hafsi, N. Ueda, S. Yoshida, M. Fukuda, Y. Fukuyasu, Y. Yamauchi, N. Itoh, *J. Am. Chem. Soc.*, **2005**, 127, 68-69.

1.4. Bioprobes based on boron-diol interactions

Boron-diol interactions are most significant when considering human health,¹ plant growth² and additionally quorum-sensing among certain bacteria.³ Boron is one of the ten most common elements in sea water and saccharides are one of the most significant classes of biomass on the planet.⁴

Currently; under investigation is the development of synthetic saccharide receptors which are based on the covalent interactions between boron and sugars. These interactions are reversible in aqueous solution.⁵ In this chapter, the current understanding of these processes will be reviewed, to provide a historical perspective on their discovery, and to classify these interactions by carbohydrate types. This information is crucial to the design and synthesis of the bioprobe for project number 1, containing boronic acid as a molecular recognition tool. The nature of the mechanism for the reversible binding between boron acids and diols has been widely exploited in sensor design. Furthermore, the use of boronic acid derivatives with carbohydrate recognition properties could provide procedures for the selective detection of specific sugars in future applications in early-stage diagnostics. The aim of this project is to design a boron-based bioprobe targeting the cell-surface sugars that will be able to recognize particular characteristic antigenic determinants for the identification of diseases, thus enabling earlier diagnosis and treatment. In this chapter, the fundamental research of boron-carbohydrate interactions will be described. However, discussion of how this translates into the design of synthetic carbohydrate receptors will also be included.

1.4.1. Boron-saccharide interactions

Due to the unique strong interaction between boronic acids and diols through reversible ester formation, there has been a great deal of interest in using boronic acids as the recognition moiety for the development of sensors for sugars. Their well-documented ability to form complexes with diols rapidly and reversibly in basic aqueous media gives them a very significant role in this field. Sugars which have prearranged *cis*-diols can form stronger complexes with boronic acids and are convenient as an interface for artificial sugar receptors. The interactions between

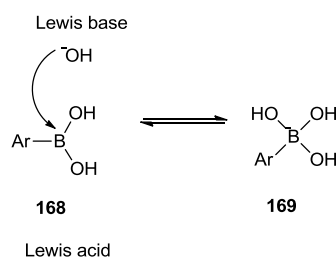
sugars and boronic acids can be combined with the use of hydrogen bonding interactions for sugar sensing in aqueous systems. This can be explained as more the strongly associated covalent structures that arise when boronic acids are connected with polyhydroxylic saccharides, allowing them to be selectively recognised by reactions at diols unit. It has been known for over forty years that the boron atom in a boronic acid becomes more acidic when bound to a saccharide. The 1,2- and 1,3-*cis* diols interact with saccharides to form five or six membered rings, respectively.⁶ In 1913, Böeseken⁷ reported the increase in acidity of boronic acids in the presence of glucose, but almost half a century passed before the group of Lorand and Edwards quantified the affinity of boric and phenylboronic acids with diols (for example catechol), and sugars (e.g. fructose, glucose).⁸

Boronic acids can be considered as electron deficient Lewis acids, and thus electron-pair acceptors (Lewis bases are electron pair-donors). A good example of interactions between the Lewis acid boron trifluoride **165** and the Lewis base triethylamine **166** is shown in Scheme 43. The covalent bond between them is formed by the electrons from the Lewis base. These types of bonds are called coordination or dative bonds.⁹



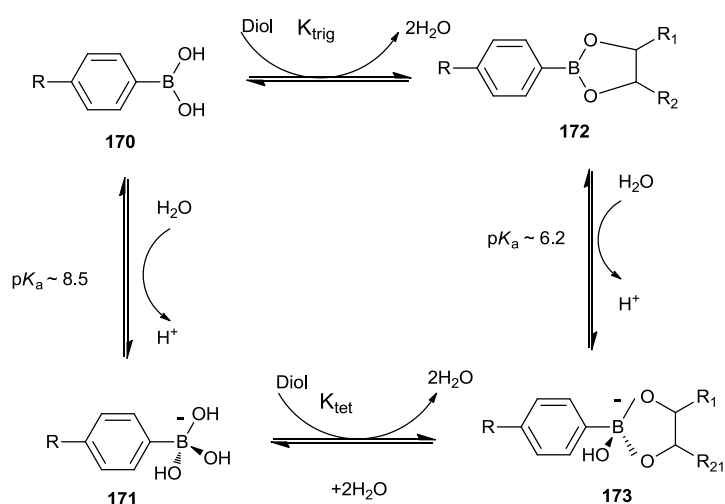
Scheme 43 Interaction between Lewis acid and base.

The geometry of boronic acids is planar trigonal as they have an sp^2 hybridized boron atom and an empty p orbital to receive electrons, explaining how they can easily react in a Lewis acid manner with anions. Another example of this interaction, shown in Scheme 44, is with hydroxide anion.^{8,9}



Scheme 44 Equilibrium between Lewis base and acid.

The equilibrium between diols and boronic acid is shown in Scheme 45. This process illustrates the unique Lewis acid feature of boronic acids and esters. The binding interaction by the esterification of **170** to form **172**, causes a decrease in the Lewis acidity which involves a reduction of the pK_a . The formation of the anionic form of the boronic species **173** is made by complexation of boronic acids. The derivative **173** is in equilibrium with dye **170** boronate ester **172** has a trigonal structure. This ester **172**, with $pK_a \sim 6.2$, is able to convert into structure **173** as shown in Scheme 35, and the pK_a of the conversion from acid **170** to dye **171** is different from ester **172** to dye **173** ($pK_a \sim 8.5$) due to the increase in acidity when diols bind to the boronic acids. The geometry of the anionic adducts is tetrahedral with a sp^3 -hybridized boron atom which is electron rich. These changes produce a significant effect on the properties of these compounds, so the pK_a of 8.8 is reserved mostly for a phenylboronic acid itself, but in the case of the adduct (boronic group + sugar), the pK_a typically will reach about 6.8 for its glucose ester and 4.5 for fructose esters. The boronate esters with low pK_a are explained by the higher affinity for specific diols to bind to phenylboronic acid (PBA), thus D-fructose binds to PBA much better than D-glucose.^{9,10,11}

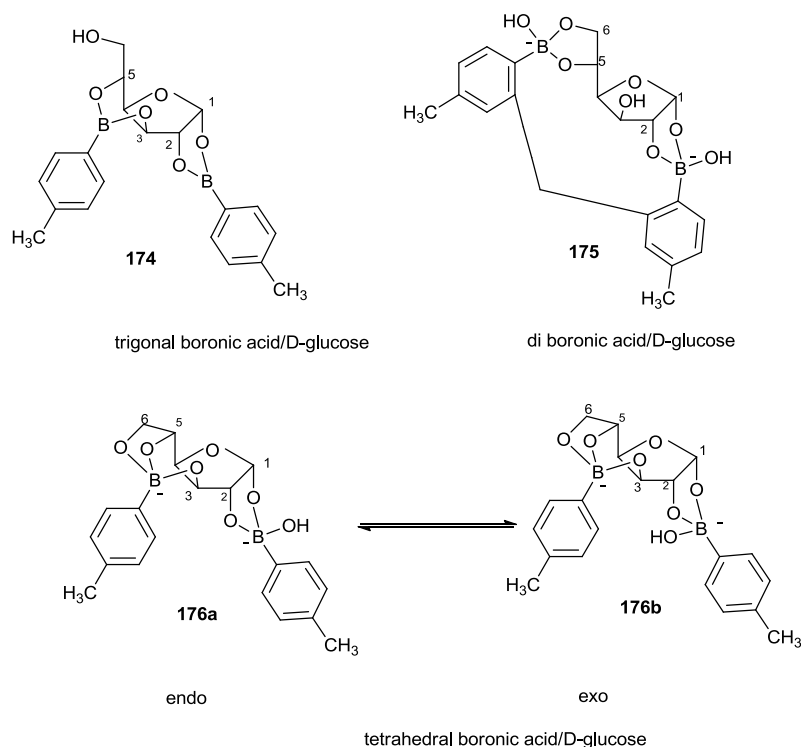


Scheme 45 The binding interaction between boronic acids and diols.

1.4.2. Bioprobes based on the complexes of boronic acids with diols

In the 1950's, the high affinity of boronic acids for sugars was first described. Structural studies of saccharide-boronic acid complexes could not be presented until much later when NMR techniques became available. From the point of view of carbohydrate bioprobes development, it is important to know the structural features in aqueous conditions. The most common models for sugars are glucose and fructose, and mono or diboronic acids. Additionally, some researchers have reported much work on conformational and structural investigations which were established by the determination of *C-H* and *H-H* coupling constants. These allowed to differentiate different adducts depending on the size of the ring and conformation of the sugar in the cyclic ester.^{12,13,14,15} The question then arose: in which form does the complex exist between glucose and phenylboronic acid? The first answer for that question was reported by Eggert and Norrid in 1995.¹⁶ They studied ester formation between the boronic acid and D-glucose using ¹³C and ¹H NMR spectroscopy in neutral non-aqueous and basic conditions. The results showed that the first binding site was position (1,2) of the furanose form of the D-glucose in both neutral non-aqueous and alkaline conditions. The boronic acid dye **174** was then formed by binding to the (3,5) positions of the furanose form of D-glucose under neutral non-aqueous conditions, (Scheme 46). Binding to positions (5,6) was observed for the diboronic acid probe **175**. However, the

boronic acid **176** was bound to positions (3,5,6) in a *tris* coordinated manner under basic conditions, as shown in Figure 26.¹⁶



Scheme 46 Examples of sugar-boronic acid interactions.

Another answer about the form of these complexes was obtained by Norrid in 1996. His group reported structural studies of the fructose complex with phenylboronic acid. The boronic acid and fructose (ratio 1:1) under alkaline conditions was shown to form a 2,3,6 tridentate complex as the major product (Figure 26). Furthermore the fructose was in furanose form in all cases and observed only traces of 2,3 *exo* and *endo* isomers were observed.¹⁵

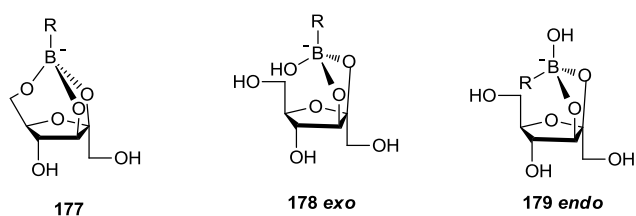


Figure 26 Example of fructose forms.

At the ratios 2:1 and 4:1 boronic acid/fructose, they observed four new complexes which are a consequence of binding to positions (2,3) and (4,5) in the fructopyranose

form with two boronic acids. These four compounds, which are diastereomers (*endo* and *exo*) are shown in Figure 27.

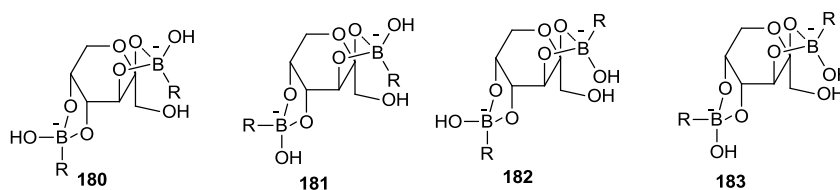
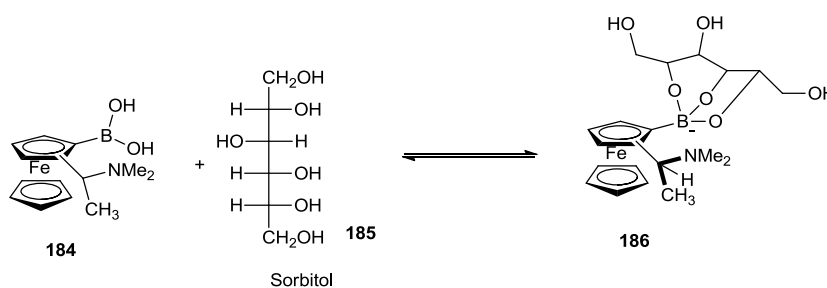


Figure 27 The structures of diastereomers.

The observations that the first boronic acid is bound to 2,3 position of D-fructose and the second boronic acid is bound to 4,5-position of the D-fructose was confirmed by Draffin *et al.*¹⁷ who reported the crystal structure of the fructopyranose complex with the phenylboronic acid.¹⁷

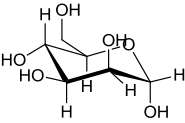
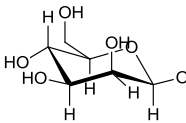
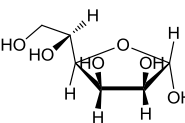
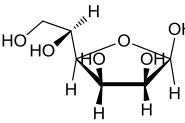
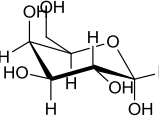
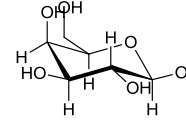
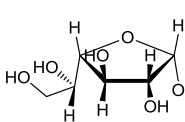
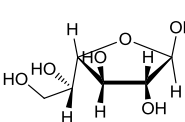
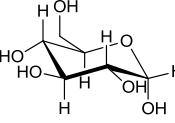
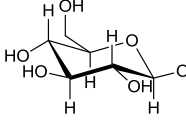
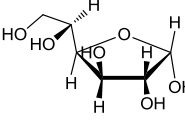
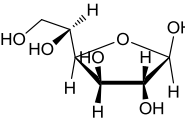
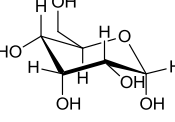
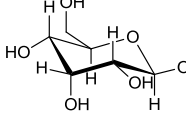
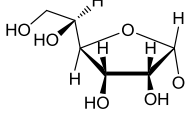
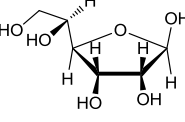
Another important sugar discussed in the literature is sorbitol. This sugar forms a trivalent complex with a boronic acid, confirmed by the studies of the reaction between D-sorbitol **185** and (*S,S*)-2-(*N,N*-dimethyl-1-aminoethyl)ferrocene boronic acid **184** by Norrid's group (Scheme 47).¹⁸ Sorbitol, as well as fructose, has the ability to bind to boronic acid in a tridentate manner a factor in the higher affinity of these mentioned sugars for boronic acids, compared to glucose or mannose.



Scheme 47 Formation of trivalent complex between sorbitol and a boronic acid derivative.

Some of the furanose and pyranose forms of sugars typically exploited in the biosensor methodology are presented in Table 1.

Table 1 Furanose and pyranose forms of sugar exploited in the biosensor methodology

name of sugar	α -Pyranose forms	β -Pyranose forms	α -Furanose forms	β -Furanose forms
D-mannose				
D-galactose				
D-glucose				
D-allose				

1.4.2.1. The events which can influence the binding event

Several factors which can affect the binding effect need to be considered when designing boronic acid-based bioprobes. The most noteworthy factors are pH, pK_a of the boronic acid, the nature and concentration of the buffer, the dihedral angle of the diol, and temperature.⁹

1.4.2.1.1. The pH and pK_a of boronic acids

The pH is influenced by the affinities of boronic acids towards diols. The higher the pH, the higher the binding constants between boronic acid and diol. Hence, for example, boronic acids with lower pK_a s have higher affinities at neutral pH.^{19,20,21} Studies of relationship between pK_a , pH and binding constant were pioneered by Wang *et al.*¹¹ This group used a three component competitive method to show the importance of pK_a and pH on the binding event. In their study, they compared the binding affinities

between a series of 25 arylboronic acids derivatives with varying diols at different pH. The outcome showed that the pKa of monosubstituted boronic acids can be predicted based on the substituent effect (σ values) using a Hammett plot. Interestingly, this suggests that the previous view that boronic acids with lower pKas have greater binding affinities at neutral pH is not necessarily correct. In fact, the optimal pH for binding is related to both the pKas of the boronic acid and the diol and it is not necessarily higher than the pKa of the boronic acid. Typically, before this publication, it was believed that higher pH favours the binding between boronic acid and a diol. The pH would need to be above the pKa of the boronic acid to see meaningful binding. On this basis, the more acidic boronic acids binding more tightly with diols will be observed. When Wang's group described the binding constants at varying pH values of various substituted phenylboronic acids with glucose, fructose and catechol it was shown that the trend of the boronic acid pKa is not essentially correct in the ranking of binding constants among different boronic acids with a diol at physiological pH. Although 2,5-difluorophenylboronic acid has a higher apparent pKa (7.6) than 3,4,6-trifluorophenylboronic acid (6.8) it can bind more effectively with glucose at pH 7.5, contrary to prediction.¹¹

The pH of the solution plays an important role as well. The binding constant between 2,5-difluorophenylboronic acid and fructose is larger than that of 3-chloro-4-fluorophenylboronic acid at pH 7.5, but lower at pH 8.5. So it was needed to consider the pH of the solution in which the binding constants were measured to understand the relative binding constants of various boronic acids with a particular diol.

Interestingly, the predicted optimal pH is 9.8 for the binding between 2,5-difluorophenylboronic acid and glucose but the highest binding constant was detected at pH 7.5. As this outcome shows, the pKas of boronic acids and diols were not the only the major factor to influence the binding constants and optimal pH, and the nature of the buffer and steric factors, need to be taken into account, as they affect the binding constants.^{11,22}

1.4.2.1.2. The pKa of the boronic esters and the stability of the boronic-acid-diol complex

The pKa values of boronic esters are lower than those of the corresponding boronic acids, and different diols have various affinities for a given boronic acid. The binding constant is generally associated with the apparent pKa value of the boronic ester, except for sugars engaged strongly in trivalent binding such as sorbitol.¹¹ The higher binding constant should be observed for lower pKa of the boronic ester and any influence on the increase of the boron Lewis acidity would be expected to improve the binding constant. Theoretically, there are two features (steric and electronic effects) which can cause the change in pKa values from boronic acid to boronic esters, and the electronic factors are probably not the dominant factor. The steric (geometric) factor can help to understand the relative affinities among different diols. Specifically, their capability to force the boron to go from trigonal to the tetrahedral form is due to the boronic ester pKa and the diol-boronic acid binding constants.

During the consideration of the issue of the conversion from trigonal to tetrahedral form, it should be noted that there is only a small distance between the two diol oxygens. The consequence of this is to have a smaller O-B-O bond angle in the ester which is similar to the sp³ form 109° and moves away from the 120° needed for the boron to stay in the trigonal form. This is why diols with small and constrained binding angles are able to bind to boronic acids with higher affinities.⁹

1.4.2.1.3. Buffer effects

Another significant factor in establishing boronic acid based receptors is the buffer. One of the common buffers in physiological conditions at pH 7.4 is phosphate. As the boronic acid is a Lewis acid and the phosphate a Lewis base, it can be expected that it will affect the complexation state of the boron atom, and potentially it is possible to interact with other Lewis bases such as water and sugars.⁹

1.4.3. The bioprobes based on fluorescent boronic acid reporter

The significant part of fluorescent bioprobes is the fluorescent reporter which can cause changes in fluorescence upon binding. In the literature

there are many examples of work towards the development of these types of reporters based on boronic acids.^{6,14,23,24} The binding between a boronic acid and diols works an on-off or off-on system to produce visible fluorescence changes. This will now be discussed with selected examples from the literature on fluorescent reporter compounds and their valuable properties.

1.4.3.1. Photoinduced Electron Transfer (PET) types of bioprobes

A significant tool to distinguish fluorescence intensity is the photoinduced electron transfer (PET) mechanism. The PET sensors possess three major parts; a fluorophore, a linker, and an acceptor. The fluorescent probes based on boronic acids for saccharide detection have to provide a strong fluorescence intensity to aid accurate detection. Additionally, the pH in the presence of sugar must be shifted to a lower pH range as the sensor can then detect sugars more sensitively at specific pH. This interaction is due to the increase in the Lewis acidity of the boronate adducts.⁹

Yoon and Czarnik, reported the first fluorescence PET bioprobe for sugars which are established on fluorophore-containing boronic acids. Their results showed that 2-anthracenylboronic acid **187** (Figure 28) could be used to detect saccharides but unfortunately the changes in fluorescence were minor.²⁵

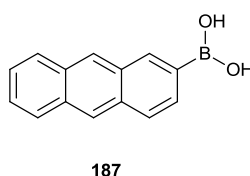


Figure 28 Structure of PET bioprobe.

Afterwards, Suenega *et al.* studied eight aromatic boronic acids, among which, acids **188** and **189** (Figure 29) are the most appropriate for sugar detection.²⁶

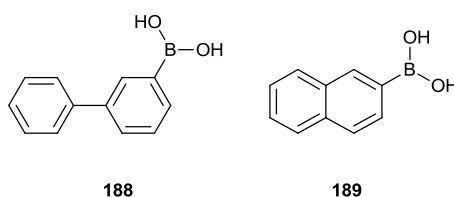
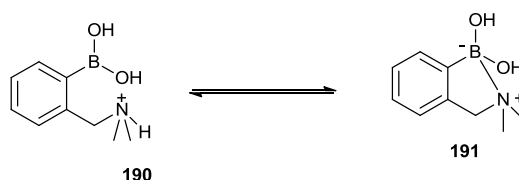


Figure 29 Example of boronic acids dyes used for sugar detection.

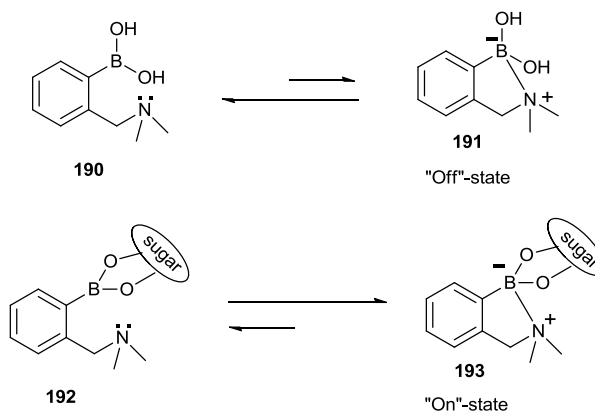
These first reported systems suffer from the disadvantage that they can only perform precise binding with saccharides at high pH, which is required to make a boronate anion, and this is problematic to attempts to address applications in biological systems. The solution to the problem was found by Wulff who incorporated an amine adjacent to the boronic acids. This forced the creation of tetrahedral sp^3 boron at or near neutral pH and it is illustrated by the equilibrium between **190** and **191** (Scheme 48). This equilibrium involves the deprotonation of an ammonium ion, after which the lone pair on the nitrogen associates itself with the empty p orbital on the boron.²⁷ The results of these investigations showed that complex **191** reacts with saccharides at neutral pH and additionally that this process is analogous to the interconversion of **171** and **173** as shown in Scheme 45. The pKa is raised from 9 to 12 by the boron-nitrogen interaction, as the Lewis acidity of the boronic acid is decreased. This interaction also lowers the pKa of the ammonium ion, which changes from 9 to 5. All these changes can be observed by ^{11}B NMR. The peak for boron in compound **190** (trigonal) appears around 28-30 ppm and in the case of compound **191**, the peak lies around 9-10 ppm. It is the tetrahedral form of the boron atom that causes the chemical shift downfield from the trigonal planar geometry.²⁸



Scheme 48 The equilibrium of **190** and **191**.

Another advantage of incorporation of an amine core is that the fluorescence intensity is controlled by its properties. Consequently, these types of system are working as off/on receptors. The 'off' state occurs when sugar is not bound to the compound and the 'free' amine can decrease of the fluorescence by PET quenching. In the case of the 'on' system, the sugar is added and the boron becomes more Lewis acidic and makes a strong bond to the amine. In this way, the cyclic esters conveniently adopt the tetrahedral form and possess a higher affinity. The lone pair on the nitrogen is no longer available as the nitrogen is bound to boron, and the fluorescence cannot now be quenched, which causes the strong fluorescence emission. Scheme 49 presents the

equilibrium between these two “off-on” systems; in the “off” state, the equilibrium is moved to the left hand side however in the “on” state the equilibrium is more in favour of the right hand side.²⁷



Scheme 49 The equilibrium between two “off-on” systems.

The first PET system for sugars was reported by James and Shinkai *et al.*,¹⁴ and such a dye **194** displays a selectivity for D-fructose as shown in Figure 30.

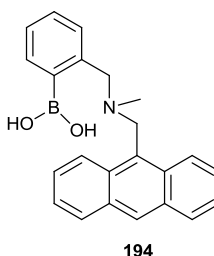
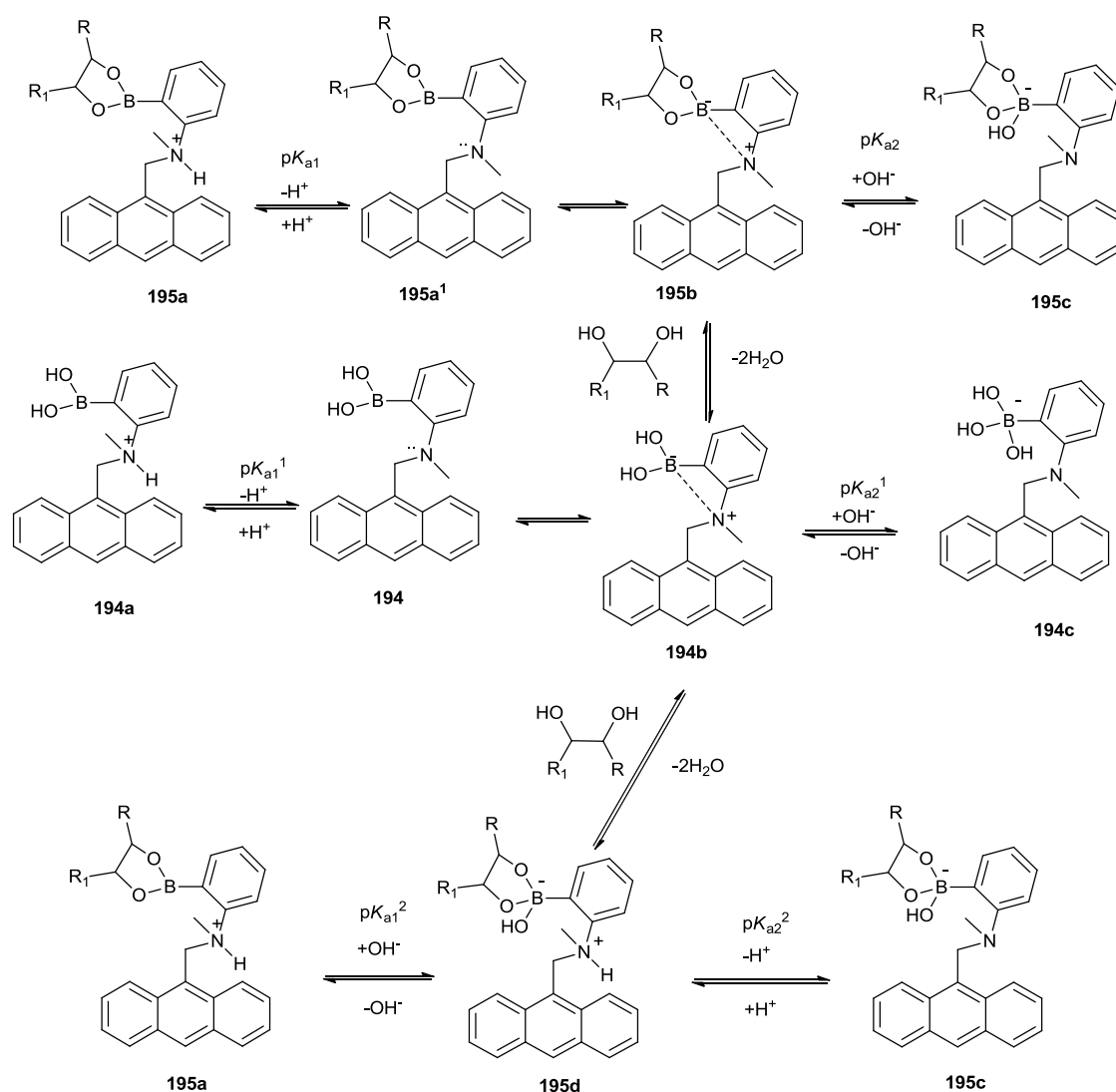


Figure 30 Structure of the first PET system for sugars.

An interesting and noteworthy development and reinvestigation of the mechanism of the changing fluorescence intensity of the Shinkai system **194** has been reported by Springsteen’s group. The initially-proposed mechanism described that the changes in the intensity of the fluorescence are due to B-N bond formation (lone pair on nitrogen is masked). W. Ni *et al.*²⁸ performed studies that suggest a more sophisticated mechanism for the complexation of boronic acid **194** with diols. The new proposal includes solvolysis which leads to protonation of the amine nitrogen, but for this to occur, the reactions need to be performed in a protic solvent such as water. The

protonation of the nitrogen atom stops the photoinduced electron transfer, resulting in reduced quenching of the anthracene fluorescence. The suggested mechanism describes the various forms of boronic-acid and boronic acid-diol structures, which are shown in Scheme 50.²⁸



Scheme 50 The new proposal of equilibrium which includes solvolysis.

To determine precisely the proposed mechanism, they examined the effect of changes in the pH profile of the reporter system in the presence and absence of a sugar, and also studied the maximal fluorescence intensity for changes caused by different sugars. The effect of sugars capable of trivalent binding to boronic acid was tested and then the B-N bond strength was taken into account. In detail, when the pH is below the first

pKa of boronic acid, the amino group can exist in the protonated form **194a**. The research shows that the first pKa is the deprotonation of amine which is due the B-N bond formation. A significant decrease of fluorescence is observed when compound **194b** is formed, in spite of formation of the B-N bond. These results suggest that the creation of B-N bond itself is not enough to completely “tie up” the lone pair electrons to stop the PET process. Increasing pH will give **194c** which no longer has a B-N bond (the hydroxide displaces the amino group).

During the addition of the diol, there are two possibilities, neither of which has been experimentally confirmed or disqualified. In the first case (the “B-N bond mechanism”) which was proposed by Shinkai and co-workers¹⁴, the pKa₁ of the ester **195a** corresponds to the deprotonation of the amino group and the formation of the B-N bond in **195b**. The pKa₂ leads to **195c** due to the replacement of the B-N bond by B-O bond. In the second case (referred to as a “hydrolysis mechanism”), which is shown in the bottom of Scheme 50, the pKa₁ corresponds to the formation of **195d** due to addition of the hydroxide to the boron and pKa₂ now corresponds to the loss of the proton from the ammonium ion to form **195c**. The main difference between these two cases is that under neutral conditions, addition of diol will give **195b** in B-N bond mechanism or **195d** in the hydrolysis mechanism.

The pH profile of the free boronic acid **195a** shows a significant fluorescence intensity decrease. These reductions are not influenced by hydroxide ion association with / dissociation from boron, but instead by deprotonation/protonation at the nitrogen. The reason that this is consistent with the hydrolysis mechanism is that the B-N bond formation can give the ester at the same pH profile as the free acid itself and if the boronate ester **195b** adopts a tetrahedral structure this will support small binding angles (the investigations by using different sugars also give to those results). The pKa values of the boronic esters of different sugars have different values which could lead to the conclusion that the B-N bond strength would also be different for **195b**. Additionally, this is supposed to sequentially influence the quenching efficiency by the lone pair electrons and consequently the maximal fluorescent intensity for a particular ester.²⁸

In reality, all saccharides offer the same maximal fluorescence intensity, which is not correct for the B-N bond mechanism. However, it fits with the hydrolysis mechanism because the fluorescent species **195d** has the same structural properties independent of the choice of the sugar. However, if hydrolysis mechanism is correct it will not be expected to observe a difference in the magnitude of the maximal fluorescence recovery. Furthermore, considering that the B-N bond formation is responsible for the loss of fluorescence intensity for sugars which are bonded in the trivalent way to a boronic acid, this should not be able to prompt the changes in the fluorescence intensity. In the cases of sorbitol and fructose (binding in a trivalent fashion), the same changes in the intensity of fluorescence were observed. This example is now correct for the B-N bond mechanism, and not consistent with the hydrolysis mechanism. Finally, the strength of B-N bond was calculated (3 kcal mol^{-1}) which is too small to “tie up” the lone pair of electrons to avoid the PET effect.²⁸

The outcome of the investigations shows that the changes in the fluorescent intensity which are occurring when a sugar binds to the boronic acid derivatives are due to a hydrolysis mechanism which gives derivative **195d**. However, the form of the sensor without sugar can be present as **194b** but after addition of sugar (because of the lowered value of pKa of the boron), the first equilibrium is described by the reaction of the boron with a water molecule to give **195d**. The protonated form is also stabilised by the presence of the anionic form of boron which is next to the amine. The effect of masking of the lone pair electrons, which eliminates the PET quenching of the anthracene fluorescence and results in a rise of the fluorescence intensity, is due to transformation of the weak B-N bond form in **194b** into the amine-protonated form **195d**. The compound **195d** represents the on-state of the system and **194b** corresponds to the off-state.²⁸ In conclusion, the hydrolysis mechanism is right for the pH profile studies of the boronic acid and its sugar and, as well, the estimation of B-N bond strength confirms this.

An interesting example of a design of a fluorescent bioprobe has been reported by Wang *et al.*²⁹ This group have developed biosensor **196**, suitable for binding D-glucarate based on the cooperative action of boronic acid and guanidium groups. D-glucarate **197** is an important biologically active carbohydrate, and is present in human

serum, vegetables and fruits, and additionally it can act as a chemopreventive agent in certain cancers. The bioprobe's use of the guanidium ion allowed the recognition of the carboxylate groups of glucarate. The outcome shows that glucarate can bind more strongly than glucuronic acid **198**. This process demonstrates that both carboxylates of glucarate are involved in the binding, through an anionic interaction with the guanidium group. The intensity of the fluorescence for the bioprobe solution is raised by 4-5 fold following the addition of glucarate (Figure 31).²⁹

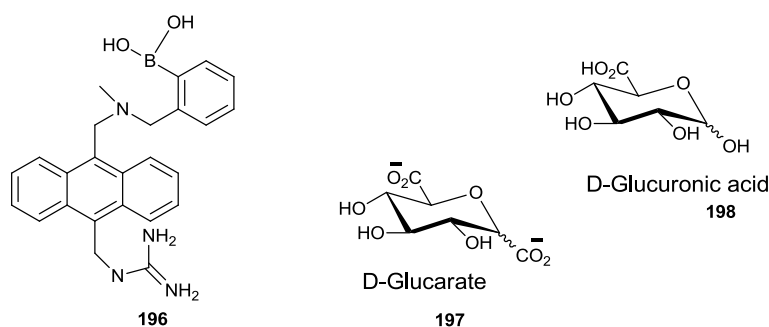
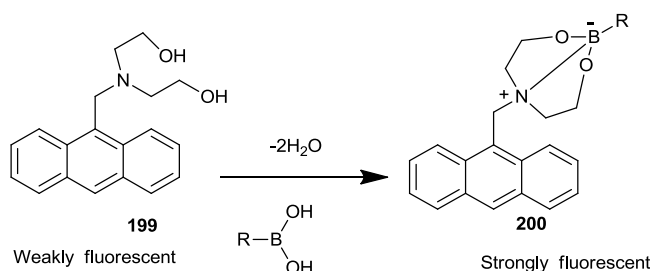


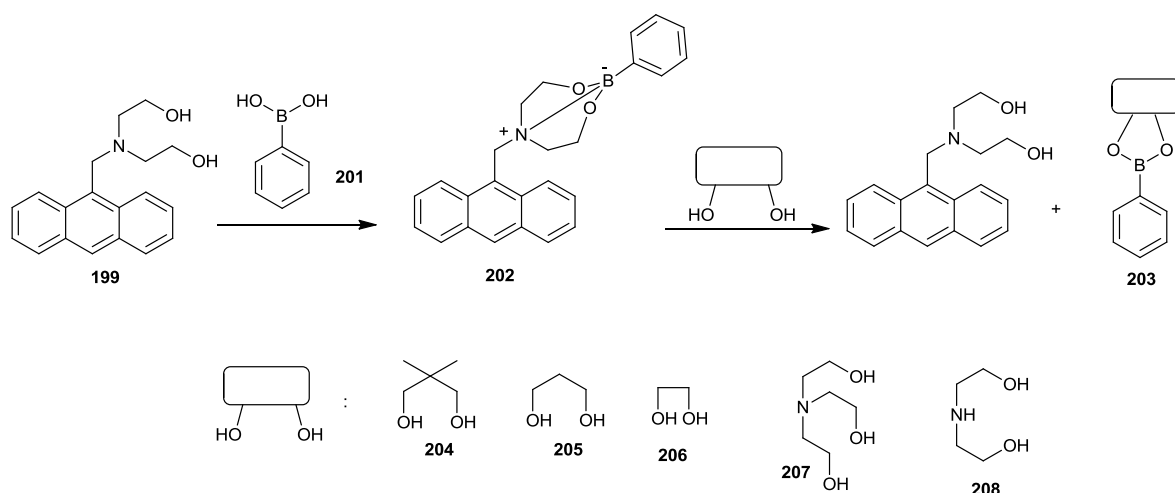
Figure 31 Biosensor suitable for binding with D-glucarate and D-glucuronic acid.

Another noteworthy example of an anthracene-based PET bioprobe **200** (Scheme 51) was developed by Spingsteen *et al.*³⁰ Their sensor for boronates used the diethanolamine recognition site **199** which acts on the same basis but the opposite way round to sugar sensors. It was proved that the high binding affinity of boronic and boric acids dyes with diethanolamine in the boronate formation process is due the manner of incorporation of diethanolamine. The lone pair on nitrogen is donated to the boron atom to form the five membered rings (boronate is stabilized). In the absence of boronic acid and boric acid, weak fluorescence was detected, but in its presence, the fluorescence intensity was increased by 16 fold at saturated concentrations.³⁰



Scheme 51 An example of an anthracene-based PET bioprobe **200**.

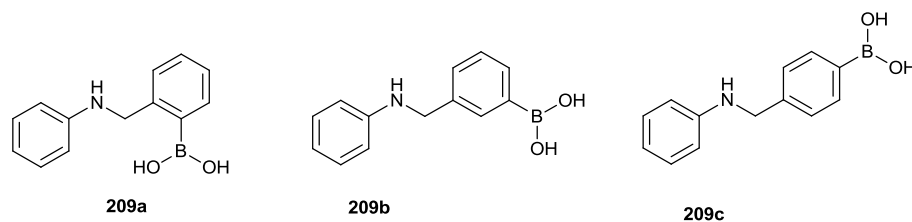
Another example worth notice is research on the same system by James *et al.*³¹ This group have found that the sensor **199** does not bind with phenylboronic acid **201** in methanol but instead chloroform was used to form a stable complex between **199** and phenylboronic acid **201**. The increase in fluorescence intensity was observed in fluorescence titrations of **199** (Scheme 52) employing rising concentrations of phenylboronic acid. The resulting cyclic boronate ester (complex **202**) has a strong B-N bond and this causes the changes in the fluorescence intensity. The fluorescence titration of complex **202** with various diols resulted in the reduction of the fluorescence intensity. The selectivity order is: **204** > **208** > **207** > **206** > **205**. Scheme 42 presents the changes in intensity which are due to reaction of **199** and phenylboronic acid **201** in chloroform to form a fluorescent complex **202**. This complex is unstable upon the addition of diols to produce complex **203** and reform **199** (which has low fluorescence because of PET). This type of methodology helps to evaluate the relative stability of adducts of general form **203**.³¹



Scheme 52 Reaction of **199** and phenylboronic acid affording fluorescent complex **203**.

A good example of a ratiometric sensor (where fluorescence changes are observed in two different wavelengths) was published in 2001 by James and co-workers. His group synthesised the monoboronic acid **209a** as a fluorescent reporter.³² They confirmed the expectations based on the fundamental binding affinity of monoboronic acids; D-

fructose showed the expected higher binding affinities with **209a** than did D-galactose and D-glucose (Scheme 53).



Scheme 53 Structures of boronic acid based dyes **209a-c**.

The same group subsequently discussed new outcomes for **209a** when compared to compounds **209b** and **209c**, which were used as controls.³³

1.4.4. Internal Charge Transfer (ICT) in bioprobes

Another process which can cause changes in spectral properties during the interaction between boronic acid and saccharides is called Internal Charge Transfer (ICT). This process is very sensitive to small changes which can affect the spectral shifts and changes in the intensity. The ICT structure has two parts in the same chromophore, an electron donor group and an electron acceptor group. These types of bioprobes have the sp^2 -hybridized boron atom of the boronic acid which acts as an electron acceptor because of the empty p-orbital on boron. This can be connected directly to the chromophore to form a conjugated system with the aromatic moiety, and the inclusion in the same molecule of a donor group can cause excited-state charge transfer. It is noteworthy that the change from sp^2 to sp^3 hybridization will lead to a boron atom which no longer has an empty p orbital and this will stop the ICT route. The lowering in the pKa value (2-3 units) can be observed following the conversion of a phenylboronic acid analogue into its ester with saccharides. The changes of the boron atom from the neutral sp^2 form to the anionic sp^3 occur when boronic ester is formed and this can happen at physiological pH, so by the addition of a sugar to the boronic ester it can be possible to cause changes in the ICT effects.^{6,34}

An example chosen to illustrate this is the simple bioprobe using a donor-acceptor dye based on the diphenyloxazole **210** which was reported by DiCesare and his co-workers. They presented the comparison of the dye **210** with sensor **211**, showing that the high

fluorescence intensity and spectral changes are due to the formation of the anionic form of the boronic acid as the pH increases (Figure 32).³⁵

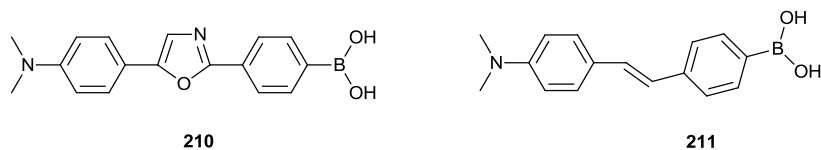


Figure 32 Structures of donor-acceptor bioprobes.

This group has also described the chalcone-analogue fluorescent probes **212** and **213** which are shown in Figure 33.³⁶

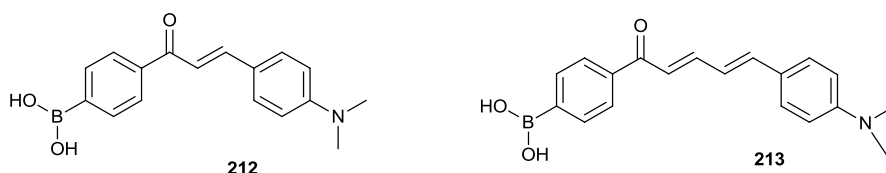


Figure 33 Chalcone based fluorescent probes.

In bioprobes **210** and **211** the boronic acid group was directly involved in the ICT, and the blue shift observed in those two probes was huge in comparison with the systems **212** and **213**. Additionally, dyes **212** and **213** showed a high affinity to D-fructose.

1.4.5. Bioprobes for glucose binding

Monitoring glucose concentrations is widely understood to be a major challenge in the management of diabetes. Enzyme-based determination methods requiring multiple and often frequent collection of blood samples are the most common way in which blood sugar concentration is determined, with glucose oxidase and hexokinase being the most common enzymes utilised in the method. When testing blood sugar levels, it is common for blood sample to be applied to a test-strip paper where the chemical monitoring system is contained. The test strip is then inserted into the meter where a reading is given. Some problems from this type of procedure occur due to the fact that the monitoring is not continuous, and the shelf-life of the test kits is limited by the lack of stability of the enzymes themselves. Chemical bioprobes can offer the answer to

these problems, by the advantage of higher stability and relatively easy manufacturing. To establish a viable design for a chemical bioprobe-based continuous monitoring device, one needs to develop glucose sensors that show high selectivity and appropriate affinity. It is not only the monitoring of glucose concentrations during treatment of diabetes that needs to be taken into account. Other analytical methods that rely on the selective recognition of D-glucose could possibly have significant applications. In humans the breakdown of glucose transport has also been correlated with diseases such as renal glycosuria³⁷, cystic fibrosis³⁸, and even human cancer³⁹. Fluorescence is one of the techniques used to monitor the blood glucose levels. Typically, mono-boronic acid derivatives have been used to develop glucose bioprobes, but with limited success. Fortunately, Shinkai discovered that di-boronic acids derivatives, in particular the 9,10-bis-(aminomethyl)anthracene skeleton **214**, are suitable as glucose binding agents with a high enough affinity to make an effective sensor. The bioprobe is another example of the use of photoinduced electron transfer (PET) (Figure 34).⁴⁰

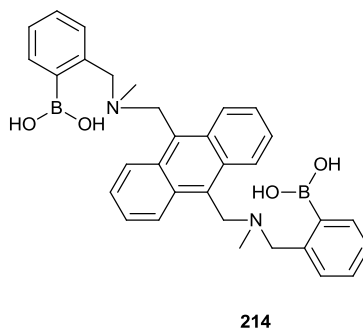


Figure 34 Bioprobe for glucose based on photoinduced electron transfer.

The results show that sensor **214** is selective for glucose because it forms a 1:1 complex between the two boronic acids and the 1,2 and 4,6-hydroxyls of glucose. Additionally, glucose binds to the boronic acids in a pyranose form and the sensor displays a clear order of selectivity for monosaccharides: D-glucose > D-allose > D-fructose ~ D-galactose.⁴⁰

Furthermore, this selectivity applies to all diboronic saccharides, but bioprobes of type **215** were the first of a series of compounds used for the ditopic recognition of monosaccharides based on a PET sensor system, Figure 35.⁴¹

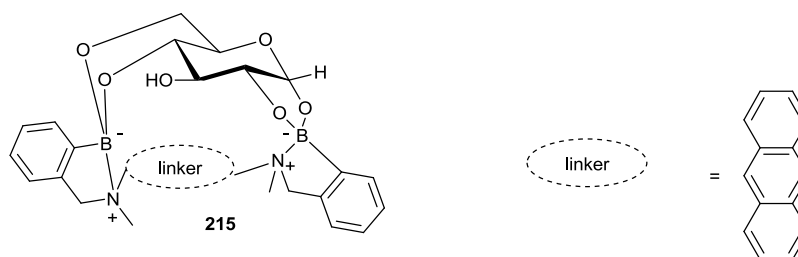


Figure 35 An example of bioprobe **215** based on a PET system.

When compared to the Shinkai **194** system, however, the two boronic acids of **216**, Figure 36 are not as well arranged to cooperatively capture D-glucose.⁴¹

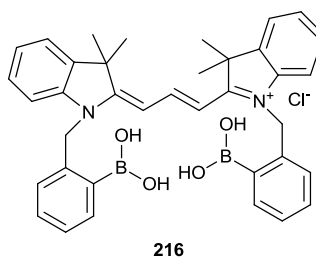
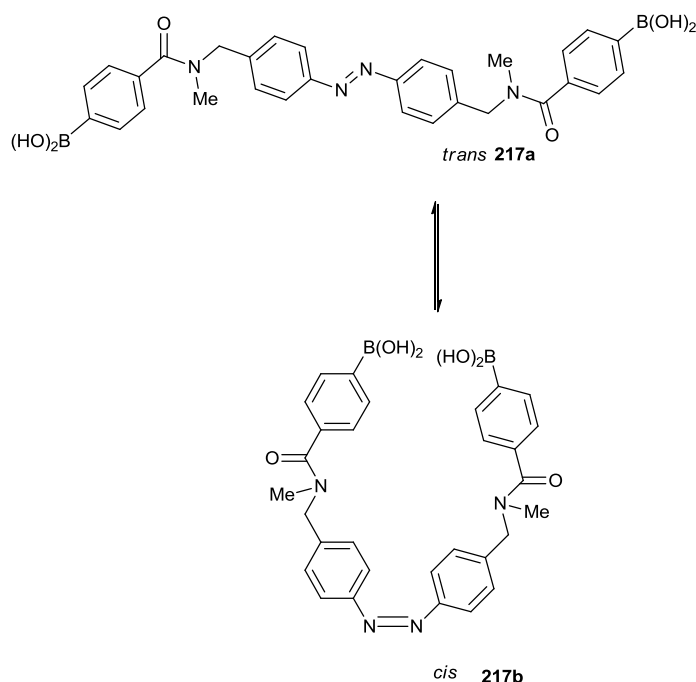


Figure 36 The structure of the bioprobe **216** which shows poor arrangement of boronic acids to bind D-glucose.

An interesting example of a more flexible structure was described by Shinkai's group⁴² which reported a photoactive azo-dye based diboronic acid **217a**, with switchable selectivity for D-glucose. The outcomes of their research indicate that by irradiation of diacid cis-**217b** with visible light it is possible for binding to occur for glucose and allose with very high selectivity (Scheme 54).⁴²



Scheme 54 Representation of photoactive azo-dye based diboronic acid.

The bioprobe **218** combines low pKa values and water solubility and also showed selectivity for glucose. Norrid's group established that glucose binds to the compound as the α -D-glucofuranose 1,2:3,5-bisboronate complex at physiological pH.⁴³

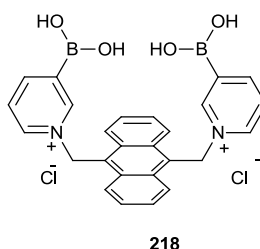


Figure 37 Structure of bioprobe **218**.

Wang's group⁴⁴ also investigated glucose sensitive diboronic acid fluorescent sensors. Three different diboronic acids were synthesised. As the outcome of their research, the bioprobe **219** was found to bind with better affinity (300 fold increases) and selectivity (1400-fold) for glucose over fructose in comparison with phenylboronic acid. Additionally, based on the structure of **219**, the phenyl ring with two acetamides connected to it in an ortho relationship gives the best (proper) orientation for

diboronic acid for binding with glucose, with the distance between the boron atoms matching perfectly the required separation. Unfortunately, the compounds **220**, **221** did exhibit sufficient selectivity and affinity for glucose at the required levels. It has been reported by Anslyn⁴⁵ that boronic acid **201** can be used in competitive assays with a separate reporter component. It is necessary that the receptor and reporter associate under sample conditions. After an initial measurement, selective dissociation of the complex between receptor and reporter can be quantified by addition of suitable analytes. As the result, the measurement of this response is observed when the reporter dissociates from the receptor.⁴⁵ The most commercially useful reagents for a competitive assay are Alizarin Red S **222** (ARS) and phenylboronic acid **201**, see Figure 38.

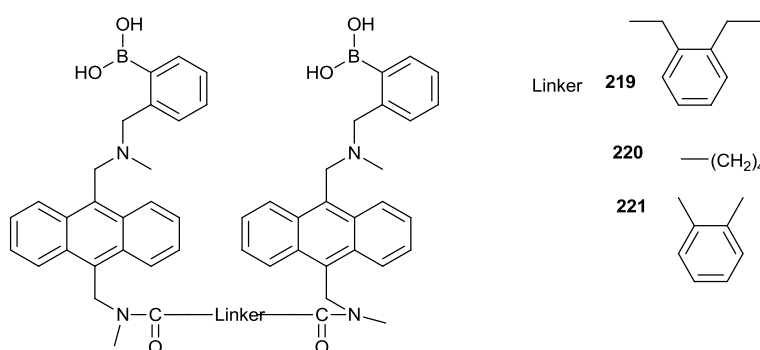
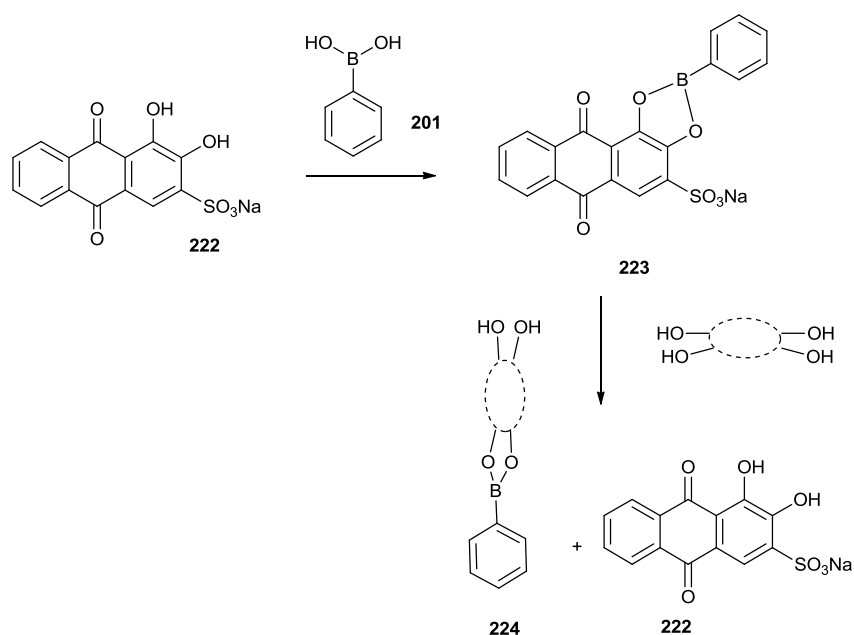


Figure 38 Bioprobes with high affinity for glucose.

Another good example of a D-glucose fluorescent bioprobe that uses ARS **222** was reported by James *et al.*³¹ The results show that upon addition of the boronic acid **201**, a new absorbance at 464 nm appears. However, another new absorbance at 530 nm is monitored when the experiments is investigated during addition of D-glucose and D-fructose to the solution containing ARS **222** and the sensor. There are some significant changes observed in absorbance and fluorescence which are due to release of free ARS as the saccharides compete for the boronic acid in solution (Scheme 55).³¹



Scheme 55 Representation of the competitive assay with Alizarin Red S **222** and phenyl boronic acid **201**.

The discussion turns now to an enantioselective and chemoselective fluorescent sensor **225** (Figure 39) for sugar acids and alcohols. The fluorescent bioprobe is well suited for use as an *in vivo* probe, for example mapping the spatial and temporal distribution of the biological analytes.^{46,47,48}

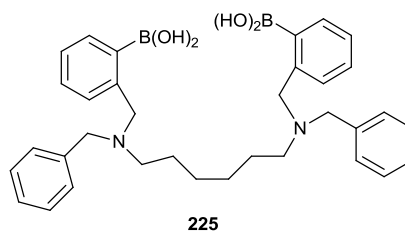


Figure 39 Structure of enantioselective and chemoselective bioprobe **225**.

These fluorescent boronic acid-based probes which have been reported to be perfect sensors for tartaric acid, D-glucuronic acid and D-glucaric acid (shown with D-sorbitol in Figure 40).^{46,47,48}

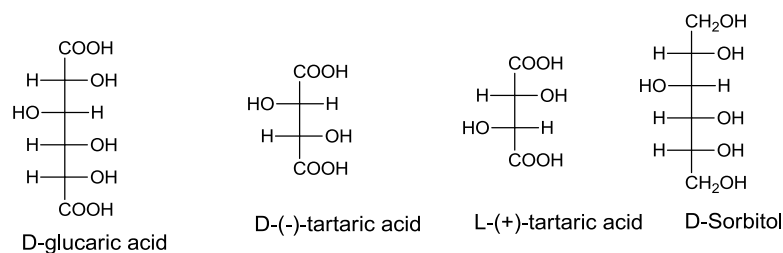


Figure 40 Structures of D-glucaric acid, D-(-)-tartaric acid, L-(+)-tartaric acid, D-sorbitol.

The chiral bioprobe **226** was designed by James *et al.*⁴⁹ in order to analyze chiral molecules such as sugars, sugar acids and sugar alcohols. In this work, anthracene is used as a suitable fluorophore for read out as a rigid linker and the chiral centres are built-up in close proximity to the binding site of the receptor. This group also synthesised the chiral monoboronic acid receptor **227** which is shown in Figure 41.⁴⁹

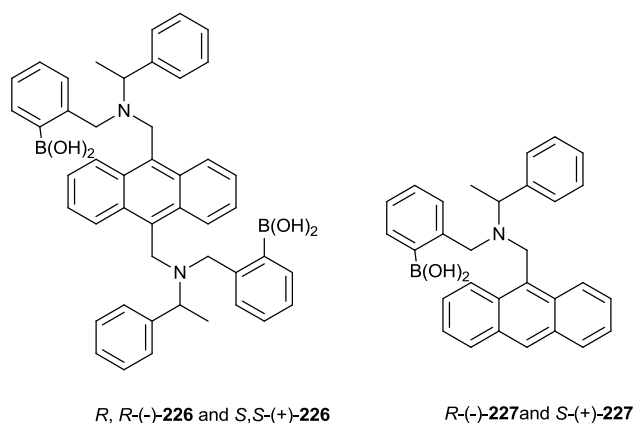


Figure 41 Structures of chiral bioprobes.

1.4.6. Boron-cell surface interactions

The development of synthetic carbohydrate receptors is a very important tool as they may serve as diagnostics to monitor changes on cell surfaces associated with disease progression in, for example, cancer, or they could be useful as drug-targeting agents to deliver chemotherapeutic agents to specific cell types. A few examples of boron-cell surface interactions will be described.

An excellent example is provided by work performed by Hageman's group which demonstrated the targeting of cell-surface structures with fluorescent dansyl

boronates to associate with *Bacillus subtilis*.⁵⁰ Additionally, they showed that the diboronate dyes can detect the agglutination of erythrocytes. Later on, Gallop advanced a technique using boronates to transfer lipophilic dyes and probes into cells. This method is called “boradaption”.⁵¹ There is commercial interest in preparation of artificial transporters for the extraction of sugars (glucose, fructose or lactose).⁵² In 2006, a significant development appeared for the use of lipophilic boronic acids as membrane transport agents for hydrophilic molecules (sialic acid and their derivatives).⁵³ The Kataoka’s group⁵⁴ reported polymeric boronates, which were used to target cell surface sialic acids to produce biological and analytical responses. The outcome of their research showed that these boronates can cause the induction of lymphocytes in the way that the natural lectins behave.⁵⁴ The technique for the precise determination of cell surface sialic acid levels has been reported by Miyahara and co-workers. They established that the use of a self-assembled monolayer on a gold electrode helps to apply the coating of boronates.^{55,56} The research in this area and development and applications of boron-carbohydrate interactions continues to expand into 21st century. Much knowledge has been obtained, specifically from the development of boronate based glucose receptors for application in sugar monitoring in diabetics. Nowadays, an increasing number of research groups are dedicated to the development of boron based receptors for complex oligosaccharides. These types of receptors are very significant in applications as diagnostics for cancer and drug targeting. Unfortunately, application of these interactions to target oligosaccharides still has limitations as not many boron-based oligosaccharide receptors have so far been developed. The answer to this challenge is to combine boron-carbohydrate interactions with several additional non-covalent interactions, H-bonding, hydrophobic, and, as in our work, to increase the information read-out from the spectroscopic study of the potentially many interconverting adducts that can form between the sensor and its target, in cell surface applications.⁹

1.4.7. References:

-
- ¹ R. I. Scorei, R. Popa, *Anti-Cancer Agents in Medicinal Chemistry*, **2010**, 10, 346-351.
- ² M. A. O'Neill, S. Eberhard, P. Albersheim, A. G. Darvill, *Science*, **2001**, 294, 846-849.
- ³ X. Chen, S. Schauder, N. Potier, A. V. Dorsselaer, I. Pelczer, B. L. Bassler, F. M. Hughson, *Nature*, **2002**, 415, 545-549.
- ⁴ X. L. Mao, J. Wu, Y. B. Ying, *Chinese Journal of Analytical Chemistry*, **2008**, 36, 1749-1755.
- ⁵ A. J. Bard, L. R. Faulkner, *Electrochemical methods: fundamentals and applications*, 2nd ed.; Wiley: New York, **2001**.
- ⁶ a) T. D. James, K. R. A. Sandanayake, S. Shinkai, *Supramol. Chem.*, **1995**, 6, 141-157;
b) T. D. James, K. R. A. Sandanayake, S. Shinkai, *Angew. Chem. Int. Ed. Engl.*, **1996**, 35, 1910-1922.
- ⁷ J. Böeseken, *Ber. Dtsch. Chem.*, **1913**, 46, 2612-2628.
- ⁸ J. P. Lorand, J. O. Edwards, *J. Org. Chem.*, **1959**, 24, 769-774.
- ⁹ D. G. Hall, *Boronic Acids: Preparation and Applications in Organic Synthesis, Medicine and Materials (Second Edition)*, Wiley-VCH Verlag GmbH & Co. KGaA, **2001**.
- ¹⁰ N. DiCesare, J. R. Lakowicz, *Tetrahedron Lett.*, **2001**, 42, 9105-9108.
- ¹¹ G. Spingsteen, B. Wang, *Tetrahedron*, **2002**, 58, 5291-5300.
- ¹² K. Tsukagoshi, S. Shinkai, *J. Org. Chem.*, **1991**, 56, 4089-4091.
- ¹³ T. D. James, T. Harada, S. Shinkai, *J. Chem. Soc., Chem. Comm.*, **1993**, 10, 857-860.
- ¹⁴ T. D. James, K. R. A. S. Sandanayake, S. Shinkai, *J. Chem. Soc., Chem. Commun.*, **1994**, 1621.
- ¹⁵ M. Bielecki, H. Eggert, J. C. Norrid, *J. Chem. Soc., Perkin Trans 2*, **1999**, 449-455.
- ¹⁶ H. Eggert, J. C. Norrid, *J. Am. Chem. Soc.*, **1995**, 117, 1479.
- ¹⁷ S. C. Draffin, P. J. Duggan, G. D. Fallon, *Acta Cryst.*, **2004**, 60, 1520-1522.
- ¹⁸ J. C. Norrid, *J. Chem. Soc., Perkin Trans. 2*, **2001**, 719-726.
- ¹⁹ M. Vanduin, J. A. Peters, A. P. G. Kieboom, H. Vanbekkum, *Tetrahedron*, **1984**, 40, 2901-2911.
- ²⁰ R. P. Singhal, B. Ramamurthy, N. Govindraj, Y. Sarwar, *J. Chromatogr.*, **1991**, 543, 17-38.

-
- ²¹ T. D. James, K. R. A. S. Sandanayake, S. Shinkai, *J. Chem. Soc., Chem. Commun.*, **1994**, 17, 477-478.
- ²² H. R. Mulla, N. J. Agard, A. Basu, *Bioorg. Med. Chem. Lett.*, **2004**, 14, 25-27.
- ²³ W. Wang, S. Gao, B. Wang, *Org. Lett.*, **1999**, 1, 1209-1212.
- ²⁴ W. Wang, S. Gao, B. Wang, *Bioorg. Chem.*, **2001**, 29, 308-320.
- ²⁵ J. Yoon, A. W. Czarnik, *J. Am. Chem. Soc.*, **1992**, 114, 5874-5875.
- ²⁶ H. Suenaga, M. Mikami, K. R. A. S. Sandanayake, S. Shinkai, *Tetrahedron Lett.*, **1995**, 36, 4825-4828.
- ²⁷ G. Wulff, *Pure Appl. Chem.*, **1982**, 54, 2093-2102.
- ²⁸ W. Ni, G. Springsteen, B. Wang, *Bioorg. Chem.*, **2004**, 32, 571-581.
- ²⁹ W. Yang, J. Yan, H. Fang, B. Wang, *Chem. Commun.*, **2003**, 792-793.
- ³⁰ G. Springsteen, W. Wang, B. Wang, *Chem. Commun.*, **2000**, 1283-1284.
- ³¹ S. Arimori, T. D. James, *Tetrahedron Lett.*, **2002**, 43, 507-509.
- ³² S. Arimori, L. I. Bosch, C. J. Ward, T. D. James, *Tetrahedron Lett.*, **2001**, 42, 4553-4555.
- ³³ L. I. Bosch, T. M. Fyles, T. D. James, *Tetrahedron*, **2004**, 60, 11175-11190.
- ³⁴ N. DiCesare, J. R. Lakowicz, *J. Photochem. Photobiol. A*, **2001**, 143, 39.
- ³⁵ N. DiCesare, J. R. Lakowicz, *Chem. Commun.*, **2001**, 2022-2023.
- ³⁶ N. DiCesare, J. R. Lakowicz, *Tetrahedron Lett.*, **2002**, 43, 2615-2618.
- ³⁷ L. J. Elsa, L. E. Rosenberg, *J. Clin. Invest.*, **1969**, 48, 1845.
- ³⁸ P. Baxter, J. Goldhill, P.T. Hardcastle, J. Taylor, *Gut*, **1990**, 31, 817.
- ³⁹ T. Yamamoto, Y. Sino, H. Fukumoto, H. Yano, *Biochem. Biophys. Res. Commun.*, **1990**, 170, 223.
- ⁴⁰ T. D. James, K. R. A. S. Sandanayake, R. Iguchi, S. Shinkai, *J. Am. Chem. Soc.*, **1995**, 117, 8982-8987.
- ⁴¹ M. Takeuchi, T. Mizuno, S. Shinkai, *Tetrahedron*, **1996**, 52, 1195-1204.
- ⁴² H. Shinmori, M. Takeuchi, S. Shinkai, *J. Chem. Soc., Perkin Trans. 2*, **1998**, 847.
- ⁴³ H. Eggert, C. Morin, J. C. Norrid, *J. Org. Chem.*, **1999**, 64, 3846-3852.
- ⁴⁴ V. V. Karnati, X. Gao, S. Gao, W. Yang, W. Ni, S. Shankar, B. Wang, *Bioorg. Med. Chem. Lett.*, **2002**, 12, 3373-3377.

-
- ⁴⁵ a) A. Metzger, E. V. Anslyn, *Angew. Chem. Int. Ed. Engl.*, **1998**, 37, 649; b) J. Lavigne, E. V. Anslyn, *Angew. Chem. Int. Ed. Engl.*, **1999**, 38, 3666. c) L. A. Cabell, M. K. Monahan, E. V. Anslyn, *Tetrahedron Lett.*, **1999**, 40, 7753.
- ⁴⁶ A. P. de Silva, H. Q. N. Gunaratne, T. Gunnlaugsson, A. J. M. Huxley, C. P. McCoy, J. T. Rademacher, T. E. Rice, *Chem. Rev.*, **1997**, 97, 1515.
- ⁴⁷ L. Pu, *Chem. Rev.*, **2004**, 104, 1687.
- ⁴⁸ M. Takeuchi, M. Yamamoto, S. Shinkai, *Tetrahedron*, **1998**, 54, 3125.
- ⁴⁹ J. Zhao, M. G. Davidson, M. F. Mahon, T. D. James, *J. Am. Chem. Soc.*, **2004**, 126, 16179-16186.
- ⁵⁰ T. J. Burnett, H. C. Peebles, J. H. Hageman, *Biochem. Biophys. Res. Commun.*, **1980**, 96, 157-162.
- ⁵¹ P. M. Gallop, M. A. Paz, E. Henson, *Science*, **1982**, 217, 166-169.
- ⁵² P. J. Duggan, T. A. Houston, M. J. Kiefel, S. M. Levonis, B. D. Smith, M. L. Szydzik, *Tetrahedron*, **2008**, 64, 7122-7126.
- ⁵³ T. M. Altamore, P. J. Duggan, G. Y. Krippner, *Bioorg. Med. Chem.*, **2006**, 14, 1126-1133.
- ⁵⁴ E. Uchimura, H. Otsuka, T. Okano, Y. Sakurai, K. Kataoka, *Biotechnol. Bioeng.*, **2001**, 72, 307-314.
- ⁵⁵ A. Matsumoto, N. Sato, K. Kataoka, Y. Miyahara, *J. Am. Chem. Soc.*, **2009**, 132, 12022-12023.
- ⁵⁶ A. Matsumoto, H. Cabral, N. Sato, K. Kataoka, Y. Miyahara, *Angew. Chem. Int. Ed.*, **2010**, 49, 5494-5497.

CHAPTER 2:

Results and Discussion Project 1

2.1. Aim of the project 1

In both of the projects comprising this work, the aim was to prepare bioprobes with not just fluorescent features but also with an IR-responding group and so, by comparing the outputs from both reporting methods, it was hoped to demonstrate the high information-content responses of IR-based systems.

Several research groups have described work on anthracene-based fluorescence reporters (See Chapter 1.4.3.1). Photoinduced electron transfer (PET) is a valuable tool in the design of the fluorescent bioprobes. As previously discussed, PET dyes are generally construct from a fluorophore and a receptor connected by a short spacer. When a guest binds to the receptor, changes occur in the oxidation/reduction potential of the receptor which can disturb the PET process and lead to changes in fluorescence.

The design of bioprobe (Figure 42) with successful anthracene based fluorophore was inspired by work of James and Shinkai et al.¹ The boronic acid dye **194** (Figure 30) showed a great binding affinity to D-fructose in 33.3% methanol-water at pH 7.77 (phosphate buffer). Based on this research, the design of bioprobe **228**, Figure 42 to prove the accuracy of the proposed IR-read out method by comparison with the well-established PET approach was investigated. In target molecule **228**, Figure 42 the amine group is important because of two roles in the system: 1) boronic acids in the presence of a neighbouring amine show increased binding of saccharides to boronic acids at neutral pH; 2) the lone pair on the amine controls the intensity of fluorescence.

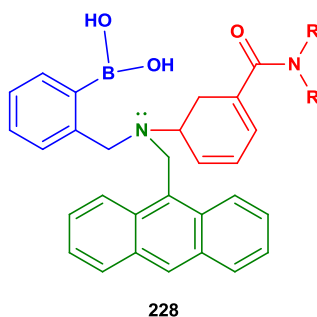


Figure 42 Structure of the target molecule **228**.

The advantages of the target compound are; it contains an anthracene portion as a fluorescence reporter group, and an organometallic tricarbonyliron portion as an IR reporter group. These features allow us to use two analytical techniques, fluorescence spectroscopy and IR spectroscopy, to detect the saccharide binding. The IR method will allow observation of the hydrogen bonding interactions, because although the sugar uses two of its OH groups to bind to the boronic acid, there will remain other OH groups on the sugar which can form hydrogen bonds with an amide group which was intended to be placed on the 1,3-cyclohexadiene ligand of the iron complex (**228b**, Figure 43). The expectation is that different sugars will show different hydrogen bonding interactions, because they have different patterns of OH groups as their substituents, and so could be distinguishable by examination of details of the IR response for both the positions of the bands and their vibrational couplings. The binding event will show a response in both the fluorescence and IR reporter groups, and so establish that the changes in the IR spectrum are indeed a consequence of the binding of the sugar by the receptor. By the plotting of a correspondence graph between these two outputs, a firm footing of the ability of the IR technique to read out the details of the sugar binding is to be achieved. In future work it could be possible to optimise the reporting protocol to improve the selectivity of response.

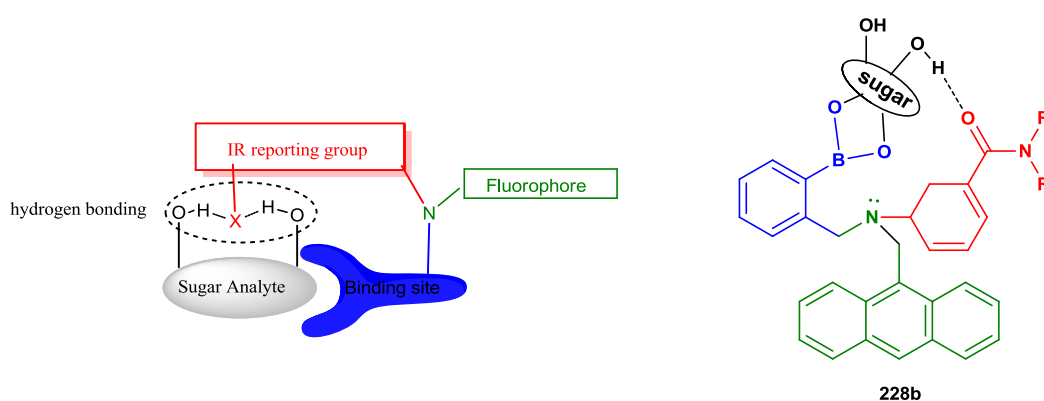
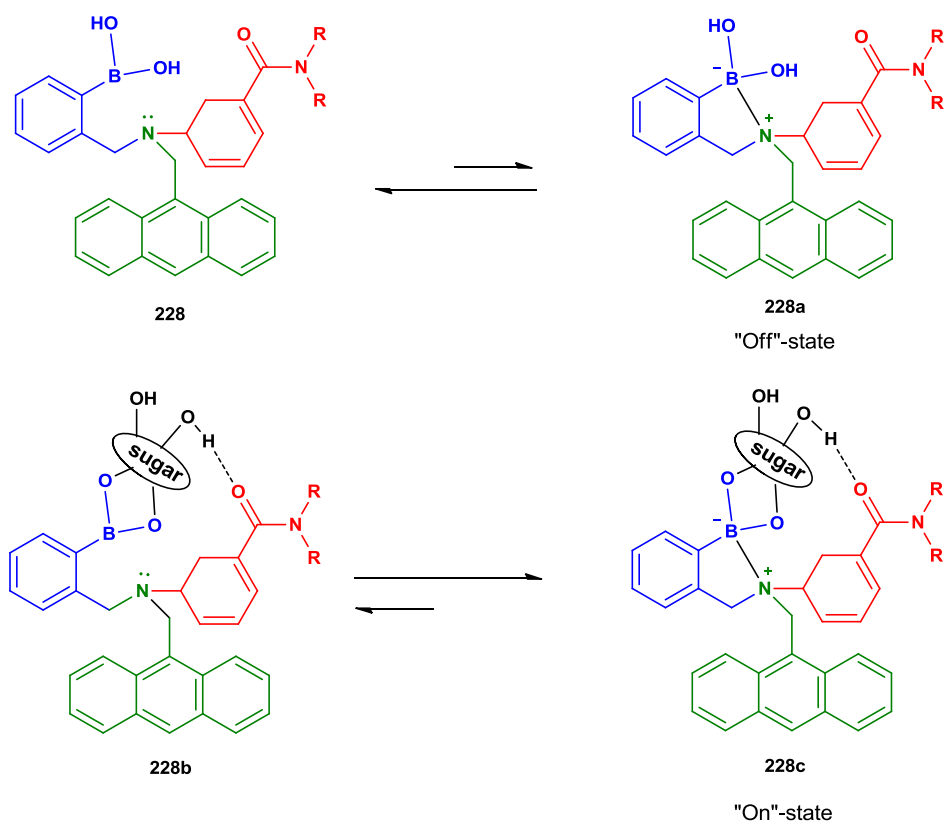


Figure 43 Representation of the hydrogen bonding interaction in the design molecule.

2.1.1. The Photoinduced Electron Transfer (PET) effect on the target bioprobe

The target molecule **228** will possess a tertiary amine attached to the boronic acid receptor site. As mentioned above, the fluorescence intensity is controlled by an

amine, so the lone pair of nitrogen can interact with the anthracene molecule and block access to the fluorescence route. Scheme 56 shows simply this effect of nitrogen lone pair donation to the anthracene molecule upon absorption of a photon, which is the basis of bioprobe design.



Scheme 56 Representation of equilibrium for off and on state in target bioprobe.

Fluorescence is best described by a Jablonski diagram as shown in Chapter 1.3 in Figure 12. To restate this briefly, the fluorescence emission is the consequence of the return of an excited electron to its ground state, and PET stops this process by transferring electrons into the ground state of the molecule (for example, the anthracene moiety in the sensor). This results in the complete occupation of the ground state orbital, and thus blocks the return of the excited electron to its ground state. In general, when photoinduced electron transfer of the nitrogen lone pair to an anthracene molecule occurs, the fluorescence is quenched. Interestingly, in the case of target bioprobes, if the sugar successfully binds to the boronic acid **228b**, the amine should become more

strongly bound to the boron centre which should now be in the form of a cyclic ester **228c** which has a higher affinity and is more easily adapted into the tetrahedral form. As a consequence, the boron-bound amine is unable to quench the fluorescence since the nitrogen lone pair is no longer available and hence a strong fluorescence is observed, “on-state”, Scheme 56. Although, as discussed in detail in Section 1.4, the results from pH profile studies of the free boronic acid and sugar (Scheme 50) showed that the hydrolysis mechanism provides a better explanation for observed changes in PET quenching, compared to the B-N mechanism, until now it has been hard to prove which mechanism is right. In developing the designs for the organoiron analogues of the boronic acid fluorescent reporter dyes the *ortho*-substituted example shown in Figure 43 could operate by either the hydrolysis mechanism or the B-N mechanism (Scheme 50), but for the alternative *meta*-substitution pattern in the arylboronate, only the hydrolysis mechanism should be applicable. The position of B(OH)₂ in the target molecule will be modified due to some difficulties in the synthesis of target molecule **228**. However, while in principle, the *ortho*-substitution should best allow the B-N bond mechanism to operate, the comparison of *ortho*- and *meta*- substitution patterns can be of value as a potential way to distinguish between the two mechanistic alternatives, so it was felt that the *meta* series was also a worthwhile goal.

2.1.2. Hydrogen bonding interaction observed by IR upon binding

As mentioned above, the target molecule is made from three important parts. The IR responding part was designed to be able to form hydrogen bonding interactions. On successful binding of saccharide to boronic acid derivative, this interaction will be observed between hydroxyl groups on the saccharide and the amide group attached to 1,3-cyclohexadiene (Figure 44). As the amide group is in conjugation with the diene system, after binding, the hydrogen bonding interactions should affect the electron density in the π -system. This should be observable by the IR method because this is sensitive to the degree of back-donation of electron density into the CO antibonding orbital (See Chapter 1.1.3, Figure 3).

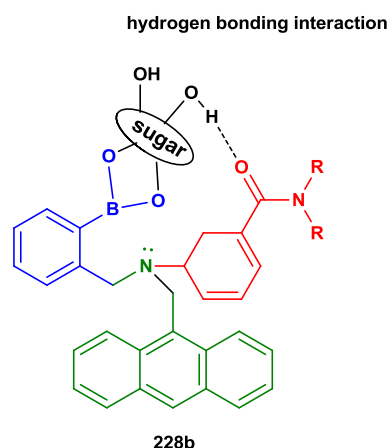
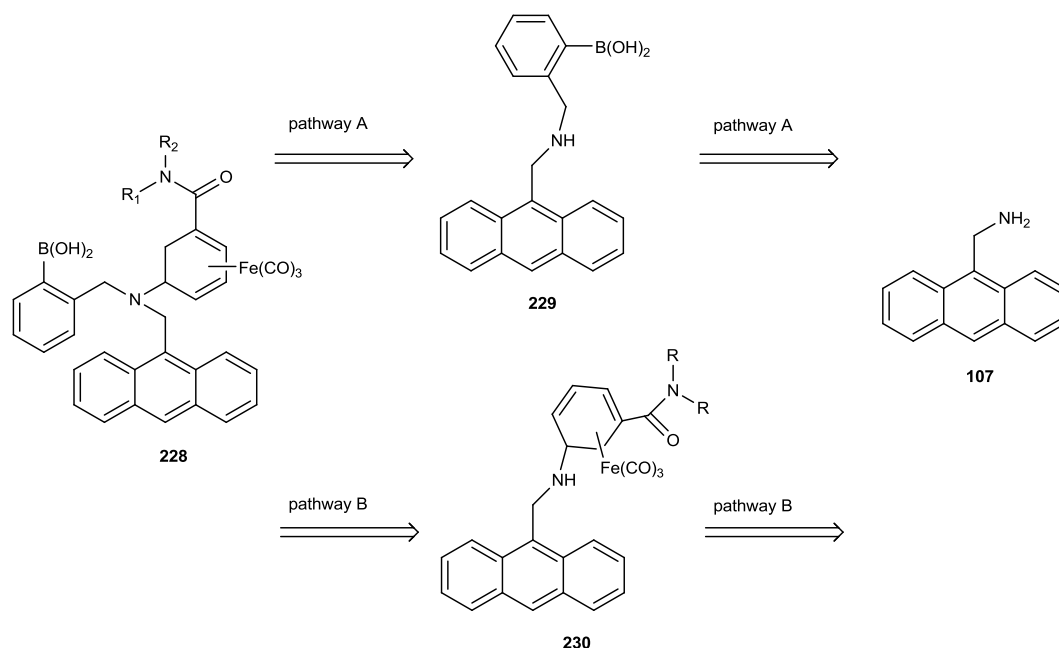


Figure 44 Representation of hydrogen bonding interaction between hydroxyl group on the saccharide and the amide group attached to 1,3-cyclohexadiene.

2.2. Results and discussion

The retrosynthetic route towards the preparation of target molecule **228** is shown in Scheme 57.



Scheme 57 Retrosynthetic route towards the preparation of desired bioprobe **228**.

There are two pathways which will be investigated to build the target structure; both pathways will involve the preparation of 9-aminomethylanthracene **107** and novel tricarbonyliron complexes. Pathway A includes reductive amination of 2-formylphenylboronic acid **256a**, followed by nucleophilic substitution of derivative **229** to give the target bioprobe **228**. In pathway B, the first step will involve the

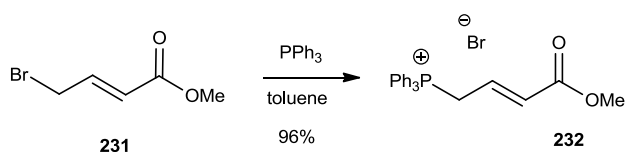
nucleophilic substitution of tricarbonyliron salt with 9-aminomethylanthracene **107**, then the *N*-alkylation of **230** to obtain desired compound **228**. This project requires the development of a synthetic route to novel iron complexes (as IR reporting groups) bearing both a 9-aminomethyl anthracene as a fluorescence reporting group and a boronic acid derivative to bind with sugars.

2.2.1. The choice and synthesis of IR reporting group

The applications of transition metals are a major interest in research in organic chemistry. Nowadays, handling air and moisture sensitive organometallic compounds for use in synthetic procedures is a straightforward process and this has led to major advances in the field of organometallic chemistry. As described in Chapter 1.2, organoiron complexes are well established in synthetic chemistry and possess excellent spectroscopic properties. Those advantages lead us to select the tricarbonyliron group as the organometalcarbonyl system for the intended applications. It was decided to explore the viability of forming iron tricarbonyl complexes of **235** and its derivatives. In course of doing so, commercially available $\text{Fe}_2(\text{CO})_9$ was used, which is more reactive and less toxic than $\text{Fe}(\text{CO})_5$. Additionally it is easier to handle a solid as opposed to a liquid. More details for iron complexation will be discussed in Results and Discussion for project 2 as the comparison of these two reagents and more details of the scope and limitations for iron complexation reactions was investigated in the course of project 2.

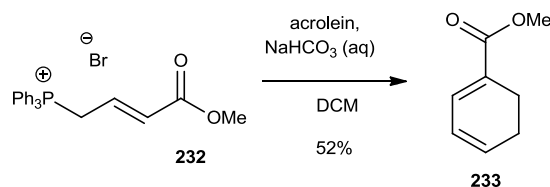
Preparation of the starting materials followed the procedure of Graden and co-workers,² who described in 2004 the synthesis of carboxylic acid iron complex **235**.

Synthesis of the Wittig salt **232** started from the commercially available methyl-4-bromocrotonate **231** by addition of triphenylphosphine in dry toluene. The reaction was stirred at room temperature for 2 days and the desired (3-methoxycarbonylallyl)-triphenylphosphonium bromide **232** was obtained in 96% yield (Scheme 58).³



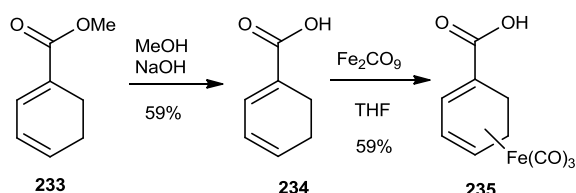
Scheme 58 Synthesis of Wittig salt **232**.

Cyclohexa-1,3-dienecarboxylic acid methyl ester **233** was synthesised by treatment of the phosphonium bromide **232** with acrolein and sodium bicarbonate. The reaction was stirred for 3 days at room temperature before being quenched to obtain the expected compound **233** in good yield (52%) (Scheme 59).³



Scheme 59 Preparation of Cyclohexa-1,3-dienecarboxylic acid methyl ester **233**.

The last two steps route (Scheme 60) started with the hydrolysis of cyclohexa-1,3-dienecarboxylic acid methyl ester **233** with methanolic sodium hydroxide to produce the cyclohexa-1,3-dienecarboxylic acid **234** in 59 % yield, followed by iron complexation of acid derivative **234** by heating for 5 hours at reflux in the presence of diironnonacarbonyl in dry THF. The ¹H NMR and ¹³C NMR spectra of the product **235** were in agreement with data reported in the literature.² The tricarbonyl(cyclohexa-1,3-dienecarboxylic acid)iron **235** was synthesised in good yield (59%) and was used as the starting material for the parallel synthesis of the target amides (Scheme 60).

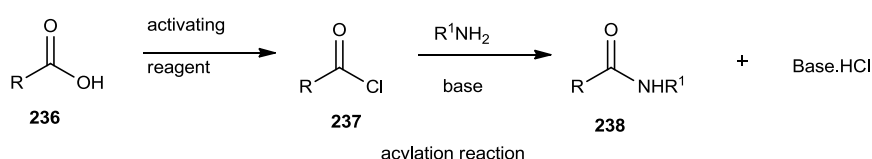


Scheme 60 Synthetic route to produced precursor **235**.

There are two potential ways to create the novel amide-bearing complexes - by an acylation reaction or by peptide coupling. As an acylation reaction was successful, it was decided to continue in this way. Nowadays, the procedures for amide synthesis have become highly developed because of the introduction of new peptide coupling reagents in organic synthesis. But still, the simple two step acylation reactions (activation of carboxylic acid followed by reaction with amines) have not been discarded in this chemistry. The key intermediate for this type of reaction is an acid chloride, which can be used for transformation into many other functional groups as

well as amides: for instance, anhydrides, esters and ketones. Additionally, this type of reaction can be used as a protecting strategy in significant synthetic methods which involve several steps, leading to many bioactive compounds (vitamins, agrochemicals, xanthenes, also conjugational peptide synthesis).⁴

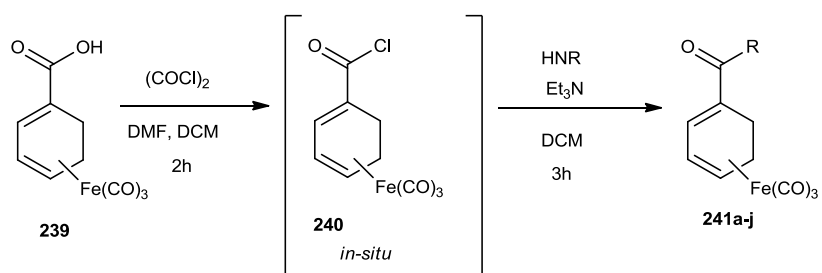
Scheme 61 shows an example of an *N*-acylation reaction, where in the first step the carboxylic acid is activated by changing it into the acid chloride and subsequent reaction with the amine.



Scheme 61 Representation of *N*-acylation reaction.

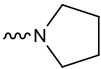
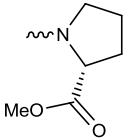
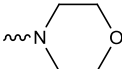
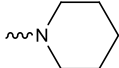
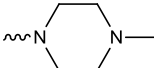
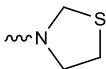
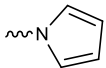
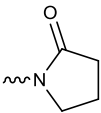
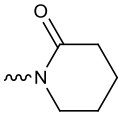
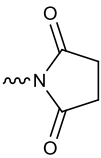
The acylation reaction is a crucial step in the synthesis of the novel tricarbonyliron complexes. The synthesis of tricarbonyl iron complexes which possess a range of different amide groups was developed. The intention is that the amide carbonyl group in conjugation with the diene complex will be suitable for the proposed hydrogen bonding interactions (see Figure 44) that should provide the basis for the differential read-out in the IR of the presence of different sugars.

As a first step, tricarbonyl(cyclohexa-1,3-dieneacyl chloride)iron **240** was made by reaction of tricarbonyl(cyclohexa-1,3-dienecarboxylic acid)iron **239** with oxalyl chloride in dry DCM in the presence of a catalytic amount of DMF to form the acyl chloride **240** *in situ*. In a series of reactions, various types of amines were added to a solution of this key intermediate **240** in dry DCM at room temperature, in the presence of triethylamine. The reaction mixture was stirred at room temperature for 3 hours before being quenched. Under these reaction conditions the desired novel tricarbonyliron complexes with different amides group **241a-f** were obtained in good yields (Scheme 62, Table 2). Analysis by IR showed vibrations at around 1974 and 2050 cm^{-1} for the $\text{Fe}(\text{CO})_3$ moiety and at about 1722 cm^{-1} for the amide carbonyl group. The use of longer reaction times was also examined but offered no improvement in yields. These reaction conditions failed for compounds **241g-j**.



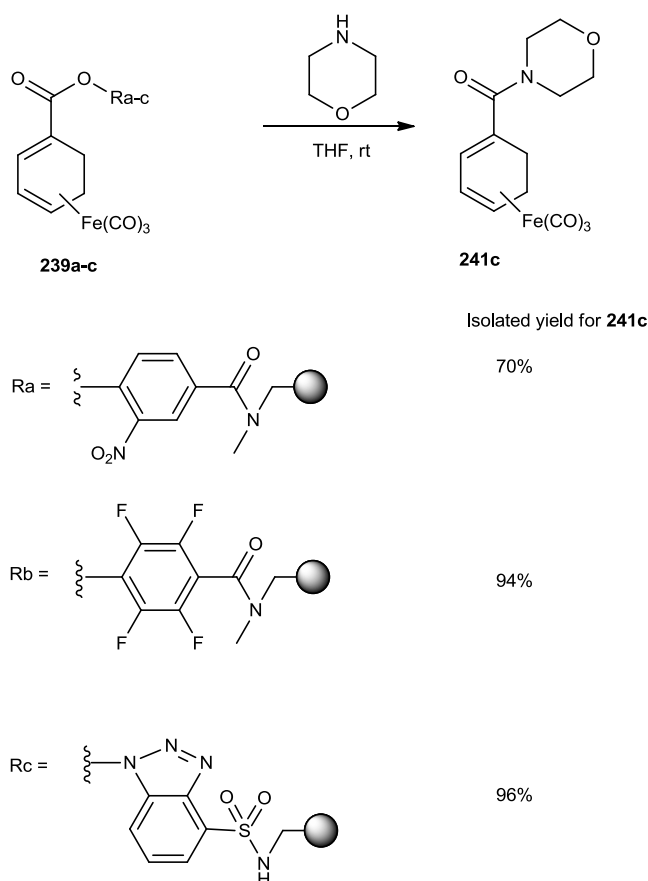
Scheme 62 The preparation of novel tricarbonyliron complexes and their salts.

Table 2 Isolated yields for different substituents under reaction conditions described in Scheme 62.

241	
R	Isolated Yield (%)
a 	81%
b 	67%
c ⁵ 	92%
d 	75%
e 	74%
f 	55%
g 	0%
h 	0%
i 	0%
j 	0%

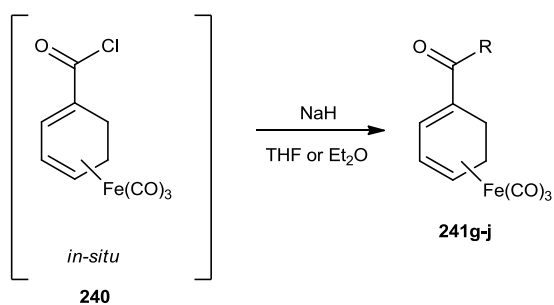
All the synthesised tricarbonyl complexes **241a-f** are new apart from the compound **241c**. In 2006, J. Eriksson and co-workers synthesised **241c** by polymer-amide cleavage, as shown in Scheme 63. Different types of active esters **239a-c** were reacted in dry THF at room temperature. The reaction was followed by HPLC using *N,N*-

dimethylbenzamide as a standard. The best results were obtained by using the ester **239a** which gave **241c** in 96 % yield. The ^1H NMR, ^{13}C NMR and IR spectrum of the product **241c** obtained by our method agreed with data reported in the literature.⁵



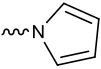
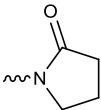
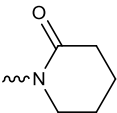
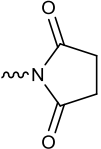
Scheme 63. The synthesis of tricarbonyliron **241c** by polymer-amide cleavage.

However, in order to optimise the reaction conditions for compounds **241g-j**, the influence of the supporting base and solvent on the course of the reaction was specifically studied. The addition of pyrrole, 2-pyrrolidinone, δ -valerolactam, and succinimide to solutions of tricarbonyl(cyclohexa-1,3-dieneacyl chloride)iron **240** in dry THF in the presence of sodium hydride was successful for only one compound. An excellent 95% yield was obtained to give derivative **241j** when the reaction was stirred for three hours at room temperature, but no yield was observed for the rest of the substrates using these same conditions (Table 3, Scheme 63). These compounds seem to be unstable under the reaction conditions and decompose upon extended reaction time. Changing the solvent to diethyl ether failed to improve results.



Scheme 63 Modification of the reaction conditions to obtain tricarbonyl iron complexes **241g-j**.

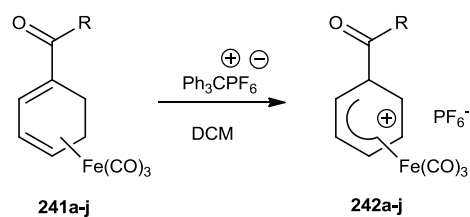
Table 3 Isolated yields for different substituents under reaction conditions described in Scheme 63.

241	
R	Isolated Yield (%)
g 	0%
h 	0%
i 	0%
j 	95%

2.2.1.1. Preparation of tricarbonyliron salts

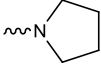
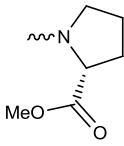
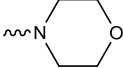
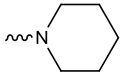
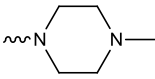
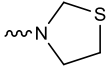
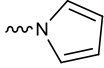
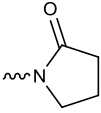
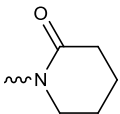
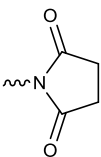
The synthesis of the tricarbonyl η^5 -cyclohexadienyl iron salts **242a-j** was approached by hydride abstraction with trityl cations (triphenylcarbenium hexafluorophosphate or triphenylcarbenium tetrafluoroborate) in dry DCM as shown in Scheme 65.^{2,6} The work-up of the reaction mixture involves the addition of diethyl ether, which causes the precipitation of tricarbonyliron salts. Unfortunately these reaction conditions did not work consistently for all the novel complexes, even when the counterion was changed from PF_6^- to BF_4^- . The best result was obtained for compound **242c** (Table 4, Scheme 65), but for the rest of the examples the salt could not be precipitated. As an

alternative, it was decided to investigate whether those salts can be used with nucleophiles *in situ* without isolation of the salts. The IR measurements after hydride abstraction show the peaks $\sim 2118\text{ cm}^{-1}$ and $\sim 2063\text{ cm}^{-1}$ that indicate the salts are formed in the solution but cannot be precipitated. The un-isolated tricarbonyliron salts can still be potentially useful in future syntheses, for example with different types of nucleophiles.



Scheme 65. The preparation of novel tricarbonyliron salts.

Table 4 Isolated yields for different substituents under reaction conditions described in Scheme 65.

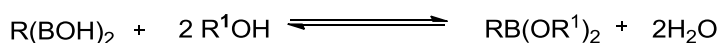
242		
R	Isolated Yield (%)	
a		0%
b		0%
c		70%
d		0%
e		0%
f		0%
g		-
h		-
i		-
j		0%

2.2.2. Choice and synthesis of the sugar sensor

It is important to understand clearly the role of the boronic acid moiety of the target molecule, and how it functions. In the introduction (Section 1.4), the importance of boronic acids specifically in carbohydrate bioprobe systems was discussed. They have

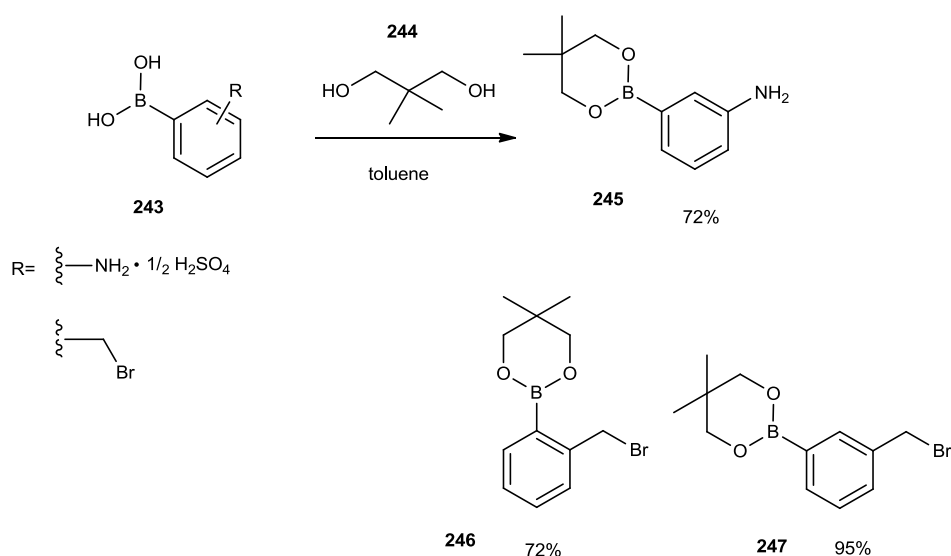
unique properties as strong organic Lewis acids. It is also significant that boronic acids can be described as “green” compounds because of their low toxicity and their ultimate degradation into boric acid which is environmentally friendly.⁷

Additionally, boronic acids are not always very convenient in purification and characterization, but their ester derivatives are often more easily handled, since the two hydroxyl groups are protected. In addition, conversion of the hydroxyl groups into other functional groups (halides) can give increased reactivity necessary for several synthetic applications. All of the boronic acids which were used in this research were commercially available but it was still necessary to perform some protection reactions of these compounds. The representative Scheme 66 describes the synthesis of boronic esters from boronic acids and alcohols or diols. The reaction is in equilibrium and the formation of the ester is favoured when this product is not soluble in the reaction solvent.⁷



Scheme 66 Equilibrium and the formation of the esters.

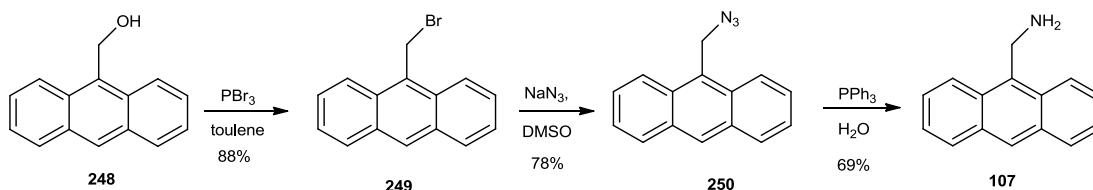
Within this project 2,2-dimethyl-1,3-propanediol **244** in dry toluene was used for protection and the reaction mixture was stirred overnight at room temperature before being quenched. The corresponding esters are listed in Scheme 67 and were obtained in good yields.



Scheme 67 Synthetic route for protection of boronic acids.

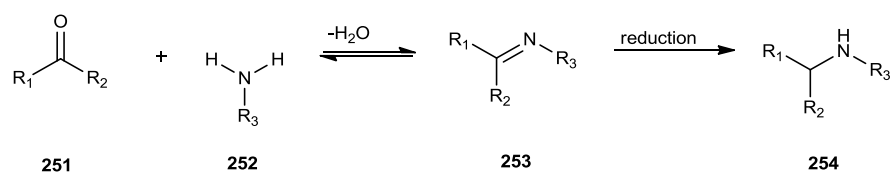
2.2.3. Choice and the synthesis of fluorescent reporting group

The choice of the 9-aminomethylantracene **107** fluorophore is based on its advantageous use in the synthesis of known bioprobes. This type of fluorophore is commercially available but is very expensive (2 g costs \$1250, at Betapharmascientific®) so it was important to find a short and easy way to prepare it. Following a literature search,⁸ an attractive way to prepare the required fluorophore **107** was identified. The first step involved bromination of 9-anthracenemethanol **248** by phosphorous tribromide in dry toluene to yield (88 %) the bromomethyl product **249** as yellow crystals. Subsequent preparation of 9-azidomethylantracene **250**, was achieved in 78 % yield by reaction of 9-bromomethylantracene **107** in presence of sodium azide in DMSO. The final step is called the Staudinger reaction⁹ and is the conversion of an azido group into an amino group. 9-Azidomethylantracene **250** was reduced by using triphenylphosphine in water with hydrolysis to produce 9-aminomethylantracene **107** in good yield (69%) (Scheme 68).



Scheme 68 Synthetic route to prepare desired fluorophore **107**.

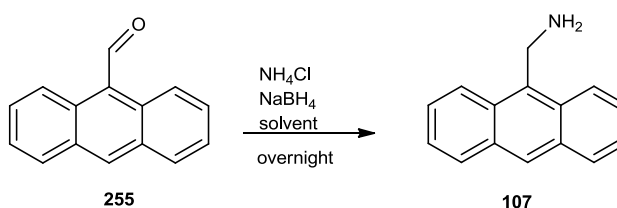
Although, the literature example is very precise and easy to follow, it was decided to investigate a shorter way to prepare this fluorophore just by simple reductive amination. In the synthesis, the number of steps were reduced from three to just one to give the desired compound **107** in good yield by this reductive amination approach. Reductive amination of aldehydes and ketones is a well-known method of preparation of secondary amines. In this type of reaction, the amine **252** will react with the carbonyl group to produce an imine **253** (reversible), which involves the loss of one molecule of water. The equilibrium between the formed imine **253** and aldehyde or ketone **251** can be moved toward imine formation by removal of the water. It is possible to isolate and reduce the imine **253** (an intermediate) with a suitable reducing agent: this is called indirect reductive amination (Scheme 69).¹⁰



Scheme 69 Representation of reductive amination.

It is also possible to perform both steps in one pot, with the imine formation and reduction occurring in sequence, which is known as direct reductive amination. In this case, the initial equilibrium can be driven by the irreversible reduction step. These methods use reducing agents which are more reactive towards imines than ketones, for example sodium cyanoborohydride (NaBH_3CN) and sodium triacetoxyborohydride [$\text{NaBH}(\text{OCOCH}_3)_3$]. Another interesting and significant transformation of the imine intermediate is catalytic hydrogenation. The disadvantage of this method, however, is that the hydrogenation conditions for the reaction are not suitable for many other reducible functional groups, for instance nitro, cyano, double, triple bond. To avoid those extra reductions, sodium cyanoborohydride is preferable.¹⁰

The shortened synthesis of the fluorophore was started from the reaction of 9-anthracenecarboxaldehyde **255** with ammonium chloride and sodium borohydride as shown in Scheme 70. In order to optimise the reaction conditions, the influence of the solvent, reducing agent and source of ammonia on the course of the reaction was specifically studied, by changing each parameter in turn while keeping the others constant. The best solvent under these conditions was found to be dichloroethane, Table 5.

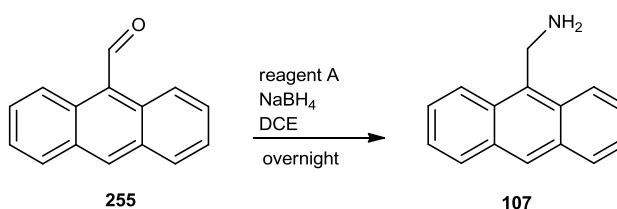


Scheme 70 Reductive amination of **255** to afford **107** by using various solvents.

Table 5 Yields and corresponding solvents applied to Scheme 70.

<u>solvent</u>	<u>Y (%)</u>
MeOH	40%
EtOH	35%
DCE	80%

Next, a comparison of different sources of ammonia for this reaction was explored (Scheme 71). Reaction with either ammonia in methanol (liquid), or ammonium chloride (powder), surprisingly showed that ammonium chloride powder gave slightly better results as we obtained the required compound in excellent yield 80% (Table 6).

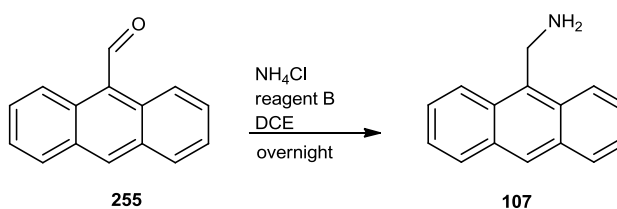


Scheme 71 Reductive amination of **255** to afford **107** by using various sources of ammonia.

Table 6 Yields and corresponding ammonia sources applied to Scheme 71.

<u>reagent A</u>	<u>Y (%)</u>
NH ₃ in MeOH	40%
NH ₄ Cl	80%

Finally, the effect of different reducing agents was shown. Reactions and yields with different reducing agents; NaBH₄, NaBH(OAc)₃, and NaBH₃CN in dry DCE are shown in Scheme 72, Table 7, respectively.



Scheme 72 Reductive amination of **255** to afford **107** by using different reducing agents.

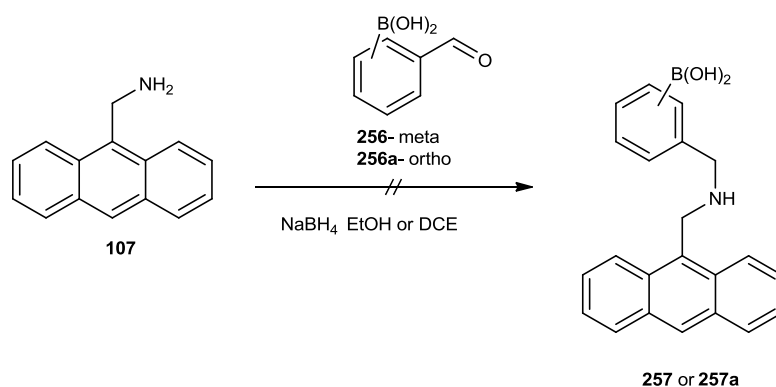
Table 7 Yields and corresponding reducing agents applied to Scheme 72.

reagent B	Y (%)
NaBH ₄	80%
NaBH(OAc) ₃	15%
NaBH ₃ CN	60%

As a conclusion concerning the reductive amination step, the best conditions were achieved by using NH₄Cl as a source of ammonia and NaBH₄ as the reducing agent in dry DCE.

2.2.4. Synthesis of the main part of the target molecule (pathway A)

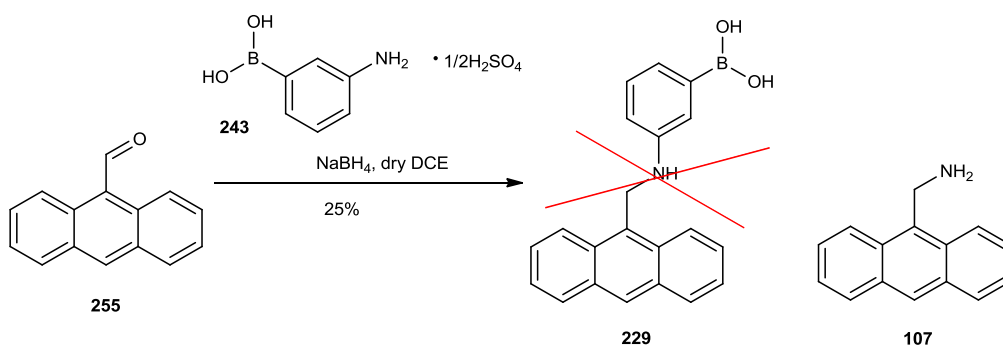
Boronic acids **256** or **256a** are commercially available and were chosen for an initial examination of the reductive amination following the known procedure from a previous PhD thesis¹¹ in which the reaction was performed in the *ortho* series, using a boronic acid prepared for the project. The *meta* and *ortho* derivatives of formylphenylboronic acid (**256**, **256a**) were reacted individually with 9-aminomethylantracene **107** in the presence of sodium borohydride but unfortunately failed to give the desired compound **257** or **257a**, Scheme 73.



Scheme 73 Unsuccessful attempt to produce molecule **257**.

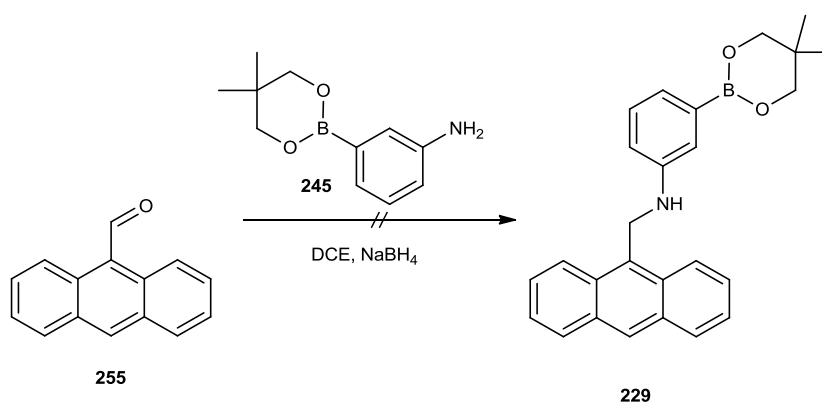
It was decided to reverse the functional groups on the two substrates and then apply the same conditions as previously for the reductive amination step. Surprisingly, this reaction also failed to give the desired building block **229** for the target molecule **228**, but instead 9-aminomethylantracene **107** was isolated, Scheme 74. The formation of

107 was confirmed by IR, ^1H -NMR and ^{13}C -NMR. The reaction was repeated several times to make sure that this product did not arise from cross-contamination.



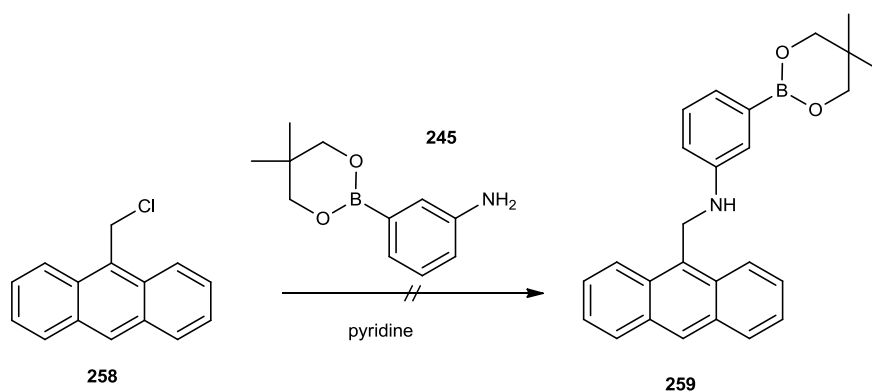
Scheme 74 Unpredictable synthesis of fluorophore **107**.

The next attempt was to use protected boronic acid derivatives under the same conditions (Scheme 75), unfortunately with no success.



Scheme 75 Unsuccessful route to achieve molecule **229**.

In the light of this observation, the use of the chloro analogue was considered instead. The previously prepared 3-(5,5-dimethyl-1,3,2-dioxaborinan-2-yl)aniline **245** and the commercially available 9-(chloromethyl)anthracene **258** were arbitrarily chosen for this study (Scheme 76). The reaction was carried out using pyridine as a solvent but unfortunately it failed to achieve the expected compound **259**.¹²

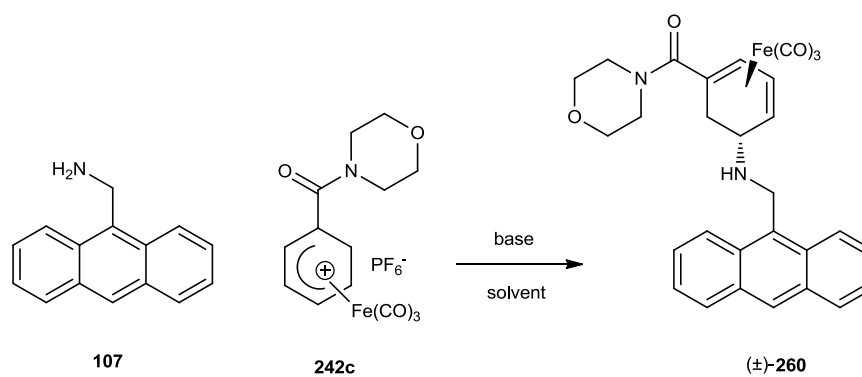


Scheme 76 Unsuccessful route towards **259**.

Facing these unsuccessful efforts to prepare the target molecule by pathway A, it was decided to move on to the pathway B which is shown in Scheme 56.

2.2.5. Reaction of tricarbonyliron salt with nucleophile (pathway B)

First, following literature conditions,^{13,14} it was attempted to prepare compound (±)-**260** by reaction of 9-aminomethylanthracene **107** and tricarbonyl[5-(morpholine-4-carbonyl)cyclohexa-2,4-dien-1-yl]iron hexafluorophosphate **242c** in dry CH₃CN and then in DCM. Unfortunately both reactions failed to provide the desired compound (±)-**260**. The new (±)-tricarbonyl{5-[(anthracen-9-ylmethyl)amino]cyclohexa-1,3-dien-1-yl}(morpholino)methanone}iron complex (±)-**260** was isolated in low yield (5%) by using dry THF as a solvent and stirring for 3 hours at room temperature. A series of experiments was then undertaken to attempt to optimise the yield of this transformation; starting by varying the choice of the supporting base (Table 8, Scheme 77). When triethylamine was used, the yield was marginally improved to 8%. It is noteworthy that changing the supporting base to dimethylaminomethyl-polystyrene (DMAM-Ps) gave the best yield (15%) for this reaction. The use of longer reaction times at room temperature, and reflux were also compared but did not improve yield. These results suggest the reaction between 9-aminomethylanthracene molecule and tricarbonyl{5-(morpholine-4-carbonyl)cyclohexa-2,4-dien-1-yl}iron hexafluorophosphate **242c** with DMAM-Ps should be considered for future investigations.



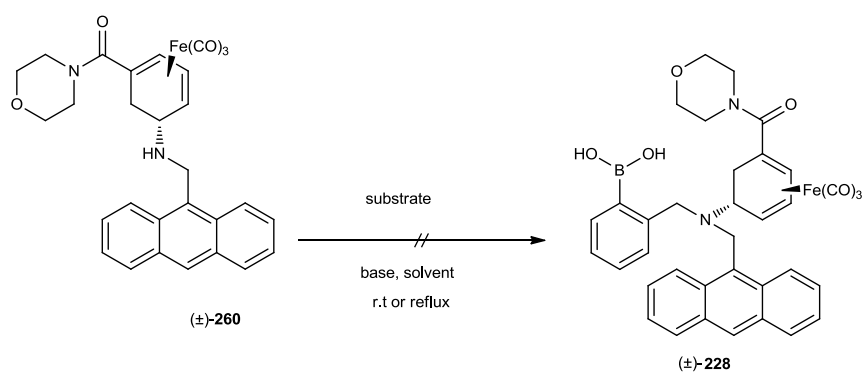
Scheme 77 Synthetic route towards compound (±)-**260** under different reaction conditions.

Table 8 Yields and corresponding supporting base and solvents applied to Scheme 77.

Solvent	Base	Y(%)
CH ₃ CN	-	0%
DCM	-	0%
THF	-	5%
THF	Et ₃ N	8%
THF	DMAM-PS	15%

2.2.6. Preparation of target molecule (±)-**228** and modified target molecules (±)-**228d** and (±)-**267**

The synthesis of the ideal target molecule with the *ortho*-substituted boronic acid was attempted *via* a second nucleophilic addition reaction with molecule (±)-**260**, by addition at room temperature of commercially available 2-bromomethylphenylboronic acid **261** followed by treatment with potassium carbonate in dry acetonitrile (CH₃CN) to give bioprobe (±)-**228** (Scheme 78). This reaction failed to proceed and no product was obtained. The supporting base was varied by using potassium bicarbonate in dry THF but this reaction also failed.

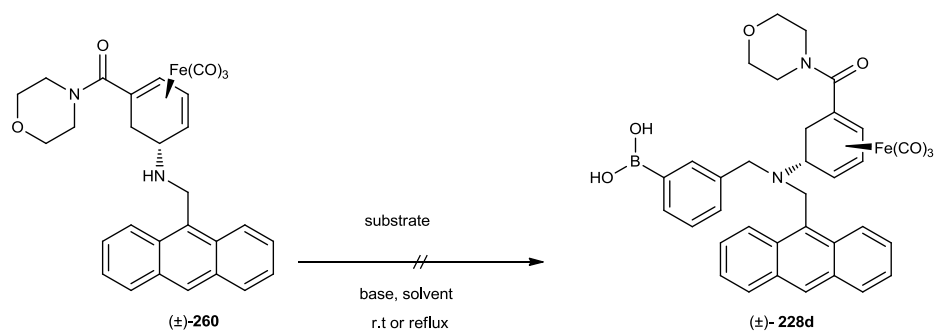


Scheme 78 Synthetic route towards preparation of ideal target molecule $(\pm)\text{-228}$.

Table 9 Reaction conditions applied to Scheme 78.

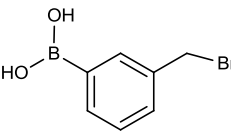
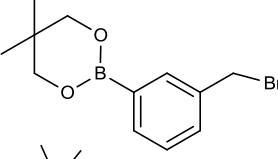
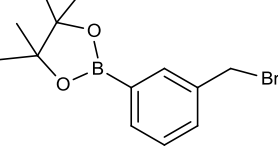
substrate	base	solvent
 261	NaH	THF
	K_2CO_3	THF or CH_3CN

Additionally the preparation of modified target molecule with a *meta*-substituted boronic acid was attempted, varying the conditions of the reaction by changing the boronic substrates, base and solvents. The reactions were carried out at room temperature and also at reflux. Unfortunately, none of these modifications allowed for isolation of the desired product $(\pm)\text{-228d}$, (Table 10, Scheme 79).

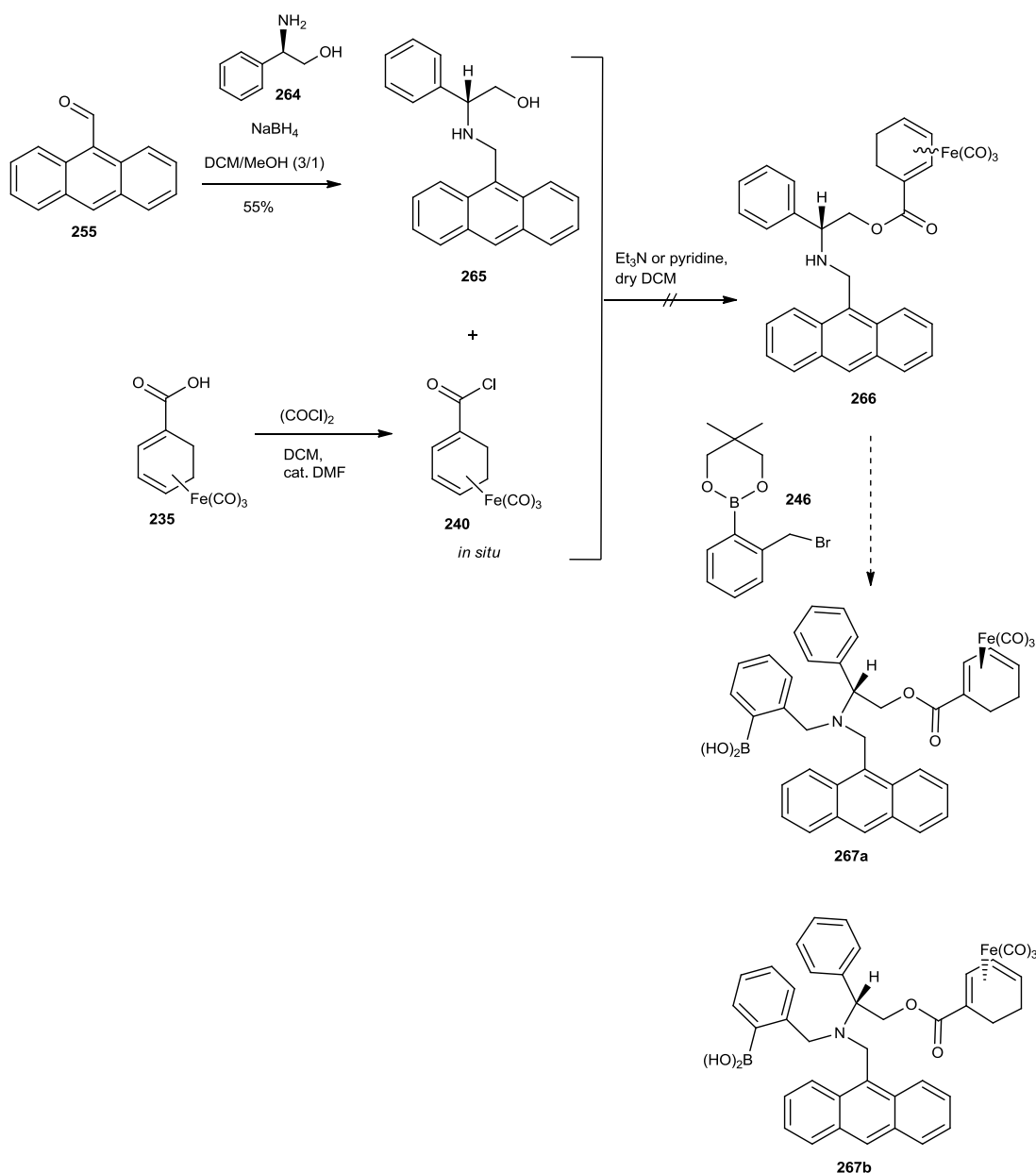


Scheme 79 Synthetic route towards preparation of modified target molecule $(\pm)\text{-228d}$.

Table 10 Reaction conditions with different substrates applied to Scheme 79.

substrate	base	solvent
 262	NaH K ₂ CO ₃	THF THF or CH ₃ CN
 247	NaH K ₂ CO ₃	THF THF or CH ₃ CN
 263	NaH K ₂ CO ₃	THF THF or CH ₃ CN

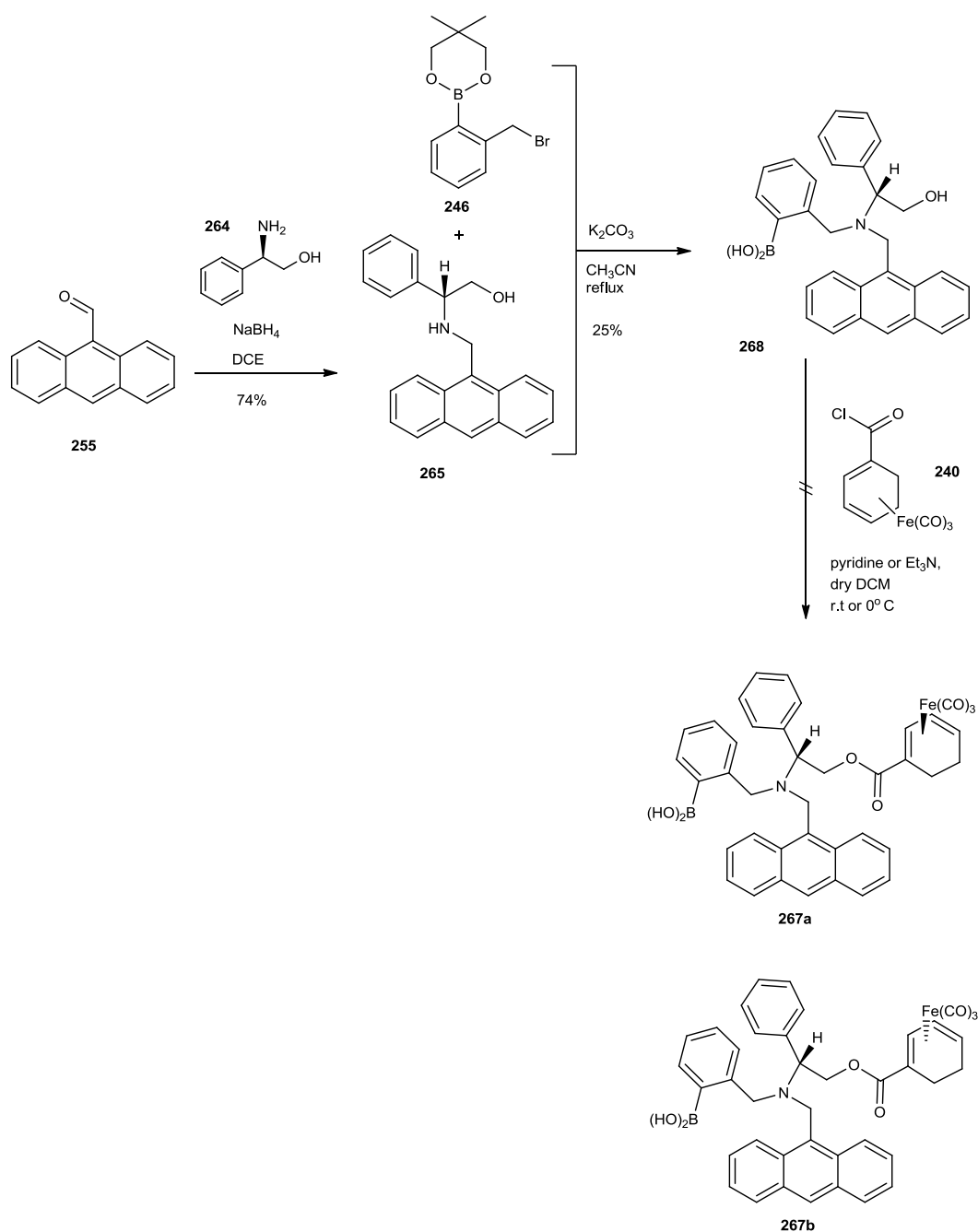
Faced with this setback, alternative methods of synthesising the changed target molecule (\pm)-**267** were examined. It was decided to prepare the molecule following the synthetic route presented in Scheme 80. Based on the literature,¹⁵ in the first step the (*R*)-2-phenyl-2-(anthracen-9-ylmethylamino)-ethanol **265** was synthesised by reductive amination in 55% yield. This time, the reductive amination of (*R*)-2-amino-2-phenyl-ethanol **264** was performed in a mixture of DCM/MeOH (3/1) in the presence of sodium borohydride. Next, an approach that required the conversion of tricarbonyl(cyclohexa-1,3-dieneacyl chloride)iron **240** in dry DCM by using triethylamine (Et₃N) or pyridine as a base, which could possibly lead to the novel compound **266**, was investigated. Subsequently a simple *N*-alkylation with 2-(2-bromomethylphenyl)-1,3,2-dioxaborinane **246** would yield the diastereoisomers **267a** and **267b**. Unfortunately, this strategy proved unsuccessful.



Scheme 80 New synthetic routes to achieve (±)-**267a-b**.

A last route for this part of project was finally considered. The previously developed conditions were applied to the reductive amination step, as follows; 9-anthracenecarboxaldehyde **255** was reacted with *(R)*-2-amino-2-phenylethanol **264**, by treatment with sodium borohydride in dry DCE, to produce the *(R)*-2-phenyl-2-(anthracen-9-ylmethylamino)-ethanol **265** in an improved yield (74 %), compared with the literature example. The next step involved reaction of *(R)*-2-phenyl-2-(anthracen-9-ylmethylamino)-ethanol **265** with 2-(2-bromomethylphenyl)-1,3,2-dioxaborinane **246** in dry acetonitrile (CH_3CN) by using potassium carbonate. The reaction mixture was refluxed for 8 hours before being worked up. The desired compound **268** was

synthesised in 25% yield. Following that, the addition of tricarbonyl(cyclohexa-1,3-dieneacyl chloride)iron **240** in the presence of a Et₃N or pyridine in dry DCM (Scheme 81) was attempted. These reactions led only to complex mixtures of products.



Scheme 81 Unproductive modification of synthetic route to achieve **267a-b**.

2.3. Conclusions

Although the target molecule was not synthesised, even after several attempts, and it was not possible to directly prove, by spectroscopic evaluation, the bioprobe approach that formed the motivation for this project, the desired target is just one step away from the point in the synthesis currently reached. In the course of the work described in this section, the novel tricarbonyliron complexes **241a-b**, **241d-f** were synthesised. These new complexes have potential utility for synthetic elaboration and have accumulated important information about the scope and limitations of the use of tricarbonyliron chemistry to address highly functionalised target structures. Some further investigations with the electrophilic cations **242a-f**, **242j** are still needed to explore their reactivity with nucleophiles by the '*in situ*' approach. To summarise the outcomes reported in this section of the thesis, development of a new way to prepare the expensive fluorophore, 9-aminomethylantracene **107** was achieved, which has an important role in the field. Subsequently, the synthesis of the main part of the target molecule was attained with interesting outcomes which can possibly guide future work to investigate these types of reactions. Results (both successful and unsuccessful) presented in this thesis provide crucial information needed to devise alternative approaches to achieve the synthesis of the first examples of this novel class of sensor structures.

2.4. References

- ¹ T. D. James, K. R. A. S. Sandanayake, S. Shinkai, *J. Chem. Soc., Chem. Commun.*, **1994**, 477-478.
- ² T. Olsson, H. Graden, J. Hallberg, N. Kann, *J. Comb. Chem.*, **2004**, 6, 783-788.
- ³ F. Bohlmann, C. Zdero, *Chem. Ber.*, **1973**, 106, 3779.
- ⁴ M. Stare, K. Laniewski, A. Westermarck, M. Sjogren, W. Tian, *Organic Process Research and Development*, **2009**, 13, 857-862.
- ⁵ J. Eriksson, T. Olsson, N. Kann, H. Gradén, *Tetrahedron Lett.*, **2006**, 47, 635-638.
- ⁶ A. J. Birch, P. E. Cross, J. Lewis, D. A. White, S. B. Wild, *J. Chem. Soc. (A)*, **1968**, 332-340.
- ⁷ D. G. Hall, *Boronic Acids: Preparation and Applications in Organic Synthesis, Medicine and Materials (Second Edition)*, Wiley-VCH Verlag GmbH & Co. KGaA, **2001**.
- ⁸ D. E. Stack, A. L. Hill, C. B. Diffendaffer, N. M. Burns, *Org. Lett.*, **2002**, 4, 4487-4490.
- ⁹ H. Staudinger, J. Meyer, *Helv. Chim. Acta*, **1919**, 2, 635-646.
- ¹⁰ S. Gomez, J. A. Peters, T. Maschmeyer, *Adv. Synth. Catal.*, **2002**, 344, 1037-1057.
- ¹¹ Seena Sudhakaran Pillai, PhD thesis, University of East Anglia, **2010**.
- ¹² M. J. Plater, I. Greig, M. H. Helfrich, S. H. Ralston, *J. Chem. Soc., Perkin Trans 1*, **2001**, 2553-2559.
- ¹³ A. J. Birch, B. M. R. Bandara, K. Chamberlain, B. Chauncy, P. Dahler, A. I. Day, I. D. Jenkins, L. F. Kelly, T.-Ch. Khor, G. Kretchmer, A. J. Liepa, A. S. Narula, W. D. Raverty, E. Rizzardo, C. H. Sell, G. R. Stephenson, D. J. Thompson, D. H. Williamson, *Tetrahedron*, **1981**, 37, 289-302.
- ¹⁴ T. Olsson, H. Graden, J. Hallberg, N. Kann, *J. Comb. Chem.*, **2004**, 6, 783-788.
- ¹⁵ L. Chi, J. Zhao, T. D. James, *J. Org. Chem.*, **2008**, 73, 4684-4687.

CHAPTER 3:

Results and Discussion Project 2

3.1. Aim of the project 2

This project describes collaboration with Prof. Pierre-Yves Renard and Pr. Anthony Romieu in University of Rouen, whereby I spent six months working under their supervision. It involved the preparation of a molecular bioprobe associating two modalities: fluorescence and infra-red, which will work as an enzyme assay to visualize enzyme activities. As described in Section 1.3, the last decade has seen a high level of interest in the synthesis of pro-fluorescent compounds to use in this type of bioprobe to advance the discovery and optimization of industrial enzymes which have become of increasing importance because of the impact they make in economically viable, mild, environmentally-friendly production processes. Furthermore, the progress of research with these types of bioprobes opens the way for advances in drug discovery efforts, medical diagnostics and in the technologies for cellular and tissue imaging.¹ The most uncomplicated and feasible bioprobes rely on a synthetic molecule that releases a coloured or fluorescent product during reaction or make a noticeable change in solution, for instance a precipitation. As well, such reactions use different types of techniques which respond indirectly to consumption of substrate or product formation. The indicator techniques can be used simply as a pH-meter, but also many bioprobes are based on NMR, IR or fluorescence.²

This project is based on bioprobes which are constructed with a cleavable active bond as a linker. These types of bioprobes typically contain three potential parts: a signalling moiety, a labelling or recognition moiety (which allows specific recognition of the targeted analyte and/or a specific reaction) and, in most of the cases, a suitable linker or spacer (which connects the two functional moieties). This project was designed by proposing a self-immolative cleavable linker to connect a recognition unit to a signalling unit which has been the most prevalent and provides the inspiration for many spectroscopic probes, through unveiling of the signalling unit once the self-immolative cleavable linker has been cleaved. The Figure 45 represents the general mechanism for this type of bioprobe.^{2,3,4}

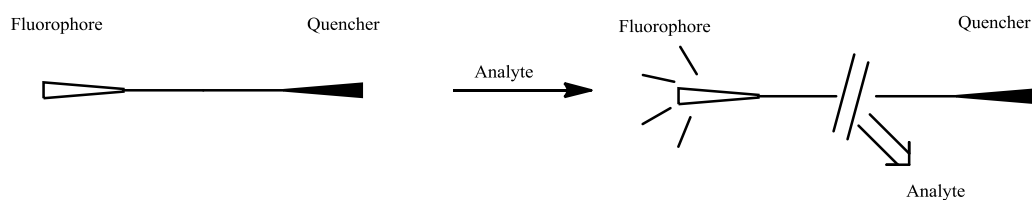


Figure 45 Representation of mechanism for pro-fluorescent bioprobe.

When the fluorophore is connected to a quencher with a cleavable active bond it emits only a weak fluorescence because of intramolecular self-quenching or fails to fluoresce at all. Afterwards, when an analyte is added and the linker in the probe is cleaved, the fluorophore is released and so is separated from the quencher, with the return of a fluorescent response. In the past few years, this design of bioprobe and the mechanism of operation has opened a novel alternative route to the specific determination of analytes with high hydrolytic reactivity and has permitted many biological processes to be monitored *in situ* and in real-time.⁵

The project is based on the synthesis and proof of model dye **268** (Figure 46) with novel fluorescent / IR reactive probes with cleavable active bonds aiming at the detection of a model protease. As in project 1, this target molecule will contain the conventional fluorophore (the aminocoumarin) and the IR-active tricarbonyliron complex, to convey the read-out information which can be validated by comparison of IR and fluorescence responses. 7-Aminocoumarins with electron-withdrawing groups at the aniline moiety generally display a high quenching of their fluorescence. Cleavage of the amide bond by a model protease (namely penicillin G acylase) will lead, through a 1-6 elimination process, to the release of the 7-aminocoumarin, and thus, to the release of the fluorescence, as well as the modification of the IR responsive $\text{Fe}(\text{CO})_3$ moiety, which should also display a significant modification on the IR signal (*vide infra*).

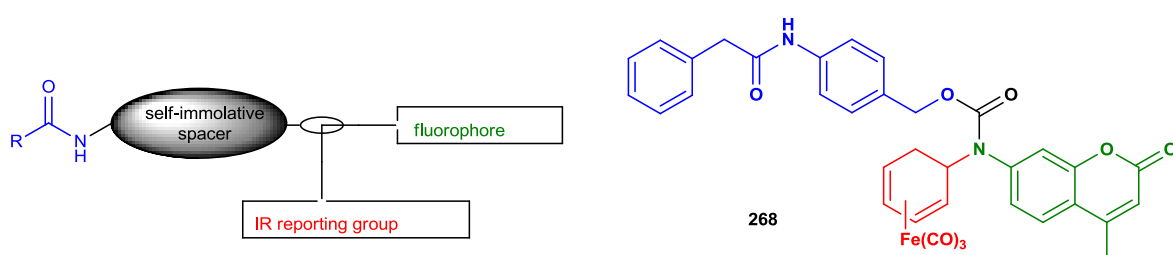
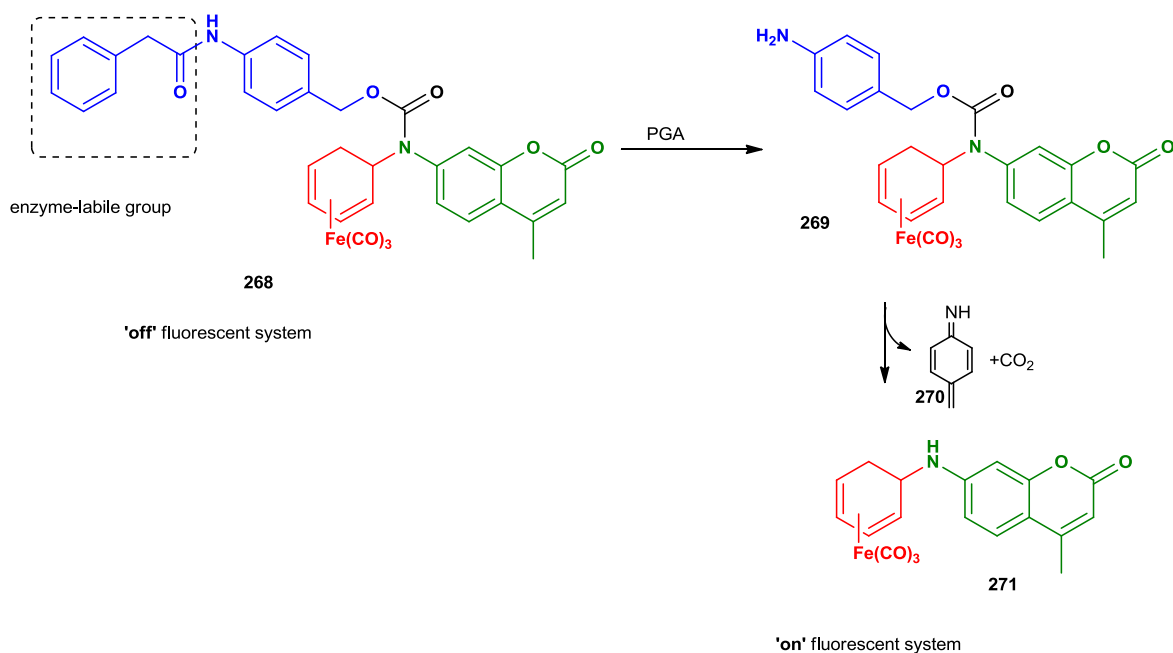


Figure 46 Representation (left) and structure (right) of target bioprobe **268**.

Pro-fluorescent bioprobes (or fluorogenic probes) are molecules in which a physical property of the fluorophore or IR-active group is changed upon interaction with an analyte (enzyme, metal cation, and reactive oxygen species) so displaying important information. As an example, for fluorophores, there will be changes in the fluorescence spectrum and/or an increase in the fluorescence quantum yield at a particular wavelength, and/or a change in some other fluorescent properties of the molecule. In some cases, the fluorogenic probes unveiled intense fluorescence only by a user-designated chemical reaction, so they present a unique selectivity and limited interferences related to the probe's concentration, excitation intensity, and emission sensitivity.⁴ These properties have made them very advantageous in many fields because they have ability to improve analytical sensitivity and can provide greater temporal and spatial sampling capabilities. Principally it is shown in the literature that bioprobes are valuable tools in challenging biomedical applications such as *in vivo* fluorescence imaging, or in the enzyme-linked immunosorbent assay (ELISA), high throughput screening of enzyme inhibitors, detection of DNA and RNA, and evaluation of cell viability.⁶

In this concept, the target is the detection of a model protease, penicillin acylase (PGA), where the biocatalyzed transformation will be combined with a domino reaction. As shown in Scheme 82, the mechanism will include the fragmentation of the compound **268** to give dye **269**, and then spontaneous 1,6 elimination to create azaquinonemethide **270** and the fluorescent compound **271**, to observe an off/on system.



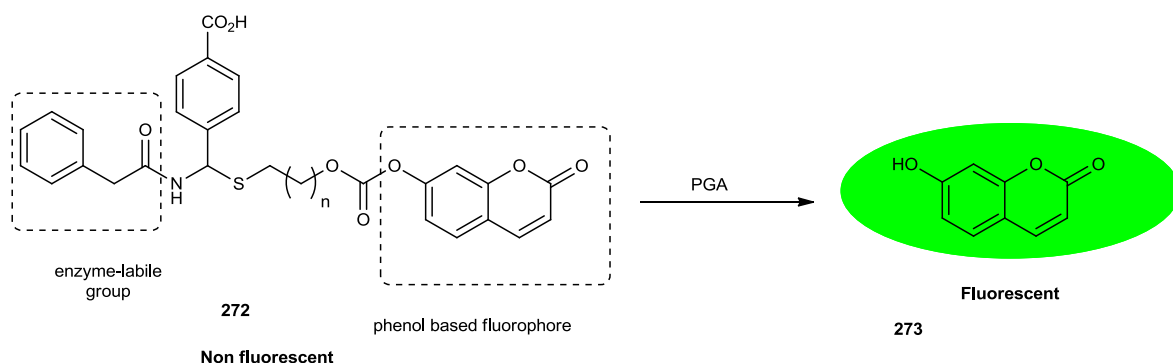
Scheme 82 The biocatalyzed transformation to release fluorescent compound **271**.

3.1.1. Choice of the self-immolative linker

There have been many examples during the last decade in which numerous self-immolative linker approaches have been advanced as the strategy of efficient prodrug designs of various pharmaceuticals which will be acceptable for the synthesis of organic compounds through many methods.^{7,8} This concept of a self-cleavable linker which plays the role of a spacer unit between the peptidyl substrate and a fluorescent label is showing a potentially additional advantage as it increases the enzymatic reactivity as well as spectral properties. Moreover, this self-immolative spacer strategy causes the reduction of the background noise associated with nonspecific hydrolysis of the resulting pro-fluorophore compared to “standard” two-component fluorogenic protease substrates. The self-decomposition of the spacer through a protease-initiated domino reaction can lead to release of fluorophores which contain an aniline, a phenol, or a thiophenol derivative.⁹ The requirement for such fluorophores to deliver a high off/on signal for this type reaction is a fluorescence modification once the aniline / phenol / thiophenol is involved in an electron withdrawing bond, of which cleavage is induced by the self immolative reaction. Among the fluorophores displaying such

properties, fluorescent amines such as 7-amino-4-methylcoumarin (AMC), rhodamine 110, or cresyl violet can be expected to give protease-activated optical probes with excellent analytical properties.

Pr. Renard's group in Rouen has a good experience in such kind of bioprobes. For instance, in 2008, his group described the synthesis of a novel self-immolative spacer system **272** which will be able to release phenol-containing compounds (Scheme 83).¹⁰



Scheme 83 Representation of novel self-immolative spacer **272** upon biotransformation.

These novel compounds for this application proved to be precisely stable under physiological conditions and activated through spontaneous decomposition of the intermediate under neutral aqueous conditions. The advantage of this dye was proved by the preparation of a fluorogenic substrate aimed at the detection of the activity of penicillin amidase whose strong fluorescence is unmasked through enzyme-domino reactions. Moreover, they could be potentially a good guide for the design of profluorophore or prodrug delivery systems appropriate for cancer imaging or chemotherapy.¹⁰

In the same year, Renard's group prepared a new class of far-red Emitting fluorogenic dye **274**, Figure 47. In their strategies, they introduced the beneficial use of a PABA derivative as a linker between peptidyl substrate and the fluorophore. This self-immolative spacer when present shows higher stability in physiological media and even better enzymatic recognition and cleavage kinetics.¹¹

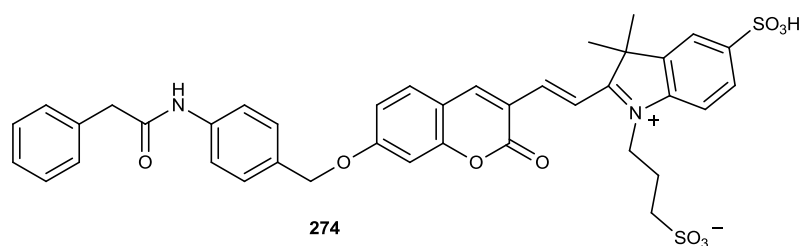


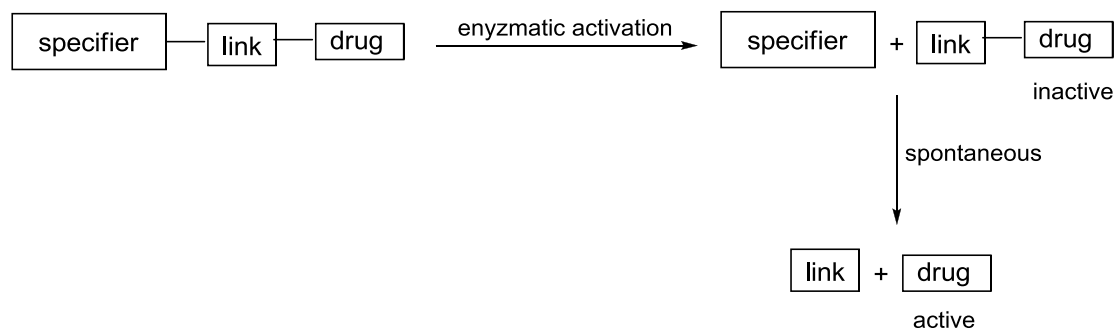
Figure 47 Representation of novel Far-Red Emitting Fluorogenic Dye **274**.

Additionally, the designed fluorogenic derivatives were projected in precise manner:

- 1) as 7-alkoxycoumarins emit more weakly when compared with 7-hydroxycoumarins they can give the pro-fluorescence properties,
- 2) the phenol group of the 7-hydroxycoumarin and an hemicyanine dye should work as a push-pull device,
- 3) the presence of one or two double bonds in the 3-position of the coumarin aims at producing the red-shift of the emission wavelength (extension of the π -conjugation of the dye),
- 4) to achieve water solubility, a sulfonate group was introduced on the hemicyanine derivative.

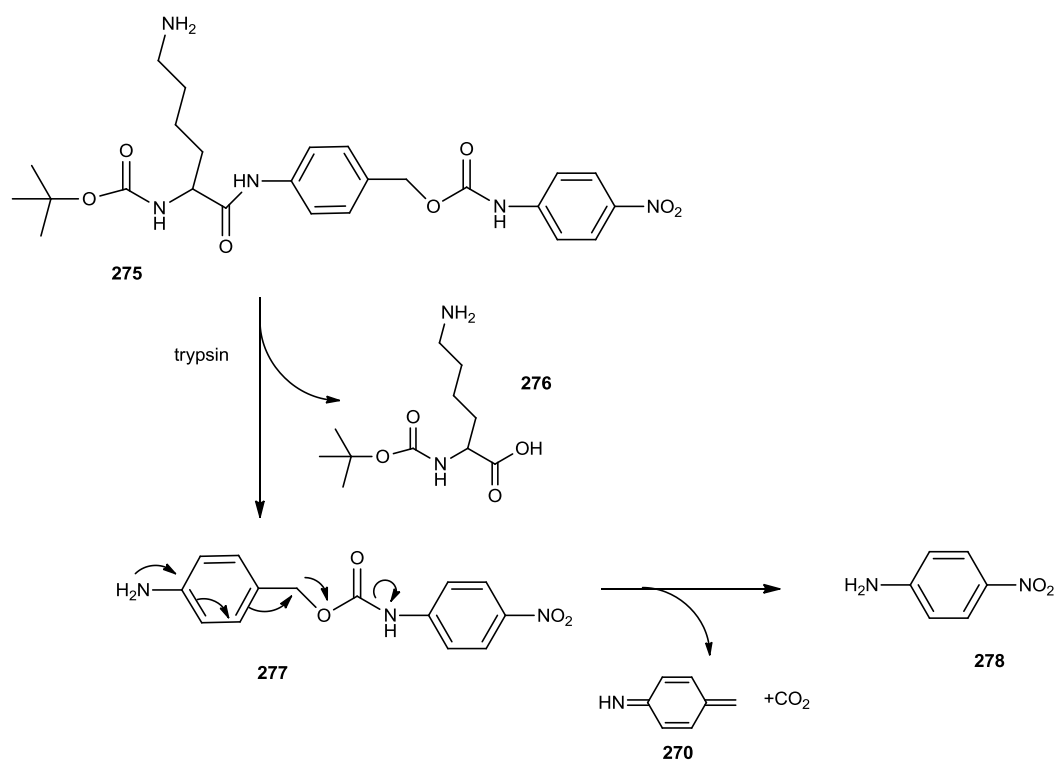
Furthermore they proved that self-immolative linkers based on PABA derivatives (the stabilising spacer is *N,N'*-dimethylethylenediamine) disassemble faster than ones with a hemithioaminal core. As a result, the PABA dyes are suitable to use to get fast-responsive probes and the hemithioaminal linker will be more useful for the preparation of tunable (bio)functionalised probes.¹¹

Noticeably Pr. Renard's group were using the commercially available *para*-aminobenzyl alcohol (PABA) as the self-immolative spacer. PABA is one of the most popular self-immolative linkers applicable in prodrug design. The pioneer in this field is Katzenellenbogen whose group described in 1981 that 4-aminobenzyl alcohol can be useful as an efficient self-immolative linker in prodrug design. In Scheme 84 is shown the design of this approach in which the linker is used as a connector between a drug and an enzymatic substrate. Noticeably, the prodrug is stable and non toxic until the enzymatic substrate is connected followed by the cleavage of substrate's bond by the enzyme to release a free active drug.¹²



Scheme 84 The design of prodrug probe in which the linker is used as a connector between a drug and an enzymatic substrate.

The utility of this self-immolative spacer was examined as well by Shabat *et al.*,¹³ they used 4-nitroaniline as a model drug and lysine as an enzymatic substrate for trypsin. In Scheme 85 is shown the reaction of trypsin with designed prodrug **275**, and as a result the release of aniline derivatives **277** was observed, which spontaneously provides azaquinonemethide **270** and free 4-nitroaniline **278**.¹³



Scheme 85 The model drug **275** and lysine as an enzymatic substrate for trypsin.

Taking all these points into account, the immolative spacer PABA was chosen as it offered the right levels of reactivity, was well-precedented in biological applications, and was commercially available.

3.1.2. Choice of the enzyme and fluorophore

After choosing the suitable spacer, confirmation of the self-immolative methodology in the context of new protease-sensitive pro-fluorescent probes was needed. It was decided to develop assays with penicillin amidase (PGA), a commercially available and widely used biocatalyst which is used in the enzymatic synthesis of β -lactam antibiotics; since it allows the deprotection of phenacetyl protected amines. This type of enzyme is not expensive, and is readily manageable in an immobilized form. Moreover, it is stable even if using reasonable amount of organic solvents (acetone or methanol, up to 40-50% in water) and can be widely used to react (either in solution or on solid phase) as a suitable reagent or catalyst in organic synthesis.¹⁴ Most known

examples include the selective deprotection of amino groups within complex molecular architectures (i.e. dendrimers¹⁵).¹⁶

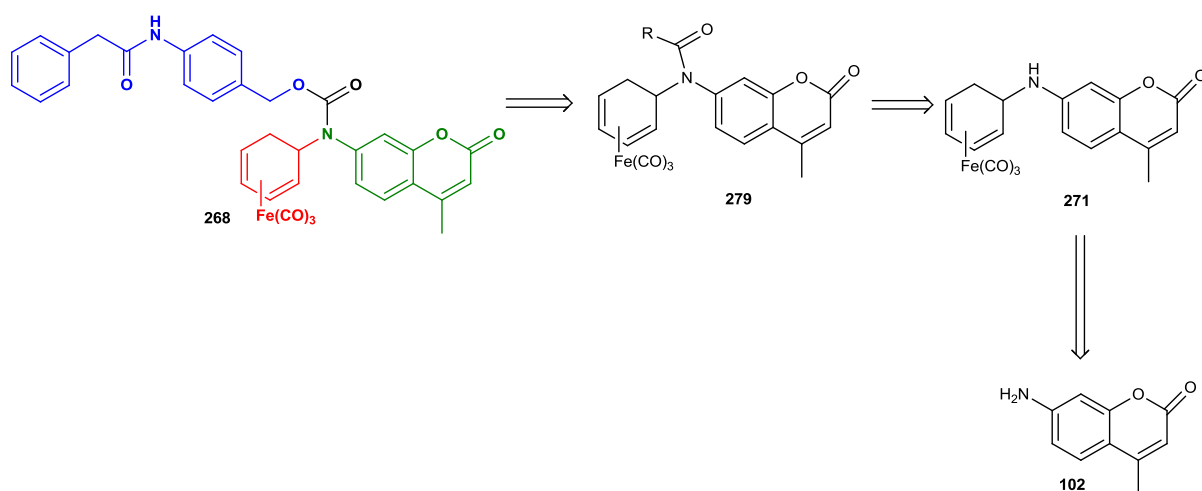
Remarkably, the studies for *in vitro* detection of PGA activity are based on the use of phenylacetamide derivatives of fluorescent amines (e.g. AMC) as fluorogenic substrates. The focus of this project is to design a novel class of PGA-sensitive pro-fluorescent probes which will check how the PABA moiety, introduced between the fluorophore and the protease-reactive group of the latent fluorophores, is fulfilling the requirements for biomolecular imaging applications:

- 1) The changes of the fluorescence intensity should be significantly increased upon reaction with the enzyme,
- 2) The bioprobe needs to be stable under physiological conditions,
- 3) The enzyme-domino reaction has to be efficient due to release the fluorophore.

The choice of the fluorophore used in the project was influenced by many factors and as *in vitro* and *in vivo* applications involve the use of fluorescent compounds exhibiting a significant emission in the range 450–750 nm (650–750 nm for *in vivo*). It was decided to work with 7-amino-4-methylcoumarin (AMC), since this fluorescent compound shows large decrease in fluorescence intensity once attached to an electron withdrawing group, is soluble in water as well as in organic media, is commercially available, and easy to handle in organic chemical reactions.¹⁶

3.2. Results and discussion

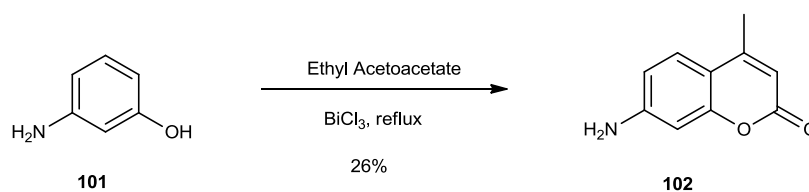
The methodology towards a preparation of the target molecule is presented as a retrosynthetic route in Scheme 86. The first step will involve the synthesis of starting materials which are 7-amino-4-methylcoumarin itself **102**, the tricarbonyliron complex derivative, and finally the introduction of the self-immolative spacer PABA. Afterwards the simple nucleophilic addition to get fluorescent derivative **271** followed by incorporation of carbonyl group in the molecule **279** which can possibly react with PABA derivative to reach a target bioprobe **268** (Scheme 86).



Scheme 86 Retrosynthetic route towards the preparation of desired bioprobe **268**.

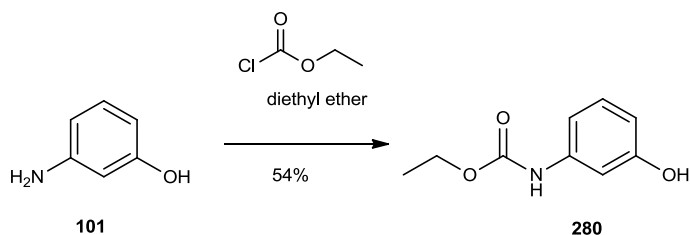
3.2.1. Preparation of 7-amino-4-methylcoumarin

Synthesis of the fluorescence reporting group **268** was investigated starting from the commercially available 3-aminophenol **101** by Pechmann condensation¹⁷ at reflux with ethyl acetoacetate in the presence of BiCl_3 as depicted in Scheme 87. Under these reaction conditions, the desired fluorophore **102** was obtained in 26% yield. The work up gave much trouble as the crude product was sticky and insoluble in most organic solvents and multicomplex products were formed.



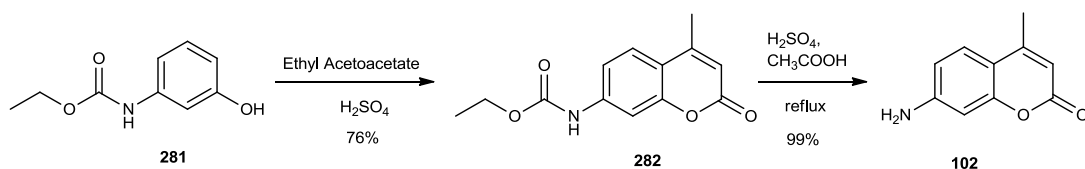
Scheme 87 Pechmann condensation to obtain fluorophore **102**.

In order to improve the yield and overcome the difficulties with the work up to isolate fluorophore **102**, after further literature investigation,¹⁸ it was decided to protect the amino group on the 3-aminophenol **101** by reaction with ethyl chloroformate in diethyl ether to obtain 3-hydroxyphenylurethane **281** (54%), Scheme 88. The reaction mixture was stirred for 2 hours at room temperature before being quenched.



Scheme 88 Protection of 3-aminophenol **101**.

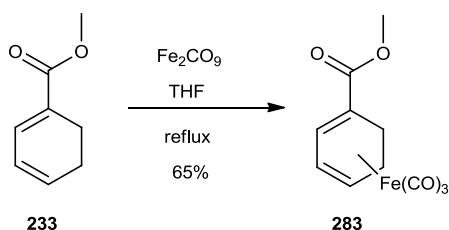
Afterwards, the addition of ethyl acetoacetate in sulphuric acid to get the protected coumarin derivative **282** in good yield (76%) was followed by the acidic deprotection of **282** which was performed by using the mixture of sulphuric acid and acetic acid at reflux for 4 hours to afford the target molecule **102** in 99% yield, Scheme 89.



Scheme 89 Improved synthetic route to obtain fluorophore **102**.

3.2.2. Preparation of tricarbonyl complex and its cation

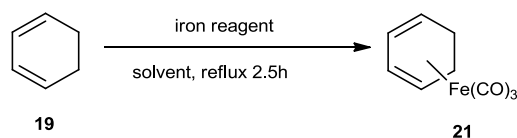
The target tricarbonyliron complexes were prepared based on the procedures reported by Birch¹⁹ and improved by Pearson *et al.*²⁰ The synthesis of tricarbonyl(η^4 -cyclohexa-1,3-dienecarboxylic acid methyl ester)iron **283** was isolated in good yield (65%) after reaction with diironnonacarbonyl in dry THF at reflux as shown in Scheme 90.



Scheme 90 Preparation of tricarbonyl iron complex **283**.

To evaluate the possibility of improved procedures, the complexation of the simple 1,3-cyclohexadiene **19** with various iron reagents using the typical reaction conditions found in the literature was also examined, Table 11. The 1,3-cyclohexadiene **19** and

iron pentacarbonyl (FeCO_5) and diironnonacarbonyl (Fe_2CO_9) in various solvents were heated at reflux for different amounts of time. Unfortunately, it was not possible to synthesise tricarbonyl(η^4 -cyclohexa-1,3-diene)iron **21** in better yield than 30%. The results are reported in Table 11.

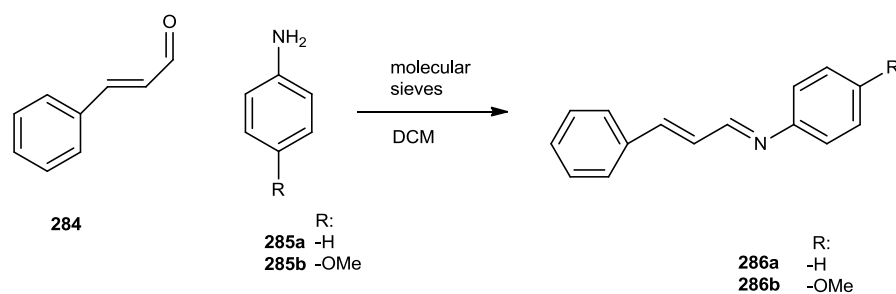


Scheme 91 Complexation of 1,3-cyclohexadiene **19** with various iron reagents to get desired **21**.

Table 11 Yields and different reaction conditions applied to Scheme 91.

Entry	Solvent	Iron Reagent	Yield (%)
1	THF	Fe_2CO_9	20%
2	Dibutyl ether	FeCO_5	15%
3	Dibutyl ether	Fe_2CO_9	20%
4	Diethyl ether	Fe_2CO_9	30%

In order to improve the reaction conditions for the iron complexation to occur in synthetically useful yields, the application of ligand exchange reagents **287a** and **287b** was investigated. Following chemistry of Pearson group,²¹ the first attempt was made using an equimolar mixture of *trans*-cinnamaldehyde **284** and suitable amine **285a** or **285b** in the presence of molecular sieves in dry DCM. The reaction was carried out overnight before solvent was removed and the products were isolated in excellent yields (Table 12, Scheme 92).

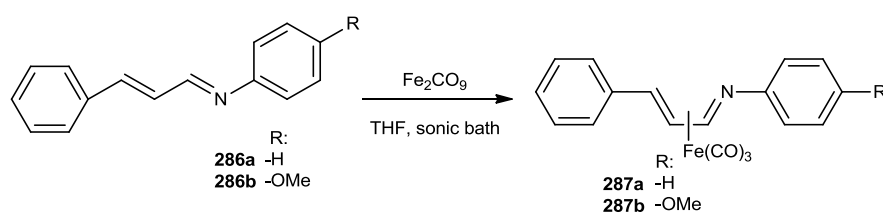


Scheme 92 Preparation of compounds **286a-b**.

Table 12 Yields applied for Scheme 92.

Entry	R	Yield (%)
1	H	89%
2	OMe	91%

Furthermore, these compounds **286a** and **286b** can be converted into ligands exchange reagents by iron complexation by using sonication of diirononacarbonyl in dry THF. This transformation also occurs in high yield as reported in Table 13, Scheme 93.²¹

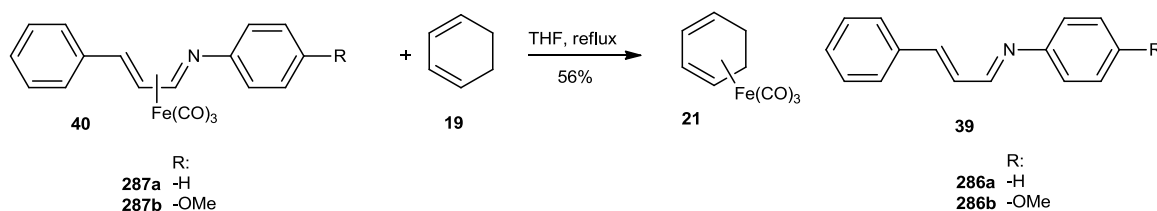


Scheme 93 Preparation of ligands exchange **287a-b**.

Table 13 Yields applied for Scheme 93.

Entry	R	Yield (%)
1	H	91%
2	OMe	97%

These two ligand exchange complexes **287a** and **287b** were used in the next step by addition of 1,3-cyclohexadiene **19** and at reflux in dry THF. The reaction mixture was refluxed for 1.5 hours before being quenched. The advantage of this reaction is that the azabuta-1,3-diene **286a** or **286b**, Scheme 94 can be recovered and reused to prepare new batches of the ligand exchange complexes. The results for this reaction are shown in Table 14.



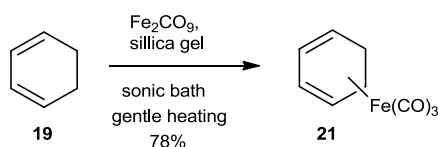
Scheme 94 Reaction with ligands exchange **287a-b** affording compound **21**.

Table 14 Yields applied for Scheme 94.

Entry	R	Yield (%)
1	H	45%
2	OMe	65%

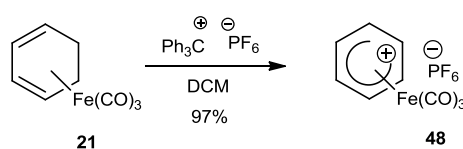
As was reported by Pearson group,²¹ the yield was increasingly improved in comparison with previous methods but it was not possible to obtain the same yield as in the literature.

Next, inspired by the Pauson group's example,²² which describes the preparation of the iron complex derivatives by using silica and without any solvent, we developed access to tricarbonyliron complexes. The desired tricarbonyl(η^4 -cyclohexa-1,3-diene)iron complex **21** was obtained in the best 78% yield through the reaction of the starting 1,3-cyclohexadiene **19** with silica gel in the presence of diironnonacarbonyl by gentle heating in a sonic bath, Scheme 95.



Scheme 95 Preparation of tricarbonyliron complex **21**.

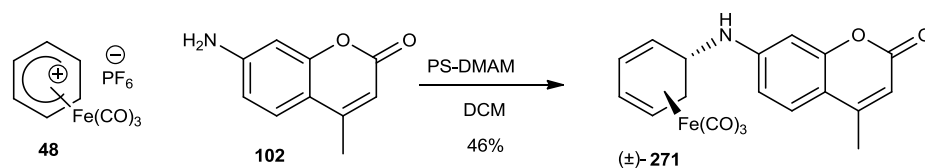
For the next step, following the classic²³ method, the desired tricarbonyl(η^5 -cyclohexa-1,3-dienylium)iron hexafluorophosphate product **48** was obtained in a good 97% yield by hydride abstraction from the starting tricarbonyliron complex **21** with triphenylcarbenium hexafluorophosphate in dry DCM. The reaction mixture was stirred for 1 hour before being quenched to obtain product **48** (Scheme 96) as yellow crystals.



Scheme 96 Preparation of salt **48**.

3.2.3. Preparation of the core of the molecule

The new fluorescent compound (\pm)-**271** was prepared by reaction of electrophilic cation **48** with 7-amino-4-methylcoumarin **102** in dry DCM in the presence of dimethylaminomethyl-polystyrene in modest 46% yield (Scheme 97).



Scheme 97 Preparation of fluorescent compound (\pm)-**271**.

The fluorescence properties of the new tricarbonyliron complex (\pm)-**271** were studied. The absorption spectrum in DMSO at 25°C indicates the absorbance maximum at 350 nm and emission at 446 nm (Figure 48) and, from a series of measurements at different concentrations, a quantum yield of 58% was calculated for compound (\pm)-**271**.

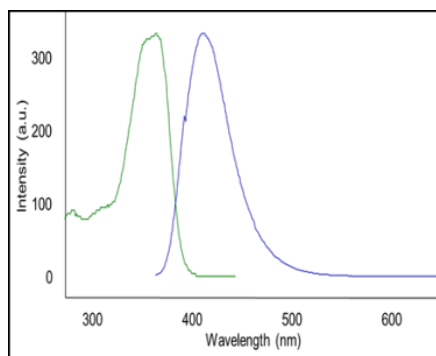
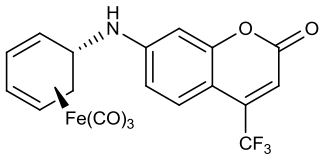
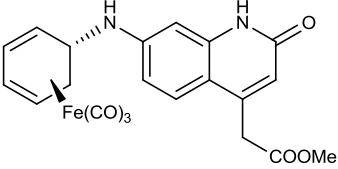
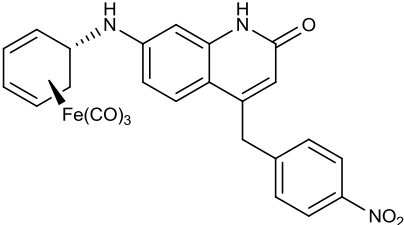
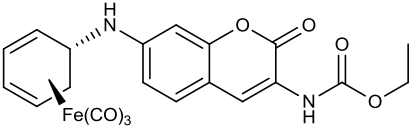
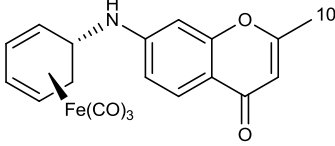


Figure 48 The excitation (350 nm) and emission (446 nm) spectra for compound (±)-**271**.

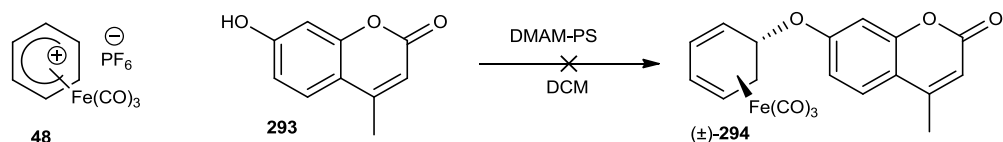
Satisfyingly, although most of the fluorophores can display fluorescence quenching in the presence of organometallic species²⁴, it was noted that (±)-**271** showed almost the same fluorescent properties as the 7-aminocoumarin itself. In order to further exploit this methodology, the scope and limitation of this reaction was investigated. The same reaction conditions were used for different types of aminocoumarins (commercially available). The results of this reaction are shown in Table 15.

Table 15 Yields for fluorescent dyes (\pm)-**288-292** by using different substrates.

Entry	Product	Yield (%)
1		(\pm)- 288 74%
2		(\pm)- 289 0%
3		(\pm)- 290 0%
4		(\pm)- 291 0%
5		(\pm)- 292 86%

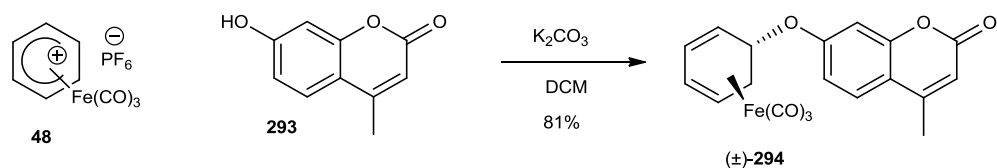
The preparation of compound (\pm)-**288** was of particular importance because it should have an enhanced quantum yield and red shift in the emission spectrum. For compound (\pm)-**289**, an increase in solubility was expected once the ester has been cleaved to a carboxylic acid. Furthermore, (\pm)-**291** can potentially be used as a scaffold for the extension of conjugation through the amine in the position 3. All of these expectations are under current investigations within our group.

Noteworthy, as for the nitro compound (\pm)-**290**, the application of this methodology to 7-hydroxy-4-methylcoumarine **293** failed to give the expected compound (\pm)-**294**, Scheme 98.



Scheme 98 Unsuccessful application of previous methodology to 7-hydroxy-4-methylcoumarin **293**.

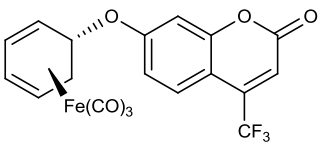
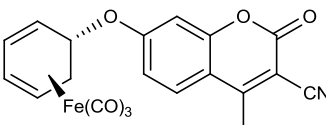
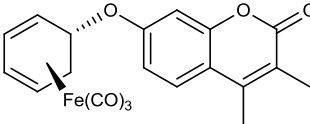
This failure was assigned to the greater fragility of the 7-hydroxycoumarin moiety **293** (as compared to 7-aminocoumarin moiety **102**) in presence of amines (both through base-mediated lactone ring opening, and 1-4 addition on the alpha-beta unsaturated ester moiety). In order to modify this methodology for the synthesis of 7-hydroxy-4-methylcoumarin derivatives, the effects of changing the supported base was evaluated. For this purpose, 7-hydroxy-4-methylcoumarin **293** was reacted with cation **48** by using potassium carbonate in dry DCM to achieve the target molecule (±)-**294** in great yield (81%) (Scheme 99).



Scheme 99 Preparation of fluorescent compound (±)-**294**.

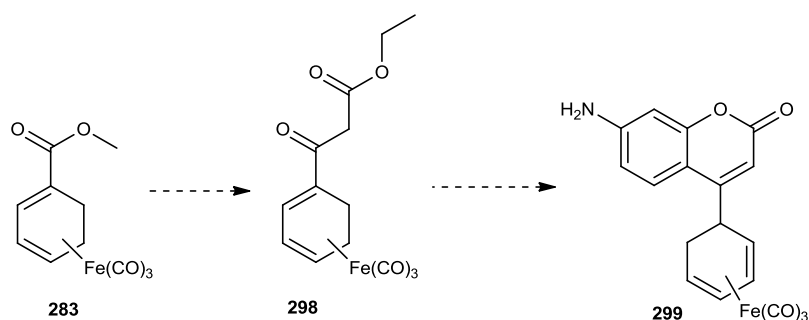
The further exploitations of these reaction conditions were investigated. As previously, using different types of 7-hydroxycoumarin (which were commercially available) under the same reaction conditions, gave the results shown in Table 16.

Table 16 Yields for fluorescent dyes (\pm)-**295-297** by using different substrates.

Entry	Product	Yield (%)
1		(\pm)- 295 78%
2		(\pm)- 296 0%
3		(\pm)- 297 0%

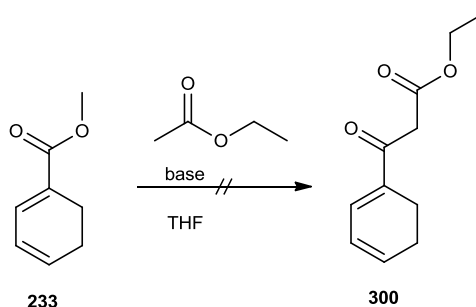
Although the reaction gave (\pm)-**295** in satisfactory yield, this reaction fate seems to be very sensitive as far as the substrate is concerned since (\pm)-**297** and (\pm)-**294** only differ by a single additional methyl group.

Finally the investigation of an alternative synthesis towards the series of 7-aminocoumarine derivative **299** which will contain the tricarbonyliron moiety in position 4, since these “carbon-linked” structures might be more robust in physiological conditions than the heteroatom-linked alternatives described above, where, particularly in the oxygen-linked series the C-O bond next to the diene complex would be labile under acidic conditions. For this purpose, the construction of the aminocoumarin moiety directly starting from already obtained iron complex **283** was envisaged, and then using a Claisen condensation to give the beta keto ester **298**, required for the Pechmann condensation, which would be followed by addition of 3-aminophenol as depicted Scheme 100.



Scheme 100 Synthetic route towards new fluorescent compound **299**.

However, starting from the previously prepared cyclohexa-1,3-dienecarboxylic acid methyl ester **233**, problems were encountered with the proposed Claisen step²⁵ when addition of ethyl acetate in the presence of different bases was investigated. The different bases were assayed for this reaction. The base was added at 0°C to the ethyl acetate/**233** reaction mixture in dry THF. The reaction was stirred at room temperature for three hours before being quenched. Under these reaction conditions the desired compound **300** was not obtained, whichever base was used (Table 17, Scheme 101).

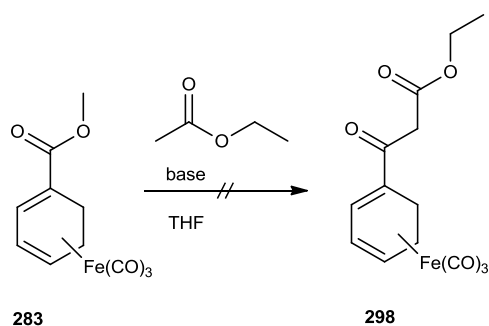


Scheme 101 Preparation of compound **300**.

Table 17 Yields applied for Scheme 89.

Entry	Base	Yield (%)
1	<i>n</i> -BuLi	0%
2	NaH	0%
3	LiHMDS	0%
4	NaHMDS	0%

After these unsuccessful attempts, the previously prepared tricarbonyl(cyclohexa-1,3-dienecarboxylic acid methyl ester)iron complex **283** was used under the same reaction conditions. Again, the desired product **298** was not formed under the conditions listed in Table 18, Scheme 102.

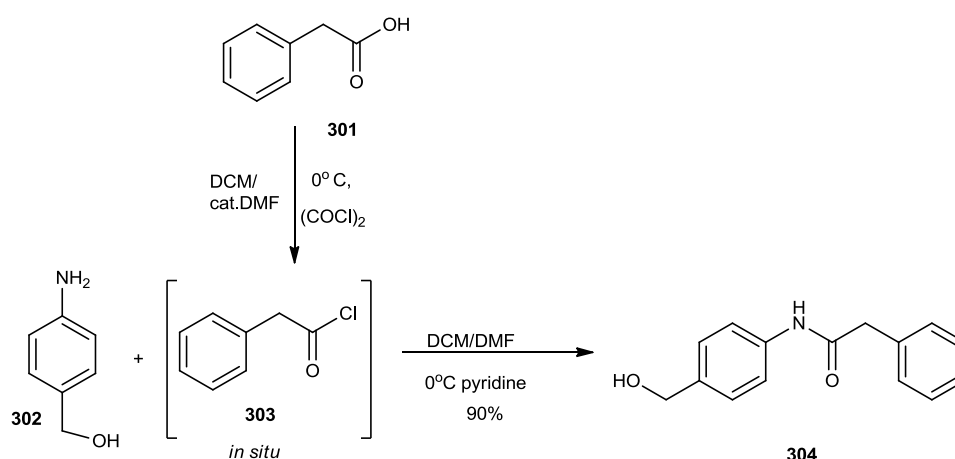
**Scheme 102** Unsuccessful attempt to obtain compound **298**.**Table 18** Yields applied for Scheme 102.

Entry	Base	Yield (%)
1	<i>n</i> -BuLi	0%
2	NaH	0%
3	LiHMDS	0%
4	NaHMDS	0%

At this stage in the project, with the oxygen-linked and nitrogen-linked structures available, the preparation of the linker and fluorophore building blocks were performed. This allowed time to make an initial study of the assembly of the first generation of tricarbonyliron-containing self-immolative linker-based biosensors, to permit their initial evaluation with their target enzyme systems. Successful results in that part of the project would then justify renewed efforts with the more stable carbon-linked structures, which, because of improved stability, might prove more practical in real applications.

3.2.4. Preparation of PABA linker

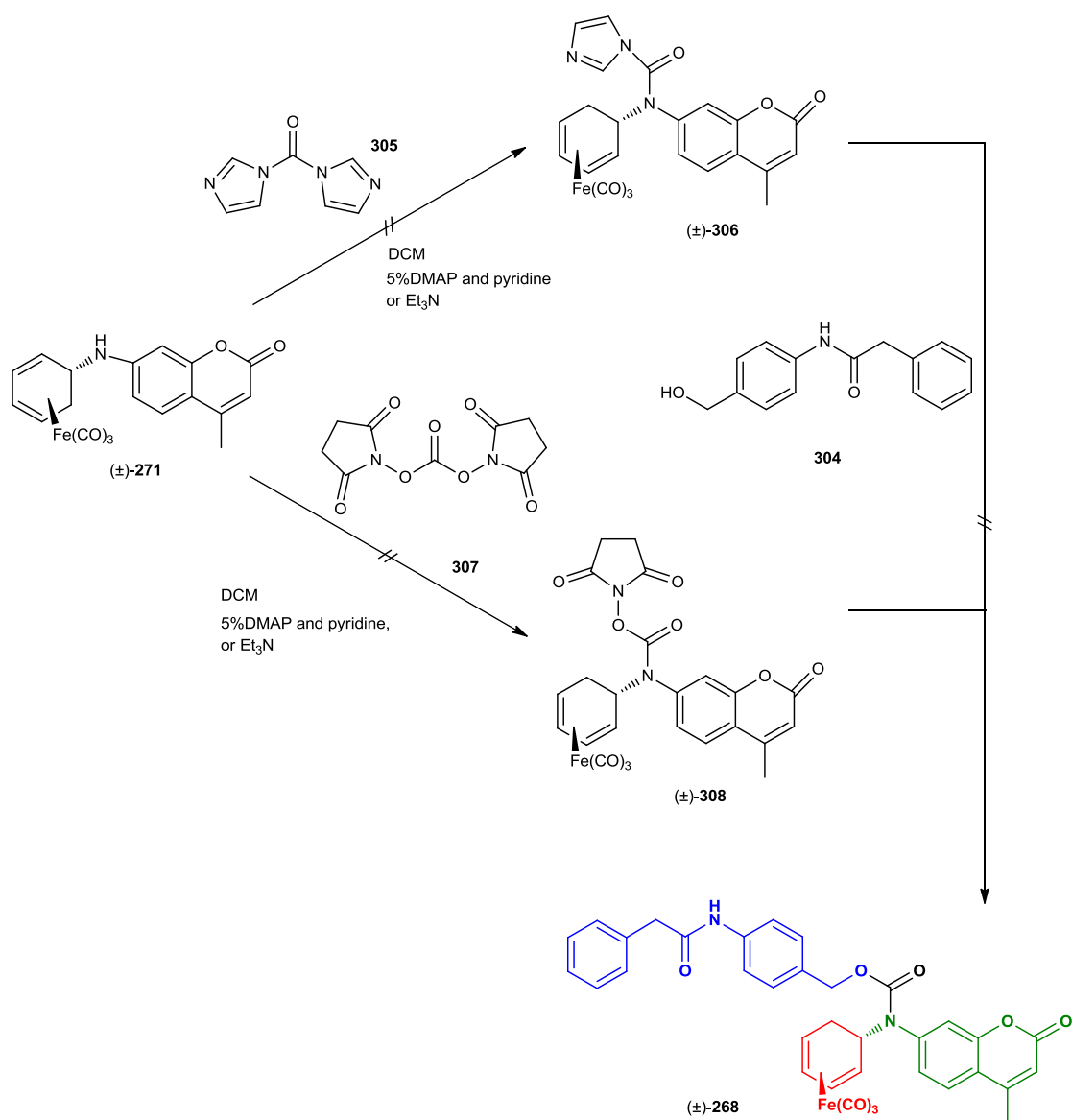
In order to prepare the self-immolative spacer phenylacetamide **304**, firstly the phenylacetyl chloride **303** was synthesised, by treatment of phenyl acetic acid **301** with oxalyl chloride in dry DCM with catalytic DMF, at 0° C.²⁶ The reaction mixture was stirred for 3 hours before being quenched. The phenylacetyl chloride **303** was used directly in the next step of the synthesis in a reaction with *p*-aminobenzyl alcohol (PABA) **302** in the presence of pyridine in a mixture of dry DCM and DMF to obtain in good yield (90%) the expected product **304** (Scheme 103).



Scheme 103 Preparation of PABA derivative **304**.

3.2.5. Preparation of target molecule (±)-268

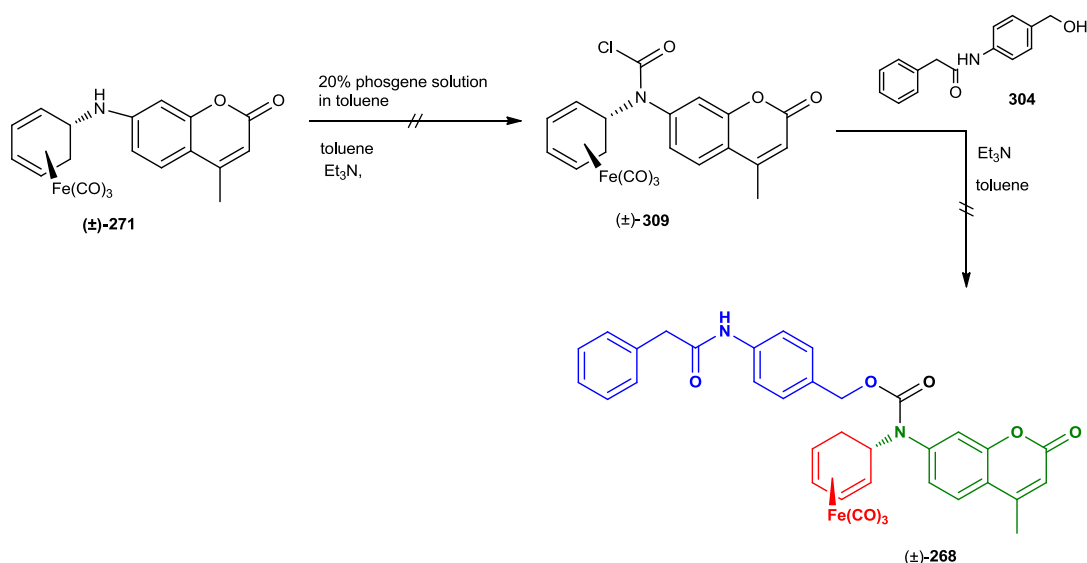
Despite the unsolved difficulties with the Claisen route to the carbon-linked 4-substituted series of regioisomers, with the nitrogen- and oxygen-linked tricarbonyliron-containing coumarins in hand (see Tables 15 and 16), and with all the other main parts needed to construct the target molecule now available, the investigation of the synthesis of the proposed novel pro-fluorescent bioprobes was performed. Two routes were investigated for this purpose. As a first attempt, it was decided to use the *N,N'*-carbonyldiimidazole - CDI²⁷ **305** with previously prepared (±)-tricarbonyl[7-(cyclohexa-2,4-dien-1-ylamino)-4-methyl-2H-chromen-2-one]iron **271** in dry DCM, in the presence of 5% of DMAP and pyridine, or triethylamine, but this failed to give compound (±)-**268**. The replacement of CDI **305** by *N,N'*-disuccinimidyl carbonate - DSC²⁸ **307** shown in Scheme 104 also did not allow to synthesise the carbamate (±)-**268**. This failure was assigned to the low nucleophile character of the aniline combined with the further electronic effect of the iron tricarbonyl complex.



Scheme 104 Synthetic route towards target compound (±)-268.

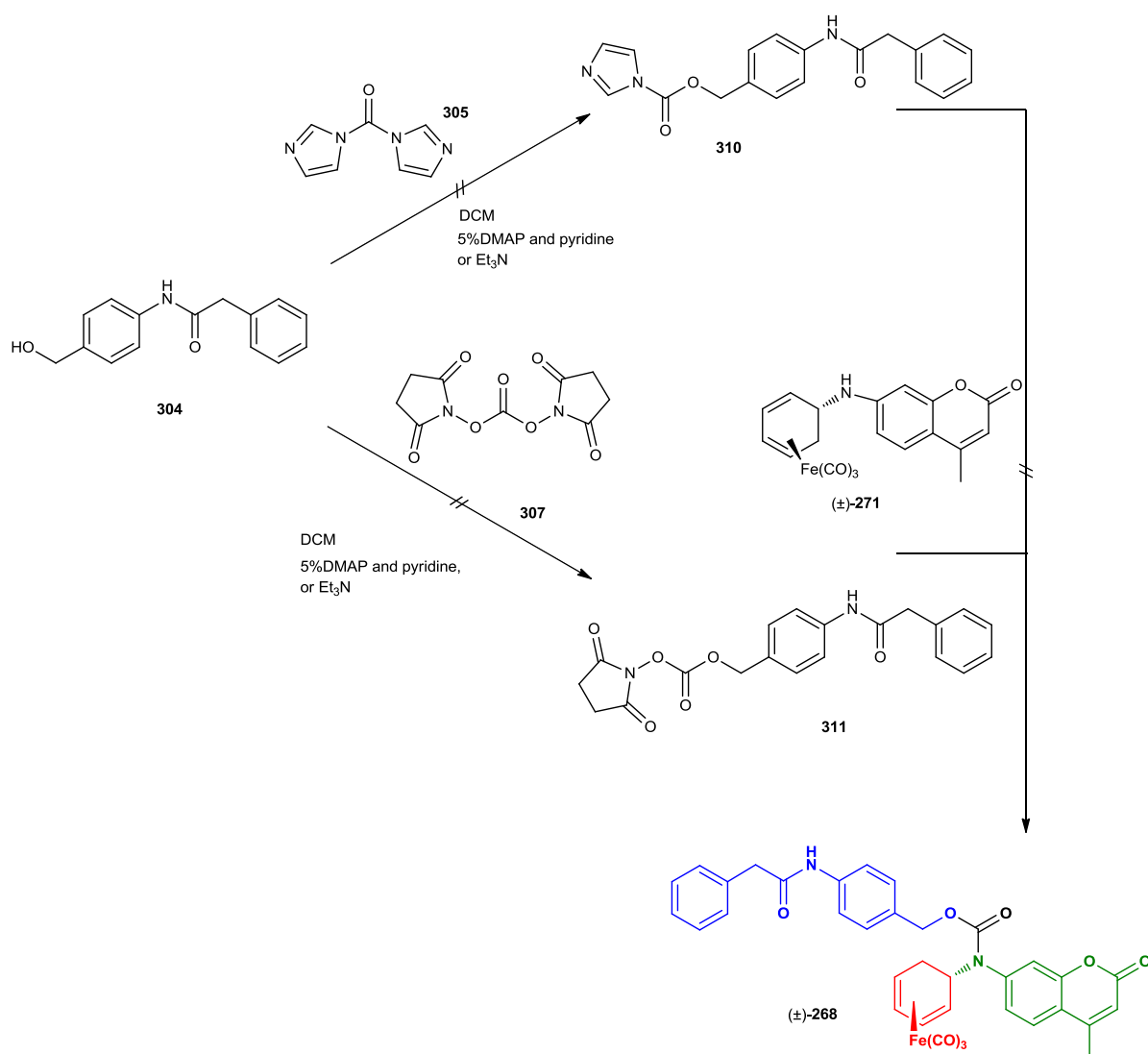
It was decided to use a more electrophilic counterpart, namely phosgene, although this reactant displays high toxicity. The last attempt for this route included the use of (±)-tricarbonyl[7-(cyclohexa-2,4-dien-1-ylamino)-4-methyl-2H-chromen-2-one]iron **271** in dry toluene followed by addition of phosgene solution (20%) in the presence of triethylamine as a supporting base.²⁹ The reaction mixture was stirred for 3 hours at room temperature. Afterwards, phenylacetamide **304** in dry toluene was added to the reaction mixture. Unfortunately this methodology, as in the previous attempts, failed to give desired target molecule (±)-**268**, Scheme 105. This procedure, when applied to

the substrate, led to mixture of compounds, which could not be identified. Similarly, the reaction failed to proceed when using reflux or longer reaction times.



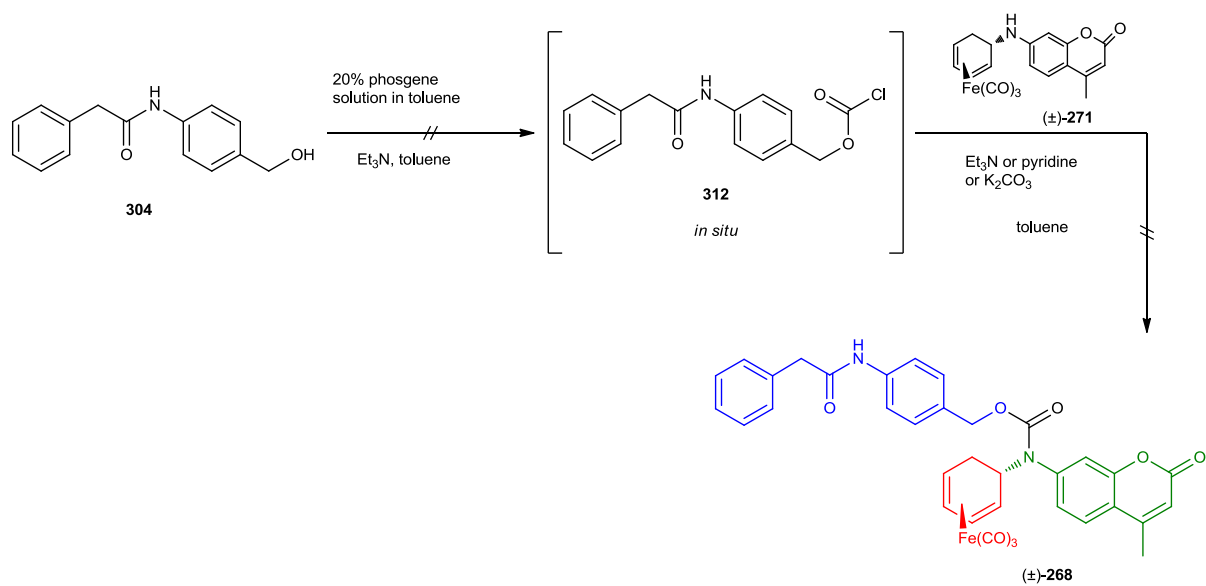
Scheme 105 Unsuccessful route towards the preparation of target molecule (±)-268 using phosgene.

It was therefore decided to investigate an alternative route, featuring the reaction of PABA derivatives with different reagents as a first step. Utilisation of the N,N' -carbonyldiimidazole - CDI **305** in dry DCM, in the presence of 5% of DMAP and pyridine, or triethylamine failed to give compound **310**. Afterwards, the use of CDI **305** by N,N' -disuccinimidyl carbonate - DSC **307** was checked but this also did not allow the synthesis of the carbamate (±)-268 (Scheme 106).



Scheme 106 Unsuccessful route towards the preparation of target molecule (±)-**268** using CDI **305** and DSC **307**.

In the last attempt, phenylacetamide **304** was used in the presence of triethylamine as a base followed by addition of 20% phosgene solution in dry toluene at 0 °C, Scheme 107. The reaction mixture was stirred for 4 hours before being quenched. Afterwards, the (±)-tricarbonyl[7-(cyclohexa-2,4-dien-1-ylamino)-4-methyl-2H-chromen-2-one]iron **271** in dry toluene was added and the reaction mixture was stirred additional 3 hours at room temperature. As previously, the reaction failed to proceed when varying the supporting bases or upon reflux or even longer reaction time.



Scheme 107 Alternative attempted route towards the preparation of target molecule (±)-268.

3.3. Conclusion

Despite the fact that it was not possible to achieve, in the time available, the synthesis of the final target molecules, the work described in this section of the thesis has further extended the definition of the scope and limitations of the commonly used tricarbonyliron chemistry when challenged by the demands of real target molecule synthesis. The novel intended applications of the target molecules as bioprobes mean that previously unexplored functionality (boronates in project 1, and now coumarins in project 2) are included in the targets, which in earlier typical cases where the tricarbonyliron methodology has been employed, have focused on natural product targets (e.g. terpenes³⁰, alkaloids³¹ in the cyclohexadienyliron series, and HETEs³² in the case of acyclic complexes). Despite the difficulties described above, in the early stage of the organoiron route, successful development of an alternative method of preparation of these complexes was achieved, which can now be applied in future synthetic work. Turning to coumarin chemistry, the reactivity of the well-known electrophilic cyclohexadienyliron complexes was checked by the reaction with 7-amino-4-methylcoumarin **102** to obtain a new fluorescent compound (\pm)-**271**. The methodology has been successfully applied to the preparation of novel series of fluorescent compounds (\pm)-**288**, (\pm)-**291**, (\pm)-**292**, (\pm)-**294**, (\pm)-**295**, which could be regarded as valuable precursors in prodrug applications. The confirmation of the retained fluorescent properties of one of these novel organometallic derivatives is itself an important achievement, providing the information needed to plan their application in further examples of bioprobe-based procedures.

3.4. References

- ¹ H. M. Ma, U. Jarzak, W. Thiemann, *New. J. Chem.*, **2001**, 25, 872-874.
- ² N. Johnsson, K. Johnsson, *ACS Chem. Biol.*, **2007**, 2, 31-38.
- ³ A. P. de Silva, H. Q. N. Gunaratne, T. Gunnlaugsson, A. J. M. Huxley, C. P. McCoy, J. T. Rademacher, T. E. Rice, *Chem. Rev.*, **1997**, 97, 1515-1566.
- ⁴ L. Prodi, F. Boletta, M. Montalti, N. Zaccheroni, *Coord. Chem. Rev.*, **2000**, 205, 59-83
- ⁵ X. Chen, M. Sun, H. Ma, *Current Organic Chemistry*, **2006**, 10, 477-489.
- ⁶ R. P. Haugland, M. T. Z. Spence, I. D. Johnson, A. Basey, *A Guide to Fluorescent Probes and Labeling Technologies*, 10th ed., Molecular Probes, Eugene, **2005**.
- ⁷ S. Brase, S. Dahmen, *Chem. Eur. J.*, **2000**, 6, 1899-1905.
- ⁸ C. Gil, S. Brase, *Curr. Opin. Chem. Biol.* **2004**, 8, 230-237.
- ⁹ S. F. Mayer, W. Kroutil, F. Kurt, *Chem. Soc. Rev.*, **2001**, 30, 332-339.
- ¹⁰ Y. Meyer, J.-A. Richard, M. Massonneau, P.-Y. Renard, A. Romieu, *Org. Lett.*, **2008**, 10, 1517-1520.
- ¹¹ J.-A. Richard, M. Massommeau, P.-Y. Renard, A. Romieu, *Org. Lett.*, **2008**, 10, 4175-4178.
- ¹² P. L. Carl, P. K. Chakravarty, J. A. Katzenellenbogen, *J. Med. Chem.*, **1981**, 24, 179-180.
- ¹³ R. Erez, D. Shabat, *Org. Biomol. Chem.*, **2008**, 6, 2669-2672.
- ¹⁴ M. Ninkovic, D. Riester, F. Wirsching, R. Dietrich, A. Schwienhorst, *Anal. Biochem.*, **2001**, 292, 228-233.
- ¹⁵ A. Gopin, S. Ebner, B. Attali, D. Shabat, *Bioconjugate Chem.*, **2006**, 17, 1432-1440.
- ¹⁶ J.-A. Richard, Y. Meyer, V. Jolivel, M. Massonneau, R. I. Dumeunier, D. Vaudry, H. Vaudry, P.-Y. Renard, A. Romieu, *Bioconjugate Chem.*, **2008**, 19, 1707-1718.
- ¹⁷ S. K. De, R.A. Gibbs, *Synthesis*, **2005**, 1231-1233.
- ¹⁸ R. L. Atkins, D. E. Bliss, *J. Org. Chem.*, **1978**, 43, 1975-1980.
- ¹⁹ A. J. Birch, P. E. Cross, J. Lewis, D. A. White, S. B. Wild, *J. Chem. Soc. (A)*, **1968**, 332-340.
- ²⁰ A. J. Pearson, *Tetrahedron*, **2010**, 66, 4943-4946.

-
- ²¹ H.-J. Knolker, G. Baum, N. Foitzik, H. Goesmann, P. Gonser, P. G. Jones, H. Rottele, *Eur. J. Inorg. Chem.*, **1998**, 993-1007.
- ²² G. F. Docherty, G. R. Knox, P. L. Pauson, *J. Org. Chem.*, **1998**, 568, 287-290.
- ²³ A. J. Birch, D. H. Williamson, *J. Chem. Soc., Perkin Trans. 1*, **1973**, 1892-1900.
- ²⁴ J. R. Lakowicz, *Principles of Fluorescence Spectroscopy*, Third Edition, Springer Science & Business Media, 5 Dec, **2007**.
- ²⁵ J. B. Tingle, E. E. Gorsline, *J. Am. Chem. Soc.*, **1908**, 40, 46-88.
- ²⁶ J. A. Richard, Y. Meyer, V. Jolivel, M. Massonneau, R. Dumeunier, D. Vaudry, H. Vaudry, P.-Y. Renard, A. Romieu, *Bioconjugate Chem.*, **2008**, 19, 1707-1718.
- ²⁷ E. K. Woodman, J. G. K. Chaffey, P. A. Hopes, D. R. J. Hose, J. P. Gilday, *Organic Process Research and Development*, **2009**, 13, 106-113.
- ²⁸ M. Morpurgo, E. A. Bayer, M. Wichek, *J. Biochem. Biophys. Meth.*, **1999**, 38, 17-28.
- ²⁹ H. Babad, A. G. Zeiler, *Chem. Rev.*, **1973**, 73, 75-91.
- ³⁰ a) A. J. Pearson, M. K. O'brien, *J. Org. Chem.*, **1989**, 54, 4663-4673; b) A. J. Pearson, P. Ham, W. O. Chi, T. R. Perrior, D. C. Rees, *J. Chem. Soc., Perkin Trans. 1*, **1982**, 1527-1534.
- ³¹ G. B. Marini-Bettolo, J. Schmutz, *Helv. Chim. Acta*, **1959**, 42, 2146-2155.
- ³² E. J. Goetzl, *Immunology.*, **1980**; 40, 709-719.

CHAPTER 4:

Experimental Part

4.1. General Methods

Chemicals of reagent grade were used as purchased unless stated otherwise. When mentioned as distilled, THF, Et₂O, and DME were freshly distilled from sodium benzophenone ketyl. DCM and acetonitrile were distilled from calcium hydride. Toluene was distilled from sodium. All non-aqueous reactions were carried out under oxygen-free nitrogen or argon using flame-dried glassware. Flash column chromatography was carried out using Davisil LC60A 40-63 micron silica (amorphous silicon dioxide). Thin layer chromatography was carried out using commercially available Macherey-Nagel pre-coated TLCsheets (ALUGRAM® SIL G/UV254 silica plates). Proton and carbon NMR spectra were recorded on a Varian UNITYplus 400 MHz spectrometer with a 5 mm Inverse detect broad band z-gradient probe, a Bruker Avance III nanobay 400 MHz spectrometer with a 5 mm broad band observe BBFOplus probe fitted with an actively shielded z-gradient coil and Bruker Avance III 500 MHz spectrometer with a 5 mm broad band observe BBFOplus smart probeTM fitted with an actively shielded z-gradient coil (500 MHz). NMR signals were measured using the residual non-deuteriated NMR solvent signal as a reference (for ¹H NMR, CDCl₃ at 7.27 ppm DMSO-d₆ at 2.50 ppm, CD₃CN at 1.94 ppm, and CD₃OD at 3.31 ppm). For ¹³C NMR, the signals of CDCl₃ at 77.0 ppm, DMSO-d₆ at 39.51 ppm, CD₃CN at 118.26 ppm, and CD₃OD at 49.00 ppm were used. Melting points were measured on a Buchi melting point B-545 apparatus. Infra-red spectra were recorded on a Perkin Elmer Spectrum 100 FT-IR spectrometer. The specific rotations were measured on an ADP 440 polarimeter from Bellingham + Stanley, and were measured in DCM at 15 mg mL⁻¹ unless otherwise stated. Chemical ionisation and high resolution mass spectra were measured at the EPSRC Mass Spectrometry Centre at the University of Wales, Swansea.

Protocol for handling and storage of Diironnonacarbonyl and Pentacarbonyliron:

- Diironnonacarbonyl and pentacarbonyliron must be stored under inert gas at -4°C in the freezer at all times. Incorrect storage results in decomposition to produce finely divided black particles of pyrophoric iron.

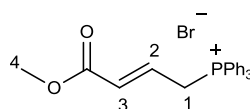
- Before use, the diironnonacarbonyl or pentacarbonyliron should be left in the fume hood for about 15-20 minutes before opening the container it is stored in, to allow the contents to come to room temperature.
- All handling of diironnonacarbonyl or pentacarbonyliron must take place in the fume hood. It must be weighed out on a balance under a blanket of argon in the fume hood. (Use an inverted funnel attached to an argon line)
- All glassware etc. that will come in contact with the diironnonacarbonyl or pentacarbonyliron should be pre-dried in an oven and then cooled in a dessicator.
- All spillages must immediately be cleaned up using acetone and all utensils used must be rinsed with acetone also. If pyrophoric iron develops and it starts to produce smoke, 1 M aqueous HCl should be used to quench the reacting iron.
- Once opened, the diironnonacarbonyl or pentacarbonyliron must be sealed under nitrogen or argon before being returned to the freezer.

Protocol for Removal and Treatment of Pyrophoric Iron, Iron Pentacarbonyl and Triirondodecarbonyl, Side Products Formed During Reaction:

- A short silica gel gravity column is performed to remove any pyrophoric iron from the reaction mixture. The silica used should then be quenched using dilute HCl and water. When safe to do so (when sufficiently diluted with water), the dilute acid solution that elutes from the column can be disposed of down the sink in the fume hood.
- Any iron pentacarbonyl formed at the end of reaction (isolated as yellow liquid in rotary evaporator trap) should be treated with the utmost care. The iron pentacarbonyl is quenched using household bleach or bromine water (prepared by shaking bromine (3g) with water (100 cm³) until a homogeneous solution is obtained) and is also disposed of down the sink when safe to do so (when sufficiently diluted with water). All glassware used is rinsed with household bleach.
- The triiron dodecarbonyl formed is a green coloured material, which is separated from the product on the second silica (flash chromatography) column. This is treated with a dilute basic solution (e.g. sodium hydroxide solution) to adjust the pH of the triiron dodecarbonyl to pH 10-11 and is then treated with bleach. This is done slowly in order to control the temperature. The resulting solution is left to stand

overnight. The solution is then adjusted to pH 7 by slow addition of dilute HCl and disposed of down the sink in the fume hood.

(3-Methoxycarbonylallyl)-triphenylphosphonium bromide (232)¹



Chemical Formula: C₂₃H₂₂BrO₂P

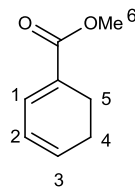
Molecular Weight: 441.2973 g/mol

Methyl-4-bromocrotonate (2.24 mL, 19.1 mmol) was added dropwise to a solution of triphenylphosphine (5.01 g, 19.1 mmol) in dry toluene (20 mL). After stirring for 2 days at room temperature, the precipitate was removed by filtration, washed with toluene and finally with petroleum ether to give the expected compound as white crystals (8.05 g, 96%).

¹H NMR (200 MHz, CDCl₃) δ 8.15 – 7.57 (Ar-*H*, m, 15H), 6.94 – 6.64 (3-*H*, m, 1H), 6.52 (2-*H*, dd, *J* = 15.5, 4.8 Hz, 1H), 5.29 (1-*H*, dd, *J* = 16.3, 1.2 Hz, 2H), 3.73 (4-*H*, s, 3H).

Data in agreement with those previously reported.¹

Cyclohexa-1,3-dienecarboxylic acid methyl ester (233)¹



Chemical Formula: C₈H₁₀O₂

Molecular Weight: 138.1638 g/mol

Saturated sodium hydrogen carbonate (108 mL) followed by acrolein (0.81 mL, 17.2 mmol) were added to a mixture of (3-methoxycarbonyl-allyl)-triphenylphosphonium bromide (7.62 g, 17.2 mmol) in DCM. The two phase reaction mixture was stirred at room temperature for 3 days. After separation of the phases, the organic phase was dried over MgSO₄, and then concentrated *in vacuo*. Purification by flash chromatography (DCM, *R_f* = 0.75) gave a colourless oil (1.25 g, 52 %).

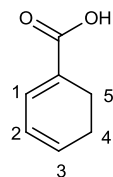
IR (NaCl) ν = 1721 (COOMe).

¹H NMR (500 MHz, CDCl₃) δ 6.99 (1-*H*, d, *J* = 5.4 Hz, 1H), 6.17 – 6.11 (2-*H*, m, 1H), 6.05 (3-*H*, ddt, *J* = 9.3, 5.4, 1.8 Hz, 1H), 3.75 (6-*H*, br. s, 3H), 2.50 – 2.40 (5-*H*, m, 2H), 2.31 – 2.22 (4-*H*, m, 2H).

¹³C NMR (126 MHz, CDCl₃) δ 168.06, 133.62, 133.36, 127.23, 124.07, 51.70, 22.97, 20.88.

Data in agreement with those previously reported.¹

Cyclohexa-1,3-dienecarboxylic Acid (234)¹



Chemical Formula: C₇H₈O₂

Molecular Weight: 124.1372 g/mol

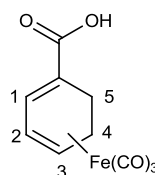
To a solution of cyclohexa-1,3-dienecarboxylic acid methyl ester (2.04 g, 14.5 mmol) in MeOH (20 mL), NaOH_(aq) was added in two portions (1M, 2x20 mL). After stirring for 3 h, the aqueous phase was washed once with petroleum ether (25 mL), acidified with concentrated aqueous HCl, and extracted with DCM (5 x 50 mL). The organic phase was dried over MgSO₄, filtered and concentrated by rotary evaporation. The residue was purified by flash chromatography (petroleum ether/ EtOAc/AcOH [79:20:1]) to afford the expected compound as white crystals (1.05 g, 59 %).

¹H NMR (500 MHz, CDCl₃) δ 7.14 (1-*H*, d, *J* = 5.4 Hz, 1H), 6.27 – 6.16 (2-*H*, m, 1H), 6.09 (3-*H*, ddt, *J* = 9.3, 5.4, 1.9 Hz, 1H), 2.52 – 2.40 (5-*H*, m, 2H), 2.37 – 2.25 (4-*H*, m, 2H).

¹³C NMR (126 MHz, CDCl₃) δ 172.96, 135.66, 134.92, 126.52, 124.10, 23.01, 20.39.

Data in agreement with those previously reported.¹

Tricarbonyl(η^4 -cyclohexa-1,3-dienecarboxylic acid)iron(235)¹



Chemical Formula: C₁₀H₈FeO₅

Molecular Weight: 264.0125 g/mol

To a slurry of diironnonacarbonyl (10.0 g, 27.5 mmol) in dry THF (15 mL) was added a solution of cyclohexa-1,3-dienecarboxylic acid (1.51 g, 11.9 mmol) in dry THF (5 mL). The reaction mixture was flushed with argon and stirred at reflux under argon for 5 h. After filtration of the mixture through a short pad of Celite, the solvent was removed *in vacuo*. **(Caution! Pentacarbonyliron is extremely toxic by inhalation).** Gradient chromatography column using a stepwise gradient of petroleum ether/EtOAc [80:20], and petroleum ether/ EtOAc/AcOH [79:20:1] afforded 1.81 g of yellow crystals (59 %).

IR (NaCl) ν =2055 (C \equiv O symmetric), 1980 (C \equiv O asymmetric), 1660 (C=O).

¹H NMR (500 MHz, CDCl₃) δ 6.07 (1-*H*, br. s, 1H), 5.39 (2-*H*, br. s, 1H), 3.42 (3-*H*, br. s, 1H), 2.33 – 2.07 (4-*H*, m, 1H), 2.06 – 1.86 (4-*H*, m, 1H), 1.80 – 1.55 (5-*H*, m, 1H), 1.52 – 1.32 (5-*H*, m, 1H).

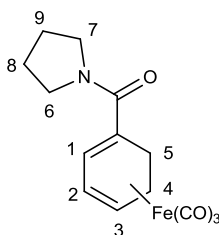
Data in agreement with those previously reported.¹

General procedures for the preparation of tricarbonyliron complexes of amide derivatives

Method A (reaction with Et₃N)²

The appropriate carboxylic acid (0.31 g, 1.14 mmol) was dissolved in dry DCM (15 mL) under argon. Two equivalents of oxalyl chloride (0.20 mL, 2.27 mmol) followed by a catalytic amount of DMF were added and reaction mixture was stirred for 2 h at room temperature. The solvent was removed *in vacuo* with a rotary evaporator (bath temperature 30 °C). The yellow oil was dried under high vacuum (6 mmHg) for 10 minutes, and then was dissolved in dry DCM (15 mL). Triethylamine (0.40 mL, 2.84 mmol, 2.5 equiv.) and the appropriate amine (2.47 mmol, 2.2 equiv.) were added and the reaction mixture was stirred at room temperature for 3-6 h (reaction monitored by TLC) to give the desired amides after flash chromatography on silica gel (Et₂O/hexane [3:1]).

Tricarbonyl[η^4 -cyclohexa-1,3-dien-1-yl(pyrrolidin-1-yl)methanone]iron (241a)



Chemical Formula: C₁₄H₁₅FeNO₄

Molecular Weight: 317.1182 g/mol

Flash chromatography (Et₂O/hexane [3:1], R_f = 0.27) gave 0.30 g, 81% of a yellowish powder.

M.p. 100-103 °C.

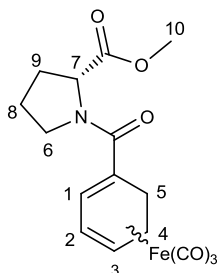
IR (NaCl) ν = 2043 (C \equiv O symmetric), 1964 (C \equiv O asymmetric), 1606 (C=O).

¹H NMR (500 MHz, CDCl₃) δ 6.16 (1-*H*, d, J = 4.0 Hz), 5.39 – 5.34 (2-*H*, dist. dd, J = 6.7, 4.0 Hz 1H), 3.82 (3-*H*, br. s, 1H), 3.63 – 3.35 (6-*H*, 7-*H*, m, 4H), 2.03 – 1.85 (8-*H*, 9-*H*, 4-*H*, m, 4H), 1.81 – 1.69 (5-*H*, m, 2H), 1.54 – 1.38 (4-*H*, m, 1H).

¹³C NMR (126 MHz, CDCl₃) δ 171.53, 85.91, 85.87, 71.79, 64.33, 48.20 (br.), 47.39, 27.06, 25.94, 23.89, 23.13.

HRMS [APCI] for [M]⁺ C₁₄H₁₄FeNO₄ requires 316.0474, found 316.0470.

Tricarbonyl[η^4 -(*R*)-methyl-1-(cyclohexa-1,3-dienecarbonyl)pyrrolidine-2-carboxylate] iron (241b)



Chemical Formula: C₁₆H₁₇FeNO₆

Molecular Weight: 375.1543 g/mol

Flash chromatography (Et₂O/hexane [3:1], *R_f* = 0.2) gave 0.29 g, 67% of a brown oil, [α]_D²⁴ = + 89 (0.0012, DCM) consisting of two diastereoisomers, as evidenced by peak doubling in the ¹H- and ¹³C- NMR spectra below.

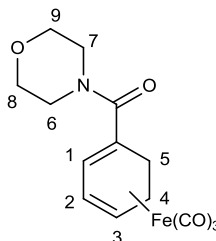
IR (NaCl) ν = 2045 (C \equiv O symmetric), 1966 (C \equiv O asymmetric), 1744 (ester C=O), 1610 (amide C=O).

¹H NMR (500 MHz, CDCl₃) δ 6.13 (1-*H*, d, *J* = 4.5 Hz, 1H), 6.12 (1-*H*, d, *J* = 4.5 Hz, 1H), 5.37 (2-*H*, dd, *J* = 5.9, 4.5 Hz, 1H), 5.32 (2-*H*, dd, *J* = 5.9, 4.5 Hz, 1H), 4.51 (7-*H*, t, *J* = 7.8 Hz, 1H), 4.45 – 4.34 (7-*H*, br. m, 1H), 3.99 – 3.87 (9-*H*, 2 overlapping m, 1H), 3.71 (10-*H*, s, 3H), 3.64 (10-*H*, s, 3H), 3.68 – 3.57 (9-*H*, 2 overlapping m, 1H), 3.44 (3-*H*, d, *J* = 5.9 Hz, 1H), 3.38 (3-*H*, d, *J* = 5.9 Hz, 1H), 2.33 – 1.69 (4-*H*, 5-*H*, 6-*H*, 8-*H*, m, 7H), 1.56 – 1.48 (4-*H*, 5-*H*, m, 1H), 1.49 – 1.39 (4-*H*, 5-*H*, m, 1H).

¹³C NMR (126 MHz, CDCl₃) δ 173.04, 172.97, 171.92, 171.83, 86.37, 86.15, 85.66, 85.44, 70.18, 69.80, 64.70, 63.75, 60.69, 60.14, 52.26, 52.09, 48.73, 48.43, 28.85, 28.72, 26.33, 26.00, 25.40, 25.38, 23.02, 22.92.

HRMS [ASAP oil] for [M⁺] C₁₆H₁₇FeNO₆ requires 376.0478, found 376.0479.

Tricarbonyl[η^4 -(cyclohexa-1,3-dienyl)-morpholin-4-yl-methanone]iron (241c)³



Chemical Formula: C₁₄H₁₅FeNO₅

Molecular Weight: 333.1176 g/mol

Flash chromatography (Et₂O/hexane, [3:1], R_f = 0.14) gave 0.36 g, 92% of a yellow solid.

M.p. 139-141 °C.

IR (NaCl) ν = 2043 (C \equiv O symmetric), 1964 (C \equiv O asymmetric), 1606 (C=O), 1409 (C=C), 1113 (C-N).

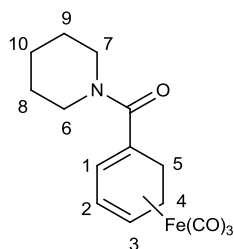
¹H NMR (500 MHz, CDCl₃) δ 6.13 (1-*H*, d, *J* = 4.0 Hz, 1H), 5.33 (2-*H*, dist. dd, *J* = 6.8, 4.0 Hz, 1H), 3.84 - 3.51 (6-*H*, 7-*H*, 8-*H*, 9-*H*, m, 8H), 3.50 - 3.44 (3-*H*, m, 1H), 1.99 (4-*H*, dddd, *J* = 15.5, 11.5, 5.3, 3.0 Hz, 1H), 1.83 (5-*H*, dd, *J* = 13.7, 8.0 Hz, 1H), 1.76 (5-*H*, dd, *J* = 13.7, 11.5 Hz, 1H), 1.45 (4-*H*, dddd, *J* = 15.5, 8.0, 5.3, 4.0 Hz, 1H).

¹³C NMR (126 MHz, CDCl₃) δ 171.99, 86.20, 85.54, 68.96, 66.85, 65.15, 45.32 (br.), 27.13, 23.56.

HRMS [+pNSI] for [M⁺] C₁₄H₁₅FeNO₅ requires 334.0372, found 334.0372.

Data in agreement with those previously reported.³

Tricarbonyl[η^4 -cyclohexa-1,3-dien-1-yl(piperidin-1-yl)methanone]iron (241d)



Chemical Formula: C₁₅H₁₇FeNO₄

Molecular Weight: 331.1448 g/mol

Flash chromatography (Et₂O/hexane [3:1], R_f = 0.43) gave 0.29 g, 75 % of yellow solid.

M.p. 89-91 °C.

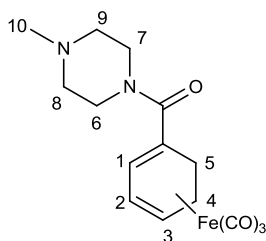
IR (NaCl) ν = 2044 (C \equiv O symmetric), 1965 (C \equiv O asymmetric), 1614 (C=O), 1429 (C=C), 1258 (C-N).

¹H NMR (500 MHz, CDCl₃) δ 6.11 (1-*H*, d, J = 4.2 Hz, 1H), 5.29 (2-*H*, dist. dd, J = 6.4, 4.2 Hz, 1H), 3.78 – 3.46 (6-*H*, 7-*H*, m, 4H), 3.46 – 3.39 (3-*H*, m, 1H), 1.99 (4-*H*, dddd, J = 15.6, 11.2, 5.6, 3.1 Hz, 1H), 1.83 (5-*H*, dd, J = 14.0, 8.0 Hz, 1H), 1.81 – 1.76 (5-*H*, br. m, 1H), 1.73 – 1.50 (8-*H*, 9-*H*, 10-*H*, m, 7H), 1.43 (4-*H*, dddd, J = 15.6, 8.0, 5.5, 4.0 Hz, 1H).

¹³C NMR (126 MHz, CDCl₃) δ 171.51, 85.74, 85.58, 70.44, 64.78, 46.23 (br.), 27.14, 26.00, 24.68, 23.77.

HRMS [ASAP] for [M⁺] C₁₅H₁₇FeNO₄ requires 332.0580, found 332.0582.

**Tricarbonyl[η^4 -cyclohexa-1,3-dien-1-yl(4-methylpiperazin-1-yl)methanone]iron
(241e)**



Chemical Formula: C₁₅H₁₈FeN₂O₄

Molecular Weight: 346.1594 g/mol

Flash chromatography (Et₂O/hexane 3:1, **R_f** = 0.43) gave 0.51 g, 74 % of yellow solid,
M.p. 101-103 °C.

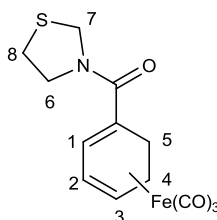
IR (NaCl) ν =2050 (C \equiv O symmetric), 1971 (C \equiv O asymmetric), 1624 (C=O), 1461, 1421 (C=C), 1263 (C-N).

¹H NMR (500 MHz, CDCl₃) δ 6.12 (1-*H*, d, *J* = 4.1 Hz, 1H), 5.30 (2-*H*, dist. dd, *J* = 6.2, 4.1 Hz, 1H), 3.97 – 3.49 (6-*H*, 7-*H*, m, 4H), 3.47 – 3.44 (3-*H*, m, 1H), 2.42 (8-*H*, 9-*H*, br. s, 4H), 2.31 (10-*H*, s, 3H), 1.99 (4-*H*, dddd, *J* = 15.0, 11.4, 5.5, 3.0 Hz, 1H), 1.82 – 1.81 (5-*H*, dd, *J* = 13.7, 8.0 Hz, 1H), 1.79 (5-*H*, dd, *J* = 13.7, 11.4 Hz, 1H), 1.47 – 1.42 (4-*H*, m, 1H).

¹³C NMR (126 MHz, CDCl₃) δ 171.71, 85.98, 85.61, 69.52, 64.98, 54.94, 46.18, 30.45, 27.19, 23.64.

HRMS [+pNSI] for [M⁺] C₁₅H₁₈FeN₂O₄ requires 347.0689, found 347.0687.

Tricarbonyl[η^4 -cyclohexa-1,3-dien-1-yl(thiazolidin-3-yl)methanone]iron (241f)



Chemical Formula: C₁₃H₁₃FeNO₄S

Molecular Weight: 335.1566 g/mol

Flash chromatography (Et₂O: hexane [3:1], R_f = 0.1) gave 0.21 g, 55 % of yellow solid.

M.p. 93-95 °C.

IR (NaCl) ν = 2050 (C \equiv O symmetric), 1979 (C \equiv O asymmetric), 1624 (C=O), 1404, 1369 (C=C), 1263 (C-N).

¹H NMR (500 MHz, CDCl₃) δ 6.11 (1-*H*, d, J = 4.2 Hz, 1H), 5.34 (2-*H*, dist. dd, J = 6.5, 4.2 Hz, 1H), 4.18 (7-*H*, s, 2H), 3.54 – 3.39 (3-*H*, m, 1H), 3.13 (8-*H* or 6-*H*, t, J = 6.4 Hz, 2H), 2.81 (8-*H* or 6-*H*, t, J = 6.4 Hz, 2H), 1.98 (4-*H*, dddd, J = 15.1, 11.0, 5.8, 3.1 Hz, 1H), 1.83 (5-*H*, dd, J = 14.0, 11.0 Hz, 1H), 1.79 (5-*H*, dd, J = 14.1, 8.0 Hz, 1H), 1.54 – 1.35 (4-*H*, m, 1H).

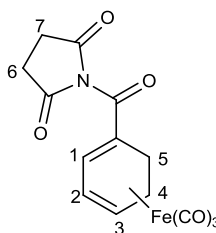
¹³C NMR (126 MHz, CDCl₃) δ 171.86, 86.29, 85.37, 71.28, 64.88, 58.67, 55.94, 30.07, 26.62, 23.26.

HRMS [+pNSI] for [M⁺] C₁₃H₁₃FeNO₄S: requires 335.9991, found 335.9987.

*Method B (Reaction with NaH)*⁴

The appropriate carboxylic acid (0.31 g, 1.17 mmol) was dissolved in dry DCM (15 mL) under argon. Two equivalents of oxalyl chloride (0.20 mL, 2.35 mmol) were added and reaction mixture was stirred for 2 h at room temperature. The solvent was removed under vacuum (bath temperature 30°C). The resultant yellow oil was dried under high vacuum (6 mmHg) for 10 minutes, and then was dissolved in dry THF. The mixture was added to a suspension of sodium hydride (0.07 g, 2.94 mmol, 2.5 equiv.) and the amine (0.26 g, 2.68 mmol, 2.2 equiv.) in dry THF. The mixture was stirred at room temperature for 3h (reaction was monitored by TLC) to give the desired amide after extraction with diethyl ether (3 x 15 mL), followed by flash chromatography on silica gel.

Tricarbonyl[η^4 -1-(cyclohexa-1,3-dienecarbonyl)pyrrolidine-2,5-dione]iron (241j)



Chemical Formula: C₁₄H₁₁FeNO₆

Molecular Weight: 345.0852 g/mol

Flash chromatography (Et₂O: hexane, 3:1, *R_f* = 0.32) gave 0.37 g, 95 % of yellow solid.

M.p. 165-167 °C.

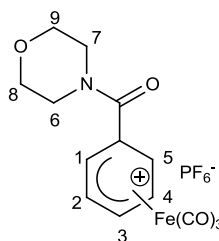
IR (NaCl) ν = 2064 (C \equiv O), 1989 (C \equiv O), 1725 (C=O), 1696 (C=O), 1335 (C=C), 1257 (C-N).

¹H NMR (500 MHz, CDCl₃) δ 6.19 (1-*H*, d, *J* = 3.9 Hz, 1H), 5.46 (2-*H*, dd, *J* = 6.6, 3.9 Hz, 1H), 3.51 (3-*H*, s, 1H), 2.78 (6-*H*, 7-*H*, s, 4H), 1.95 (4-*H*, dddd, *J* = 15.1, 11.0, 5.7, 3.5 Hz, 1H), 1.79 (5-*H*, dd, *J* = 14.2, 8.5 Hz, 1H), 1.71 (5-*H*, ddd, *J* = 14.2, 11.0, 2.5 Hz, 1H), 1.54 (4-*H*, dddd, *J* = 15.1, 8.5, 5.5, 3.3 Hz, 1H).

¹³C NMR (126 MHz, CDCl₃) δ 174.55, 173.44, 88.67, 86.94, 66.87, 63.83, 29.16, 26.25, 22.21.

HRMS [APCI] for [M⁺] C₁₄H₁₁FeNO₆ requires 346.0009, found 346.0008.

**Tricarbonyl[η^5 -5-(morpholine-4-carbonyl)cyclohexa-2,4-dien-1-ylum]iron
hexafluorophosphate (242c)**



Chemical Formula: C₁₄H₁₉F₆FeNO₅P

Molecular Weight: 482.1135 g/mol

Following the procedure reported by Birch *et al.*,⁵ to a solution of tricarbonyl-[(cyclohexa-1,3-dienyl)-morpholin-4-yl-methanone]iron (0.54 g, 1.62 mmol) in dry DCM (15 mL) was added to a solution of triphenylcarbenium hexafluorophosphate (0.75 g, 1.95 mmol, 1.2 equiv.) in dry DCM (15 mL). The reaction mixture was stirred for 40 minutes at room temperature and poured into wet Et₂O. The resulting yellow precipitate was washed twice with Et₂O (15 mL) and dried *in vacuo* to provide 0.35 g of yellow crystals in 70 % yield.

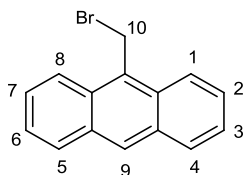
IR (NaCl) ν = 2118 (C \equiv O symmetric), 2063 (C \equiv O asymmetric), 1634 (C=O), 839 (P-F).

¹H NMR (500 MHz, CD₃CN) δ 6.98 (2-*H*, t, *J* = 5.2 Hz, 1H), 6.12 (1-*H*, d, *J* = 5.2 Hz, 1H) 5.78 (3-*H*, dist. dd, *J* = 5.2, 7.0 Hz, 1H), 4.40 (4-*H*, dist dd, *J* = 6.3, 7.0 Hz, 1H), 3.71 – 3.49 (6-*H*, 7-*H*, 8-*H* or 9-*H*, m, 6H), 3.24-(8-*H* or 9-*H*, m, 2H), 2.22 (5-*H*, br. s, 1H), 2.18 (5-*H*, br. s, 1H).

¹³C NMR (126 MHz, CD₃CN) δ (C-N inside the morpholine ring is not observed), 165.47, 102.76, 101.73, 85.96, 81.64, 66.91, 64.28, 27.78.

HRMS [+pNSI] for [M⁺] C₁₄H₁₄FeNO₅ requires 332.0216, found 332.0217.

9-Bromomethylantracene (249)⁶



Chemical Formula: C₁₅H₁₁Br

Molecular Weight: 271.1518 g/mol

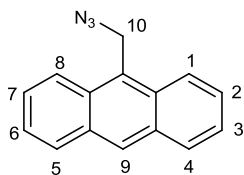
Phosphorus tribromide (2.30 g, 8.49 mmol) was added dropwise to the suspension of 9-hydroxymethylantracene (1.52 g, 7.29 mmol) in toluene (50 mL). The mixture was stirred at room temperature for 1 h until it becomes homogeneous and then saturated sodium carbonate solution (15 mL) was added slowly. The organic phase was separated and washed with water, brine and dried over magnesium sulphate. After filtration, the solvent was removed *in vacuo* and compound was purified by flash chromatography column (ether/hexane 1:1) to give the title compound as a yellow powder (1.71 g, 88 %); **M.p.** 143-144 °C (lit.⁶: 143-146°C).

¹H NMR (500 MHz, CDCl₃) δ 8.48 (9-*H*, s, 1H), 8.30 (8-*H*, 1-*H*, d, *J* = 8.2 Hz, 2H), 8.04 (5-*H*, 4-*H*, d, *J* = 8.5 Hz, 2H), 7.65 (7-*H*, 2-*H*, ddd, *J* = 8.9, 6.5, 1.3 Hz, 2H), 7.51 (6-*H*, 3-*H*, ddd, *J* = 8.2, 6.6, 0.8 Hz, 2H), 5.53 (2-*H*, s, 2H).

¹³C NMR (126 MHz, CDCl₃) δ 131.70, 129.83, 129.39, 129.30, 127.98, 126.90, 125.49, 123.62, 27.09.

Data in agreement with those previously reported.⁶

9-Azidomethylantracene (250)⁶



Chemical Formula: C₁₅H₁₁N₃

Molecular Weight: 233.2679 g/mol

To a solution of 9-bromomethylantracene (1.59 g, 5.86 mmol) in DMSO (62 mL) was added in one portion, sodium azide (0.39 g, 5.98 mmol). The reaction mixture was stirred for 3.5 h at 65 °C. The mixture was then cooled to room temperature and poured into H₂O (50 mL) and extracted with EtOAc (3 x 30 mL). The organic phase was washed with brine and dried over MgSO₄. After filtration, the solvent was evaporated *in vacuo* to give the expected product (1.02 g, 78 %).

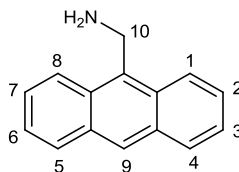
M.p. 82-83 °C (lit.⁶: 80-83°C).

¹H NMR (500 MHz, CDCl₃) δ 8.49 (9-*H*, s, 1H), 8.29 (8-*H*, 1-*H*, d, *J* = 8.9 Hz, 2H), 8.04 (5-*H*, 4-*H*, d, *J* = 8.4 Hz, 2H), 7.60 (7-*H*, 2-*H*, dd, *J* = 8.3, 6.2 Hz, 1H), 7.51 (6-*H*, 3-*H*, dd, *J* = 16.6, 9.3 Hz, 1H), 5.30 (10-*H*, s, 1H).

¹³C NMR (126 MHz, CDCl₃) δ 131.5, 130.8, 129.4, 129.1, 127.0, 125.9, 125.3, 123.6, 46.4.

Data in agreement with those previously reported.⁶

9-aminomethylantracene (107)



Chemical Formula: C₁₅H₁₃N

Molecular Weight: 207.2704 g/mol

Method A (Staudinger reaction)⁶

Under a nitrogen atmosphere, 9-azidomethylantracene (1.01 g, 4.57 mmol) was dissolved in anhydrous THF (15 mL). Triphenylphosphine (1.26 g, 4.79 mmol, 1.05 equiv.) was added at 0 °C. The reaction was removed from the ice bath and stirred at room temperature for 2 h before H₂O (1.21 g, 14.7 equiv., 67.1 mmol) was added and stirred for an additional 2.5 h. The reaction was monitored by TLC, eluting with ethyl acetate: hexane (5:1). When the starting material was completely converted into product, Et₂O (60 mL) was added. The mixture was cooled to 0 °C, followed by addition of 10% aq. HCl (30 mL). The salt was collected by vacuum filtration and dissolved in EtOAc (50 mL), and the solution was cooled to 0 °C. Concentrated aqueous ammonia solution NH₄OH (40 mL) was added until the pH became 12, followed by addition of H₂O (50 mL). The organic layer was separated. The aqueous layer was again extracted with EtOAc (2 × 30 mL). The combined organic phase was washed with brine and dried over MgSO₄. After filtration the solvent was evaporated *in vacuo* to afford the crude product as yellow powder which was recrystallised from chloroform/hexane to give the title compound as yellow needles (0.62 g, 67%).

Method B (reductive amination reaction)⁷

To a solution of 9-anthracenealdehyde (1.01 g, 4.89 mmol, 1 equiv.) in dry DCE (50 ml) under nitrogen, was added ammonium chloride (0.65 g, 12.2 mmol, 2.5 equiv.). The resulting solution was stirred for 2 h at room temperature, after which, the reducing agent (19.6 mmol, 4 equiv.) was added. The reaction mixture was stirred overnight. The aqueous layer was extracted with DCM (2 x 30 ml) and the combined organic layers were dried over MgSO_4 filtered and evaporated. Crude material was then purified by silica gel column chromatography (diethyl ether/ hexane [1:1]) affording the desired amine. (for yields, See Tables 4, 5, 6 Chapter 2)

Method C (reductive amination with different reagents)

9-Anthracenealdehyde (0.36 g, 1.74 mmol) was dissolved in dry DCE (20 mL), then 3-aminophenylboronic acid hemisulfate salt (0.32 g, 1.74 mmol) was added and the mixture was stirred for 2 h. After that time NaBH_4 (0.26 g, 6.96 mmol) was added in portions. After stirring overnight at room temperature, the solution was acidified with 1M HCl, followed by extraction with DCM (3 x 10 mL). The organic phase was dried over MgSO_4 , filtered, and concentrated by rotary evaporation. The residue was purified by flash chromatography column (diethyl ether/ hexane [1:1]) to give the expected compound as a yellow powder (0.14 g, 25 %).

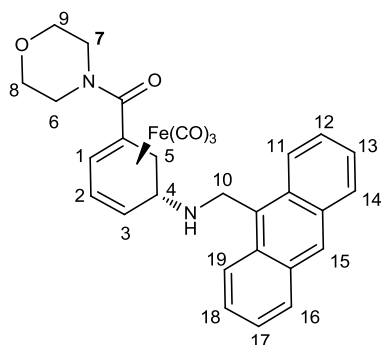
M.p. 102-103 °C (lit.⁶: 101-102°C).

^1H NMR (400 MHz, CDCl_3) δ 8.31 (9-*H*, s, 1H), 8.24 (8-*H*, 1-*H*, d, J = 8.7, 2H), 7.95 (5-*H*, 4-*H*, d, J = 8.4, 2H), 7.47 (7-*H*, 2-*H*, J = 8.7, 7.9, 1.3, ddd, 2H), 7.39 (6-*H*, 3-*H*, ddd, J = 8.4, 7.9, 1.1, 2H), 4.74 (10-*H*, s, 2H).

^{13}C NMR (100 MHz, CDCl_3) δ 131.5, 129.5, 129.2, 128.1, 128.0, 127.0, 125.4, 123.7, 46.5.

Data in agreement with those previously reported.⁶

(±)-Tricarbonyl{ η^4 -5-[(anthracen-9-ylmethyl)amino] cyclohexa-1,3-dien-1-yl}(morpholino)metha-none }iron (260)



Chemical Formula: C₂₉H₂₆FeN₂O₅

Molecular Weight: 538.3721 g/mol

A solution of 9-aminomethylantracene (0.36 g, 1.74 mmol, 2.2 equiv.) in dry THF (15 mL) was added dropwise to a mixture of tricarbonyl[5-(morpholine-4-carbonyl)cyclohexa-2,4-dien-1-ylum}iron hexafluorophosphate (0.19 g, 0.79 mmol) and DMAM-PS (0.58 g, loading 3 mmol of base/g) in dry THF (15 mL). The reaction was stirred overnight at room temperature and was monitored by FT-IR and TLC. The reaction mixture was filtered and the solvent was evaporated under vacuum. The yellow solid was purified by column chromatography on silica (eluent Et₂O/Hexane [1:1]) and the title compound was obtained as a light yellow powder (0.07 g, 15 %, R_f = 0.17 for Et₂O/Hexane [3:1]). (for yields, See Table 7 Chapter 2)

M.p. 196-198 °C.

IR (NaCl) ν = 2052 (C \equiv O symmetric), 1977 (C \equiv O asymmetric), 1725 (C=O).

¹H NMR (500 MHz, CDCl₃) δ 8.46 (15-*H*, s, 1H), 8.27 (11-*H*, 19-*H*, d, J = 8.8 Hz, 2H), 8.01 (14-*H*, 16-*H*, d, J = 8.3 Hz, 2H), 7.54 (18-*H*, 12-*H*, ddd, J = 8.8, 6.6, 1.1 Hz, 2H), 7.48 (13-*H*, 17-*H*, dist. dd, J = 8.3, 6.6 Hz, 2H), 6.24 (1-*H*, d, J = 4.2 Hz, 1H), 5.48 (2-*H*, dd, J = 6.8, 4.2 Hz, 1H), 5.45 (diastereotopic 10-*H*, d, J = 11.1 Hz, 1H), 5.37 (diastereotopic 10-*H*, d, J = 11.1 Hz, 1H), 4.41 (4-*H*, dm, J = 9.3 Hz, 1H), 3.74 – 3.59 (6-*H*, 7-*H*, 8-*H*, 9-*H*, m, 6H),

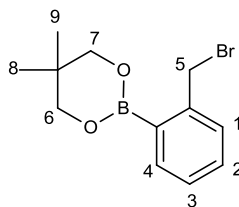
3.51 – 3.43 (6-*H*, 7-*H*, 3-*H*, m, 3H), 2.27 (5-*H*, dd, $J = 14.7, 9.3$ Hz, 1H), 1.65 (N-*H*, br. s), 1.49 (5-*H*, dd, $J = 14.7, 4.4$ Hz, 1H).

^{13}C NMR (126 MHz, CDCl_3) δ 171.43, 131.56, 130.95, 129.26, 128.75, 128.30, 126.51, 125.14, 124.06, 86.98, 85.76, 66.79, 63.75, 62.59, 61.81, 45.43 (br.), 30.50.

*General procedure for the synthesis of protected boronic acid derivatives*⁸

The appropriate (bromo)- or (amino) phenyl boronic acid derivative (2.33 mmol, 1 equiv.) and 2,2-dimethyl-1,3-propanediol (2.56 mmol, 1.1 equiv.) in dry toluene (5 mL) were stirred overnight. The solvent was removed under reduced pressure and the residue was taken up with DCM (30 mL) and extracted with water (3x 10 mL). The organic layer was dried over MgSO₄ and evaporated to obtain the expected compound.

2,2-Dimethylpropane-1,3-diyl (o-(bromomethyl)phenyl)boronate (246)⁹



Chemical Formula: C₁₂H₁₆BBrO₂

Molecular Weight: 282.9692 g/mol

Light yellow oil, 0.47 g 72%,

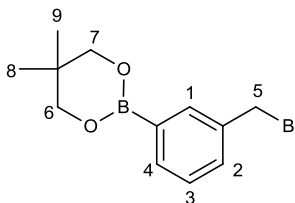
IR (NaCl) ν = 1599 (aromatic).

¹H NMR (500 MHz, CDCl₃) δ 7.72 (4-*H*, d, *J* = 7.5 Hz, 1H), 7.31 – 7.25 (2-*H*, 3-*H*, m, 2H), 7.21 – 7.16 (1-*H*, m, 1H), 4.84 (5-*H*, s, 2H), 3.72 (6-*H*, 7-*H*, s, 4H), 0.98 (8-*H*, 9-*H*, s, 6H).

¹³C NMR (126 MHz, CDCl₃) δ (¹³C resonance for aromatic C bonded to B not observed), 143.69, 135.73, 130.69, 130.35, 127.74, 72.56, 34.65, 31.93, 22.09.

Data in agreement with those previously reported.⁹

2-[3-(Bromomethyl)phenyl]-5,5-dimethyl-1,3,2-dioxaborinane (247)⁹



Chemical Formula: C₁₂H₁₆BBBrO₂

Molecular Weight: 282.9692 g/mol

White solid 0.63 g, 95 %,

M.p. 105-108°C

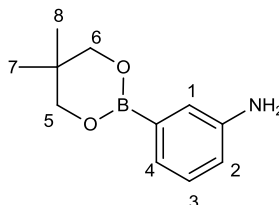
IR (NaCl) ν = 1477 (aromatic)

¹H NMR (500 MHz, CDCl₃) δ 7.83 (4-*H*, s, 1H), 7.74 (3-*H*, d, *J* = 7.4 Hz, 1H), 7.49 – 7.45 (2-*H*, m, 1H), 7.34 (1-*H*, t, *J* = 7.5 Hz, 1H), 4.52 (5-*H*, s, 2H), 3.78 (6-*H*, 7-*H*, s, 4H), 1.03 (8-*H*, 9-*H*, s, 6H).

¹³C NMR (126 MHz, CDCl₃) δ (¹³C resonance for aromatic C bonded to B not observed), 137.04, 134.55, 134.07, 131.50, 128.24, 72.47, 34.01, 32.03, 22.04.

Data in agreement with those previously reported.⁹

3-(5,5-Dimethyl-1,3,2-dioxaborinan-2-yl)aniline (245)¹⁰



Chemical Formula: C₁₁H₁₆BNO₂

Molecular Weight: 205.0612 g/mol

Grey powder, 0.34 g 72 %,

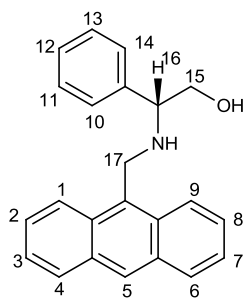
IR (NaCl) ν = 3443 (-NH₂), 3360 (B-O)

¹H NMR (500 MHz, CDCl₃) δ 7.25 – 7.20 (1-*H*, m, 1H), 7.20 – 7.12 (2-*H*, 3-*H*, m, 2H), 6.80 – 6.73 (4-*H*, m, 1H), 3.76 (5-*H*, 6-*H*, s, 4H), 3.62 (bs, 2H), 1.02 (7-*H*, 8-*H*, s, 6H).

¹³C NMR (126 MHz, CDCl₃) δ (¹³C resonance for aromatic C bonded to B not observed), 145.79, 128.66, 124.24, 120.48, 117.63, 72.37, 31.93, 21.98.

Data in agreement with those previously reported.¹⁰

(*R*)-2-phenyl-2-(anthracen-9-ylmethylamino)-ethanol (265)¹¹



Chemical Formula: C₂₃H₂₁NO

Molecular Weight: 327.4189 g/mol

To a solution of 9-anthracenecarboxylaldehyde (1.60 g, 7.76 mmol) in dichloroethane was added the (*R*)-2-amino-2-phenyl-ethanol (1.00 g, 7.29 mmol) in dry DCE (10 mL). The mixture was refluxed for 6 h. After the mixture had cooled to room temperature, NaBH₄ (0.51 g, 13.5 mmol) was added slowly, followed by stirring for 4 h at room temperature. The solvent was removed under vacuum and the residue taken up with DCM and then washed with saturated NaCl solution (3 × 50 mL). The organic phase was dried over anhydrous MgSO₄, filtered, and evaporated to dryness. The crude product was purified by flash column chromatography (silica gel, DCM/MeOH [50/1]). 1.84 g of yellowish foam was obtained with 74 % yield.

M.p. 89-92°C.

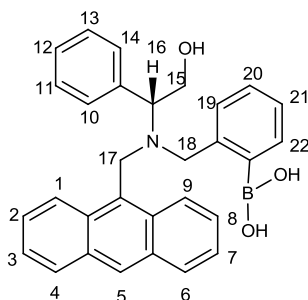
IR (NaCl) ν = 3058 (O-H, N-H), 1673 (aromatic C=C).

¹H NMR (500 MHz, CDCl₃) δ 8.40 (5-*H*, s, 1H), 8.12 (1-*H*, 9-*H*, d, *J* = 8.5 Hz, 2H), 8.02 – 7.96 (4-*H*, 6-*H*, m, 2H), 7.50 – 7.38 (m, 9H), 4.66 (17-*H*, d, *J* = 12.4 Hz, 1H), 4.59 (17-*H*, d, *J* = 12.4 Hz, 1H), 4.06 (16-*H*, dd, *J* = 9.1, 4.5 Hz, 1H), 3.73 (15-*H*, dd, *J* = 11.0, 4.5 Hz, 1H), 3.56 (15-*H*, dd, *J* = 10.9, 9.2 Hz, 1H), 2.26 (bs, 2H).

¹³C NMR (126 MHz, CDCl₃) δ 140.39, 131.66, 130.66, 130.48, 129.29, 129.00, 128.22, 127.71, 127.65, 126.34, 125.12, 124.17, 66.61, 65.40, 43.55.

Data in agreement with those previously reported.¹¹

(2-(((anthracen-9-ylmethyl)(2-hydroxy-1-phenylethyl)amino)methyl)phenyl)boronic acid (268)¹¹



Chemical Formula: C₃₀H₂₈BNO₃

Molecular Weight: 461.3592 g/mol

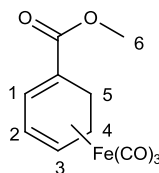
To a mixture of 2-phenyl-2-(anthracen-9-ylmethylamino)-ethanol (0.30 g, 0.88 mmol) in dry MeCN (10 mL) was added K₂CO₃ (0.49 g, 3.51 mmol) and 2-(2-bromomethylphenyl)-1, 3, 2-dioxaborinane (0.36 g, 1.41 mmol) and the mixture was refluxed for 8 h. The reaction mixture was cooled to room temperature and the solvent was removed under vacuum and the residue was taken up with H₂O (10 mL). The aqueous phase was extracted with DCM (3 × 30 mL), and the combined organic extracts were washed with brine (2 × 20 mL) and dried over anhydrous MgSO₄. The solvent was removed under vacuum and the residue purified by column chromatography (silica gel, DCM/MeOH [20:1]) to give 0.11 g of the expected compound (27%).

IR (NaCl) ν = 3207 (B-OH), 3063 (-OH).

¹H NMR (500 MHz, CDCl₃) δ 8.41 (5-*H*, s, 1H), 8.24 (1-*H*, 9-*H*, d, *J* = 8.0 Hz, 2H), 7.95 (4-*H*, 6-*H*, d, *J* = 8.0 Hz, 2H), 7.55 – 7.32 (2-*H*, 3-*H*, 7-*H*, 8-*H*, 10-*H*, m, 5H), 7.24 – 7.21 (22-*H*, m, 1H), 7.17 – 7.05 (11-*H*, 12-*H*, 13-*H*, 14-*H*, m, 4H), 6.67 (19-*H*, 20-*H*, 21-*H*, d, *J* = 7.5 Hz, 3H), 5.22 (15-*H*, d, *J* = 14.2 Hz, 1H), 5.01 (15-*H*, d, *J* = 14.2 Hz, 1H), 4.59 (17-*H*, d, *J* = 6.5 Hz, 1H), 4.56 (17-*H*, d, *J* = 6.5 Hz, 1H), 4.04 (dd, *J* = 10.8, 6.0 Hz, 1H), 3.99 – 3.94 (18-*H*, m, 1H), 3.92 – 3.82 (18-*H*, m, 1H).

Data in agreement with those previously reported.¹¹

Tricarbonyl(η^4 -cyclohexa-1,3-dienecarboxylic acid methyl ester)iron (283)⁵



Chemical Formula: C₁₁H₁₀FeO₅

Molecular Weight: 278.0391 g/mol

To a slurry of diironnonacarbonyl (3.05 g, 8.38 mmol) in dry THF (2 mL) was added the solution of cyclohexa-1,3-dienecarboxylic acid methyl ester (0.50 g, 3.64 mmol) in dry THF (3 mL). The reaction mixture was flushed with argon and stirred at reflux under argon for 5 h. **(Caution! Pentacarbonyliron is extremely toxic by inhalation).** After filtration of the mixture through a short pad of Celite, the solvent was removed *in vacuo*. Gradient column chromatography using a stepwise gradient of petroleum ether/EtOAc [80:20], and petroleum ether/ EtOAc/AcOH [79:20:1] afforded 0.65 g of yellow crystals (65 %).

IR (NaCl) ν = 2056 (C \equiv O symmetric), 1982 (C \equiv O asymmetric), 1715 (COOMe).

¹H NMR (500 MHz, CDCl₃) δ 6.04 (1-*H*, bs, 1H), 5.36 (2-*H*, s, 1H), 3.70 (6-*H*, bs, 3H), 3.37 (3-*H*, bs, 1H), 2.29 – 1.33 (4-*H*, 5-*H*, m, 4H).

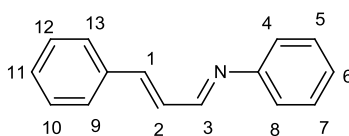
¹³C NMR (126 MHz, CDCl₃) δ 210.34, 172.72, 88.60, 85.30, 64.81, 63.32, 51.67, 25.25, 23.00.

Data in agreement with those previously reported.⁵

General procedure for the preparation of 1-azabuta-1,3-diene derivatives¹²

Trans-cinnaldehyde (82.8 mmol, 1 equiv.) and suitable amine (82.8 mmol, 1 equiv.) were dissolved in dry DCM (120 mL) containing molecules sieves. The reaction mixture was left overnight. The solvent was removed by vacuum and solid was dried over high vacuum for few hours.

1,4-Diphenyl-1-azabuta-1,3-diene (286a)¹²



Chemical Formula: C₁₅H₁₃N

Molecular Weight: 207.2704 g/mol

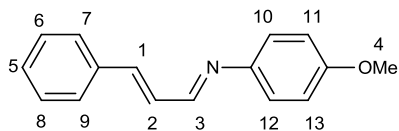
Pale yellow needles, 15.3 g, 89 %

¹H NMR (500 MHz, CDCl₃) δ 8.19 (3-*H*, dd, *J* = 7.1, 1.2 Hz, 1H), 7.52 – 7.43 (1-*H*, 2-*H*, m, 2H), 7.40 – 7.26 (Ar-*H*, m, 5H), 7.20 – 7.03 (Ar-*H*, 13-*H*, m, 5H).

¹³C NMR (126 MHz, CDCl₃) δ 161.78, 151.83, 144.17, 135.71, 129.73, 129.30, 129.05, 128.71, 127.63, 126.25, 121.05.

Data in agreement with those previously reported.¹²

1-(4-Methoxyphenyl)-4-phenyl-1-azabuta-1,3-diene (286b)¹²



Chemical Formula: C₁₆H₁₅NO

Molecular Weight: 237.2964 g/mol

17.8 g, 91 % yellowish crystals.

M.p. 121-122 °C (lit.¹² : 122°C).

¹H NMR (500 MHz, CDCl₃) δ 8.31 – 8.28 (3-*H*, m, 1H), 7.57 – 7.50 (7-*H*, 9-*H*, m, 2H), 7.42 – 7.32 (5-*H*, 6-*H*, 8-*H*, m, 3H), 7.23 – 7.19 (10-*H*, 12-*H*, m, 2H), 7.12 (1-*H*, 2-*H*, d, *J* = 4.6 Hz, 2H), 6.94 – 6.91 (11-*H*, 13-*H*, m, 2H), 3.83 (4-*H*, s, 3H).

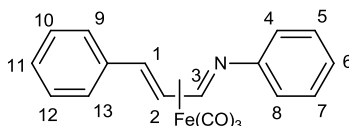
¹³C NMR (126 MHz, CDCl₃) δ 159.65, 158.54, 144.67, 143.16, 135.90, 129.51, 129.02, 128.90, 127.52, 122.35, 114.55, 55.60.

Data in agreement with those previously reported.¹²

General procedure for the preparation of η^4 -1-azabuta-1,3-diene)tricarbonyliron complexes¹²

A mixture of 1-azabuta-1,3-dienes (69.6 mmol, 1 equiv.) and diironnonacarbonyl (104.4 mmol, 1.5 equiv.) in dry THF (120 mL) was sonicated at room temperature for 24 h. **(Caution! Pentacarbonyliron is extremely toxic by inhalation).** The mixture was concentrated by rotary evaporation followed by flash chromatography (Et₂O/pentane [1:10]) of the residue on silica gel.

Tricarbonyl[(1-4- η)-1,4-diphenyl-1-azabuta-1,3-diene]iron (287a)¹²



Chemical Formula: C₁₈H₁₃FeNO₃

Molecular Weight: 347.1457 g/mol

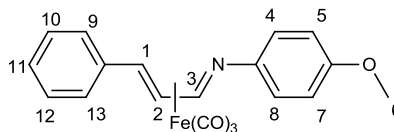
Red crystals, 22.3 g, 92 %.

IR (NaCl) ν = 2051 (C \equiv O symmetric), 1980 (C \equiv O asymmetric).

¹H NMR (500 MHz, CDCl₃) δ 7.58 – 6.70 (3-*H*, 4-*H*, 5-*H*, 5-*H*, 7-*H*, 8-*H*, 9-*H*, 10-*H*, 11-*H*, 12-*H*, 13-*H*, m, 11H), 5.80 (2-*H*, s, 1H), 3.47 (1-*H*, s, 1H).

Data in agreement with those previously reported.¹²

Tricarbonyl[(1-4-η)-1-(4-methoxyphenyl)-4-phenyl-1-azabuta-1,3-diene]iron (287b)¹²



Chemical Formula: C₁₉H₁₅FeNO₄

Molecular Weight: 377.1717 g/mol

Red crystals, 22.9 g, 94 %.

M.p. 139 °C (dec).

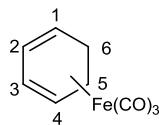
IR (NaCl) ν = 2051 (C \equiv O symmetric), 1985 (C \equiv O asymmetric).

¹H NMR (500 MHz, CDCl₃) δ 7.49 – 6.59 (3-*H*, 4-*H*, 5-*H*, 7-*H*, 8-*H*, 9-*H*, 10-*H*, 11-*H*, 12-*H*, 13-*H*, bm, 10H), 5.61 (2-*H*, s, 1H), 3.69 (6-*H*, s, 3H), 3.32 (1-*H*, s, 1H).

¹³C NMR (126 MHz, CDCl₃) δ 155.54, 146.70, 139.13, 129.05, 128.91, 127.54, 126.98, 126.74, 122.69, 122.38, 114.57, 114.44, 104.43, 74.08, 62.04, 55.57.

Data in agreement with those previously reported.¹²

Tricarbonyl(η^4 -cyclohexa-1,3-diene)iron (21)¹³



Chemical Formula: C₉H₈FeO₃

Molecular Weight: 220.0030 g/mol

Method A (reaction with Fe₂CO₉ in different solvent)¹²

To the suspension of diironnonacarbonyl (5.01 g, 16.5 mmol) in dry THF (7 mL) was added 1,3-cyclohexadiene (0.57 g, 7.17 mmol) and the mixture refluxed for 6 h. **(Caution! Pentacarbonyliron is extremely toxic by inhalation).** The reaction mixture was filtered through a short pad of Celite and solvent was removed. The residue was dissolved in petroleum ether for purification on flash chromatography on neutral aluminium oxide to afford the product as yellow oil. (For yields, see Table 12, Chapter 3)

Method B (reaction with FeCO₅)^{13,14}

Following the procedure reported by Birch¹³ and improved by Pearson *et al.*,¹⁴ 1,3-cyclohexadiene (0.57 g, 7.17 mmol) was dissolved in dry *n*-Bu₂O (24 mL) and iron pentacarbonyl was added (3.9 g, 19.9 mmol). The reaction mixture was refluxed for 43 h and then filtered through Celite. **(Caution! Pentacarbonyliron is extremely toxic by inhalation).** The filter pad was rinsed with *n*-Bu₂O. The solvent was removed by rotary evaporation, followed by flash chromatography (petroleum ether/EtOAc [80:20]). (For yields, see Table 12, Chapter 3)

*Method C (reaction with ligand exchange **287a** and **287b**) general method¹²*

1,3-Cyclohexadiene (1.20 mL, 12.5 mmol) was dissolved in dry THF (25 mL). The solution was transferred into a solution of the azadiene complex (3.22 mmol) in dry THF (100 mL). The reaction mixture was refluxed for 1.5 h, and then cooled to room

temperature. The solvent was evaporated *in vacuo* to a volume of 1 mL. The residue was purified by flash chromatography (pentane) on silica gel to afford expected compound as yellow oil. (For yields, see Table 16, Chapter 3)

Method D (modified reaction with Fe₂CO₉ and silica on sonic bath based on procedure reported by Pauson et al.¹⁵)

1,3-Cyclohexadiene (0.57 g, 7.17 mmol) was mixed with diironnonacarbonyl and silica (5 g per g of Fe₂CO₉) and placed in the sonic bath at 50 °C for 24 h. **(Caution! Pentacarbonyliron is extremely toxic by inhalation)**. After cooling, the mixture was separated by flash chromatography (hexane:diethyl ether [1:1]) to give 1.22 g, 78 % of yellow liquid.

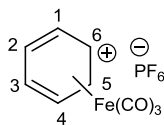
IR (ATR) ν = 2059 (C \equiv O symmetric) ,1981 (C \equiv O asymmetric).

¹H NMR (200 MHz, CDCl₃) δ 5.33 – 5.23 (2-*H*, 3-*H*, m, 2H), 3.34 – 3.08 (1-*H*, 4-*H*, m, 2H), 1.90 – 1.43 (5-*H*, 6-*H*, m, 4H).

¹³C NMR (50 MHz, CDCl₃) δ 212.36, 85.47, 62.57, 23.99.

Data in agreement with those previously reported.^{12,13}

Tricarbonyl(η^5 -cyclohexa-1,3-dienylium)iron hexafluorophosphate (48)¹³



Chemical Formula: C₉H₇F₆FeO₃P

Molecular Weight: 363.9593 g/mol

To a solution of triphenylcarbenium hexafluorophosphate (10.9 g, 2.82 mmol) in dry DCM (30 mL) was added dropwise a solution of tricarbonyl(η^4 -cyclohexa-1,3-diene)iron (5.16 g, 2.35 mmol) in dry DCM (30 mL). The reaction mixture was stirred for 1 hour at ambient temperature and wet diethyl ether (700 mL) was added. The yellow precipitate was filtered and washed three times with diethyl ether (150 mL) to give pure tricarbonyl (η^5 -cyclohexadienylium)iron hexafluorophosphate as yellow crystals (8.27 g, 97 %).

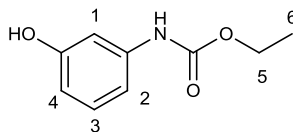
IR (NaCl) ν = 2125 (C \equiv O symmetric), 2084 (C \equiv O asymmetric).

¹H NMR (500 MHz, CD₃CN) δ 7.14 (2-*H*, t, *J* = 5.5 Hz, 1H), 5.82 (1-*H*, 3-*H*, t, *J* = 6.3 Hz, 2H), 4.23 (4-*H*, 6-*H*, t, *J* = 6.8 Hz, 2H), 2.92 (5-*H*, dt, *J* = 15.8, 6.2 Hz, 1H), 1.89 (5-*H*, br. s, 1H).

¹³C NMR (126 MHz, CD₃CN) δ 102.49, 90.00, 65.42, 24.03.

Data in agreement with those previously reported.^{12,13}

3-Hydroxyphenylurethane (281)¹⁶



Chemical Formula: C₉H₁₁NO₃

Molecular Weight: 181.1885 g/mol

Ethyl chloroformate (5.00 g, 46.1 mmol) was added to a mixture of 3-aminophenol (5.00 g, 46.1 mmol) in dry diethyl ether (200 mL). The reaction mixture was stirred for 2 h at room temperature. The grey mixture was crystallized from toluene/cyclohexane (100 mL/200 mL) to give colourless crystals (4.24 g, 54 %).

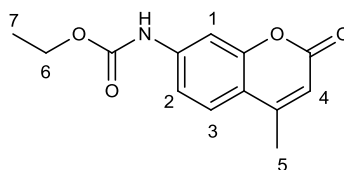
M.p. 93-94 °C (lit.¹⁶: 94-95°C)

¹H NMR (300 MHz, CDCl₃) δ 7.36 (1-*H*, s, 1H), 7.13 (3-*H*, t, *J* = 8.1 Hz, 1H), 6.73 – 6.52 (2-*H*, 4-*H*, m, 2H), 6.47 (N-*H*, O-*H*, br. s, 2H), 4.23 (5-*H*, q, *J* = 7.1 Hz, 2H), 1.31 (6-*H*, t, *J* = 7.1 Hz, 3H)

¹³C NMR (50 MHz, CDCl₃) δ 157.04, 154.14, 139.06, 130.10, 110.83, 110.61, 106.08, 61.78, 14.62.

Data in agreement with those previously reported.¹⁶

7-Carbethoxyamino-4-methylcoumarin (282)¹⁶



Chemical Formula: C₁₃H₁₃NO₄

Molecular Weight: 247.2466 g/mol

Ethyl acetoacetate (3.80 mL, 29.8 mmol) was added to the suspension of 3-hydroxyphenylurethane (4.21 g, 25.1 mmol) in 70% H₂SO₄ (58 mL) and stirred for 4 h at room temperature. The mixture was poured into water/ice giving white crystals. Recrystallization from absolute ethanol yielded colourless needles (4.75 g, 77%).

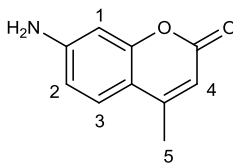
M.p. 185-186 °C (lit.¹⁶ : 186-188°C).

¹H NMR (200 MHz, DMSO-d₆) δ 8.62 (1-*H*, s, 1H), 7.64 (2-*H*, d, *J* = 8.7 Hz, 1H), 7.51 (N-*H*, s, 1H), 7.36 (3-*H*, d, *J* = 8.7 Hz, 1H), 6.18 (4-*H*, s, 1H), 4.15 (6-*H*, q, *J* = 7.1 Hz, 2H), 2.35 (5-*H*, s, 3H), 1.24 (7-*H*, t, *J* = 7.1 Hz, 3H).

¹³C NMR (50 MHz, DMSO-d₆) δ 160.10, 153.86 (2C), 153.37, 153.21, 142.90, 125.96, 114.27, 111.85, 104.40, 60.74, 18.03, 14.47.

Data in agreement with those previously reported.¹⁶

7-Amino-4-methylcoumarin (102)



Chemical Formula: C₁₀H₉NO₂

Molecular Weight: 175.1840 g/mol

*Method A (deprotection of 7-carbethoxyamino-4-methylcoumarin)*¹⁶

7-Carbethoxyamino-4-methylcoumarin (6.89 g, 27.9 mmol) in conc. H₂SO₄ (25 g) and glacial acetic acid (25 g) was heated at reflux. After 4 h, the mixture was poured into ice/water (100 mL) and left overnight. To the resulting suspension was added 50% aq. NaOH (50 mL) with cooling by addition of ice chips, until pH~10. The yellow precipitate was filtered and washed with ice water (3 x 50 mL) and purified by crystallization from ethanol to give yellow needles (4.89 g, 99 %).

*Method B (without a solvent)*¹⁷

To a mixture of *p*-aminophenol (0.49 g, 4.58 mmol), ethyl acetoacetate (0.39 mL, 3.05 mmol) was added, followed by a catalytic amount of BiCl₃. The reaction mixture was stirred at reflux for 4 h. The purification by gradient chromatography EtOAc/DCM [7:3] to provide expected compound (0.21 g, 26 %).

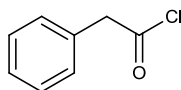
M.p. 222-223 °C (lit. M.p.¹⁶ : 223°C)

¹H NMR (500 MHz, DMSO-d₆) δ 7.40 (3-*H*, d, *J* = 8.6 Hz, 1H), 6.56 (2-*H*, dd, *J* = 8.6, 2.2 Hz, 1H), 6.40 (1-*H*, d, *J* = 2.2 Hz, 1H), 6.09 (N-*H*₂, s, 2H), 5.90 (4-*H*, *J* = 1.1 Hz, 1H), 2.29 (5-*H*, d, *J* = 1.1 Hz, 3H).

¹³C NMR (126 MHz, DMSO-d₆) δ 160.70, 155.43, 153.72, 153.05, 126.18, 111.14, 108.81, 107.45, 98.49, 18.00.

Data in agreement with those previously reported.^{16,17}

Phenylacetyl chloride (303)¹⁸

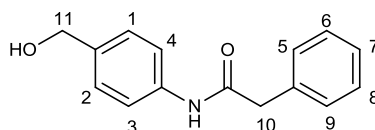


Chemical Formula: C₈H₇ClO

Molecular Weight: 154.5936 g/mol

At 0°C, to a mixture of phenylacetic acid (2.01 g, 14.7 mmol) in dry DCM (10 mL) oxalyl chloride (1.27 mL, 14.7 mmol) was slowly added, followed by a few drops of DMF. The reaction mixture was stirred at room temperature for 3 h and evaporated to give the expected acid chloride which was used in the following reaction. The yield was assumed to be quantitative.

***N*-(4-(hydroxymethyl)phenyl)-2-phenylacetamide(304)¹⁸**



Chemical Formula: C₁₅H₁₅NO₂

Molecular Weight: 241.2851 g/mol

Phenylacetyl chloride (0.53 mL, 4.01 mmol) was added dropwise to a solution of *p*-aminobenzyl alcohol (0.52 g, 4.21 mmol). At 0 °C, dry pyridine (0.68 mL, 8.4 mmol) was added to the reaction mixture. The reaction was stirred under argon for 1.5 h and checked by TLC, and then purified by chromatography column (DCM/EtOAc, 7:3) to give white solid (0.87 g, 90 %).

¹H NMR (200 MHz, CD₃OD δ 7.54 (3-*H*, 4-*H*, d, *J* = 8.5 Hz, 2H), 7.39 – 7.24 (1-*H*, 2-*H*, 5-*H*, 6-*H*, 7-*H*, 8-*H*, 9-*H*, m, 7H), 4.56 (10-*H*, s, 2H), 3.68 (11-*H*, s, 2H).

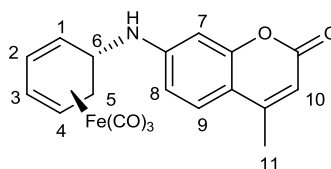
¹³C NMR (50 MHz, CD₃OD δ 172.28, 138.97, 138.65, 136.84, 130.13, 129.58, 128.58, 127.94, 121.23, 64.84, 44.68.

Data in agreement with those previously reported.¹⁸

General procedure for the synthesis of substituted 7-aminocoumarin derivatives

To a solution of the appropriate 7-amino-4-methyl-chromen-2-one (2.86 mmol, 1 equiv.) in dry THF (22 ml) was added dimethylaminomethyl-polystyrene (3-4 mmol/g base loading, 1.15 equiv.) followed by tricarbonyl(η^5 -cyclohexadienyl)iron hexafluorophosphate (3.29 mmol, 1.15 equiv.). The reaction mixture was stirred overnight and progress was monitored by TLC. The solvent was removed by rotary evaporation, and the obtained residue was purified by column chromatography (Et₂O/hexane [1:1]) followed by preparative TLC.

(±)-Tricarbonyl[η^4 -7-(cyclohexa-2,4-dien-1-ylamino)-4-methyl-2H-chromen-2-one]iron (271)



Chemical Formula: C₁₉H₁₅FeNO₅

Molecular Weight: 393.1711 g/mol

Yellow solid (0.51 g, 46 %).

M.p. 196-198 °C.

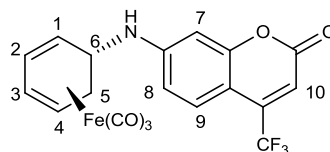
IR (NaCl) ν = 2047 (C \equiv O symmetric), 1967 (C \equiv O asymmetric), 1708 (C=O), 1606 (C=C).

¹H NMR (500 MHz, CDCl₃) δ 7.32 (9-H, d, J = 8.6 Hz, 1H), 6.39 (8-H, dd, J = 8.6, 2.3 Hz, 1H), 6.35 (7-H, d, J = 2.3 Hz, 1H), 5.97 (10-H, d, J = 1.0 Hz, 1H), 5.58 (2-H, dist. dd, J = 6.0, 4.4 Hz, 1H), 5.41 (3-H, dist. dd, J = 6.0, 4.4 Hz, 1H), 4.11 (N-H, d, J = 7.6 Hz, 1H), 4.02 (6-H, ddd, J = 10.1, 7.6, 3.6 Hz, 1H), 3.17 (1-H, ddd, J = 6.0, 3.6, 1.2 Hz, 1H), 3.04 (4-H, ddd, J = 6.0, 3.8, 1.8 Hz, 1H), 2.47 (5-H, ddd, J = 15.1, 10.1, 3.8 Hz, 1H), 2.32 (11-H, d, J = 1.0 Hz, 3H), 1.44 (5-H, d, J = 15.1 Hz, 1H).

¹³C NMR (126 MHz, CDCl₃) δ 211.03, 161.92, 155.99, 152.95, 150.57, 125.74, 110.93, 110.46, 109.81, 98.87, 87.63, 84.03, 60.66, 56.97, 51.45, 32.68, 18.65.

HRMS [ASAP] for [M⁺] C₁₉H₁₅FeNO₅ requires 394.0372, found 394.0370.

(±)-Tricarbonyl[η^4 -7-(cyclohexa-2,4-dien-1-ylamino)-4-(trifluoromethyl)-2H-chromen-2-one]iron (288)



Chemical Formula: C₁₉H₁₂F₃FeNO₅

Molecular Weight: 447.1425 g/mol

Bright yellow powder (0.95 g, 74%).

M.p. 183-185 °C.

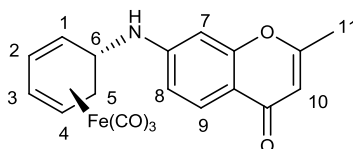
IR (NaCl) ν = 2050 (C \equiv O), 1970 (C \equiv O), 1718 (C=O), 1606 (C=C).

¹H NMR (500 MHz, CDCl₃) δ 7.43 (9-*H*, d, *J* = 8.3 Hz, 1H), 6.43 (7-*H*, 8-*H*, overlapping s and d, *J* = 8.2 Hz, 2H), 6.37 (10-*H*, s, 1H), 5.64 (2-*H*, t, *J* = 5.0 Hz, 1H), 5.55 (3-*H*, t, *J* = 5.0 Hz, 1H), 4.32 (N-*H*, d, *J* = 6.7 Hz, 1H), 4.07 – 3.94 (6-*H*, m, 1H), 3.18 – 3.10 (1-*H* or 4-*H*, m, 1H), 3.08 – 3.01 (1-*H* or 4-*H*, m, 1H), 2.48 (5-*H*, ddd, *J* = 15.0, 10.5, 4.0 Hz, 1H), 1.45 (5-*H*, partially obscured d, *J* = 15.0 Hz, 1H).

¹³C NMR (126 MHz, CDCl₃) δ 210.97, 160.37, 157.22, 151.36, 142.02 (q, *J*_{C-F} = 32.6 Hz) 126.54 (q, *J*_{C-F} = 1.9 Hz), 122.06 (q, *J*_{C-F} = 275.4 Hz) 111.55, 109.18 (q, *J*_{C-F} = 5.9 Hz), 104.30, 98.84, 87.85, 84.05, 60.20, 56.92, 51.46, 32.81.

HRMS [ASAP] for [M⁺] C₁₉H₁₂F₃FeNO₅ requires 448.0090, found 448.0080.

(±)-Tricarbonyl[η⁴-7-(cyclohexa-2,4-dien-1-ylamino)-2-methyl-4H-chromen-4-one]iron (292).



Chemical Formula: C₁₉H₁₅FeNO₅

Molecular Weight: 393.1711 g/mol

Pale yellow powder (0.96 g, 86 %).

M.p. 211-213 °C.

IR (NaCl) ν = 2047 (C≡O), 1966 (C≡O), 1645 (C=O), 1593 (C=C).

¹H NMR (500 MHz, DMSO) δ 7.62 (9-*H*, d, *J* = 8.8 Hz, 1H), 6.78 (N-*H*, d, *J* = 7.4 Hz, 1H), 6.61 (8-*H*, dd, *J* = 8.8, 2.0 Hz, 1H), 6.35 (7-*H*, br. d, *J* = 2.0 Hz, 1H), 5.96 (10-*H*, bs, 1H), 5.82 (2-*H*, dist. dd, *J* = 5.7, 4.5 Hz, 1H), 5.63 (3-*H*, dist. dd, *J* = 6.1, 4.5 Hz, 1H), 3.94 (6-*H*, ddd, *J* = 10.1, 7.4, 3.7 Hz, 1H), 3.29 (1-*H* or 4-*H*, ddd, *J* = 6.1, 3.7, 1.2 Hz, 1H), 3.17 (4-*H*, ddd, *J* = 5.7, 3.9, 1.7, 1H), 2.39 (5-*H*, ddd, *J* = 15.0, 10.1, 3.9 Hz, 1H), 2.29 (11-*H*, s, 3H), 1.43 (5-*H*, br. d, *J* = 15.0 Hz, 1H).

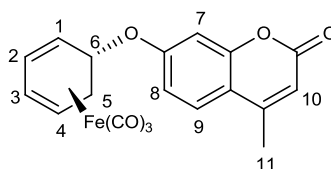
¹³C NMR (126 MHz, DMSO) δ 211.83, 175.72, 164.63, 158.42, 152.45, 125.60, 112.55, 109.28, 95.56, 87.53, 85.20, 61.98, 58.28, 50.05, 31.42, 30.67, 19.76.

HRMS [ASAP] for [M⁺] C₁₉H₁₅FeNO₅ requires 394.0372, found 394.0370.

General procedure for the synthesis of substituted hydroxyl coumarin derivatives

To a solution of the appropriate 7-hydroxy-4-methyl-chromen-2-one (4.12 mmol, 1 equiv.) in dry DCM (10 mL) was added potassium carbonate (8.24 mmol, 2 equiv.) followed by tricarbonyl(η^5 -cyclohexadienylum)iron hexafluorophosphate (4.74 mmol, 1.15 equiv.). The reaction mixture was stirred overnight and progress was monitored by TLC. The salt was collected by filtration purified by column chromatography (Et₂O: hexane, 3:1).

(±)-Tricarbonyl[η^4 -7-(cyclohexa-2,4-dien-1-yloxy)-4-methyl-2H-chromen-2-one]iron (294)



Chemical Formula: C₁₉H₁₄FeO₆

Molecular Weight: 394.1559 g/mol

R_f = 0.3, a brown solid (1.31 g, 81 %).

M.p. 103-105 °C.

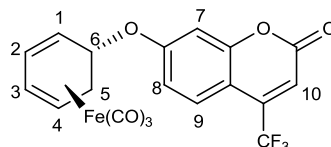
IR (NaCl) ν = 2046 (C \equiv O), 1966 (C \equiv O), 1694 (C=O), 1604 (C=C).

¹H NMR (500 MHz, CDCl₃) δ 7.45 (9-*H*, d, *J* = 8.8 Hz, 1H), 6.71 (8-*H*, dd, *J* = 8.8, 2.3 Hz, 1H), 6.66 (7-*H*, d, *J* = 2.3 Hz, 1H), 6.12 (10-*H*, s, 1H), 5.64 (2-*H*, dist. dd, *J* = 5.2, 5.0 Hz, 1H), 5.55 (3-*H*, dist. dd, *J* = 5.4, 5.2 Hz, 1H), 4.82 (6-*H*, ddd, *J* = 10.1, 3.1, 2.8 Hz, 1H), 3.12 (1-*H*, ddd, *J* = 5.0, 3.1, 1.5 Hz, 1H), 3.01 (4-*H*, ddd, *J* = 5.4, 3.8, 1.7 Hz, 1H), 2.51 (5-*H*, ddd, *J* = 15.3, 10.0, 3.8 Hz, 1H), 2.37 (11-*H*, s, 3H), 1.68 (5-*H*, d, *J* = 15.3 Hz, 1H).

¹³C NMR (126 MHz, CDCl₃) δ 210.79, 161.37, 161.35, 155.35, 152.62, 125.71, 113.66, 113.16, 112.07, 102.52, 87.90, 85.03, 75.80, 57.52, 55.30, 31.56, 18.77.

HRMS [ASAP] for [M⁺] C₁₉H₁₄FeO₆ requires 393.0056, found 393.0053.

(±)-Tricarbonyl[η^4 -7-(cyclohexa-2,4-dien-1-yloxy)-4-(trifluoromethyl)-2H-chromen-2-one]iron (295).



Chemical Formula: C₁₉H₁₁F₃FeO₆

Molecular Weight: 448.1272 g/mol

Brown solid (1.44 g, 78 %).

M.p. 182-185 °C.

IR (NaCl: ν = 2052 (C \equiv O), 1974 (C \equiv O), 1738 (C=O), 1610 (C=C).

¹H NMR (500 MHz, CDCl₃) δ 7.58 (9-*H*, dq, J = 9.0 Hz, J_{H-F} = 1.5 Hz, 1H), 6.77 (8-*H*, dd, J = 9.0, 2.4 Hz, 1H), 6.72 (7-*H*, d, J = 2.4 Hz, 1H), 6.60 (10-*H*, br. s, 1H), 5.65 (2-*H*, dist. dd, J = 5.5, 5.0 Hz, 1H), 5.56 (3-*H*, dist. dd, J = 5.4, 5.0 Hz, 1H), 4.85 (6-*H*, ddd, J = 9.5, 3.1, 2.8, 1H), 3.18 (1-*H*, ddd, J = 5.5, 3.1, 1.3 Hz, 1H), 3.02 (4-*H*, ddd, J = 5.4, 3.8, 1.7, 1H), 2.52 (5-*H*, ddd, J = 15.4, 9.5, 3.8 Hz, 1H), 1.69 (5-*H*, d, J = 15.4 Hz, 1H).

¹³C NMR (126 MHz, CDCl₃) δ 210.66, 162.28, 159.50, 156.42, 141.71 (q, J_{C-F} = 32.8 Hz), 126.54 (q, J_{C-F} = 2.1 Hz), 121.73 (q, J_{C-F} = 275.5 Hz), 114.21, 112.27 (q, J_{C-F} = 5.6 Hz), 107.06, 102.90, 87.97, 85.01, 76.11, 57.06, 55.13, 31.58.

4.2. References

-
- ¹ T. Olsson, H. Graden, J. Hallberg, N. Kann, *J. Comb. Chem.*, **2004**, *6*, 783-788.
- ² A. J. Pearson, M. Zettler, A. Pinkerton, *J. Chem. Soc., Chem. Commun.*, **1987**, 264-266.
- ³ J. Eriksson, T. Olsson, H. Garden, *Tetrahedron Lett.*, **2006**, *47*, 635-638.
- ⁴ T. Quiroz, D. Corona, A. Covarruvias, J. G. Avila-Zarraga, M. Romero-Ortega, *Tetrahedron Lett.*, **2007**, *48*, 1571-1575.
- ⁵ A. J. Birch, D. H. Williamson, *J. Chem. Soc., Perkin Trans.1*, **1973**, 1892-1900.
- ⁶ D. E. Stack, A. L. Hill, C. B. Diffendaffer, N. M. Burns, *Org. Lett.*, **2002**, *4*, 4487-4490.
- ⁷ S. Gomez, J. A. Peters, T. Maschmeyer, *Adv. Synth. Catal.*, **2002**, *344*, 1037-1052.
- ⁸ A. Pesciulli, V. Smout, T. E. Storr, E. A. Mitchell, Z. Elias, W. Herrebout, D. Berthelot, L. Meerpoel, B. U. W. Maes, *Chem. Eur. J.*, **2013**, *19*, 10378-10387.
- ⁹ D. Stones, S. Manku, X. Lu, D. G. Hall, *Chem. Eur. J.*, **2004**, *10*, 92-100.
- ¹⁰ T. R. Jackson, J. S. Springall, D. Rogalle, N. Masumoto, H. Ch. Li, F. D'Hooge, S. P. Perera, A. T. A. Jenkins, T. D. James, J. S. Fossey, J. M. H. van den Elsen, *Electrophoresis*, **2008**, *29*, 4185-4191.
- ¹¹ L. Chi, J. Zhao, T. D. James, *J. Org. Chem.*, **2008**, *73*, 4684-4687.
- ¹² H-J. Knolker, G. Baum, N. Foitzik, H. Goesmann, P. Gonser, P. G. Jones, H. Rottele, *Eur. J. Inorg. Chem.*, **1998**, 993-1007.
- ¹³ A. J. Birch, P. E. Cross, J. Lewis, D. A. White, S. B. Wild, *J. Chem. Soc. (A)*, **1968**, 332-340.
- ¹⁴ A. J. Pearson, *Tetrahedron*, **2010**, *66*, 4943-4946.
- ¹⁵ G. F. Docherty, G. R. Knox, P. L. Pauson, *J. Org. Chem.*, **1998**, *568*, 287-290.
- ¹⁶ R. L. Atkins, D. E. Bliss, *J. Org. Chem.*, **1978**, *43*, 1975-1980.
- ¹⁷ R. A. Gibbs, S. K. De, *Synthesis*, **2005**, *8*, 1231-1233.
- ¹⁸ J. A. Richard, Y. Meyer, V. Jolivel, M. Massonneau, R. Dumeunier, D. Vaudry, H. Vaudry, P.-Y. Renard, A. Romieu, *Bioconjugate Chem.*, **2008**, *19*, 1707-1718.